Techno-economic analysis of integrated sugarcane biorefinery scenarios for the production of 2,3-butanediol, 1,3-butadiene, polyhydroxybutyrate (PHB) or citric acid.

by

Mirelle René Gouws

Thesis presented in partial fulfilment of the requirements for the degree

of

MASTER OF ENGINEERING
(CHEMICAL ENGINEERING)

in the Faculty of Engineering
at Stellenbosch University

The financial assistance of the National Research Foundation (NRF) towards this research is hereby acknowledged. Opinions expressed and conclusions arrived at, are those of the author and are not necessarily to be attributed to the NRF.

Supervisor:

Prof. Johann F. Görgens

Co-Supervisor:
Dr. Eunice Sefakor Dogbe

March 2023

DECLARATION

By submitting this thesis electronically, I declare that the entirety of the work contained therein is my own, original work, that I am the sole author thereof (save to the extent explicitly otherwise stated), that reproduction and publication thereof by Stellenbosch University will not infringe any third-party rights and that I have not previously in its entirety or in part submitted it for obtaining any qualification.

Date: March 2023

ABSTRACT

To prevent the closures of South African sugar mills currently experiencing economic strain, biorefineries annexed to existing sugar mills - utilizing residues and/or by-products from the mill - for profitable biochemical and/or biofuel production, have been suggested. Residues and/or by-products readily available at a sugar mill include sugarcane molasses, first-generation (1G) feedstock, and sugarcane bagasse and brown leaves from harvesting residues, second generation (2G) feedstock.

The study considered the economic feasibility of individually producing either 2,3-butanediol (2,3-BDO), 1,3-butadiene (1,3-BD), polyhydroxybutyrate (PHB) or citric acid at a biorefinery annexed to an existing sugar mill. Two biorefinery scenarios were developed for 2,3-BDO, PHB and citric acid, utilizing either 1G or integrated 1G2G feedstock. For 1,3-BD however, four scenarios were developed, where two scenarios produce 1,3-BD with 2,3-BDO as intermediate product and two produce 1,3-BD with ethanol as intermediate product.

The study involved process development based on literature data, simulation of the production processes using Aspen Plus® software, conducting techno-economic analyses to determine the primary economic indicator, minimum selling price (MSP), and conducting sensitivity analyses to assess which factors had the largest impact on the MSP of each scenario. Finally, the greenhouse gas emissions (GHG) of each scenario was determined using the RSB GHG Calculator Tool.

The MSPs determined for 2,3-BDO, 1,3-BD, PHB and citric acid were 1.91 and 2.28 $/kg; 4.08, 4.55, 5.71 and 5.72 $/kg; 6.81 and 7.23 $/kg; and 2.44 and 2.60 $/kg, respectively. The 2,3-BDO and PHB biorefinery scenarios were all deemed profitable with regards to the respective market prices of 2.63 $/kg and 7.6 $/kg. The 1,3-BD and citric acid scenarios were all deemed unprofitable, with market prices of 1.05 $/kg and 0.8 $/kg. The difference in MSPs can overall be attributed to the yields of the various processes, although, the yield is not the only decisive factor. Citric acid, with an exceptional overall yield, had a higher MSP compared to 2,3-BDO, with a lower overall yield, due to the high capital cost associated with aerobic fermentation of citric acid versus microaerobic fermentation of 2,3-BDO.

Producing 1,3-BD with 2,3-BDO as intermediate product was more economical with MSPs of 4.08 and 4.55 $/kg compared to producing 1,3-BD with ethanol as intermediate with MSPs of 5.71 and 5.72 $/kg. This was mainly attributed to low catalytic selectivities and conversions of the latter as well as the high capital costs associated with the two-step catalytic upgrading of ethanol to 1,3-BD. Furthermore, utilizing 1G feedstock at a biorefinery proved to be more economical compared to utilizing 1G2G feedstock. The inferior economics of a 1G2G biorefinery can be attributed to the significant utility and capital cost contributions associated with 2G feedstock processing. Specifically the high capital cost of enzymatic hydrolysis equipment and the high energy consumption associated with the concentration of the hemicellulose hydrolysate prior to fermentation. The PHB scenarios were the only scenarios with notable GHG emissions. The low utility requirements of these scenarios meant that most of the biogas produced in the wastewater treatment plant was flared, releasing large quantities of CO_2 into the atmosphere.

OPSOMMING

Om die sluiting van Suid-Afrikaanse suikermeulens, wat tans ekonomiese druk ervaar, te voorkom, is bioraffinaderye wat aan bestaande suikermeulens geannekseer is – wat residu en/of neweprodukte vanaf die meule benut – voorgestel vir winsgewende biochemiese en/of biobrandstandstof produksie. Residu en/of neweprodukte wat geredelik vanaf 'n suikermeul beskikbaar is, sluit in suikerrietmolasse, eerstegenerasie (1G) grondstof, en suikerrietbagasse en bruin blare vanaf oesreste, tweedegenerasie (2G) grondstof.

Die studie het die ekonomiese uitvoerbaarheid oorweeg om individueel óf 2,3-butaandiol (2,3-BDO), 1,3-butadieen (1,3-BD), polihidroksiebutiraat (PHB) óf sitroensuur te produseer by 'n bioraffinadery wat aan 'n bestaande suikermeul geannekseer is. Twee bioraffinadery-scenario's is ontwikkel vir 2,3-BDO, PHB en sitroensuur, met die gebruik van óf 1G grondstof óf geïntegreerde 1G2G grondstof. Vir 1,3-BD is daar egter vier scenario's ontwikkel, waar twee scenario's 1,3-BD produseer met 2,3-BDO as tussenproduk en twee scenario's 1,3-BD produseer met etanol as tussenproduk.

Die studie behels prosesontwikkeling gebaseer op literatuurdata, simulasie van die produksieprosesse deur gebruik te maak van Aspen Plus® sagteware, die uitvoer van tegno-ekonomiese analises om die primêre ekonomiese aanwyser, die minimum verkoopprys (MSP), te bepaal, en die uitvoer van sensitiwiteitsanalises om te bepaal watter faktore die grootste impak op die MSP van elke scenario het. Laastens is die kweekhuisgasvrystellings (GHG) van elke scenario bepaal met behulp van die RSB GHG berekeningsgereedskap.

Die MSP's wat vir 2,3-BDO, 1,3-BD, PHB en sitroensuur bepaal was, is 1.91 en 2.28 $/kg; 4.08, 4.55, 5.71 en 5.72 $/kg; 6.81 en 7.23 $/kg; en 2.44 en 2.60 $/kg, onderskeidelik. Die 2,3-BDO en PHB bioraffinadery scenario's word almal as winsgewend beskou met betrekking tot hulle onderskeie markpryse van 2.63 $/kg en 7.6 $/kg. Die 1,3-BD en sitroensuur scenario's word almal as onwinsgewend beskou, met markpryse van 1.05 $/kg and 0.8 $/kg. Die verskil in MSP's kan oor die algemeen toegeskryf word aan die opbrengste van die verskillende prosesse, alhoewel die opbrengs nie die enigste deurslaggewende faktor is nie. Sitroensuur, met 'n uitsonderlike algehele opbrengs, het 'n hoër MSP in vergelyking met 2,3-BDO, met 'n laer algehele opbrengs, as gevolg van die hoër kapitaalkoste wat met aërobiese fermentasie van sitroensuur geassosieer word in vergelyking met die mikroaerobiese fermentasie van 2,3-BDO.

Die vervaardiging van 1,3-BD met 2,3-BDO as tussenproduk is meer ekonomies met MSP's van 4.08 en 4.55 $/kg in vergelyking met die vervaardiging van 1,3-BD met etanol as tussenproduk met MSP's van 5.71 and 5.72 $/kg. Dit kan hoofsaaklik toegeskryf word aan die lae katalitiese selektiwiteite en omskakelings van die laasgenoemde sowel as die hoë kapitaalkoste wat met twee-stap katalitiese opgradering van ethanol na 1,3-BD geassosieer word. Verder was die gebruik van 1G grondstof by 'n bioraffinadery meer ekonomies in vergelyking met die gebruik van 1G2G grondstof. Die substandaarde ekonomiese resultate van 'n 1G2G bioraffinadery kan toegeskryf word aan die aansienlike energie- en kapitaalkostes wat met die verwerking van 2G grondstof geassosieer word. Spesifiek die hoë kapitaalkoste van ensiematiese hidrolise-toerusting en die hoë energieverbruik wat met die konsentrasie van die hemisellulose hidrolisaat voor fermentasie geassosieer word. Die PHB scenario's was die enigste scenario's met noemenswaardige GHG uitlaatings. Die lae energie- en hitteverbruik van dié scenario's

het beteken dat meeste van die biogas wat in die afvalwatersuiweringsaanleg vervaardig is, opgevlam word, wat groot hoeveelhede CO_2 in die atmosfeer vrystel.

ACKNOWLEDGEMENTS

The following parties are thanked for their respective contributions in the finalization and delivering of this thesis:

The National Research Foundation of South Africa for their financial support .

My main supervisor, Prof Johann Görgens for the oppportunity to conduct a Masters in this important research field and the invaluable knowlegde I could obtain from it.

My co-supervisor Dr Sefakor Dogbe for the unfaltering assistance and guidance throughout the entire process.

The research group members, especially Cara Van Heerden, for their willingness to share information and always lend a helping hand.

My family and friends, for supporting, motivating and believing in me and being a sounding board whenever I needed one.

Most importantly, our Lord and Savior, Jesus Christ, for the unconditional love and abundant blessings provided to me. I dedicate this thesis to You.

TABLE OF CONTENTS

LIST OF FIGURES

LIST OF TABLES

NOMENCLATURE

SYMBOL/ACRONYM	DESCRIPTION
1,3-BD	1,3-Butadiene
1,4-BDO	1,4-Butanediol
2,3-BDO	2,3-Butanediol
5-HMF	5-hydroxymethylfurfural
CEST	Condensing-Extraction Steam Turbine
CHP	Combined Heat and Power
EH	Enzymatic Hydrolysis
FCI	Fixed Capital Investment
FOC	Fixed Operating Cost
GHG	Greenhouse gasses
HHPS	High-High Pressure Steam (63 bar)
HPS	High Pressure Steam (28.6 bar)
IEC	Installed Equipment Cost
Int	Intermediate
IRR	Internal Rate of Return
ISBL	Inside Battery Limits
LPS	Low Pressure Steam (2.62 bar)
LSF	Liquid Surface Fermentation
MPS	Medium Pressure Steam (10 bar)
NPV	Net Present Value
NREL	National Renewable Energy Laboratory
PHA	Polyhydroxyalkanoate
PHB	Polyhydroxybutyrate
SF	Submerged Fermentation
SHcF	Separate Hydrolysis and co-Fermentation
SmSF	Simultaneous Saccharification and Fermentation
SpHF	Separate Hydrolysis and Fermentation
SSF	Solid State Fermentation
TCI	Total Capital Investment
TEA	Techno-economic analysis
TEE	Triple Effect Evaporator
TPC	Total Production Cost
VOC	Variable Operating Cost
WWT	Wastewater treatment

1 INTRODUCTION

1.1 Background

The survival of South African sugar mills is currently being threatened by a number of factors *inter alia* decreasing sugar prices, high energy costs and the inability to compete with lower-priced producers (Gorgens F; Mandegari, M A; Farzad, S; Daful, A G; Haigh, 2016). In an attempt to prevent the closures of South African sugar mills and the extinction of the industry, the incorporation of biorefineries into existing sugar mills has been suggested. The proposed biorefinery will utilize residues and/or by-products produced at the sugar mill, in order to produce profitable biochemicals and/or biofuels (O'Hara, 2016).

Residues and/or by-products readily available at a sugar mill include sugarcane molasses, first-generation (1G) feedstock, which contains glucose, sucrose and fructose which can be extracted through little to no pre-treatment requirements, and sugarcane bagasse and brown leaves from harvesting residues, second generation (2G) feedstock, which contains glucose, xylose and arabinose which can be extracted using various pre-treatment methods and enzymatic hydrolysis (Rackemann, Zhang & Doherty, 2016; Zhang, Harrison & O'Hara, 2016). These feedstocks are advantageous for biochemicals or biofuel production since they are readily available, rich in sugar content and cost-effective (Das Bhowmik, Brinin, Williams, *et al.*, 2016; Laluce, Leite, Zavitoski, *et al.*, 2016; O'Hara, 2016). Sugarcane molasses and bagasse (and brown leaves) have readily been utilized in studies that aim to develop renewable, economically competitive bioprocesses with the aim to replace the currently dominating unsustainable fossil-fuel based chemical and fuel production processes. 2,3-butanediol, 1,3-butadiene, polyhydroxybutyrate (PHB), and citric acid can be produced through biological processes such as fermentation or catalytic conversion by utilizing a carbon-source as substrate.

2,3-butanediol (BDO) has a wide range of applications including use as an antifreeze agent and the production of printing inks, moistening and softening agents and fumigants. This versatile compound can also be converted to other valuable compounds such as methyl ethyl ketone and 1,3-butadiene (also investigated in this study). The increasing interest in 2,3-BDO can mainly be attributed to these derivatives and therefore a number of studies report the market volume of 2,3-BDO as the combined market volume of its derivatives at 32 million tons per year (Mailaram, Narisetty, Ranade, *et al.*, 2022; Rosales-Calderon & Arantes, 2019). The market volume of 2,3-BDO as a standalone product has been reported as 14 million tons per year (Dowe, 2021; Zhang, 2021). To the knowledge of the writer a distinct bio-based market has not yet been established for 2,3-butanediol and this is therefore representative of the combined bio-based and fossil-based 2,3-BDO produced globally.

1,3-butadiene (1,3-BD) is mainly used for the production of synthetic rubbers with styrene butadiene rubber (SBR) and polybutadiene rubber (PBR), used for the manufacturing of tyres, being its primary downstream products (Miyazawa, Tanabe, Nakamura, *et al.*, 2020; Pomalaza, Arango Ponton, Capron, *et al.*, 2020a; Tripathi, Palanki, Xu, *et al.*, 2019). Evidently, the main industry driving the demand for 1,3-BD is the automobile industry. The global market of butadiene has been estimated at 13 - 16 million tons per year in 2019, with a large portion still owed to the fossil-based version (Brencio, Maruzzi, Manzolini, *et al.*, 2022; Haque, Gupta, Nazier, *et al.*, 2021).

Polyhydroxybutyrate (PHB) is a polymer that has the potential to replace non-biodegradable plastic materials, currently causing major environmental pollution in oceans (Saratale, Cho, Saratale, *et al.*, 2021). Considering PHB shares qualities with currently used synthetic plastic material, this biodegradable polymer has a wide range of applications in food packaging, tissue engineering, and overall plastic manufacturing industries (Kaur, Khajuria, Parihar, *et al.*, 2017; Saratale *et al.*, 2021). A major limitation to the entry of PHB into the bioplastic market is the high costs of PHB production. This has repeatedly been attributed to high raw material costs (>50%), small production volumes and purification costs (Kaur *et al.*, 2017; Saratale *et al.*, 2021). However, an increasing number of studies are aiming at developing bacterial strains that exhibit improved production rates, using cost-effective substrates. Nevertheless, the global market volume of PHB remains small at approximately 40 kt/y (Price, Kuzhiumparambil, Pernice, *et al.*, 2020; Saratale *et al.*, 2021)

Citric acid is part of a group of organic acids, being the most widely used member in the industry. This 'Generally Regarded as Safe' (GRAS) status awarded compound has a plethora of applications in industries including, among various others, the food and beverage (approx. 70%), pharmaceutical, personal care and detergent and cleaners industries (Carsanba, Papanikolaou, Fickers, *et al.*, 2019; Mores, Vandenberghe, Magalhães Júnior, *et al.*, 2021). Preservative, antioxidant, blood anticoagulant and flavouring agent are among the various uses (Bankar & Dr Geetha, 2018a; Ciriminna, Meneguzzo, Delisi, *et al.*, 2017). The global market of citric acid is estimated at 2 million tonnes per year of which more than 99% is owed to bio-based production (Bastos & Ribeiro, 2020; Ciriminna *et al.*, 2017; Mores *et al.*, 2021)

1.2 Project Scope

This study will consider the individual production of various biochemicals at a biorefinery annexed to an existing South African sugar mill. The biochemicals are: 2,3-butanediol (2,3-BDO), 1,3-butadiene (1,3-BD), polyhydroxybutyrate (PHB) and citric acid (CA). Furthermore, for each of the biochemicals considered, a minimum of two scenarios will be considered, differentiated by the type of feedstock utilized. The first scenario will utilize first-generation (1G) feedstock i.e., sugarcane molasses, and the second scenario will consider integrated first- and second-generation feedstock i.e., combined sugarcane bagasse and brown leaves from harvesting residues. Additional scenarios for the various products will also be considered if multiple, equally attractive, production pathways exist for a specific chemical.

The objectives of this study include:

1. Conduct literature research on the bio-based production of 2,3-BDO, 1,3-BD, PHB, and citric acid.
2. Develop production processes for each of the four products from first-generation feedstock and integrated first- and second-generation feedstock.
3. Simulate the production process scenarios using Aspen Plus® Software.
4. Execute a techno-economic analysis in Microsoft Excel for each scenario.
5. Conduct a basic environmental assessment for each scenario using the RSB®(Roundtable on Sustainable Biomaterials) GHG Calculator Tool.
6. Use the mass and energy balance results generated from the simulations as well as the results of the techno-economic analysis and the environmental assessment to highlight important insights

and conclusions regarding biorefinery development. Insights and conclusions concern *inter alia* microbial selection, different feedstock highlights and challenges, capital and operational cost pressure points, required production improvements for economic viability and environmental concerns.

2 THEORY / LITERATURE REVIEW

2.1 The sugarcane biorefinery concept and available feedstock from sugarcane

In this study the proposed biorefineries are annexed to an existing sugar mill, where wastes and/or by-products produced during the sugar production process are diverted to the biorefinery as feedstock. The main categories of feedstock available at a sugar mill include first-generation (1G) feedstock (i.e., molasses) and second-generation (2G) feedstock (i.e., lignocelluloses such as bagasse and harvest residues). A sugar mill already consists of essential infrastructure including, among others, boilers, electricity generating equipment and cooling towers. Furthermore, support services like maintenance is already in place (O'Hara, 2016). These already installed equipment and support services can generally be shared between the sugar mill and the biorefinery (Gorgens F; Mandegari, M A; Farzad, S; Daful, A G; Haigh, 2016).

2.1.1 First generation feedstock

Following the harvest of the sugarcane, the stalks either go through a milling or diffusion process to allow for juice extraction (Dogbe, 2020). The juice undergoes clarification, concentration, crystallization and centrifugation to obtain raw crystalline sugar, the final product at a basic sugar mill. Molasses is the fluid product obtained when the crystalline sugar is separated from the crystal-liquid mixture by centrifugation. This crystallization and separation are usually repeated in three steps to maximize crystalline sugar recovery. The resulting A-molasses from the first step is usually processed in the second step to obtain B-molasses, which can then further be processed in a third step to obtain C-molasses as the final by-product (Dogbe, 2020; Harrison, 2016). In this study A-molasses is extracted and utilized as 1G feedstock in the biorefinery for product formation. This is done considering decreasing sugar demands reduces the necessity to recover maximum sugar and furthermore A-molasses is more pure compared to B- and C-molasses, which will reduce the complexity of purification and separation processes taking place in the biorefinery (Dogbe, Mandegari & Görgens, 2020). Evidently, diverting A-molasses to an annexed biorefinery will reduce raw sugar and C-molasses production by the sugar mill. The cost of A-molasses will therefore need to take this revenue reduction into account.

Molasses contains glucose, fructose and sucrose that can be used for the production of various biochemicals through means of fermentation. First-generation feedstock has some advantages compared to 2G feedstock, including little to no pre-treatment requirements, high yields and simplified separation and purification processes due to less impurities (Rackemann *et al.*, 2016). A-molasses does however contain traces of heavy metals that can sometimes be inhibitory, depending on the tolerance of the specific microorganisms employed for fermentation (Bozorg, Vossoughi, Kazemi, *et al.*, 2015).

2.1.2 Second generation feedstock

The fibrous material that is left after juice extraction is called sugarcane bagasse. The bagasse, together with the brown leaves as harvesting residues collected from the sugarcane fields, is the second-generation feedstock available at a sugar mill. When green harvesting methods are employed, the brown leaves are left in the field with tops to decompose, adding organic matter and nutrients back into the soil.

However in this study the tops remain in the field whilst the brown leaves are used with sugarcane bagasse as lignocellulosic feedstock, for biochemical production or for steam and electricity generation (Nieder-Heitmann, 2019).

These abundant agricultural residues (bagasse and brown leaves) primarily consist of plant cell walls that are rather recalcitrant and require additional pre-treatment and enzymatic hydrolysis steps to extract the fermentable sugars from them. Cellulose (32-45%), hemicellulose (20-32%) and lignin (17-32%) are the main constituents of these plant cell walls, compositions depending on among other things, the climate, sugarcane variety and soil conditions (Alokika, Anu, Kumar, *et al.*, 2021; Koekemoer, 2018). A variety of fermentable sugars, which can be used for biochemical production, are extractable from the cellulose and hemicellulose components, but not from lignin. Glucose is the main fermentable sugar to be obtained from cellulose whereas glucose, xylose and arabinose are some of the sugars to be derived from hemicellulose (Zhang *et al.*, 2016).

2.1.3 Integrated 1G2G feedstock

To benefit from the increased quantity of fermentable material associated with 2G feedstock, despite the higher costs of pre-treatment and enzymatic hydrolysis, integrated 1G2G feedstock has been suggested. The combination of both 1G and 2G feedstock will lead to larger production volumes, which can lead to economy of scale benefits. Furthermore the addition of molasses to the sugarcane bagasse and brown leaves hydrolysate will lead to the dilution of inhibitors which can result in more efficient fermentation processes (Dias, Cavalett & Filho, 2016). Van der Westhuizen, (2013) has confirmed the economic benefits of using integrated 1G2G feedstock as opposed to the sole use of 1G or 2G feedstock. It was found that an integrated 1G2G ethanol biorefinery scenario was the most economically feasible scenario, followed by a 1G-only and finally 2G-only ethanol biorefinery concept (Van der Westhuizen, 2013). However, this does not represent the outcome for biorefineries producing other biochemicals and the most economic option will depend largely on the various production processes.

2.2 Biochemical production process

Biochemical production from first generation feedstock is a much simpler process compared to using second generation feedstock, considering the fermentable sugars are already available. The only production process steps required when 1G feedstock is utilized include fermentation, usually preceded by a seed train for microbial growth, and a final separation and purification process to obtain the final biochemical product. These are however the production steps of a basic biochemical production process, further process steps such as catalytic upgrading can also be involved, depending on the specific biochemical being produced.

Biochemical production from second generation (2G) feedstock is more complex as various pre-processing steps are required to release the fermentable sugars from the lignocellulosic material. The type and number of pre-processing steps required will vary depending on the specific biochemical being produced. Nevertheless, the most basic process steps required for a 2G feedstock utilizing production process includes pretreatment, enzymatic hydrolysis, sometimes detoxification, fermentation and final

separation and purification (Zhang *et al.*, 2016). In this section the various process steps required for biochemical production from both first- and second-generation feedstock will be discussed.

2.2.1 Pre-treatment of lignocellulosic biomass (2G feedstock)

Pre-treatment is the first step required for the processing of 2G feedstock for the purpose of extracting the fermentable sugars from the lignocellulosic biomass, sugarcane bagasse and brown leaves from harvesting residues. Pre-treatment aims to expose and disrupt the cellulose fibres by increasing the surface area and porosity (Zhang *et al.*, 2016). This results in enhanced digestibility of the cellulose during enzymatic hydrolysis (Alokika *et al.*, 2021; Leibbrandt, 2010). Another purpose of pre-treatment is delignification. Lignin is one of the barriers that limit the efficiency of enzymatic hydrolysis, which can be attributed to ineffectual binding of the enzymes (Anu, Kumar, Rapoport, *et al.*, 2020; Bu, Wang, Deng, *et al.*, 2021). A strong correlation (R^2 = 0.965) between delignification and enzymatic digestibility was observed when peroxyformic acid pre-treatment was employed and it was furthermore found that enzymolysis efficiency could be increased from 20% to 100% following the removal of an additional 58% lignin (Bu *et al.*, 2021).

Finally, pre-treatment is also required to solubilize hemicelluloses to extract soluble and fermentable sugars. It has also been reported that the presence of hemicellulose with cellulose, hinders the enzymatic hydrolysis of cellulose and therefore effective solubilization and separation of hemicellulose prior to or during enzymatic hydrolysis is also essential (Anu *et al.*, 2020; Bu *et al.*, 2021). A remarkable hemicellulose solubilization of 92.7% was achieved by employing a steam explosion pre-treatment strategy at 200°C on sugarcane straw (Oliveira, Pinheiro, Souto-Maior, *et al.*, 2013). Furthermore, by also delignifying the lignocellulosic biomass with sodium hydroxide, enzymatic hydrolysis efficiency of the solid cellulose increased from 58.8% to 85.1% (Oliveira *et al.*, 2013).

Various pre-treatment methods are available that can be categorized as chemical, physical or biological. Physical and biological processes employed as the sole pre-treatment processes are not feasible for industrial implementation due to low productivity, poor selectivity and high energy requirements leading to increased cost (Nieder-Heitmann, 2019; Zhang *et al.*, 2016). Furthermore, physical pre-treatment techniques do not remove lignin (Naleli, 2016).

An extensive literature study regarding various pre-treatment methods has been conducted by Nieder-Heitmann, (2019). Pre-treatment methods were ranked based on a number of criteria such as high sugar yield, temperature, cost effectiveness, effect on enzymatic digestibility etc. The superior methods were found to be dilute acid pre-treatment and alkaline pre-treatment, followed closely by Steam Explosion (STEX), Ammonia Fibre Expansion (AFEX^{TM}) and ionic liquid solvent pre-treatment. However, alkaline pre-treatment, AFEX^{TM} and ionic liquid pre-treatment have limitations that prevent their industrial application such as difficulty with scale-up due to high costs and complex downstream processing (Alokika *et al.*, 2021; Makhetha, 2016; Nieder-Heitmann, 2019).

In addition to the literature study, Nieder-Heitmann (2019) also conducted a techno-economic study to evaluate the effect of various pre-treatment methods on the economic feasibility of a succinic acid

biorefinery annexed to an existing sugar mill. The study concluded that steam explosion (STEX) a hydrothermal pre-treatment method (sometimes also referred to as physicochemical pre-treatment process) was the most profitable, followed by SO_2-catalysed STEX, AFEX™ and dilute acid pre-treatment. Considering dilute acid pre-treatment and STEX pre-treatment were the leading methods established by Nieder-Heitmann, (2019), they will furthermore be discussed in this section.

2.2.1.1 Dilute acid pre-treatment

The dilute acid treatment or hydrolysis is an industrially feasible pre-treatment method that has been studied extensively. The treatment allows for the hemicellulose to be solubilized into monomers after being treated by a diluted acid such as the commonly used sulphuric acid (Koekemoer, 2018). Following hemicellulose solubilization, the liquid hemicellulose stream and the solid cellulignin can undergo separate enzymatic hydrolysis procedures to extract the various fermentable sugars, although often times only cellulignin undergoes enzymatic hydrolysis. This is because many microorganisms are not capable of utilizing xylose for biochemical or biofuel production or that the acidic pre-treatment already produces the hemicellulose sugars as monomers (Alokika *et al.*, 2021; Guragain & Vadlani, 2017). Nevertheless, it will be economically beneficial when both the hemicellulose and cellulose can be utilized for biochemical production.

The efficiency of dilute acid pre-treatment is increased by increasing the severity of operating conditions such as pH and temperature, which leads to good cellulose hydrolysis during subsequent enzymatic digestion (Zhang *et al.*, 2016). However, increased digestibility of cellulose and hemicellulose hydrolysis lead to the increased formation of inhibitory compounds. These compounds negatively affect the microbial efficiency during fermentation and complicate downstream processing (Cha, Jang, Kim, *et al.*, 2020; Koekemoer, 2018; Nieder-Heitmann, 2019).

Benjamin *et al*. (2014) conducted pre-treatment and enzymatic hydrolysis optimization experiments on bagasse samples from a range of sugarcane cultivars, and achieved a glucose recovery and overall sugar recovery of 98.7% and 66.1%, respectively, at a temperature of 190°C and residence time of 10 min. Dilute sulphuric acid was used as pre-treatment, where prior to enzymatic hydrolysis, 93% of the glucose was recovered to the water insoluble solids (WIS) and 78.4% of the xylose was recovered to the solubilized hemicellulose liquor, which gives promising results for when the cellulose and hemicellulose derived sugars need to be separated for fermentation (Benjamin, García-Aparicio & Görgens, 2014). It is important to note that these are the best results obtained for when both glucose and xylose can be utilized during fermentation.

2.2.1.2 Steam explosion pre-treatment

Steam explosion is another industrially feasible process due to high yields, cost-effectiveness, energy efficiency and high solids loading potential (50%) (Koekemoer, 2018; Petersen, 2012). The treatment involves the application of saturated steam at high temperatures (160 - 260°C) for a certain amount of time, after which the reactor, containing the biomass, is decompressed rapidly, causing an ‘explosion’ of the water inside the biomass. This extreme force causes the degradation and/or partial defibrillation of

the biomass (Koekemoer, 2018; Naleli, 2016; Wallace, 2013). During the steam explosion process, the hemicellulose is partially hydrolysed resulting in the formation of acids that subsequently act as catalysts for further hemicellulose hydrolysis (Koekemoer, 2018). In addition to these catalysts formed from hemicellulose, other catalysts such as SO_2 or H_2SO_4 can be added to aid in the pre-treatment process (Petersen, 2012). Similar to dilute acid treatment, inhibitors can also be formed during this process where the quantity depends on the severity of the conditions.

Another study investigated the effect of different operating temperature and duration of uncatalyzed steam pre-treatment on sugarcane bagasse as well as harvesting residues. Different optimal operating conditions were found for sugarcane bagasse and harvesting residues. The operating conditions for bagasse that resulted in maximum hemicellulose recover or combined sugar yield was at 202.2°C and 5 min and 215°C and 5 min respectively, whereas for harvesting residues all criteria were maximized in a range of 198-200°C and 8-12 min (Hamann, 2020).

Despite a number of examples available where promising sugar yields were obtained using uncatalyzed steam pre-treatment, various studies have observed the benefits of using catalysts such as H_2SO_4 or SO_2 (Carrasco, Baudel, Sendelius, *et al.*, 2010a; Silveira, Chandel, Vanelli, *et al.*, 2018). Using sulphuric acid as catalyst generally allows for more glucose to be released from the lignocellulose material as opposed to using SO_2 as catalyst or no catalyst at all. On the other hand, using SO_2 as catalyst the combined sugar yield of glucose and xylose is generally favoured (Martín, Galbe, Nilvebrant, *et al.*, 2002). In a study by Martin, et al., (2002) a glucose yield of 56% and xylose yield of 61% yield was observed for an SO_2-catalysed steam pre-treatment process. Furthermore, another study observed that employing SO_2 as catalyst, 44.3 $g_{glucose}/100g_{CDW}$ and 22.6 $g_{xylose}/100g_{CDW}$ were obtained, which corresponds to 91.7% and 81.7% of the theoretical yields (Carrasco, Baudel, Sendelius, *et al.*, 2010b).

2.2.1.3 Inhibitors formed during pre-treatment.

During pre-treatment of sugarcane lignocelluloses, a number of inhibitors can be formed. These inhibitory compounds affect cell growth as well as metabolism, the extent thereof depends on the tolerance of the microorganism employed during fermentation (Kim, Park, Song, *et al.*, 2013). Not only does inhibitor tolerance differ between microorganisms, but inhibitor tolerance also varies between different metabolically engineered strains of the same microorganism.

The majority of inhibitors are formed as a results of hemicellulose degradation, such as furfural, acetic acid, 5-HMF and formic acid, however 5-HMF and phenolic compounds can also form during the degradation of cellulose and lignin respectively (Chandel, da Silva & Singh, 2011; Leibbrandt, 2010; Ourique, Rocha, Gomes, *et al.*, 2020). The type of inhibitors formed as well as their respective concentrations depend on the type of biomass and pre-treatment used, as well as the specific conditions under which pre-treatment is conducted (Ourique *et al.*, 2020). Acid hydrolysis with 2.5% HCl reportedly results in a slurry of pre-treated sugarcane bagasse and hydrolysate which contains 1.89 $g.L^{-1}$ furans (e.g., 5-HMF), 2.75 $g.L^{-1}$ phenolics (e.g., vanillin) and 5.45 $g.L^{-1}$ acetic acid (Chandel *et al.*, 2011).

When choosing the most optimal pre-treatment conditions both cellulose digestibility as well as inhibitor formation need to be considered. Generally, for both dilute acid and steam explosion, higher cellulose digestibility relates to more severe conditions such as high temperatures, which in effect lead to higher inhibitor concentrations. Nevertheless, other process interventions are available to address the complications associated with inhibitors. Microorganisms with a high tolerance toward inhibitors can be chosen for fermentation, however it can be that no high-tolerating, highly efficient microorganism is available for the production of a certain biochemical. Alternatively, an additional detoxification step can be included that removes most of the inhibitors from the sugars obtained from pre-treatment and enzymatic hydrolysis, which will however negatively impact the economic feasibility of a biochemical production process considering that no cost-effective detoxification steps are currently available (Jiang, Fang, Zhao, *et al.*, 2015; Leibbrandt, 2010; Nieder-Heitmann, 2019).

Nevertheless, detoxification is sometimes essential for optimal microbial growth and fermentation efficiency. The detoxification technique used should take the type and concentration of inhibitors formed during pre-treatment as well as the tolerance of the microorganism to be used during fermentation into consideration (Van der Westhuizen, 2013). Frequently used detoxification techniques include evaporation, membrane extraction filtration, ion exchange, over liming, activated charcoal and extraction with organic solvents. An extensive review by Özüdoğru, (2018) has previously been conducted describing the methodology as well as advantages and disadvantages of each technique.

2.2.2 Enzymatic hydrolysis

During enzymatic hydrolysis, enzymes such as cellulases (endoglucanase, β-glucosidase etc.) and hemicellulases (xylanase, β-xylosidase etc.) are used to break down cellulose and hemicellulose, that remain in the pre-treated solids, into their various monomer components (Nieder-Heitmann, 2019; Zhang *et al.*, 2016). Enzymes are expensive, which previously limited the use of enzymatic hydrolysis compared to acid hydrolysis, until the discovery of the enzyme producing microorganism, *Trichoderma reesei* which naturally secretes high titres of biomass-degrading enzymes (Anu *et al.*, 2020; Zhang *et al.*, 2016). A portion of the hydrolysate produced during pre-treatment can be diverted to on-site enzyme production, reducing costs significantly (Nieder-Heitmann, 2019; Zhang *et al.*, 2016).

Various factors affect the efficiency of enzymatic hydrolysis including, but not limited to, temperature, pH, enzyme dosage, solids loading and residence time. Enzyme dosage should be carefully chosen, a high dosage will reduce residence time which subsequently increases productivity and reduced capital cost. However, high enzyme dosage will require a larger portion of the feedstock to be diverted to the enzyme production plant and increase the size of the enzyme production plant which, will consequently increase capital and operating costs (Benjamin *et al.*, 2014; Nieder-Heitmann, 2019).

2.2.3 Seed Train and Fermentation

A seed train, which precedes fermentation, allows for adequate microbial growth in smaller bioreactors before the microorganisms are inoculated into the main fermentation bioreactors (Hernández Rodríguez, Pörtner & Frahm, 2013). This process step generally uses 10% (w/w) or less of the feedstock stream

intended for fermentation (Humbird, Davis, Tao, *et al.*, 2011). The seed train is essential in minimizing the lag phase that often occurs during a fermentation process by promoting exponential microbial growth (Nieder-Heitmann, 2019). The seed train usually does not consist of just one fermenter, but rather a number of fermenters increasing in size, as the volume of microbial inoculum increases in a stepwise manner. The product from each individual seed train fermenter acts as inoculum to the next seed train fermenter until a sufficient amount of microbial growth has occurred and the microorganism can be added to the main fermenters.

The potential of a biochemical production process on industrial scale largely depends on the fermentation process developed. The fermentation process, or specifically the efficiency of the specific microorganism employed, is a key factor to consider when developing a production process. From an economic perspective, the concentration of product in the fermentation broth, i.e., the titre, has a significant impact on the recovery process further downstream, whereas yield highly influences the amount of saleable product produced from a set amount of feedstock (Lee & Choi, 1998). Furthermore, volumetric productivity impacts the equipment sizing and capital cost, specifically the equipment cost due to longer residence times requiring larger bioreactors or a larger number of bioreactors (Choi & Lee, 1999b; Van Der Merwe, 2010; Naleli, 2016). Nevertheless, titre or yield should not be sacrificed to enhance productivity (Van Der Merwe, 2010).

The National Institute of Health (NIH) has categorized microorganisms into four Risk Groups (RG) based on their pathogenicity for healthy adult humans. RG1 is the least pathogenic group, containing all microorganisms not harmful, and with no record of causing disease. The severity of pathogenicity increases with the group number to RG4 with a record of causing serious or lethal diseases and no preventative measures or treatment available (NIH, 2019). For citric acid and polyhydroxybutyrate fermentation, promising results were obtained from Risk Group 1 microorganisms. However, the most promising fermentation results for 2,3-BDO have been obtained from Risk Group 2 (RG2) microorganisms (Kuenz, Jäger, Niemi, *et al.*, 2020). Nevertheless, the pathogenicity of Risk Group 2-4 microorganisms make them undesirable for large-scale biochemical production, especially at a sugar mill producing food-grade products (Shrivastav, Lee, Kim, *et al.*, 2013). Safety regulations need to be adhered to, which implies that only Risk Group 1 microorganisms should be considered (Celińska & Grajek, 2009).

2.2.4 Further Downstream Processes

Following fermentation, the general downstream process would be the separation and purification of the final product. This usually involves an initial centrifuge that separates the solid biomass from the fermentation broth (Dunn, Adom, Sather, *et al.*, 2015). Subsequently, separation and purification processes are used to recover the final saleable product, which could either mean separation from the other fermentation broth constituents or extraction from the cells, when the product is intracellularly produced.

Another downstream process relevant to this study that could be part of the biochemical production process, is catalytic upgrading. This would be the case when the product produced during fermentation is not the final product and further processing is required to obtain the final saleable biochemical.

Evidently, the further downstream processes are particular to the specific biochemical being produced and detailed descriptions will be given for each biochemical in their respective sections.

2.3 Production of bio-based 2,3-Butanediol

2,3-Butanediol (2,3-BDO), also referred to as 2,3-butylene glycol or 2,3-dihydroxybutane (Sabra, Quitmann, Zeng, *et al.*, 2011) has the chemical formula $C_4H_{10}O_2$. 2,3-Butanediol can be produced through the fermentation of a carbon source as substrate, facilitated by microorganisms. Most studies investigating 2,3-BDO fermentation have utilized glucose (Lee & Seo, 2019). However, production from more cost-effective substrates such as lignocellulosic biomass could be the key to commercially establish the bioproduction of 2,3-BDO. Currently there are limited, major companies operating in the commercialization of bio-based 2,3-BDO, including LanzaTech, Orochem Technologies Inc., Global Bio-Chem Technology Group and GS Caltex Corporation. Of these companies, GS Caltex Corporation is the only company producing 100% bio-based 2,3-BDO using cassava as feedstock and a combination of recovery techniques all based on the physical properties of 2,3-BDO (Song, Park, Chung, *et al.*, 2019a; Tinôco, Borschiver, Coutinho, *et al.*, 2021) Other feedstock used by major companies include corn starch and waste gases (Tinôco *et al.*, 2021)

To the knowledge of the writer all studies conducted on the production of 2,3-BDO from sugarcane lignocellulose, made use of RG2 microorganisms. However, numerous studies are available describing the production of 2,3-BDO using RG1 microorganisms, from A-molasses and pure forms of the sugars that can be extracted from sugarcane bagasse.

2.3.1 Fermentation of sugar for 2,3-butanediol production

2.3.1.1 2,3-BDO producing microorganisms utilizing sugarcane derived sugars

Risk Group 1 microorganisms readily utilized in studies to produce 2,3-BDO from sugarcane derived sugars include *Bacillus amyloliquefaciens, Bacillus licheniformis*, recombinant *Escherichia coli, Saccharomyces cerevisiae* and *Klebsiella oxytoca.* The most promising 2,3-BDO production results can be found in Table 1 and will briefly be discussed in this section.

Most microorganisms prefer hexose sugars such as glucose as opposed to pentose sugars such as xylose and therefore only start consuming xylose once glucose is depleted, a phenomenon referred to as carbon catabolite repression. Furthermore, it has been reported that once the microorganism has switched to xylose consumption, it could no longer consume glucose, despite additions of the monosaccharide to the fermentation broth (Guragain & Vadlani, 2017).

For an industrially viable process, a strain capable of simultaneously utilizing pentose and hexose sugars in a mixture is favourable (Ji, Nie, Huang, *et al.*, 2011; Li, Li, Wang, *et al.*, 2014). *Zymomonas mobilis,* a microorganisms that has previously been shown to effectively produce ethanol (Humbird *et al.*, 2011) has been metabolically engineered to produce 2,3-BDO. This microorganism is capable of utilizing a whole slurry hydrolysate containing both glucose, xylose and arabinose for 2,3-BDO production. In a study using *Z. mobilis* as the microorganisms in a designed and modelled 2,3-BDO production system, a titre of 97 g/L

was assumed for batch fermentation (Davis, Grundl, Tao, *et al.*, 2018). This titre is however based on targeted projection, and much lower titres of only approximately 40 g/L has been achieved experimentally (Davis *et al.*, 2018). Further work has however been conducted by NREL, where *Z. mobilis* was used to produce 2,3-BDO at a titre of 87 g/L and 125 g/L on large scale (100L) and bench scale respectively, utilizing deacetylated mechanically refined (DMR) corn stover liquor (Dowe, 2021).

Table 1: Various microorganisms and substrates utilized to produce 2,3-BDO employing fed-batch feeding strategies.

Microorganism	Substrate	Yield ($g.g^{-1}$)	Titre ($g.L^{-1}$)	Productivity ($g.L^{-1}.h^{-1}$)	Reference
K. oxytoca KMS5005-73T	Glucose	0.49	117.4	1.2	(Jantama, Polyiam, Khunnonkwao, *et al.*, 2015)
B. licheniformis MW3	Glucose	0.492	90.1	2.82	(Ge, Li, Li, *et al.*, 2016)
B. amyloliquefaciens TUL 308	Sugarcane molasses + feeding of glucose	0.47	60.83	0.44	(Sikora, Kubik, Kalinowska, *et al.*, 2016)
B. licheniformis DSM 8785	Glucose	0.4	144.7	1.14	(Jurchescu, Hamann, Zhou, *et al.*, 2013)
K. oxytoca PBDH	Glucose	0.4	116	3.1	(Park, Rathnasingh & Song, 2015)
B. amyloliquefaciens 18025	Sugarcane molasses	0.4	48.7	0.83	(Maina, Mallouchos, Nychas, *et al.*, 2019)
S. cerevisiae BD5X-TXmNP	Xylose + Glucose	0.3*	96.8	0.58	(Kim, Sim, Kim, *et al.*, 2017)
B. amyloliquefaciens 18025	Sugarcane molasses + VHP cane sugar	0.265*	64.197*	0.526*	(Maina, Mallouchos, *et al.*, 2019)

**Calculated from available information and rounded where applicable*

When *B. licheniformis* produced 74 $g.L^{-1}$ 2,3-BDO from a lignocellulosic material, corn stover hydrolysate, glucose and xylose were consumed simultaneously, albeit at different rates. Furthermore, it was reported that the pure sugars were still more efficiently consumed when processed individually (Li, Li, *et al.*, 2014). A promising strain genetically engineered to utilize xylose as substrate for 2,3-BDO production is *S. cerevisiae* BD5X-TXmNP (Kim *et al.*, 2017). The study found that the highest titre of 96.8 g/L was observed in a fed-batch fermentation process, where the feed consisted of xylose as well as a small continuous stream of glucose (<1 g/L), which provides cofactors to improve the utilization of xylose. Interestingly, carbon catabolite repression is not observed when the glucose concentrations is very low compared to xylose concentration (Cortivo, Machado, Hickert, *et al.*, 2019; Ourique *et al.*, 2020).

There exists a significant gap in research regarding the utilization of sugarcane molasses to produce 2,3-BDO from RG1 microorganisms. To the knowledge of the writer the only promising study obtained uses *B. amyloliquefaciens* 18025, which achieves a yield of 0.4 g/g, 80% of the theoretical maximum yield (Maina, Mallouchos, *et al.*, 2019; Wang, Hu, Liu, *et al.*, 2016). Two studies attempted to improve 2,3-BDO production from sugarcane molasses by using very high polarity (VHP) cane sugar or glucose as feeding medium after the initial sugarcane molasses was depleted. The pure sugar feedings are beneficial considering less impurities are fed into the system however, to justify the high cost of VHP cane sugar and pure glucose feedings, the titres need to be significantly higher than the titres of 60.83 g/L and 64.2 g/L achieved (Maina, Mallouchos, *et al.*, 2019; Sikora *et al.*, 2016).

Despite the lack of promising studies investigating 2,3-BDO production from sugarcane molasses, a plethora of studies have been conducted on the utilization of sucrose, fructose and glucose as sole substrates or as a mixture. *B. licheniformis* is a promising strain for the production of 2,3-BDO. *B. licheniformis* has been shown capable of utilizing sugars such as sucrose and fructose for 2,3-BDO production at efficiencies comparable to utilizing glucose (Song, Rathnasingh, Park, *et al.*, 2018). Genetically engineered *B. licheniformis* ATCC 14580 could produce 103 $g.L^{-1}$ of 2,3-BDO from inulin-derived fructose and glucose by simultaneous saccharification and fermentation (SSF) (Li, Chen, Li, *et al.*, 2014).

A study that obtained high titres and yields of 2,3-BDO (117.4 g/L and 0.49 g/g, respectively) in a fed-batch fermentation used the engineered strain *K. oxytoca* KMS005-73T. Not only has it been shown that the microorganisms can produce 2,3-BDO using a minimal AM1 fermentation medium, but low concentration of by-products were also observed, with 1.5 g/L acetate being the dominating by-product. Furthermore, shake-flask experiments proved that this strain can utilize sugarcane molasses at a similar extent to glucose for 2,3-BDO production (Jantama *et al.*, 2015).

Few promising studies were found where *S. cerevisiae* was the microorganism of choice to produce 2,3-BDO, using sugarcane-derived sugars. A common observation with metabolically engineered *S. cerevisiae* strains for 2,3-BDO production is the accumulation of glycerol and ethanol as by-products (Kim *et al.*, 2017). For a 2,3-BDO titre of 132.4 g/L from pure glucose, a yield of only 0.34 g/g was obtained with high concentrations of by-products up to 25.3 g/L of glycerol (Choi, Kim, Kim, *et al.*, 2016). In a continuous fermentation process with a productivity of 7.64 $g.L^{-1}.h^{-1}$, approximately 10% more glycerol was produced compared to 2,3-BDO (Yamada, Nishikawa, Wakita, *et al.*, 2018). Due to the ease of metabolically engineering *S. cerevisiae*, by-product formation can be reduced when using *S. cerevisiae* to produce 2,3-BDO. However, to the knowledge of the writer this has not yet been investigated.

2.3.1.2 Optimal Fermentation Conditions

During 2,3-BDO fermentation, several by-products are also formed which can include succinate, lactate, formate, acetate, ethanol, glycerol and acetoin (Erian, Gibisch & Pflügl, 2018; Guragain & Vadlani, 2017; Jantama *et al.*, 2015; Jurchescu *et al.*, 2013; Kim *et al.*, 2017; Park, Song, Lee, *et al.*, 2013) depending on the microorganism used as well as the fermentation conditions. The formation of by-products reduces 2,3-BDO production efficiency and furthermore complicates downstream processing, leading to significantly higher costs (Guragain & Vadlani, 2017). To minimize by-product formation a couple of strategies have been adopted.

Most studies have started with investigating the effects of metabolically engineering a strain to delete the genes encoding enzymes responsible for by-product formation. A second strategy adopted by various studies considers the optimization of certain fermentation parameters. Parameters include *inter alia* temperature, pH, aeration, substrate concentration and nutrients used. These parameters can reduce by-product formation whilst additionally increasing production efficiency. There are no fixed parameters for 2,3-BDO production and are rather dependent on the specific microorganism used (Maina, Mallouchos, *et al.*, 2019). For example, the most optimal temperatures for 2,3-BDO fermentation have

been given as 30°C and 40°C (Maina, Mallouchos, *et al.*, 2019; Okonkwo, 2017). However, it has also been reported that the optimal temperature for *B. licheniformis* is as high as 50°C (O'Hair, Jin, Yu, *et al.*, 2020).

A nitrogen source is required for 2,3-BDO fermentation as well as cell growth (Maina, Mallouchos, *et al.*, 2019). Various nitrogen sources are available among which yeast extract is most commonly used for bench-scale experiments. Despite the effectiveness of this nitrogen source, its high cost is problematic for large-scale application (Erian *et al.*, 2018). Other nitrogen sources such as corn steep liquor (CSL) has been deemed as a suitable replacement for yeast extract (Adlakha & Yazdani, 2015; Häßler, Schieder, Pfaller, *et al.*, 2012). However, the viability of replacing yeast extract with CSL is also dependent on the microorganism.

B. licheniformis 18025 could not produce 2,3-BDO with similar efficiency when CSL was used instead of yeast extract. Furthermore, CSL favoured the formation of acetoin instead of 2,3-BDO (Maina, Mallouchos, *et al.*, 2019). In contrast, replacing yeast extract with corn steep liquor using *B. licheniformis* GSC3102 resulted in insignificant decreases in 2,3-BDO production (Song, Rathnasingh, *et al.*, 2018). Evidently it is not only microorganism specific but also strain specific. Surprisingly, fermentation mediums without nitrogen sources have also been developed and shown to support efficient 2,3-BDO fermentation using recombinant *E. coli* and *K. oxytoca* strains (Erian *et al.*, 2018; Park *et al.*, 2013).

The conversion of acetoin (a precursor of 2,3-BDO) to 2,3-BDO, is a reversible process (Kuenz *et al.*, 2020). Consequently, numerous studies have combined the production of 2,3-BDO and acetoin as the total 2,3-BDO product. However, to obtain a saleable product it is important to optimize conditions to ensure an acetoin-free 2,3-BDO fermentation broth. Two ruling factors affecting the preference of 2,3-BDO formation over that of acetoin includes initial substrate concentration and aeration.

At too low substrate concentrations, 2,3-BDO is converted to acetoin (Kuenz *et al.*, 2020). Furthermore, too high substrate concentrations inhibit cell metabolism and growth, affecting 2,3-BDO production (Li, Li, *et al.*, 2014). Fed-batch fermentation is a strategy capable of overcoming both these substrate limitations, achieving high 2,3-BDO titres by controlling the substrate concentrations (Guragain, Chitta, Karanjikar, *et al.*, 2017; Guragain & Vadlani, 2017). Specific substrate concentrations are dependent on the specific microorganism employed.

The optimum aeration that minimizes by-product formation and ensures high 2,3-BDO fermentation falls between highly aerobic and anaerobic, i.e. intermediate aeration (Guragain *et al.*, 2017). Under highly aerobic conditions, acetoin production is favoured, whilst low to medium aeration conditions favour 2,3-BDO production (Kim *et al.*, 2017; Maina, Stylianou, Vogiatzi, *et al.*, 2019; Ourique *et al.*, 2020). Various studies have developed multi-stage aeration strategies, optimizing the aeration according to the various cell growth stages. Aerobic conditions were determined to be optimal during the growth phase, allowing for preferential biomass accumulation and suppression of by-product formation, after which 2,3-BDO formation should be favoured by changing to microaerobic conditions (Erian *et al.*, 2018; Kim *et al.*, 2017; Park *et al.*, 2013)

2.3.2 Separation and Purification of 2,3-Butanediol

The downstream processing of 2,3-BDO is the major limitation, preventing the industrial application of producing this bioproduct. Despite no azeotrope formation between 2,3-BDO and water, 2,3-BDO has a high affinity for water, a very low concentration in a fermentation broth and a higher boiling point (≈180°C) compared to water (Birajdar, Rajagopalan, Sawant, *et al.*, 2015; Haider, Abdul, Hussain, *et al.*, 2018; Song, Park, Chung, *et al.*, 2019b). Consequently 2,3-BDO separation on large-scale using only conventional distillation will not be an economically favoured process, due to the high energy demands (Harvianto, Haider, Hong, *et al.*, 2018a; Li & Wu, 2016). GS Caltex has developed a demo-scale 2,3-BDO production plant with a separation and purification process consisting of a combination of centrifugation, evaporation, distillation, ion exchange and electrodialysis (Song, Park, *et al.*, 2019a). Downstream processing of 2,3-BDO reportedly accounts for more than 50% of total production cost (Van Duc Long, Hong, Nhien, *et al.*, 2018), however recent studies have aimed at developing new techniques to reduce these costs. Tinôco et al. (2021) suggests a 2,3-BDO titre of at least 80 $g.L^{-1}$ is required to ensure cost-effective downstream processing.

Generally, 2,3-BDO downstream processing has an initial microbial biomass removal operation, using membrane filtration or centrifugation, after which the separation and purification are executed to obtain the saleable product of 98% 2,3-BDO (Dai, Zhang & Xiu, 2011; Shao & Kumar, 2009). Decolorization and/or deodorization techniques such as activated carbon and neutralization agent addition can alternatively be final steps, depending on the 2,3-BDO application (Song, Park, *et al.*, 2019a).

Various techniques have previously been investigated and successfully shown to separate and purify 2,3-BDO, however the limitation is rather associated with the economic feasibility of large-scale implementation of these techniques. Many techniques have been developed, however in this study only the most promising techniques, solvent extraction (and salting-out extraction), heat integration distillation and the combination of the aforementioned processes, will be discussed.

Other techniques that have been mentioned by other studies for 2,3-BDO separation have major limitations making them unfeasible for industrial application. These techniques include membrane technology such as nanofiltration and reverse osmosis, which is limited to membrane fouling and very low processing time, and reactive extraction, where the major limitation is the corrosion from the required acid catalysts (HCL or H_2SO_4) as well as the difficulty to recycle these catalysts (Li, Wu, Zhu, *et al.*, 2016; Priya, Dureja, Rathi, *et al.*, 2021; Tinôco *et al.*, 2021). The addition of anti-corrosion devices has been proposed as a solution, however, this technology has not been developed to an industrially feasible extent (Harvianto, Haider, Hong, *et al.*, 2018b).

It is important to note that work is currently being conducted by NREL as part of a 2030 target project, where the aim is to reduce the minimum selling price of 2,3-BDO production process from lignocellulosic biomass to $2.47/gallon gasoline equivalent. One facet of this project is the optimization of the separation and purification section of the production process. Considering the 2,3-BDO will be catalytically upgraded to more valuable chemicals, the purity achieved by the developed separation and purification processes is as low as 50%. One outcome of the project was the development of a separation

and purification process consisting of both a vacuum evaporation and membrane pervaporation step. The newly developed separation and purification process resulted in a 13% reduction in energy consumption compared to a base case, which is a two-stage vacuum evaporation process (Church, Sun, Yan, *et al.*, 2021). However, no information has been made available concerning the cost differences between the two processes.

2.3.2.1 Solvent Extraction and Salting-out/Sugaring-out extraction

Solvent extraction, also referred to as liquid-liquid extraction, achieves separation by having two immiscible liquid components of which the product to be separated is preferably miscible with one of the liquid components and the other fermentation broth constituents preferably miscible with the other liquid component (Fu, Li, Sun, *et al.*, 2020). It has readily been investigated for the separation of 2,3-BDO and is one of the only two processes to be implemented for large-scale production, the other being distillation (Tinôco *et al.*, 2021). Solvent extraction performs the task of separating 2,3-BDO from *inter alia* impurities and water after which another technique such as distillation is employed to perform the purification of 2,3-BDO (Haider, Harvianto, Qyyum, *et al.*, 2018). Compared to conventional distillation, the combined solvent extraction and distillation system has proved to reduce total annualized costs by up to 25.8%, primarily due to the reduced reboiler and condenser duty of the distillation column considering the largest portion of water is already separated from 2,3-BDO during extraction, prior to distillation (Harvianto *et al.*, 2018b).

Solvent extraction has benefits such as low energy requirement and ease of operation (Fu et al., 2020; Tinôco et al., 2020), however as with most techniques there are also limitations. A large amount of solvent is required for standard 2,3-BDO extraction (Birajdar, Rajagopalan, Sawant, et al., 2015b; Dai, Zhang & Xiu, 2011b), consequently the recovery and reuse of the solvent is essential to deem this technique economically feasible (Harvianto et al., 2018b). A strategy to mitigate this limitation is the addition of a salt, such as K_2HPO_4, to the solvent extraction process (Fu et al., 2020). This procedure referred to as salting-out, reduces solvent consumption by increasing the 2,3-BDO extraction efficiency (Dai et al., 2011b; Harvianto et al., 2018b). Sugaring-out has also been suggested however only a low recovery of 68.79% has been achievable using glucose (Priya et al., 2021). Figure 1 shows how these separation techniques can be incorporated, which will furthermore be referred to as salting-out extraction/sugaring-out extraction. Evident from Figure 1 is that an additional distillation process is still required for solvent extraction or salting-out extraction because the solvent and product extracted need to be separated from one another to obtain the saleable product.

In a study comparing various 2,3-BDO downstream processing techniques, it was found that the most promising results were obtained from salting-out extraction using ammonium sulphate and isopropyl alcohol as salt and solvent, respectively. The study, along with various others found that by increasing the salt concentration, the separation efficiency greatly increases and the amount of solvent required decreases (Priya *et al.*, 2021; Xie, Zhang, Zhou, *et al.*, 2017). Furthermore, using a fermentation broth containing >80 $g.L^{-1}$ of 2,3-BDO produced from glucose as substrate (cell free), 20% ammonium sulphate ($(NH_4)_2SO_4$) and 20% isopropyl alcohol could initially recover 86% 2,3-BDO in the top-phase. A second

extraction was additionally conducted on the bottoms phase using the recovered isopropyl alcohol (rotary evaporator) after which a 99% recovery of 2,3-BDO was achieved (Priya *et al.*, 2021).

Compared to conventional solvent extraction however, the salting-out extraction requires additional steps to recover the salt for reuse, which will naturally increase costs. These additional steps have also not readily been investigated for large-scale processes, neither has the effect of reusing solvent and salt on the separation efficiency (Priya *et al.*, 2021). Furthermore, if the salt is not effectively recovered, salt build up can occur which leads to solid formation, potentially causing damage to the equipment and blockages (Harvianto *et al.*, 2018b).

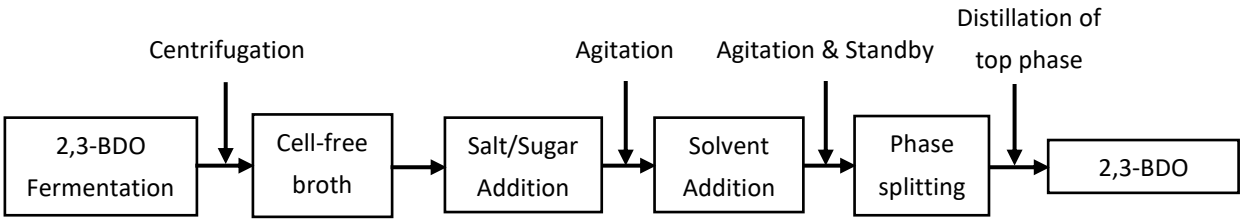

Figure 1: 2,3-BDO recovery process from salting-out extraction/sugaring-out extraction and distillation. (Redrawn from (Priya et al., 2021)).

2.3.2.2 Heat integration distillation

2,3-Butanediol recovery using conventional distillation is a simple process because 2,3-BDO does not form an azeotrope with water. However, this process requires high amounts of energy to evaporate water due to the low concentrations of 2,3-BDO generally found in a fermentation broth as well as the high boiling point of 2,3-BDO at 177°C. This high energy demand leads to conventional distillation being uneconomical for industrial application (Harvianto *et al.*, 2018b; Li *et al.*, 2016). To reduce the energy demand and subsequent costs associated with it, heat integrated distillation has been suggested (Haider, Abdul, *et al.*, 2018).

In a paper by Haider, et al. (2018) a number of heat integration configurations were developed and compared to an optimized conventional, side stream distillation column. Comparisons were based on energy cost and total annualized cost of the various configurations. 2,3-BDO recovery and purity were set parameters for all configurations, at 90wt% and 99wt%. Heat integration of vacuum flash distillation (HI-VFD) and heat integration of a dual column configuration (HI-DC) proved to result in the highest savings of energy cost and total annualized cost. The energy costs were reduced by 66.6% and 51% for HI-VFD and HI-DC respectively. Furthermore, the total annualized costs were reduced by 61.2% and 55% for HI-VFD and HI-DC respectively (Haider, Abdul, *et al.*, 2018).

2.4 Production of bio-based 1,3-Butadiene

1,3-Butadiene (1,3-BD), with the chemical formula, C_4H_6, is considered a very important unsaturated C4 compound, due to its key role in the production of polymers (Baerdemaeker, Feyen, Mu, *et al.*, 2015; Larina, Remezovskyi, Kyriienko, *et al.*, 2019; Pomalaza, Vofo, Capron, *et al.*, 2018). The predominant fossil-based commercial production of 1,3-butadiene is by the steam cracking process, where the main

incentive of the process however, is to produce ethylene, with 1,3-BD only produced as a by-product (Cheong, Shao, Tan, *et al.*, 2016). Furthermore, a recent deviation in the steam cracking process has seen the utilization of lighter hydrocarbons, which result in a significantly lower BD-to-ethylene ratio, compared to the utilization of heavier hydrocarbons such as naphtha (Baerdemaeker *et al.*, 2015; Pomalaza, Arango Ponton, Capron, *et al.*, 2020b). This has resulted in lower amounts of 1,3-BD being produced by the current commercial processes employed, despite the demand for the valuable chemical increasing.

To attempt at meeting global demands for bio-based 1,3-BD and prevent the inevitable price increase that will follow the decreasing supply, considerable efforts have been made to investigate the on-purpose production of 1,3-BD (Samsudin, Zhang, Jaenicke, *et al.*, 2020). Furthermore, the development of bio-based processes have also been an important objective, considering the significant carbon footprint of the current, unsustainable, fossil-fuel based steam cracking process (Pomalaza *et al.*, 2020b).

The dominating on-purpose bio-based processes investigated, have been the conversion of either bioethanol or bio-based C4 alcohols, such as 2,3-BDO or 1,4-BDO, to 1,3-butadiene (Kuznetsov, Kumar, Ardagh, *et al.*, 2020; Samsudin *et al.*, 2020). The interest in the ethanol-to-butadiene process is in fact a revitalization of the process, following obsoletion after the Second World War, when the inexpensive steam cracking process was developed (Pomalaza *et al.*, 2020b).

To the knowledge of the writer, there are only two industrial examples of bio-based 1,3-BD processes currently available. One is an ethanol-to-butadiene prototype plant in Bassens, France, constructed as part of a 10-year project by Michelin, IFP Energies Nouvelles and Axens (Michelin, 2019; Samsudin *et al.*, 2020). Another is a project by LanzaTech and Invista, aiming to produce 1,3-BD via 2,3-BDO, that has been produced by syngas fermentation. As of 2018, the large scale production of 2,3-BDO from the syngas was already developed, whilst the large scale conversion of 2,3-BDO to 1,3-BD was still in progress (Duan, Yamada & Sato, 2016; LanzaTech, 2018; Makshina, Dusselier, Janssens, *et al.*, 2014).

2.4.1 Catalytic Upgrading of 1,3-Butadiene

The efficiency of a bio-based 1,3-butadiene production process is determined by a number of parameters including conversion of substrate, 1,3-BD selectivity, yield and productivity ($g_{BD}.g_{cat}^{-1}.h^{-1}$), which are all encompassed by the key factor, catalyst efficiency (Dai, Zhang, Yu, *et al.*, 2017; Pomalaza *et al.*, 2018). Efficient catalysts are of utmost importance to increase the profitability of this production process, due to reduced amount of feedstock that will be required per ton 1,3-BD produced, lowering raw material cost (Cabrera Camacho, Alonso-Fariñas, Villanueva Perales, *et al.*, 2020).

2.4.1.1 1,3-Butadiene production, with ethanol as intermediate product

The production of bioethanol, especially from 1G feedstock, is already a mature process, using well-established technologies with an abundance of research already conducted to improve ethanol yields from 1G feedstock, as well as to integrated 1G and 2G sugarcane feedstock (Ayodele, Alsaffar & Mustapa, 2020; Mandegari, Farzad & Görgens, 2017; Ponce, Miranda, Maciel Filho, *et al.*, 2015). The main process

steps of first-generation bioethanol production are fermentation and distillation, with pretreatment and enzymatic hydrolysis included for the second-generation bioethanol production (Ayodele *et al.*, 2020).

The microorganism most commonly used for cost-competitive bioethanol production is *S. cerevisiae*, due to multiple factors *inter alia*, high yields and productivities achieved, anaerobic operation and a high tolerance toward inhibitors (de Andrade, Maugeri Filho, Maciel Filho, *et al.*, 2013; Khan, Dwivedi, Engineering, *et al.*, 2013; Moonsamy, 2021). Optimal conditions vary depending on the *S. cerevisiae* strain employed, but generally comprise of temperature ranging 30-40°C and pH ranging 3.7-5.5 (Ayodele *et al.*, 2020; Basso Carlos, Basso Olitta & Rocha Nitsche, 2011).

A common process used in distilleries, especially those located in Brazil, is the Melle-Boinot process, which is a fed-batch process with cell recycle. The recycled cells are treated with a dilute sulphuric acid solution, before being combined with the sugar feedstock and fermentation medium (Basso Carlos *et al.*, 2011; Dias, Junqueira, Filho, *et al.*, 2009; Ensinas, Codina, Marechal, *et al.*, 2013). This process is preferred to another commonly employed strategy, continuous fermentation, due to higher productivities and yields achieved of the specific products as well as ease of maintenance (Basso Carlos *et al.*, 2011).

For the bioethanol production from 2G feedstock, various strategies can be employed. Separate hydrolysis and fermentation (SpHF) and simultaneous saccharification and fermentation (SmSF) are common strategies, where both have multiple advantages. The most prominent advantages include the shorter processing times and reduced equipment associated with the SmSF strategy, whereas for SpHF the conditions can be made optimal for both enzyme used in the hydrolysis step and the yeast used in the fermentation step. Furthermore, cell recycle is much easier when the SpHF strategy is employed compared to the SmSF, due to complexity of lignin and yeast separations (Ayodele *et al.*, 2020; Humbird *et al.*, 2011; Moonsamy, 2021).

Distillation is used for the separation and purification of hydrous ethanol (approximately 92-95%), whereafter more complex technologies can be employed such as azeotropic distillation or molecular sieves when anhydrous ethanol (>99%) is required (Ayodele *et al.*, 2020; Ensinas *et al.*, 2013; Humbird *et al.*, 2011). The minimum required ethanol concentration in the fermentation broth, going to distillation, for an industrially feasible process has been reported as 40 g/L (Ayodele *et al.*, 2020).

1,3-Butadiene (1,3-BD) can be produced from ethanol using an appropriate catalyst. Various studies have mentioned two proven methods, using a similar mechanism, to produce 1,3-BD from ethanol. The first involves direct conversion of ethanol to 1,3-BD using multifunctional catalysts and is referred to as the Lebedev or one-stage process. The second involves two steps where ethanol is initially, partially converted to acetaldehyde, after which the ethanol-acetaldehyde mixture is converted to 1,3-butadiene and is referred to as the Ostromislensky process (Burla, Fehnel, Louie, *et al.*, 2012; Pomalaza *et al.*, 2020b; Pomalaza, Capron, Ordomsky, *et al.*, 2016).

Naturally the one-stage process will have lower capital costs due to less process steps, however it is seldom that high conversion and selectivity are simultaneously achieved in the one-stage process (Dai *et al.*, 2017). Furthermore the one-stage process requires higher temperatures and cannot be optimized for

the various stages of the process as with the Ostromislensky process (Bin Samsudin, Zhang, Jaenicke, *et al.*, 2020).

In addition to catalyst efficiency, temperature additionally affects 1,3-BD production from ethanol. The reactions conducted during the conversion of ethanol to 1,3-BD are all endothermic and therefore require a thermal source (Burla *et al.*, 2012). The optimal temperature is dependent on the type of catalyst used and have been reported to range between 300°C and 700°C. Various promising 1,3-BD producing catalysts from ethanol with their subsequent performance and optimal temperatures can be found in Table 2.

Table 2: Promising catalysts for the production of 1,3-BD from ethanol.

Catalyst	Conversion (%)	1,3-BD Selectivity (%)	Productivity ($g_{BD}.g_{cat}^{-1}.h^{-1}$)	Temperature (°C)	Reference
2%Zn-8%Y/beta	100	75	0.12	623	(Dai *et al.*, 2017)
$Hf_{2.5}Zn_{16}$	99.2	71	0.264	360	(De Baerdemaeker, Feyen, Müller, *et al.*,
1A g/4ZrO_2/SiO_2-SBA16	99	70.5	0.09	325	(Dagle, Flake, Lemmon, *et al.*, 2018)
Zr/MCF	96	73	0.64	235[a] 400[b]	(Dagle *et al.*, 2018)
Mg-SiO_2	95	77	1.35	450	(Huang, Men, Wang, *et al.*, 2017)
ZnTa-TUD-1	94	73	2.13	400	(Pomalaza *et al.*, 2018)
Copper-chromite/Tanta-silica	50%[a] 44.5%[b]	92%[a] 55%[b]	-	312[a] 350[b]	(Burla *et al.*, 2012)

[a]First catalytic upgrading reaction. [b]Second catalytic upgrading reaction

A major challenge for catalytic processes is catalytic stability and deactivation from coking deposition on active sites (Dagle *et al.*, 2018; Pomalaza *et al.*, 2016). Due to this deposition, catalyst efficiency rapidly decreases with increasing time of production. However, recent 1,3-BD studies have focused on selecting or developing catalysts with high stability, tolerance to coking and especially potential for regeneration, for use in the production process. Oxidation/reduction treatment has reportedly been effective in complete regeneration of an Ag/ZrO_2/SiO_2 catalyst system (Dagle *et al.*, 2018). Other regeneration processes that have been reported includes a simple calcination process and/or heat treatment in air for regeneration of a range of catalyst (Baylon, Sun & Wang, 2016; Cai, Zhu, Chen, *et al.*, 2018; Cheong *et al.*, 2016; Dai *et al.*, 2017; Pomalaza *et al.*, 2020b).

Another factor to consider, that affects the efficiency of 1,3-BD production from ethanol, is the water content of the ethanol feed mixture. Processes using anhydrous ethanol as feed achieves higher conversion and selectivity compared to ethanol-water mixtures (Larina *et al.*, 2019; Pomalaza *et al.*, 2020b). The water adsorbs onto the surface of the catalyst which affects the catalyst surface active sites, reducing efficiency (Kyriienko, Larina, Balakin, *et al.*, 2021; Larina *et al.*, 2019). It will be beneficial if a catalyst can be developed or discovered that can efficiently utilize a water-ethanol mixture (50-80%) for 1,3-BD production (Larina *et al.*, 2019). This is because additional steps associated with the purification

and concentration of ethanol from its fermentation broth are reduced or completely eliminated, which will obviously reduce costs (Pomalaza *et al.*, 2020b).

2.4.1.2 1,3-Butadiene production with C4 alcohols as intermediate products

The conversion of C4 alcohols to 1,3-BD is, in effect, very similar to the conversion of ethanol to 1,3-BD. Similarities include but are not limited to: both are catalytic processes that operate at high temperatures (200-700°C) and both ethanol and butanediols can be produced from renewable, cost-effective feedstock such as lignocellulosic biomass (Duan *et al.*, 2016; Pomalaza *et al.*, 2020b; Sun, Li, Yang, *et al.*, 2020). Most studies reviewed, that investigate the production of 1,3-BD with C4 alcohols as intermediate products, use the C4 alcohol, 2,3-BDO. This could be due to the increased attention given to the production of 2,3-BDO as a result of the diverse applications of its derivatives (Sun, Li, *et al.*, 2020). Furthermore, it has been reported that the production by pathway engineering is more complex for 1,4-BDO compared to 2,3-BDO (Zhang, 2021).

A major by-product produced when 2,3-BDO is dehydrated to 1,3-BD is methyl ethyl ketone (MEK). Various studies have even investigated the co-production of 1,3-BD and MEK (Pomalaza *et al.*, 2020b; Song, Yoon & Lee, 2018). Considering MEK cannot be converted to 1,3-butadiene like other unsaturated alcohols produced as intermediates in the dehydration process, the aim is to reduce its selectivity for a 1,3-BD process (Sun, Li, *et al.*, 2020). This has been successfully achieved by developing appropriate catalysts. A 1,3-BD selectivity of >90% was achieved using a CsH_2PO_4-SiO_2 catalyst with a single bed system (Tsukamoto, Sakami, Ito, *et al.*, 2016). Similarly, a double catalyst bed composed of Sc_2O_3 and Al_2O_3 respectively, could reach a selectivity of 94% alongside an impressive 100% conversion of 2,3-BDO.

Evidently, the production of 1,3-BD from BDO has higher selectivities compared to when ethanol is utilized (Table 2). However, interestingly most techno-economic studies still make use of the lignocellulosic biomass-to-ethanol-to-1,3-BD route. This could potentially be due to the processes involving ethanol being more established and mature compared to those involving butanediols such as 2,3-BDO, however to the knowledge of the writer this has not been reported in literature (Song, Yoon & Lee, 2017a).

2.4.2 Separation and Purification of 1,3-Butadiene

The recovery process of 1,3-butadiene from the crude butadiene product containing solution, is a relatively simple process. Nevertheless, the catalytic process with the highest selectivity should be favored because it will reduce downstream processing cost, by reducing the amount of by-products formed and subsequent process steps required to separate these by-products from 1,3-BD (Jones, 2014; Pomalaza *et al.*, 2016). Various papers have investigated optimized extractive distillation, however they were primarily concerned with the separation of 1,3-BD from the C4 cut (C4 hydrocarbons) mixture produced during the current steam cracking method (Mantingh & Kiss, 2021).

The most common byproducts formed during the conversion of ethanol to 1,3-BD, albeit dependent on the specific catalyst employed, include *inter alia* acetaldehyde, ethylene, diethyl ether and croton aldehyde, which all require a simple process to separate from 1,3-BD (Li, Pang, Jaegers, *et al.*, 2020;

Miyazawa *et al.*, 2020). Conventional distillation with multiple distillation columns and a decanter has been deemed sufficient for 1,3-BD recovery at a purity of >98%, from a solution containing the abovementioned by-products. Furthermore, unreacted ethanol and acetaldehyde can be recovered at >97% and >59% respectively in this simple configuration, which can be recycled back to the process (Burla *et al.*, 2012; Farzad, Mandegari & Görgens, 2017).

The separation and purification of high purity 1,3-butadiene from a product mixture obtained when 2,3-BDO is converted to 1,3-BD is, however, slightly more complex, due to the presence of 1-butene which has a similar boiling point to 1,3-BD (Kuznetsov *et al.*, 2020; Song, Yoon, Seo, *et al.*, 2019). In a techno-economic study comparing conventional distillation and extractive distillation for the recovery of 1,3-BD from a 2,3-BDO-to-1,3-BD product mixture found that the price of 1,3-BD was too low to justify the additional costs associated with extractive distillation to produce 1,3-BD with a high recovery of 99% compared to 94% achievable from their conventional distillation configuration (Song, Yoon, *et al.*, 2019).

2.5 Production of Polyhydroxybutyrate

Polyhydroxybutyrate (PHB) is the most commonly known and researched polyhydroxyalkanoate (PHA) (Koller, 2018; Sabapathy, Devaraj, Anburajan, *et al.*, 2021). Polyhydroxyalkanoates (PHAs) are a group of biopolymers, distinctively known for their biodegradability, making them an environmentally sustainable choice compared to other plastics such as polypropylene or polyethylene, with which they share similar properties (Directorate-General Energy, 2015; Samrot, Samanvitha, Shobana, *et al.*, 2021). In particular, PHB and polypropylene have comparable properties including melting temperature and tensile strength (Valappil, Misra, Boccaccini, *et al.*, 2007).

The chemical structure of PHAs is depicted in Figure 2 (McAdam, Fournet, McDonald, *et al.*, 2020), the *R*-functional group of polyhydroxybutyrate being methyl. The bioplastic has specific characteristics including brittleness, high crystallinity, thermoplasticity and high glass transition and melting temperatures (Koller, 2018; Marciniak & Możejko-Ciesielska, 2021). PHB is currently being produced on a commercial scale by companies such as Biomer in Germany, Goodfellow in UK, PHB Industrial (BIOCYCLE®) in Brazil and Metabolix (Mirel) in the USA, to name a few (Directorate-General Energy, 2015; Singh & Yakhmi, 2017).

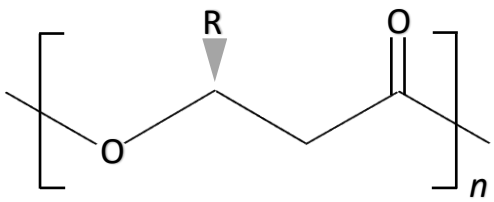

Figure 2: Chemical structure of PHAs (Redrawn from McAdam, et al., (2020))

Despite multiple companies currently producing PHB, the production cost of these bioplastics is still too high to compete with fossil-based plastic, the primary motive for commercial production of PHB remains the environmental benefits (Marciniak & Możejko-Ciesielska, 2021). Several strategies that have been suggested to reduce the high production cost include the utilization of cost effective waste material to

produce high yields of PHB, metabolic engineering of microorganisms or produce PHB more efficiently and simplified production processes, specifically relating to the separation and purification of PHB (Bharti & Swetha, 2016; Favaro, Basaglia, Casella, *et al.*, 2019; Marciniak & Możejko-Ciesielska, 2021).

Of the various strategies suggested, the utilization of cost-effective substrates has already been implemented in commercial production processes. The substrates used to commercially produce polyhydroxybutyrate are soybean oil, corn oil or palm oil and sugarcane by the companies Biomer and PHB Industrial, respectively (Ashby, 2013; Biocycle, 2012). Nevertheless, implementing only this strategy has not reduced the production cost of PHB sufficiently and further research and optimization of the production process is required to potentially replace fossil fuel-based plastics altogether.

Interestingly, some papers mention the use of sugarcane bagasse fibers as fillers that can be entrapped in the PHB matrix, leading to reduced production cost and potentially improved biodegradability (Marciniak & Możejko-Ciesielska, 2021). However, this changes thermal and mechanical properties of the bioplastic and to the knowledge of the writer the commercial viability of this is yet to be determined (Sabapathy *et al.*, 2021).

2.5.1 Fermentation of Sugars to Produce Polyhydroxybutyrate

Polyhydroxybutyrate are produced as granules inside the cytoplasm of microbial cells, i.e., intracellularly as an energy reserve (García-Torreiro, Lu-Chau & Lema, 2016; Samrot *et al.*, 2021). Table 3 summarises the sugarcane-based feedstock and microorganisms used for the production of PHB, and the corresponding results obtained. From Table 3 it is clear that the accumulated PHB can make-out quite a large portion of the cell mass after fermentation, with PHB contents of up to 94% reported (Samrot *et al.*, 2021). Various microorganisms can produce PHB during fermentation of sugarcane-derived sugars, which can all be arranged into two categories.

The first category consists of microorganisms that cannot produce PHB during the growth phase. For PHB fermentation employing a category 1 microorganism, sufficient carbon and nutrients are initially required for optimal biomass accumulation, after which a PHB accumulation phase is initiated by applying nutrient limitation. These types of microorganisms produce PHB when under stress, such as phosphate, oxygen or nitrogen limitation with an excess of carbon (García-Torreiro *et al.*, 2016). Microorganisms falling in the first category include *Cupriavidus necator* and *Halomonas boliviensis* (García-Torreiro *et al.*, 2016; Kaur *et al.*, 2017).

The second category contain microorganisms that can produce PHB during the growth phase, i.e., biomass growth and PHB accumulation. Microorganisms falling in this category include *Alcaligenes latus* and recombinant *E. coli* (Kaur *et al.*, 2017). Although nutrient limitation is not a requirement for PHB production when category 2 microorganisms are employed, it highly increases PHB production efficiency when some sort of nutrient control is applied (Huu Phong, Minh Khuong, Hop, *et al.*, 2017). From the microorganisms and associated PHB production efficiencies listed in Table 3, most if not all have reached the promising PHB yields by either oxygen, nitrogen and/or phosphate nutrient limitations.

Table 3: Microorganisms used for the production of PHB from sugars obtainable from a sugar mill and corresponding results obtained.

Microorganism	Substrate	PHB ($g.L^{-1}$)	PHB (% of CDW)	CDW ($g.L^{-1}$)	Productivity ($g_{PHB}.L^{-1}.h^{-1}$)	Reference
Recombinant *E. coli*	Glucose	141.6	73	194.1	4.63	(Choi, Lee & Han, 1998)
Recombinant *E. coli*	Glucose	101	65.7	153.7	2.8	(Wang & Lee, 1997a)
Alcaligenes latus	Sucrose	98.7	88	111.7	4.94	(Wang & Lee, 1997b)
Halomonas TD01	Glucose	64.68	84	77	1.16	(Tan, Xue, Aibaidula, *et al.*, 2011)
Cupriavidus necator	Glucose	63	77	81	1.85	(Atlić, Koller, Scherzer, *et al.*, 2011)
Yangia sp.	Fructose	53	67.5	78.5	1	(Huu Phong *et al.*, 2017)
Bacillus megaterium BA-019	Sugarcane molasses	41.6	46	90.7	1.73	(Kanjanachumpol, Kulpreecha, Tolieng, *et al.*, 2013)
Burkholderia sacchari	Sucrose	36.5	52	70.2	1.29	(de Sousa Dias, Koller, Puppi, *et al.*, 2017)
Halomonas boliviensis	Glucose	35	72.9	48	0.58	(García-Torreiro *et al.*, 2016)
Bacillus sacchari IPT 101	Xylose + Glucose	34.8	58	60	0.47	(Silva, Taciro, Michelin Ramos, *et al.*, 2004)
Recombinant *E. coli*	Beet molasses	31.6	80	39.5	1	(Liu, Li, Ridgway, *et al.*, 1998)

In addition to the capability of *E. coli* to produce PHB during the growth and accumulation phase, the microorganism has numerous other advantages, making it an excellent candidate for commercial PHB production. The advantages include but are not limited to fast microbial growth, high PHB accumulation content inside the cells and the achievement of high PHB yields from a vast range of substrates, which include sugars extractable from residues and/or by-products available at a sugar mill, such as molasses and sugarcane lignocellulose. The last-mentioned advantage can be attributed to the ease of genetic engineering *E.coli*, allowing it to be modified to utilize the specific substrate available (Kaur *et al.*, 2017; Marciniak & Możejko-Ciesielska, 2021). Furthermore, *E. coli* has advantages associated with the recovery of PHB from the cells that will be discussed in *Section 2.5.2.*

In addition to nutrient control, other operating conditions affecting PHB production efficiency include pH, temperature, fermentation technique and feeding strategy (Bharti & Swetha, 2016; Samrot *et al.*, 2021). Submerged fermentation is the dominating fermentation technique used for PHB production, whilst solid state fermentation (SSF) has been investigated, difficulty of controlling operating conditions is a major drawback of this fermentation technique making it unsuitable for commercial PHB production (Koller, 2018).

Furthermore, fed-batch fermentation is considered the leading feeding strategy for PHB production and is by-far the strategy most commonly found in PHB production studies. All entries in Table 3 used fed-batch fermentation strategies, aside from the study using *Halomonas* TD01 and the study using *Cupriavidus necator*, which made use of a continuous fermentation strategy (Atlić *et al.*, 2011; Tan *et al.*, 2011). Due to the sensitivity of the PHB fermentation process concerning nutrient concentrations, the fed-batch feeding strategy allows for optimal control, which could explain the efficiency of this strategy for PHB production (Kanjanachumpol *et al.*, 2013).

The type of monomer sugars preferred for the production of PHB is completely dependent on the type of microorganism employed; generally, hexose sugars such as glucose and fructose are preferred to pentose sugars such as xylose (Clifton-García, González-Reynoso, Robledo-Ortiz, *et al.*, 2020). Evident from Table 3, studies investigating PHB production have primarily focused on the utilization of hexose sugars and very few have ventured into genetic engineering of microorganism to also utilize pentose sugars.

A number of studies have also investigated the production of PHB utilizing lignocellulosic biomass such as sugarcane bagasse, however, primarily on shake flask scale. To the knowledge of the writer the highest cell dry weight (CDW) and PHB concentration obtained from sugarcane bagasse was found to be 9 g/L and 5 g/L respectively (Getachew & Woldesenbet, 2016).

2.5.2 Separation and purification of polyhydroxybutyrate

The separation and purification of PHB involves the extraction of the PHB granules that have accumulated within the cells. This is another crucial section of the PHB production process that requires optimization in order to reduce the overall PHB production cost (Bharti & Swetha, 2016)(Marciniak & Możejko-Ciesielska, 2021). Following fermentation, microbial cells containing the PHB need to be harvested from the fermentation broth usually with methods such as filtration or centrifugation (McAdam *et al.*, 2020). The isolated cells can then be treated by various techniques to eventually extract PHB and obtain the required product purity.

The appropriate downstream processing technique for the extraction of PHB depends *inter alia,* largely on the type of microorganism employed (i.e., difficulty or ease of breaking down cell wall), the PHB content of the cells (%), the desired quality and purity of the PHB product and finally, the effect of the chosen technique on the molecular weight and thermal properties of PHB (Koller, Niebelschütz & Braunegg, 2013; Nieder-Heitmann, 2019). Furthermore, high temperatures and strong chemicals are unfavorable for PHB extraction because these harsh conditions cause major polymer degradation. Numerous methods of PHB extraction have been mentioned in literature, of which only the most promising and most commonly employed techniques will be discussed here.

Solvent extraction is the techniques most commonly used and studied for PHB extraction, where an appropriate solvent such as chloroform is capable of disrupting the cell wall of the microorganisms and simultaneously extract the PHB in its amorphous state into the solvent where it then crystallizes causing minimal polymer degradation (Rameshwari & Meenakshisundaram, 2014). This technique is used due to

its efficiency and ability to achieve high PHB recovery (up to 94%) and purity (up to 99%) (Kaur *et al.*, 2017; Pagliano, Galletti, Samorì, *et al.*, 2021; Samrot *et al.*, 2021). A major limitation of this technique, however, is the large amount of solvent required (up to 20-fold of the biomass weight), which is not only harmful to the environment but also expensive leading to an economically unfeasible production process (Marciniak & Możejko-Ciesielska, 2021; McAdam *et al.*, 2020; Pagliano *et al.*, 2021; Samrot *et al.*, 2021).

Another PHB extraction method is cell lysis or biomass degradation, which can be conducted by using either chemicals or enzymes (Price, Kuzhiumparambil, Pernice, *et al.*, 2020b). Enzyme degradation has a number of promising attributes including gentle conditions causing minor polymer degradation and high selectivity, however as mentioned in section 2.2.2 (Enzymatic hydrolysis), enzymes are costly and will most likely lead to an economically unfeasible PHB production process (Kaur *et al.*, 2017; Nieder-Heitmann, 2019).

Alternatively, cell lysis is a promising technique when using cost-effective chemicals, which include alkaline compounds such as NaOH and KOH (Samrot *et al.*, 2021). Cell lysis using alkaline compounds require mild conditions (30°C and 0.1-0.2 M), which leads to insignificant cell degradation, causing little to no change to the molecular weight of PHB (Koller *et al.*, 2013; Pagliano *et al.*, 2021). Furthermore the low residence time of 1 hour required and high purity (98.5%) and recovery (91.3%) achieved, makes this an industrially feasible extraction technique for PHB production (Choi & Lee, 1999a; Nieder-Heitmann, 2019). Important to consider however is that this technique has shown to be very promising to extract PHB from the microorganism *E. coli* only, which has a thin cell wall compared to many other microorganisms employed for PHB production.

It is also important to note that cell lysis using other chemicals such as hypochlorite has been deemed unfeasible due to the high polymer degradation this substance causes (Choi & Lee, 1999a; McAdam *et al.*, 2020). The combination of hypochlorite with chloroform has been mentioned as a way to mitigate this effect, nevertheless alkaline compounds still cause less degradation (Chaijamrus & Udpuay, 2008; Valappil *et al.*, 2007).

2.6 Production of bio-based Citric Acid

Citric Acid, with the chemical formula $C_6H_8O_7$ and IUPAC name 2-hydroxypropane-1,2,3-trocarboxylic acid, is part of a group of organic acids, being the most widely used member. Citric Acid is a white crystalline powder and is currently sold either in its monohydrate form, $C_6H_8O_7 \cdot H_2O$, or in its anhydrous form, where the latter accounts for the larger portion of the market demand (Behera, Mishra & Mohapatra, 2021).

The production of citric acid through biological processes is industrial well-established, with approximately 99% of citric acid production from fermentation (Mores *et al.*, 2021). However, the current challenge for commercial producers of citric acid is the development of processes that are more economical and environmentally friendly with enlarged production capacities, to keep up with the increasing product demand (Show, Oladele, Siew, *et al.*, 2015). The dominating cause for the rising

interest in citric acid seems to be an increased awareness by consumers of the digestive benefits of citric acid (Behera *et al.*, 2021).

As of 2015, 59% of all citric acid was produced in China by companies including Weifang Ensign Industry Co., Ltd.; Huangshi Xinghua Biochemical Co. Ltd.; RZBC Group Co., Ltd and COFCO Biochemical (Anhui) Co.,Ltd. Other companies, elsewhere in the world include *inter alia* Gadot Biochemical Industries Ltd. (Israel), Cargill® (USA), ADM® (USA) and Jungbunzlauer (Switzerland) (Behera *et al.*, 2021; Ciriminna *et al.*, 2017).

Companies currently producing citric acid at large scale, predominantly utilize starch based materials such as sweet potato and corn as raw materials. One company, Vogelbush Biocommodities, specifically makes use of a mixture of starch hydrolysates, raw sugar and beet or cane molasses for the production of citric acid (Vogelbusch Biocommodities, 2020). This suggests the potential of an economically attractive citric acid production process from integrated 1G2G feedstock available from an existing sugar mill.

2.6.1 Fermentation of Sugars the Produce Citric Acid

The citric acid fermentation can be performed using one of three techniques, solid state fermentation (SSF), liquid surface fermentation (LSF) or submerged fermentation (SF). SSF and LSF are based on the growth of microorganisms on the surface of the solid or liquid substrate, directly obtaining nutrients from the substrate. The latter is also referred to as liquid stationary fermentation, where the fermentation medium containing sugars is inoculated with spores (usually *Aspergillus niger*) once it has been placed into shallow stainless-steel trays stacked in a fermentation chamber (Narayanamurthy, Ramachandra, Rai, *et al.*, 2008). This varies from submerged fermentation where the substrate, microorganism and nutrients are all submerged in a fermentation broth (Bankar & Dr Geetha, 2018b).

The two former techniques (SSF & LSF) have various advantages compared to submerged fermentation including low energy requirements, simplified equipment and downstream processing techniques and finally, reduced waste generation (Kim, Lee & Lee, 2015). Despite these attributes, SSF and LSF are merely used in small and medium scale productions due to difficulties with scale-up, uneven dispensation of oxygen and nutrients and intensive labor requirements (Bankar & Dr Geetha, 2018b; Kim *et al.*, 2015; Mores *et al.*, 2021).

Submerged fermentation has, however, been shown readily acceptable for industrial/large scale implementation, often making use of beet and cane molasses as substrate (Bakhiet & Al-Mokhtar, 2015). Advantages include reduced labor and higher yield compared to SSF and LSF. Additionally, the process can be automated, which allows for the development of a standardized process (Bankar & Dr Geetha, 2018b; Mores *et al.*, 2021). Despite high equipment installation cost, increased complexity of citric acid purification and the need for pretreatment of lignocellulosic material (i.e., sugarcane bagasse), the many limitations of SSF and LSF still means that submerged fermentation is the most suitable technique for citric acid fermentation. Currently 80% of the citric acid produced globally is by submerged fermentation (Özüdoğru, 2018).

2.6.1.1 Citric acid producing microorganisms utilizing sugarcane derived sugars

Currently, commercial citric acid is predominantly produced by the microorganism *A. niger* using substrates such as glucose, sucrose or the low-cost alternative, molasses (Abdullah-Al-Mahin, Sharifuzzaman, Faruk, *et al.*, 2012a; Carsanba *et al.*, 2019). Furthermore, *A. niger* is a favored microorganism not only to produce citric acid, but also other organic acids (Dezam, Vasconcellos, Lacava, *et al.*, 2017). The microorganism has various advantages including high organic acid yields, stability and reduced by-product formation (Abdullah-Al-Mahin, Sharifuzzaman, Faruk, *et al.*, 2012b; Bakhiet & Al-Mokhtar, 2015).

A. niger has readily been shown capable of fermenting various alternative carbon sources including *inter alia* sugarcane molasses (Ikram-Ul, Ali, Qadeer, *et al.*, 2004), cassava (Wang, Tan, Yu, *et al.*, 2021; Yu, Zhang, Sun, *et al.*, 2018) and corn hydrolysate (Wang, Li, Zhu, *et al.*, 2017). However, the production of citric acid by *A. niger* is very sensitive to trace metal ions present in molasses, and clarification would be required for optimal production (Kim *et al.*, 2015; Show *et al.*, 2015). Furthermore, detoxification of pre-treated lignocellulosic biomass will be a crucial step due to the low tolerance *A. niger* exhibits toward inhibitors such as furfural, HMF, vanillin and formic acid (Zhou, Meng & Bao, 2017). The strain has shown to utilize sugarcane bagasse to produce citric acid, however, primarily by solid surface fermentation (Bakhiet & Al-Mokhtar, 2015; Bastos & Ribeiro, 2020).

A. niger cannot directly utilize sucrose to produce citric acid, however it does produce the necessary invertase enzymes required to hydrolyze sucrose to glucose and fructose, which can be utilized (Alekseev, Dubina & Komov, 2015; Bizukojc & Ledakowicz, 2004). Interestingly, in a repeated fed-batch cultivation experiment, it was observed that at low citric acid concentrations (approx. <30 g/L) the fructose uptake rate by *A. niger* was similar to that of glucose. However, as the citric acid concentration increased (approx. >30 g/L) the fructose uptake rate drastically decreased as the glucose uptake rate increased, leaving fructose as residual sugar (Bizukojc & Ledakowicz, 2004). Furthermore, *A. niger* has the ability of utilizing xylose to produce citric acid, albeit less efficiently compared to glucose (Show *et al.*, 2015; Soccol, Vandenberghe, Rodrigues, *et al.*, 2006). To the knowledge of the writer no recent papers have investigated the simultaneous utilization of xylose and glucose to produce citric acid using *A. niger*.

Another microorganism readily studied for the production of citric acid is the yeast, *Yarrowia lipolytica*. A major limitation of using yeast to produce citric acid is the co-production of isocitric acid, which complicates the purification of citric acid when present at concentrations above approximately 5% (Förster, Aurich, Mauersberger, *et al.*, 2007). However, due to the ease of metabolically engineering *Y. lipolytica*, this by-product formation can be reduced (Cavallo, Nobile, Cerrutti, *et al.*, 2020).

Other advantages of *Y. lipolytica,* include a higher tolerance toward high substrate concentrations and metal ions compared to *A. niger*, which in effect means that a wider range of substrates can be utilized for citric acid production without the requirement of clarification or detoxification (Carsanba *et al.*, 2019; Konzock, Zaghen & Norbeck, 2021; Tan, Chen, Wang, *et al.*, 2016). Important to note is that *Y. lipolytica* is not as tolerant to inhibitors produced during pre-treatment and detoxification will most likely be required if high concentrations of inhibitors are present. Various studies have investigated the production

of citric acid from sucrose, glucose and xylose using *Y. lipolytica*, however to the knowledge of the writer no studies have been conducted on the utilization of sugarcane molasses or sugarcane bagasse and brown leaves from harvesting residues.

Y. lipolytica has been shown to only utilize fructose following the depletion of glucose (Förster *et al.*, 2007). In a study utilizing sucrose in a repeated fed-batch scheme to produce citric acid, 100 g/L residual fructose was still present in the fermentation broth when all glucose was consumed following sucrose hydrolysis, by strain *Y. lipolytica* H222-S4(p67ICL1) T5 (Moeller, Zehnsdorf, Aurich, *et al.*, 2013). Furthermore, *Y. lipolytica* is not naturally able to utilize xylose, however appropriate metabolically engineering can give a strain the ability to utilize xylose. Low concentration feedings of glucose has also shown to enhance citric acid production, by reducing the lag phase (Konzock *et al.*, 2021). Glucose addition was kept very low at 4 mg/L to avoid carbon catabolite repression, which was observed when equal amounts of glucose and xylose were used as substrate for citric acid production (Ledesma-Amaro, Lazar, Rakicka, *et al.*, 2016).

Table 4 contains the most promising citric acid production results from *A. niger* and *Y. lipolytica*. Another microorganisms *Candida oleophila* has also been shown to produce citric acid from glucose at a concentration of 167 g/L (Anastassiadis & Rehm, 2006). However only one study has reported on this microorganism and reviews on citric acid production primarily focuses on *A. niger* and *Y. lioplytica* as citric acid producing strains.

Table 4: Various microorganisms and substrates utilized for citric acid production.

Microorganism	Substrate	Yield ($g.g^{-1}$)	Titre ($g.L^{-1}$)	Productivity ($g.L^{-1}.h^{-1}$)	Feeding strategy	Reference
C. oleophila ATCC 20177	Glucose	0.5	167	1.5	Repeated fed-batch	(Anastassiadis & Rehm, 2006)
Y. lipolytica SWJ-1b	Glucose	0.89	101	0.42	Fed-batch	(Tan *et al.*, 2016)
Y. lipolytica H222-S4(p67ICL1) T5	Sucrose	0.82	140	0.73	Fed-batch	(Förster *et al.*, 2007)
A. niger GCB-75	Sugarcane molasses	0.76	113.6	0.79	Batch	(Ikram-Ul *et al.*, 2004)
Y. lipolytica XYL+	Xylose	0.53	79.4	-	Batch	(Ledesma-Amaro *et al.*, 2016)
Y. lipolytica XYL+	Xylose and Glucose	0.27	102.8	-	Fed-batch	(Ledesma-Amaro *et al.*, 2016)

2.6.1.2 Optimal Fermentation Conditions

The operating conditions that have the largest impact on the efficiency of citric acid production as well as the operating costs of the process, apart from the carbon source, is the nitrogen source, substrate concentration, concentration of metal ions, pH, temperature, and oxygen demand (Behera *et al.*, 2021; Carsanba *et al.*, 2019; Cavallo *et al.*, 2020).

The formation of citric acid results in the reduction of pH of the fermentation broth and therefore, microorganisms capable of operating optimally in low pH will be beneficial (Sun, Gong, Lv, *et al.*, 2020).

Furthermore, at low pH, citric acid is favored as opposed to by-products such as oxalic acid and gluconic acid and the risk of contamination is reduced (Mores *et al.*, 2021). *A. niger* has been reported to have an optimal pH range of 3.8-6, which could reduce the need for pH regulation (Sun, Gong, *et al.*, 2020). For *Y. lipolytica* strain H222-S4(p67ICL1) T5 an optimal pH of 6.8 was determined (Förster *et al.*, 2007).

One of the main incentives of adding a nitrogen source to the citric acid fermentation medium is the pH reduction it brings about (Mores *et al.*, 2021). Expensive nitrogen sources such as yeast extract is unfavorable for large-scale production processes (Cavallo *et al.*, 2020). Corn Steep Liquor (CSL), a cost-effective alternative, has been shown to give similar or slightly better results compared to yeast extract, when *Y. lipolytica* was used for citric acid production. Furthermore, only 0.5 $g.L^{-1}$ CSL was required to achieve similar results to 1 $g.L^{-1}$ YE (Cavallo *et al.*, 2020). The concentration of the nitrogen source needs to carefully be considered seeing as a high concentration of nitrogen promotes biomass growth, whilst a low nitrogen concentration promotes citric acid production. And although biomass growth is required for high yields and productivity of citric acid, excessive growth uses a large quantity of the carbon source required for citric acid production (Wang *et al.*, 2021).

Another important variable pertaining to the nitrogen source is the carbon to nitrogen ratio (C/N), especially when *Y. lipolytica* is used for citric acid production (Carsanba *et al.*, 2019). A high C/N molar or elemental ratio is required for optimal citric acid production. C/N ratios of 20:1 to 30:1 have been reported as a general requirement. However, the C/N ratio is ultimately dependent on the specific strain used for citric acid production and can differ with variations of other operating parameters such as temperature (Yadvika, Santosh, Sreekrishnan, *et al.*, 2004). In a study optimizing citric acid production from *Y. lipolytica* observed that an optimal C/N molar ratio was as high as 367, which resulted in a yield of 0.77 $g.g^{-1}$. The optimal yield was 10% and 30.5% higher compared to the yield at a C/N molar ratio of 167 and 567 respectively (Carsanba *et al.*, 2019).

Oxygen demand also majorly influences citric acid production, insufficient oxygen supply has been reported to inhibit the functioning of enzymes, more specifically the enzyme responsible for citric acid synthesis. Furthermore, the need for sufficient oxygen supply is promising for scale up potential. A 2.3-fold increase in productivity has been observed when a citric acid production process was scaled up from shake flasks to a 5L- stirred tank bioreactors, primarily due to sufficient aeration and agitation achievable in the bioreactors (Cavallo *et al.*, 2020). This could imply that the productivity would increase even further when scaled up to an industrial-sized reactor.

2.6.2 Separation and Purification of Citric Acid

It has been reported that downstream processing constitutes up to 40% of the production cost of citric acid and therefore should be selected carefully, considering economics as well as environmental impact (Mores *et al.*, 2021). In line with a current industrial citric acid production plant, the separation and purification of citric acid from a fermentation broth include various steps such as mycelium filtration, purification, evaporation, crystallization, centrifugation and finally drying to achieve anhydrous citric acid crystals at >99.8% purity (MacAringue, Li, Li, *et al.*, 2020; Pasternack, Mead & Davenport, 1934; Vogelbusch Biocommodities, 2020).

Various purification techniques have been investigated for citric acid fermentation, among which calcium salt precipitation, adsorption and solvent extraction are the most promising and common techniques and will furthermore be discussed in detail.

2.6.2.1 Calcium Salt Precipitation

The most frequently used and most established recovery technique for citric acid production is calcium salt precipitation. This technique has already been commercially implemented for citric acid production and has various advantages including high selectivity and high product purity (Li, Jiang, Feng, *et al.*, 2015). The technique involves the addition of a calcium salt ($Ca(OH)_2$ or $CaCO_3$) to the citric acid fermentation broth, after which precipitation of calcium citrate occurs. Following filtration and washing of the precipitate to remove any impurities, the calcium citrate is treated with sulphuric acid to solubilize the citric acid. Depending on the application of the citric acid, various treatments such as crystallization and drying can be employed to subsequently purify citric acid (Cavallo *et al.*, 2020; Li *et al.*, 2015).

A major limitation of the technique is the production of gypsum when calcium is solubilized from calcium citrate and large quantities of wastewater is produced from washing of the precipitate. From an environmental perspective these wastes make calcium salt precipitation a very unfavored process, and processing of the wastes would reduce its environmental impact. However, treating of gypsum will be uneconomical (Dhillon, Brar, Verma, *et al.*, 2011; Mores *et al.*, 2021; Wu, Peng, Arlt, *et al.*, 2009). Furthermore, the raw material cost (calcium salt and sulphuric acid) contributes largely to operational costs (Mores *et al.*, 2021).

2.6.2.2 Solvent extraction

Solvent extraction is a promising alternative for citric acid recovery compared to calcium salt precipitation, considering the reduced amount of waste being produced (Araújo, Coelho, Balarini, *et al.*, 2017; Behera *et al.*, 2021). Furthermore it has been reported that solvent extraction is less labor intensive and more economical compared to calcium salt precipitation (Wang, Cui, Li, *et al.*, 2020). Solvent extraction or specifically reactive extraction has also been commercially implemented, customarily using a tertiary amine for extraction and subsequently water for back extraction (Mores *et al.*, 2021). Following the solvent extraction the aqueous citric acid solution undergoes one or a combination of evaporation, crystallization and decolorization, depending on the application (Araújo *et al.*, 2017; Behera *et al.*, 2021).

Solvent extraction as sole recovery method cannot recover citric acid from a fermentation broth containing <15% (w/w) citric acid, which is common for a fermentation broth, to meet the purity requirements of pharmacopoeia and food (Mores *et al.*, 2021; Wang *et al.*, 2020). Therefore, for optimization and additionally cost reduction, a combination of evaporation, solvent extraction and crystallization has been suggested, which led to a recovery and purity of 100% and >99.8% respectively (Baniel, et al., 2008).

Recovery of the solvent for solvent extraction is beneficial for the economic feasibility of the process and will furthermore contribute to reducing the environmental impact of the process (Wang *et al.*, 2020). The recovery will also lead to reduced raw material and subsequently operational costs (Mores *et al.*, 2021).

2.6.2.3 Adsorption

Another recovery process, adsorption, has also readily been studied for the recovery of citric acid. This process, like solvent extraction does not produce large quantities of by-products such as gypsum (calcium sulphate), consumes little energy and in the case of packed columns has ease of operation and less solvent loss compared to solvent extraction (Bankar & Dr Geetha, 2018b; Mores *et al.*, 2021).

The basic principle of the method is the use of adsorbents placed in compacted columns, agitated tanks or simulated moving beds (Mores *et al.*, 2021). The chosen adsorbent should have a high selectivity to citric acid. Following adsorption and separation from fermentation broth, an eluent or desorbent liquid is then used to release the citric acid from the resin. Similar to previously described processes, evaporation, crystallization, drying and/or decolorization are finally applied to produce the required purity and form of citric acid (Delgado Dobladez, Águeda Maté, Uribe Santos, *et al.*, 2019).

Organic solvents such as methanol, water and acids have been suggested as appropriate eluents for adsorption (Delgado Dobladez *et al.*, 2019; Dhillon *et al.*, 2011; Wang *et al.*, 2020; Wu *et al.*, 2009). The choice of eluent is a crucial economical step for this recovery technique. Tailor-made tertiary poly(4-vinylpyridine) (PVP) resin has been suggested as a promising adsorbent due to its high adsorption capacity and high citric acid selectivity at low and moderate pH (Mores *et al.*, 2021). Furthermore the bonding strength of citric acid to the PVP resin is weak enough that citric acid can easily be desorbed using deionized water (Wu *et al.*, 2009).

A major limitation of the adsorption technique is the large amount of desorbent required to release citric acid from the adsorbent. This leads to a very dilute citric acid extract that will complicate subsequent purification and lead to large amounts of waste liquid (Bankar & Dr Geetha, 2018b). However, this limitation can be mitigated by recycling the desorbent. When water is solely used as eluent it can be recycled to the fermentation section, due to the presence of minerals and residual sugars (Wu *et al.*, 2009). Furthermore, tertiary poly(4-vinylpyridine) (PVP) resin can be regenerated by methanol and ethanol, consequently the organic solvent can be repurposed after being used as eluent (Mores *et al.*, 2021).

Another major limitation of adsorption is the challenges associated with resin shelf life, disposal, regeneration and recovery (Dhillon *et al.*, 2011). Due to the decrease of resin capacity over time, easy, efficient and economical recovery and regeneration of resin is crucial, yet this technology has not been established (Dhillon *et al.*, 2011; Mores *et al.*, 2021; Wang *et al.*, 2020). Wang, et al. (2020) reported that raw material cost of ion exchange surpassed that of calcium salt precipitation due to the large amount of solvent required for the regeneration of resin.

In addition to conventional adsorption, ion exchange, simulated moving bed technology and *in situ* adsorption processes have been investigated for citric acid recovery. Ion exchange merely uses ion exchange resins to remove anion and cation impurities in subsequent steps. Hydrochloric or sulphuric acid are common eluents used for ion exchange (Wang *et al.*, 2020). Simulated moving bed essentially uses a similar principle to ion exchange, however the number of steps is reduced increasing productivity and reducing chemical consumption (Wang *et al.*, 2020). Wu et al. (2009) achieved a purity and recovery

of 99.8% and 97.2% respectively using simulated moving bed technology, tailor-made tertiary PVP resins as adsorbents and a fermentation broth containing impurities and residual sugar as feed.

Finally, *in situ* recovery is a technique where recovery is combined with fermentation, which means that the product is recovered as it is produced. This is not limited to adsorption techniques, solvent extraction and membrane separation have also been used for *in situ* product removal strategies (Li *et al.*, 2015). However, for citric acid recovery *in situ* adsorption processes have primarily been studied. *In situ* product recovery has various advantages including increased productivity, reduced post-recovery waste streams and reduced cost associated with additional downstream processing steps (Dhillon *et al.*, 2011; Jianlong, Xianghua & Ding, 2000). Furthermore, due to the continuous removal of citric acid, pH changes and product inhibition on the microorganism is avoided, leading to increased sugar utilization and consumption (Dhillon *et al.*, 2011; Jianlong *et al.*, 2000; Li *et al.*, 2015). However, it has been observed that microbial cells can also adsorb to resin (Jianlong *et al.*, 2000).

2.7 Techno-economic analysis

To determine the economic feasibility of a biorefinery scenario, a thorough techno-economic analysis is required. A techno-economic analysis consists of the capital expenditures (CAPEX), the operational expenditures (OPEX) and finally the discounted cash flow rate of return (DCFROR) analysis. The industrial feasibility of a bioproduction process is moreover dependent on the environmental impact of the process. Although a life cycle analysis is outside the scope of this project, a Greenhouse Gas Emissions (GHG) assessment will be conducted using the RSB® GHG Calculator Tool, for each scenario.

2.7.1 Capital Expenditures (CAPEX)

The capital expenditures include the cost of equipment to be purchased and installed as well as various other direct and indirect capital costs including *inter alia* site development, warehouses, field expenses, contingency and office and construction (Gorgens F; Mandegari, M A; Farzad, S; Daful, A G; Haigh, 2016; Humbird *et al.*, 2011; Sorrels & Walton, 2017). The cost of equipment to be purchased and installed naturally depend on the size and number of pieces of equipment required. This can be determined by manual calculations using Microsoft Excel or alternatively using Aspen Economic Analyser in Aspen Plus®. The latter gives best sizing and cost estimations for generic equipment including pumps, compressors, flash drums and heat exchangers (Gorgens F; Mandegari, M A; Farzad, S; Daful, A G; Haigh, 2016). The former is then used for specialized equipment. These calculations can be done by using the module cost technique described by Turton, *et al.*, (2018) or alternatively quoted values can be obtained from reliable literature sources (Davis *et al.*, 2018; Humbird *et al.*, 2011) and updated for capacity and time. Equation 1 is used to scale the equipment to the desired capacity following a quote obtained for a certain defined capacity (Dheskali, 2017).

$$C_p = \frac{CEPCI_t}{CEPCI_{t0}} C_{p,0} \left(\frac{X}{X_0}\right)^n \qquad 1$$

In Equation 1 the C_p represents the purchased equipment cost in the current year of calculation (project year), X represents the capacity, the exponent ‘n’ is a scaling factor reflecting economy-of-scale

dependencies and finally CEPCI represents the Chemical Engineering Plant Cost Index (CEPCI), of which the two latter parameters are obtainable from literature (Humbird *et al.*, 2011; Jenkins, 2020; Nieder-Heitmann, 2019; Sorrels & Walton, 2017). The subscript '0' refers to the specific parameter in the year the quote was issued.

Following the determination of the purchased equipment cost, an installation factor can be used to determine installed equipment cost (Humbird *et al.*, 2011). The various capital cost components are used to determine two main capital parameters, the Fixed Capital Investment (FCI) and the Total Capital Investment (TCI) (Gorgens F; Mandegari, M A; Farzad, S; Daful, A G; Haigh, 2016).

2.7.2 Operational expenditures (OPEX)

Operation expenditures include fixed and variable operational costs, as well as annual capital charge, where the latter refers to the cost of e.g., catalysts or enzyme which is not continually replaced during operating but only every few months or years. Fixed operational costs include the property taxes and insurance, labour, maintenance and additional overhead costs, incurred irrespective of production capacity (Davis *et al.*, 2018; Nieder-Heitmann, 2019). The salaries, methods of estimating the number of operating staff and labour indices can be obtained from literature (Gorgens F; Mandegari, M A; Farzad, S; Daful, A G; Haigh, 2016; Humbird *et al.*, 2011; United States Department of Labor US, 2020). Variable operating costs are costs which are not fixed and vary with capacity. The costs can be determined using the mass and energy balances obtained from Aspen Plus® software as well as the chemical costs and cost indices, obtainable from literature. Costs include raw material and waste disposal costs (Nieder-Heitmann, 2019).

2.7.3 Profitability indicators

A commonly used profitability indicator used to determine the economic feasibility of a biorefinery scenario, is the minimum selling prices (MSP), determined at a specified or desired internal rate of return (Nieder-Heitmann, 2019). The MSP is determined by conducting a discounted cash flow rate of return (DCFROR) analysis, using predetermined parameters including among others, interest rate, plant life and construction start-up period (Humbird *et al.*, 2011; Nieder-Heitmann, 2019).

3 METHODOLOGY

In the following section, the steps that were followed to conduct the study and to obtain interpretable results will be discussed. Following an extensive literature review, production processes were selected and developed for 2,3-BDO, 1,3-BD, PHB and citric acid. The process selection was based on the most optimal production routes to aim at developing the most profitable scenarios. The developed processes were then simulated using Aspen Plus® software to obtain the mass and energy balances required to conduct a techno-economic analysis. A thorough techno-economic analysis and subsequent sensitivity analysis was thereafter conducted for each biorefinery scenario using Microsoft Excel, to determine the economic indicator, minimum selling price (MSP) and to assess which factors had the largest impact on the MSP of each scenario, respectively. Finally, the environmental impact of each biorefinery scenario was evaluated by determining the greenhouse gas emissions (GHG) using the RSB GHG Calculator Tool. The following sections will discuss the aforementioned steps in further detail.

3.1 Process Description and Simulation Development

The various biorefineries developed in this study are all annexed to an existing sugar mill. In this section, detailed descriptions of each developed biorefinery scenario will be given. Furthermore, general aspects common to the biorefinery scenarios such as feedstock compositions and flowrates, utility production facilities and facilities shared with the annexed sugar mill, will also be specified. Certain steps of the production processes were sectioned and, as far as possible, sections that fell into similar production step categories were similarly numbered. A guide is given in Table 5. When a certain process section consisted of two or more sub-sections, the specific sub sections was indicated with a hyphen. For example, the CHP plant, which is process section 500, consists of both a boiler and CEST unit. When referring to the boiler of the CHP plant it will therefore be: S500-1, and for the CEST unit: S500-2.

Table 5: Biorefinery process sections naming guide

Section	Production step
100	All pre-processing of 2G feedstock. This includes pretreatment and enzymatic hydrolysis as well as any other units that aid these two processes.
200	All fermentation processes, including seed trains, fermentation, and hydrolysis of sucrose.
300	All separation and purification processes of the fermentation broths produced.
400	Wastewater treatment plant
500	Combined Heat and Power Plant
600	All other utilities. This includes the cooling water tower, chilled water package and process water storage.
700	This section is only applicable to the 1,3-BD scenarios. This includes all steps associated with catalytic conversion. The separation and purification following catalytic upgrading is also included in this section.
800	This section is only applicable to the 1,3-BD scenarios. This includes the thermal fluid heater producing molten salt.

The biorefinery scenarios have all been designated a letter, to simplify the process of referring to a specific biorefinery scenario. In this study 10 biorefinery scenarios were developed. In Table 6 each biorefinery scenario developed, alongside the designated letter is presented. For 2,3-BDO, PHB and citric

acid only two scenarios were developed, one utilizing 1G feedstock and the other utilizing 1G2G feedstock. For 1,3-BD, four scenarios were developed, where two scenarios produce 1,3-BD with 2,3-BDO as intermediate product and the other two produce 1,3-BD with ethanol as intermediate product. For the respective 1,3-BD production pathways, one scenario utilizes 1G feedstock whilst the other utilizes 1G2G feedstock.

Table 6: Biorefinery scenarios developed in this study and their respective designated letter.

SCENARIO	PROCESS DESCRIPTION
A	1G 2,3-BDO
B	1G2G 2,3-BDO
C	1G 1,3-BD (BDO)
D	1G2G 1,3-BD (BDO)
E	1G 1,3-BD (ETH)
F	1G2G 1,3-BD (ETH)
G	1G PHB
H	1G2G PHB
I	1G Citric Acid
J	1G2G Citric Acid

3.1.1 Feedstock available from the sugar mill

For the 1G scenarios, A-molasses was the feedstock employed for product formation and bagasse was used (where applicable) as feedstock to the combined heat and power plant (CHP) (*S500*). A-molasses, with a flowrate of 25 433 kg/h is available from the sugar mill, at a temperature of 56°C and a composition of 69.8% sucrose, 15.1% glucose and 15.1% fructose on a dry basis, with 22.07% water (Dogbe *et al.*, 2020). Bagasse with a total flowrate of 30484 kg/h and composition of 40.7% cellulose, 22.5% hemicellulose, 25.5% lignin, 3.8% ash and 7.5% extractives, is available (Dogbe, Mandegari & Görgens, 2019a). It is important to note that the 1G biorefineries only use the necessary amount of bagasse and does not use all the bagasse available from the sugar mill.

For the 1G2G scenarios, A-molasses as well as a portion of the available 2G-feedtsock from the sugar mill is used for product formation, whilst the remainder of the 2G-feedtsock is used for combustion in the CHP plant. The percentage of available 2G-feedtsock being used for combustion is referred to as the bypass ratio and was individually determined for each scenario, based on the energy requirements (Farzad, Mandegari, Guo, *et al.*, 2017). The total 2G-feedstock available to the biorefinery has a flowrate of 63702 kg/h and composition of 40.4% cellulose, 24.4% hemicellulose, 24.6% lignin, 3.4% ash and 7.3% extractives (Dogbe, 2020).

3.1.2 Utilities available from sugar mill and produced at the biorefinery

All utilities obtained and produced will be discussed in this section. Limited electricity and steam are available from the sugar mill. If the steam and electricity requirements of a biorefinery exceeded this amount a new CHP plant will have to be constructed to provide the additional required steam and electricity. The CHP plants were all designed to produce minimal excess electricity and steam.

Furthermore, the energy requirements of the various biorefineries were all reduced by manually implementing a heat integration network throughout each process.

3.1.2.1 Sugar mill

The sugar mill to which the biorefineries are annexed is based on an average sugar mill found in South Africa, processing 300 t/h sugarcane (Mandegari *et al.*, 2017). The sugar mill itself also has a number of utility production systems, which include a cooling tower, chilled water package and combined heat and power plant (CHP), providing all cooling utilities, steam and electricity required by the sugar mill. Originally the existing sugar mill boiler, with an efficiency of 65%, had an assumed steam-on-cane ratio of 45% (Dogbe, 2020; Dogbe, Mandegari & Görgens, 2019b). However, with further research and technological development it was found that a steam-on-cane ratio of 40% can now be assumed (Dogbe *et al.*, 2019b). This is beneficial to an annexed biorefinery, considering 15 t/h HPS (@360°C and 28.6 bar) is available from the existing boiler, due to the increased efficiency. The biorefinery however still pays for the raw materials consumed to produce the HPS, which corresponds to 6660 kg/h bagasse and 5681 kg/h 2G feed for the first-generation and integrated first -and second-generation scenarios, respectively.

When A-molasses is extracted from the sugar mill, as is the case with a 1G and 1G2G biorefinery scenario, the LPS (@130°C and 2.62 bar) requirement of the mill reduces by 15.5 t/h. This takes place due to A-molasses not being processed to B- and C-molasses anymore. As a consequence, the existing mill design will produce excess LPS which can be utilised by the biorefineries at no cost to the annexed biorefinery. Furthermore, for all biorefinery scenarios (1G and 1G2G) the sugar mill produces 1857.5 kW excess electricity, also available to the biorefinery at no cost. Table 7 provides a summary of all utilities available from the sugar mill CHP plant. No other utility facilities are shared between the sugar mill and annexed biorefinery.

Table 7: Summary of all utilities available to the biorefinery, produced by the existing sugar mill CHP plant.

Utility	Unit	Quantity	Additional expense to biorefinery
High-Pressure Steam (@360°C and 28.6 bar)	t/h	15	✓
Low Pressure Steam (@130°C and 2.62 bar)	t/h	15.5	✗
Electricity	kW	1857.5	✗

3.1.2.2 Wastewater Treatment Plant (S400 in all relevant Scenarios)

The wastewater treatment plant consists of an anaerobic biodigester unit, aerobic digestion unit and reverse osmosis unit. The feed to the anaerobic biodigester consists of the cooling tower blowdown (*CTBLOWD*) from *Section 600*, ammonia (*NH3*), and various liquid waste streams produced within the production process (*T2*, *S22* and *EFFLUENT* in Figure 3). The feed stream (*S3*) is initially cooled to 35°C, the temperature at which anaerobic digestion takes place (Humbird *et al.*, 2011).

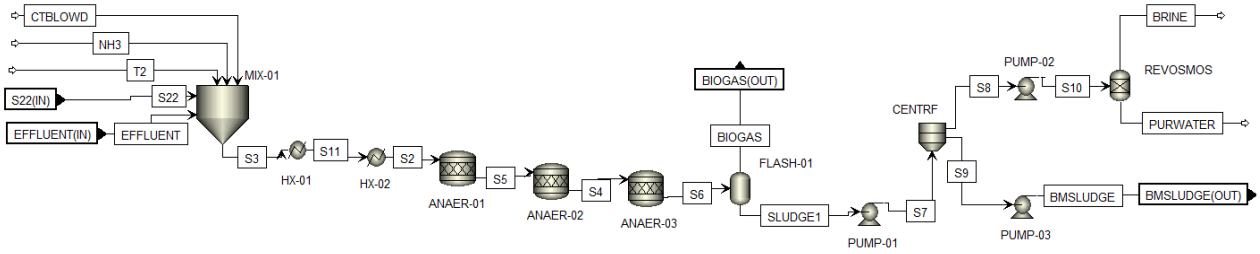

Figure 3: Wastewater Treatment Plant, flowsheet modelled in Aspen Plus®

The anaerobic biodigester unit itself was based on a similar simulation by Nieder-Heitmann (2019) and was simulated using three *RStoic* units in Aspen Plus®, representing the various stages of reactions taking place in an anaerobic biodigester. The various stages include the hydrolysis stage, acidogenesis and acetogenesis stage, and finally the methanogenesis stage (Nieder-Heitmann, 2019). The reactions used, can be found in Table 8.

For each individual scenario, the components in the feed stream to the anaerobic digester was considered and reactions were added where applicable. Following the anaerobic biodigester units, a flash drum (*FLASH-01*) has been simulated to represents the biogas that would have been emitted from the anaerobic biodigester unit (*BIOGAS*). The biogas is sent to the CHP plant for combustion via blowers, that have been accounted for in the TEA.

Table 8: Stoichiometric reactions used in the anaerobic biodigester reactors of Section 400 (Nieder-Heitmann, 2019).

Stoichiometric Reactions
ANAER-01: Hydrolysis stage
$C_6H_{12}O_6(Glucose) + 0.1115\ NH_3 \rightarrow 0.1115\ C_5H_7NO_2\ (Biomass\ Sludge) + 0.744\ C_2H_4O_2\ (Acetic\ Acid) + 0.5\ C_3H_6O_2\ (Propionic\ Acid) + 0.4409\ C_4H_8O_2\ (n-Butyric\ Acid) + 0.6909\ CO_2 + 1.0254\ H_2O$
$3\ C_5H_{10}O_5\ (Xylose) + 7.5\ C_2H_4O_2$*
$3\ C_5H_{10}O_5\ (Arabinose) \rightarrow\ C_3H_6O_2 + C_4H_8O_2 + C_5H_{10}O_2\ (Isovaleric\ Acid) + 3\ CO_2 + 3\ H_2O$ *
$3\ C_4H_6O_4\ (Succinic\ Acid) + 3\ H_2O \rightarrow 4.5\ C_2H_4O_2 + C_4H_8O_2 + 3\ CO_2 + 3\ H_2O$
$C_{12}H_{22}O_{11}(Cellobiose) + H_2O \rightarrow 4\ C_2H_6O\ (Ethanol) + 4\ CO_2$ *
ANAER-02: Acidogenesis and Acetogenesis stages
$C_5H_{10}O_2 + 0.0653\ NH_3 + 0.5543\ CO_2 + 0.8044\ H_2O \rightarrow 0.0653\ C_5H_7NO_2 + 0.8912\ C_2H_4O_2 + 0.4454\ CH_4 + C_3H_6O_2 + 0.0006\ H_2$ *
$C_4H_8O_2\ + 0.0653\ NH_3 + 0.5543\ CO_2 + 0.8038\ H_2O + 0.0006\ H_2 \rightarrow 0.0653\ C_5H_7NO_2 + 1.8909\ C_2H_4O_2 + 0.446\ CH_4$
$C_3H_6O_2\ + 0.06198\ NH_3 + 0.314336\ H_2O \rightarrow 0.06198\ C_5H_7NO_2 + 0.9345\ C_2H_4O_2 + 0.660412\ CH_4 + 0.160688\ CO_2 + 0.00055\ H_2$
$C_2H_6O + H_2O \rightarrow C_2H_4O_2 + 2\ H_2$
$2\ CO_2 + 4\ H_2 \rightarrow\ C_2H_4O_2 + 2\ H_2O$
ANAER-03: Methanogenesis stage
$14.497\ H_2 + 0.0836\ NH_3 3.8334\ CO_2 \rightarrow 3.4154\ CH_4 + 7.4996\ H_2O + 0.0836\ C_5H_7NO_2$
$C_2H_4O_2 + 0.022\ NH_3 \rightarrow 0.022\ C_5H_7NO_2 + 0.945\ CH_4 + 0.066\ H_2O + 0.945\ CO_2$

*Only present in 1G2G scenarios

The slurry exiting the anaerobic biodigester (*SLUDGE1*) is further processed by aerobic digestion. For simplification purposes, the aerobic digestion step has merely been simulated as a centrifuge (*CENTRF*), achieving 90% solids removal. The entirety of the aerobic digestion equipment as well as the energy usage

of the individual pieces of equipment has however been accounted for in the techno-economic analysis along with additional operational costs such as the raw material cost of caustic, required for neutralization (Humbird *et al.*, 2011). The aforementioned were scaled from Humbird *et al*. (2011) using the mass flowrate of the stream entering the simulated centrifuge. Aerobic digestion equipment include inter alia an aerobic digester blower, aerobic sludge screw, centrifuge feed pump, centrifuge and aeration digester (Humbird *et al.*, 2011). The final sludge produced from the aerobic digestion step (*BMSLUDGE*) is also sent to the CHP plant for combustion.

The overflow from *CENTRF* is pumped (*PUMP-02*) to the reverse osmosis unit at a pressure of 25 bar, where the final purified water (*PURWATER*) and waste brine (*BRINE*) are produced. The reverse osmosis unit is merely simulated as a separation block in Aspen Plus®, where 90% of the water and 10% of the extract, ash and biomass sludge in *S10* are separated to *PURWATER* (Nieder-Heitmann, 2019). The purified water stream is recycled to sections in the production process that required fresh water, whilst the brine is sent to municipal wastewater treatment, and has been cost accordingly.

3.1.2.3 Combined Heat and Power Plant (S500-1 & S500-2 in all relevant Scenarios)

In instances where the existing sugar mill is not able to provide all the required energy of the annexed biorefinery, a combined heat and power plant is required. Consequently, for most of the simulation a CHP was designed and included. The combined heat and power (CHP) plant consisted of a combustor, high-high pressure boiler and turbogenerator (Humbird *et al.*, 2011). The CHP plant plays a key role in making the biorefinery energy self-sufficient. The combustor and high-high pressure boiler are simulated in *Section 500-1* (Figure 4), whereas the turbogenerator is simulated in *Section 500-2* (Figure 5).

In *S500-1* the various streams making up the feed (*S5*) to the combustor (*COMBUST*) will differ for each scenario. Generally, these streams consist of the bagasse (1G scenarios) or bagasse and brown leaves (1G2G scenarios), depicted by stream *B2* in Figure 4, the biogas and biomass sludge streams from the wastewater treatment plant (*S400* in all scenarios), the biomass separated from the fermentation broth and any other solid waste streams produced in the production process (e.g., cellulignin). All the feed streams, together with sufficient oxygen (*AIR*) are sent to the combustor for heat generation. The combustion reactions taking place in the combustor of all scenarios can be found in

Table 9. All reactions have an assumed conversion of 98% (Mandegari, Farzad & Görgens, 2018). Naturally there will be additional reactions for the specific scenarios, depending on the combustible components present in the feed stream to the combustor.

The combustion gas (*S6*) exiting the combustor, is used to heat the boiler feed water to produce steam (*HX-02*) and furthermore used to preheat the air to the combustor (*HX-01* & *HX-03*). The combustion gases (flue gas), at a temperature of 149°C (design specification) following heat exchange, enters a baghouse where particulate ash is removed, whereafter the gas is exhausted to the outside air through a stack (Humbird *et al.*, 2011). The baghouse and stack have been represented in the simulations as a separator block (*BAGHOUSE*), having the flue gas exit at the top and the ash exiting at the bottom.

The amount of air sent to the combustor was controlled by a design specification in the simulation. The amount of air was varied, to ensure the stream leaving the combustor (*S6*) is at a temperature of 870°C (Leibbrandt, 2010; Nieder-Heitmann, 2019; Özüdoğru, 2018). The heat exchanger responsible for heat exchange between the flue gas and the boiler (*HX-02*), has been specified with an outgoing temperature of 278°C (Humbird *et al.*, 2011; Nieder-Heitmann, 2019). The heat exchanged with the boiler has an assumed loss of 5% (*SPLIT*).

Table 9: Stoichiometric reactions used in the combustor of Section 500-1 (Assumed fractional conversion of 98% for all reactions).

Stoichiometric Reaction
$C_6H_{10}O_5\ (Cellulose) + 6\ O_2 \rightarrow 5\ H_2O + 6\ CO_2$
$CH_4 + 2O_2 \rightarrow 2\ H_2O + CO_2$
$C_4H_6O_4\ (Succinic\ Acid) + 3.5\ O_2 \rightarrow 3\ H_2O + 4\ CO_2$
$C_{12}H_{22}O_{11}(Cellobiose) + 12\ O_2 \rightarrow 11\ H_2O + 12\ CO_2$ *
$C_5H_8O_4\ (Xylan) + 5\ O_2 \rightarrow 4\ H_2O + 5\ CO_2$
$C_5H_8O_4\ (Arabinan) + 5\ O_2 \rightarrow 4\ H_2O + 5\ CO_2$
$C_6H_{10}O_5\ (Mannan) + 6\ O_2 \rightarrow 5\ H_2O + 6\ CO_2$
$C_6H_{10}O_5\ (Galactan) + 6\ O_2 \rightarrow 5\ H_2O + 6\ CO_2$
$C_8H_8O_3(Lignin) + 8.5\ O_2 \rightarrow 4\ H_2O + 8\ CO_2$
$C_5H_{10}0_5(Xylose) + 5\ O_2 \rightarrow 5\ H_2O + 5\ CO_2$
$C_5H_{10}0_5(Arabinose) + 5\ O_2 \rightarrow 5\ H_2O + 5\ CO_2$
$C_6H_{12}O_6(Extract) + 6O_2 \rightarrow 6\ H_2O + 6\ CO_2$
$C_6H_{12}O_6(Glucose) + 6O_2 \rightarrow 6\ H_2O + 6\ CO_2$
$C_5H_4O_2(Furfural) + 5\ O_2 \rightarrow 2\ H_2O + 5\ CO_2$ *
$C_2H_4O_2\ (Acetic\ Acid) + 2\ O_2 \rightarrow 2\ H_2O + 2\ CO_2$
$C_5H_7NO_2\ (Biomass\ Sludge) + 5\ O_2 \rightarrow 2\ H_2O + 5\ CO_2 + NH_3$

*Only present in 1G2G scenarios

The boiler unit includes a softener, deaerator, surge tanks and pumps, and the unit has been appropriately cost as such in the TEA (Humbird *et al.*, 2011). In the Aspen Plus® simulation however only the deaerator and one pump has been simulated. The boiler feed water (*BFW*) initially goes through the deaerator, removing air and other non-condensable components, whereafter it is pumped at a pressure of 62.2 atm (*PUMP-01*) and heated to 176°C (*HX-04* and *HX-05*), prior to entering the boiler unit (*BOILER*). The boiler unit has been simulated as a flash drum, where high-high pressure steam (*HHPS*) at 452°C is produced (Mandegari *et al.*, 2018). The temperature of the *HHPS* is achieved by determining, by means of a design specification in Aspen Plus®, the amount of boiler feed water required to obtain an outgoing stream at the required temperature.

In Figure 4*, HX-04* has been highlighted by a blue, dashed line block. This has been done to indicate that this is a section of *S500-1* that varies for the different scenarios, depending on the heat integration network of the process. It might be that only high-pressure steam (HPS) is used to heat the boiler feed water, or even that 2 or 3 heat exchangers, part of the heat integration network, is used to heat the boiler feed water, effectively reducing the HPS usage of *HX-05*.

The condensing-extraction turbine for the various scenarios will differ, depending on the utility requirements. Nevertheless, the condensing-extraction turbine for a typical scenario will be described

using stream names and units from Figure 5. The utilities produced in the CEST unit include electricity and three steam utilities, with pressure and temperature specifications depicted in Table 10.

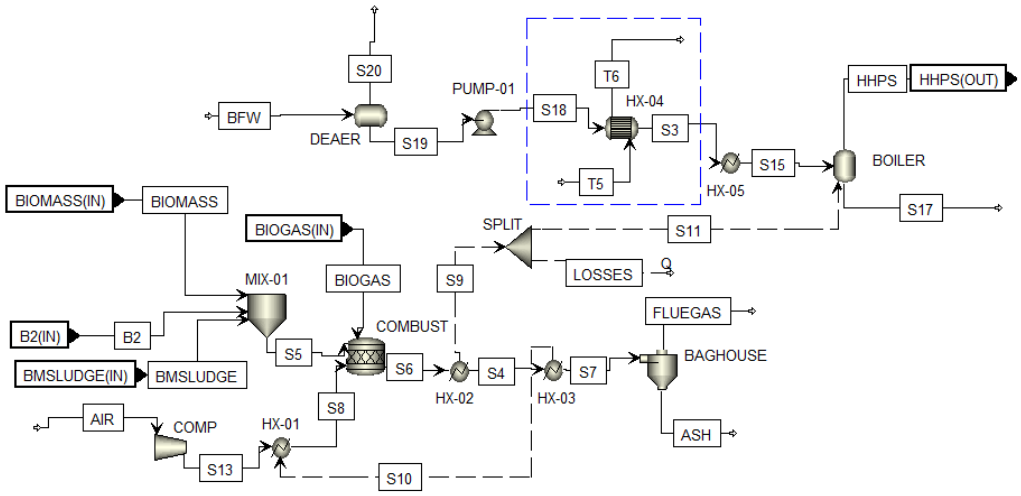

Figure 4: New High-High Pressure Boiler, part of the Combined Heat and Power Plant, flowsheet modelled in Aspen Plus®.

Table 10: Specifications of the steam utilities used in the biorefinery scenarios.

Utility	Temperature (°C)	Pressure (bar)
High-Pressure Steam (HPS)	232	28.6
Medium-Pressure Steam (MPS)	180	10
Low-Pressure Steam (LPS)	130	2.62

The high-high pressure steam (*HHPS*) produced by the boiler unit in *Section 500-1* at a pressure and temperature of 62.2 atm and 452°C respectively, enters a multistage turbine with various extraction ports and a final condenser. Whilst extracting the various steam utilities, the multistage turbine shaft turns a generator to produce electricity (Humbird *et al.*, 2011). In reality, the turbogenerator is only one unit and has been cost as such in the TEA, however, in the Aspen Plus® simulations the turbine and extraction ports are represented by individual units.

The first extraction is that of the HPS utility (*TURB-01* and *SPLIT-01*), the second is the MPS utility (*TURB-02* and *SPLIT-02*) and the third is the LPS utility (*TURB-03* and *SPLIT-03*). The final turbine (*TURB-04*) in Figure 5 represents the final condenser. The work streams (*S13*, *S10*, *S16* and *S1*) emanating from the turbines (*TURB-01*, *TURB-02*, *TURB-03* and *TURB-04*) in Figure 5 all make up the turbine shaft that will be used to turn a generator to produce electricity.

High-pressure steam and medium-pressure steam are extracted at their correct pressures, whilst LPS is extracted at a pressure between 4.7 and 9 bar, depending on the electricity requirements of the biorefinery, and is further reduced to 2.62 bar by a let-down valve (*VALVE*). Despite being at the correct pressures, the extracted streams also need to be de-superheated to obtain the correct temperatures, specified in Table 10. De-superheating involves the addition of condensate at 90°C and 1 bar to the extracted steam streams, subsequently reducing the temperatures. In Figure 5 this has been represented by *MIX-01*, *MIX-02* and *MIX-03*, where the condensate streams are *H2O*, *H2O1* and *H2O2*.

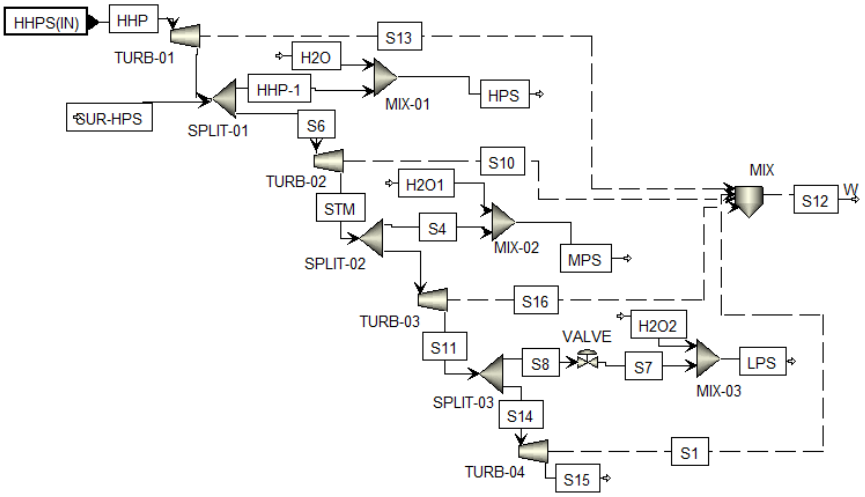

Figure 5: Condensing-Extraction Turbine, part of the Combined Heat and Power Plant, flowsheet modelled in Aspen Plus®

3.1.2.4 Other Utilities (S600 in all relevant Scenarios)

Section 600 consists of all utilities that have not been simulated but merely accounted for in the TEA. Depending on the specific scenario, *S600* can consist of a cooling water tower and chilled water package, a process water storage, a refrigerant system, and a gas engine.

Cooling water at a temperature of 28°C and 2 bar is produced in a cooling water tower. As an addition to the cooling water tower a chilled water package produces chilled water at a temperature of 4°C and 2 bar. It has been assumed that both the cooling water and chilled water package are similar to what has been designed by Humbird, et al,. (2011). In addition to the installed equipment cost of the tower and additional package, the electricity required to produce the cooling utilities were also accounted for. This was done using a coefficient of performance (COP), where the specific cooling requirement (kW) was divided by the COP, to determine the corresponding electricity usage. The COP for the cooling tower is 11.95 and 7 for the chilled water package (Petersen, Brown, Xavier, *et al.*, 2021).

Refrigerant employed in this study is ammonia at -30°C. The refrigerant system required to continuously supply refrigerant to the biorefinery has been developed by Luyben, 2017. For a system requiring 1 MW refrigerant, the compressor of the system uses 0.714 MW electricity, and the heat exchanger requires 1.714 MW cooling water. In the Aspen Plus® simulation the refrigerant utility has been specified with a cooling value of -2.175 kJ/(kg.K)(The Engineering Toolbox, 2022). The refrigerant is continuously circulated, however a make-up stream of 0.1% was assumed to account for leakages.

The process water storage merely consists of a process water tank, a process water circulations pump, and a make-up water pump (Humbird *et al.*, 2011). The input to the process water tank consists of the purified water from *Section 400: Wastewater Treatment Plant*, and the make-up water stream. The required size of the make-up water stream was determined by summing the total waste requirements of the biorefinery and subtracting it from the purified water produced in S400.

The gas engine is an alternative power generating facility. The gas engine is an internal combustion engine, where the biogas is combusted, and the expanding combustion gases is used to power the gas engine. The power generation achieved by a gas engine was estimated using Equation 2:

$$Power\ (kW) = HHV\left(\frac{MJ}{kg}\right) \times biogas\ flowrate\ \left(\frac{kg}{h}\right) \times efficiency(\%) \times 0.2778 \qquad 2$$

The HHV of the biogas was estimated as the higher heating value of methane times the methane content of the biogas. Furthermore, internal combustion engine efficiencies of up to 47.5% have been reported (Haga, 2011). However, to be conservative an efficiency of 30% was assumed.

3.1.2.5 Thermal fluid heater (S800 in all relevant Scenarios)

For the scenarios that required a higher heating source than the steam being produced in the CHP plant, a thermal fluid heater was included in the design. In this study this was only required for the 1,3-BD scenarios that used catalytic conversion. The most commonly used thermal fluid (apart from water) is thermal oil. However, to the knowledge of the writer the maximum temperature at which thermal oils are stable is 400°C (Zarza Moya, 2012). Considering the high temperatures at which 1,3-BD catalytic upgrading takes place (E.g., 401°C, 350°C or 312°C), another type of thermal fluid was employed. Thermal fluids with decomposition temperature >400°C, are molten salts, commonly consisting of 60% $NaNO_3$ and 40% KNO_3 (Reddy, 2011). The decomposition temperature of common molten salts are between 500°C and 600°C (approx. 565°C), with a melting point of 220°C (Mohammad, Brooks & Akbar Rhamdhani, 2017).

For the design of the thermal fluid heater, the combustion chamber (*COMBUST*) was designed similar to that of the high-high pressure boiler combustion chamber (*Section 500-1*), with the temperature of the combustion chamber specified as 870°C, the flue gas exiting at a temperature if 149°C (*FLUEGAS*) and the air (*S5*) preheat temperature at approximately 185°C (Mandegari *et al.*, 2018). A portion of the heat produced during combustion is used to heat the molten salt (at minimum temperature) to 555°C (*HX-02* and *HX-04*) whilst other portions of the heat produced during combustion are used firstly as an additional source of heat to the boiler (*HX-05*) and secondly to preheat the air entering the combustion chamber (*HX-01* and *HX-03*).

The minimum temperature of the molten salt differs for the various scenarios. However, as a general rule, the molten salt minimum temperature is 10°C higher compared to the highest catalytic reactor operating temperature in the process. Furthermore, the highest temperature of the molten salt (555°C) was arbitrarily chosen to be well below the decomposition temperature, whilst not too low that excessive amounts of molten salt is required.

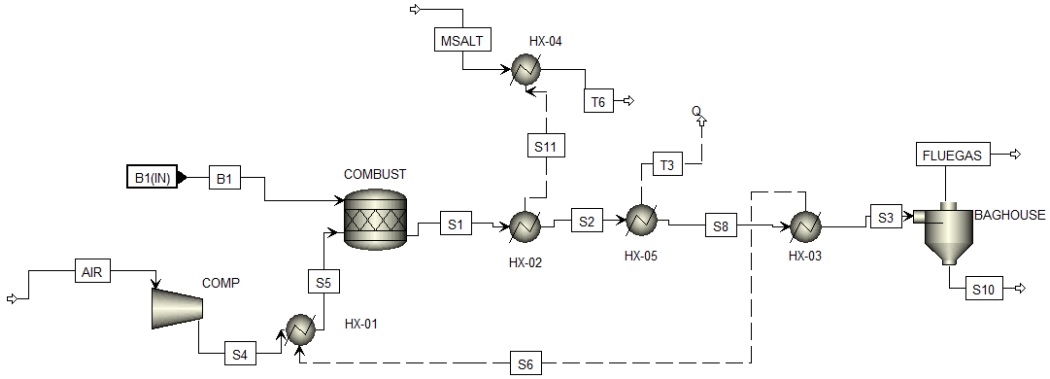

Figure 6: Thermal fluid (Molten Salt) heater, flowsheet modelled in Aspen Plus®

3.1.3 General process sections

In this sections all process sections that have been similarly designed and simulated for a number of the biorefinery scenarios will be discussed. For each general process section a screenshot of the Aspen Plus® simulation was also included. Not all sections discussed here are applicable to all the biorefinery scenarios. The general sections applicable to the various biorefinery scenario will become evident in the individual scenario process descriptions.

3.1.3.1 Section 100: Pretreatment and Enzymatic Hydrolysis

The pretreatment method employed for all the 1G2G scenarios, except for PHB (Scenario H), is SO_2-catalyzed steam pretreatment. The pretreatment and enzymatic hydrolysis section of Scenario H will be discussed in section **Error! Reference source not found.**.

Due to the high cost of SO_2, the on-site production of SO_2 seems to be a more economic option for a large-scale process (Tao, Aden, Elander, *et al.*, 2011). Furthermore, sulphur burning produces large quantities of heat which can be utilized as part of the heat integration network of the overall process. This has been implemented and, in the simulations, *HX-03* exchanges a portion of this heat produced with the CHP plant, where it is used to heat the boiler feed water.

Generally, the sulphur dioxide production process consists of a sulphur furnace where molten sulphur is atomized and sprayed into the furnace containing dry, compressed air. In Aspen Plus® the solid Sulphur (*SULPHUR*) at 25°C is sent through a heat exchanger (*HX-01*) where it is heated to approximately 117°C to ensure melting of the elemental sulphur. The molten sulphur is then pumped (*PUMP-01*) at a pressure of 7 bar to the furnace to be atomized through the nozzles (Louie, 2005). The Sulphur furnace (*SO2FURN*) has been simulated as an *RGibbs* unit in Aspen Plus®, with a heat duty specified as -300 MJ/kg mol of S(ℓ) (King, Davenport & Moats, 2013).

For the SO_2 production process, dry (dehumidified) air at a temperature of 120°C (King, et al., 2013) is required, considering SO_2 forms H_2SO_4 when coming into contact with water. The most traditional method of dehumidification involves cooling of the air to approx. 6°C (42-44°F) by passing it over a cooling coil containing either water, glycol, or refrigerant, in order to condense the condensable component i.e., water (Pillai & Desai, 2018). In the Aspen Plus® simulation the air is cooled to 6.7°C (*HX-02*), whereafter

it is flashed (*FLASH-01*) to remove any condensed water and finally compressed (*COMP*) to 120°C before being sent to the SO_2 furnace.

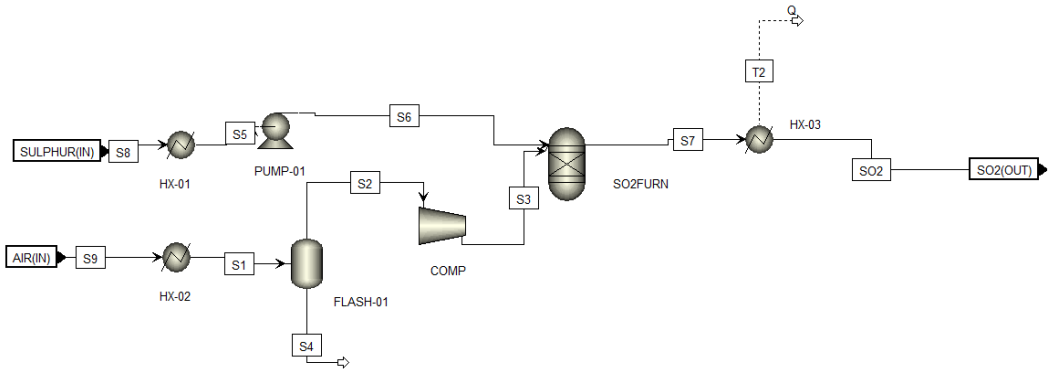

Figure 7: Section 100-1 flowsheet modelled in Aspen Plus®

The portion of 2G feed that has been sent to the biorefineries for product formation (*2GFEED*) is diluted to a moisture content of 75% before being heated through heat integration (*HX-01*) and sent to the steam pretreatment reactor (*STEAMPRE*). Other steam pretreatment operating specification include an SO_2 content of 2% w/w, based on water content of 2G feedstock, 190°C and a pressure of 17 bar (1.7 MPa) (Carrasco *et al.*, 2010a). The temperature of 190°C is maintained by injecting high-pressure steam (*STM*)(@232°C and 28.6 bar) into the reactor. The amount of high-pressure steam (HPS) required for the pretreatment is determined by a design specification, where *STM* is regulated to ensure that the stream exiting the steam pretreatment reactor (*S5*) is at a temperature of 190°C.

At these operating conditions and a residence time of 5 min, a hemicellulose hydrolysate can be obtained containing xylose, 15.1 g/100gDM along with glucose, 2.4 g/100gDM and arabinose, 1.4 g/100gDM using a continuously operated plug flow reactor (Carrasco *et al.*, 2010a; Nieder-Heitmann, 2019). Inhibitors formed during the pre-treatment include acetic acid and furfural at approximately 2.35 g/100gDM and 0.35 g/100gDM respectively (Carrasco *et al.*, 2010a). The pre-treatment process was simulated using the *RStoic* unit in Aspen Plus® with reactions presented in Table 11.

Table 11: Stoichiometric reactions used in the SO_2 catalyzed steam-pretreatment reactor (Carrasco *et al.*, 2010a; Humbird *et al.*, 2011).

Stoichiometric Reactions
Pre-treatment
$Cellulose + H_2O \rightarrow Glucose$
$Cellulose + H_2O \rightarrow Glucose\ Oligomers$
$Cellulose + H_2O \rightarrow 3Acetic\ Acid$
$Xylan + H_2O \rightarrow Xylose$
$Xylan + H_2O \rightarrow Xylose\ Oligomers$
$Xylan \rightarrow Furfural + 2H_2O$
$Arabinan + H_2O \rightarrow Arabinose$

Following the steam pre-treatment, a flash drum (*FLASH-01*) has been simulated to represent the vapors that would have been emitted from the steam pre-treatment process via blowers. The vapor stream from the flash drum (*S6*) is desulphurized, whilst the liquid-solid stream (*S7*) is sent through a centrifuge to

separate the liquid hemicellulose hydrolysate (*HEMICELL*) stream and the solid cellulignin (*S10*) stream (Humbird *et al.*, 2011). It was assumed that a 50% liquid load of solids would be appropriate to achieve a 100% solids separation in the centrifuge (Nieder-Heitmann, 2019).

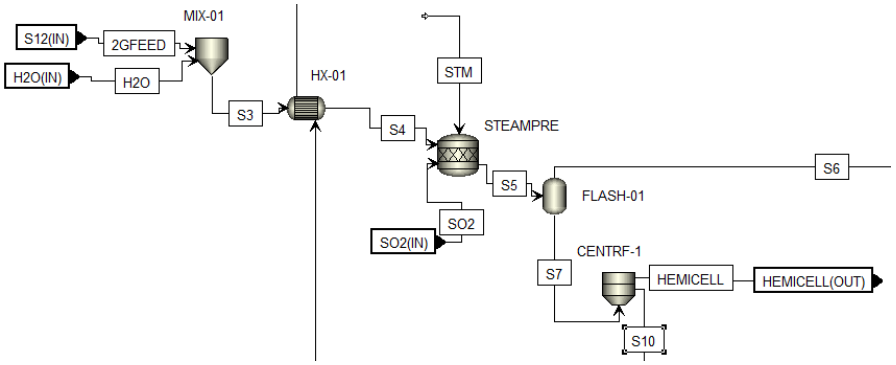

Figure 8: Pretreatment component of Section 100-2 modelled in Aspen Plus®

The SO_2 present in *S6* is removed by using a limestone slurry wet scrubber system. This is the most common desulphurization process used in industry, which makes use of a limestone slurry (*LIMESTON*) with solid loading of 10-15wt% (Srivastava, Jozewicz & Singer, 2001). A total of 95% SO_2 is removed by reacting with the limestone ($CaCO_3$) to produce calcium sulphite ($CaSO_3$) which, when sparged with air (*COMP*), the calcium sulphite reacts with oxygen to produce gypsum ($CaSO_4$) (Roy & Sardar, 2015). The scrubber (*SO2SCRUB*) has been simulated using the *RStoic* unit in Aspen Plus® and the reactions can be found in Table 12.

A flash drum (*FLASH-02*) has been simulated to represent vapors that would have been emitted from the SO_2 scrubber and will not be accounted for in the TEA. Furthermore, the gypsum is then separated from the liquid stream exiting *FLASH-02* in a centrifuge (*CENTRF-2*). The gypsum can be sold as a byproduct or alternatively sent to municipal waste treatment, which the latter has been chosen for this scenario.

The liquid stream from *CENTRF-2*, predominantly consists of water and can therefore be recycled to be used as water used to make up the limestone slurry. A bleed stream of 3% has been assumed to prevent the build-up of impurities. Due to limitations of the Aspen Plus® software, the recycle circuit has not been simulated, but has been accounted for in the TEA.

Table 12: Reactions taking place in a limestone slurry wet scrubber system for the removal of SO_2.

Stoichiometric Reactions	Fractional Conversion
Limestone slurry wet scrubber system	
$CaCO_3 + SO_2 \rightarrow CaSO_3 + CO_2$	0.95
$CaSO_3 + 0.5\ O_2 \rightarrow CaSO_4$	1

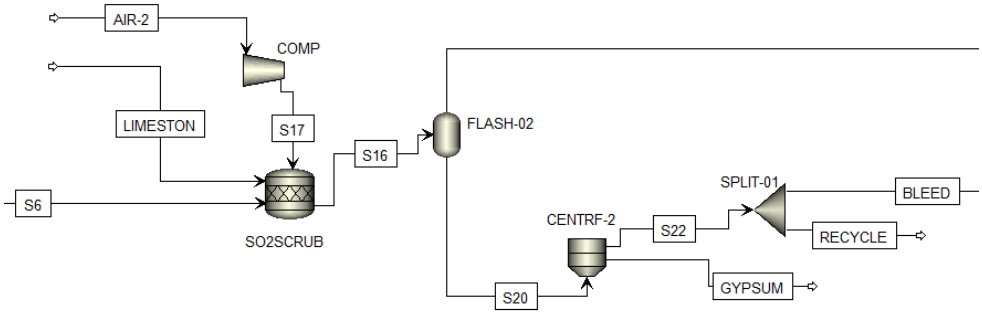

Figure 9: SO_2 Removal component of Section 100-2 modelled in Aspen Plus®

As per the suggestion of Frederick (2013) it was assumed that a portion of the entrained inhibitors from the cellulignin is removed by washing the solid stream (*S10*) from *CENTRF-1* in Figure 8 with 1.5 times the volumetric flowrate of the solids originally loaded for pre-treatment. The washing step was simulated using the *SWash* unit in Aspen Plus® (*WASH*). The liquid-to-solid ratio of the *SWash* unit was selected to ensure at least 75% of the inhibitors were removed from the cellulignin. The washing water containing 75% of the inhibitors (*WASHOUT*) is mixed (*MIX-02*) with the bleed stream from the SO_2 removal unit (Figure 9) and the vapor stream from *FLASH-02* in Figure 9. The combined stream from *MIX-02* (*WASTE*) is sent to the wastewater treatment plant.

Enzymatic hydrolysis is the following step required to hydrolyze the cellulose contained in the washed cellulignin (*S13*) to glucose. The solids are initially diluted (*DILUT*) to a 25wt% solids loading and heated to 50°C by means of heat integration (*HX-02*) with the overhead stream of *FLASH-02* in Figure 9, prior to undergoing enzymatic hydrolysis (Davis *et al.*, 2018). The batch enzymatic hydrolysis process initially starts with a screw mixer that combines the solid cellulignin from pretreatment (*S18*) and the cellulase enzymes (*CELLULAS*) produced at the on-site cellulase production plant. The mixture is then fed into various continuous, high-solids vertical tower reactors, where the mixture stays for a total of 24 hours. The pumpable slurry is then subsequently sent to batch reactors for 96 hours for the completion of enzymatic hydrolysis (Davis *et al.*, 2018; Humbird *et al.*, 2011). The entire enzymatic hydrolysis process has merely been simulated using a single *RStoic* unit in Aspen Plus® (*ENZYHDR*), however all units have appropriately been accounted for in the TEA by using the mass flowrate to the enzymatic hydrolysis unit to scale from equipment costs given in Humbird *et al*. (2011) and Davis *et al*. (2018). The reactions and fractional conversions used in *ENZYHDR* can be found in Table 13.

Table 13: Stoichiometric reactions used in the enzymatic hydrolysis reactor (Davis *et al.*, 2018; Humbird *et al.*, 2011).

Stoichiometric Reaction	Fractional Conversion
Enzymatic Hydrolysis	
$Cellulose + H_2O \rightarrow Glucose$	0.9
$Cellulose + H_2O \rightarrow Glucose\ Oligomers$	0.04
$Cellulose + 0.5\ H_2O \rightarrow 0.5\ Cellobiose$	0.012
$Cellobiose + H_2O \rightarrow 2\ Glucose$	1

Due to the high cost of enzymes, it is considered more economical to produce the cellulase enzymes on-site. The on-site cellulase production plant has not been simulated in Aspen Plus®. Simulation of the

plant would have been superfluous, considering sufficient information was available from literature to size, cost and determine total energy usage of the plant. For sizing and costing purposes, the appropriate quantity of enzyme required for a 10 $mg_{protein}/g_{cellulose}$ dose was determined using the mass flowrate of cellulose to the enzymatic hydrolysis equipment (Davis *et al.*, 2018; Humbird *et al.*, 2011).

The stream exiting the enzymatic hydrolysis operation (*S14*) is separated by a centrifuge (*CENTRF-3*) into an unhydrolyzed cellulignin solids stream (*CELLULIG*) and the glucose-rich liquid stream (*S15*). The solids stream (*CELLULIG*) is sent to the boiler for combustion, whilst *S15* is split (*SPLIT-02*) into appropriate portions to *Section 200-2* (*GFERM* &*GSEED*), *Section 200-3* (*XSEED* & *XFERM*) and the cellulase production plant (*ENZYMEPR*). The split fractions of the various stream exiting *SPLIT-02* have been determined by conducting mass balances in excel.

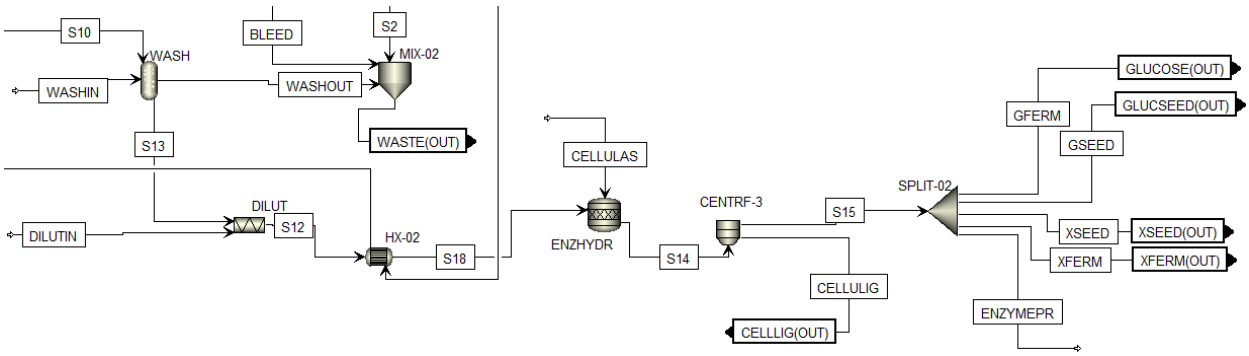

Figure 10: Enzymatic Hydrolysis component of Section 100-2 modelled in Aspen Plus®

3.1.3.2 Section 200-1: Dilution, Sterilization and Hydrolysis of A-molasses

All the biorefinery scenarios require dilution and sterilization of the A-molasses. However, hydrolysis is only applicable to scenarios where the microorganisms employed for fermentation cannot naturally hydrolyze sucrose. The A-molasses is initially sterilized to 121°C (*HX-01*) to ensure no microbes are available that could potentially affect the fermentation process (Ikram-Ul *et al.*, 2004). Following sterilization, the A-molasses is diluted (*MIX*) by clean, recycled water from the wastewater treatment plant prior to being sent to seed train and fermentation. The A-molasses is diluted prior to hydrolysis to reduce the risk of crystallisation in the hydrolysis reactor. The concentration of sugars after dilution depends on the sugar concentration required for each individual fermentation process. Finally, sucrose is hydrolyzed (*HYDR*) to glucose and fructose using invertase at a dose of 25g / 3000g sucrose, a temperature of 55°C and a residence time of 6 hours (Bratu, Stoica & Buruleanu, 2008).

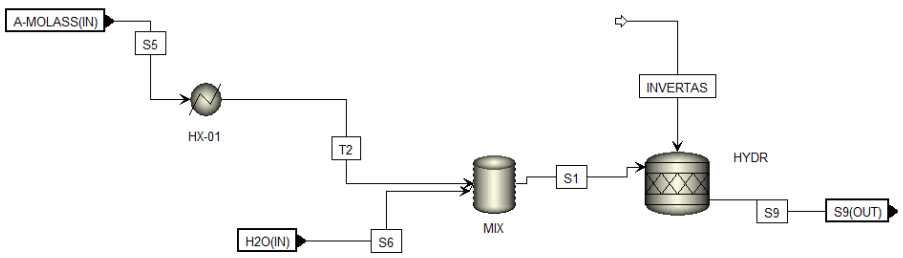

Figure 11: Section 200-1 flowsheet modelled in Aspen Plus®

3.1.3.3 Section 200-2 (&3): Seed Train and Fermentation

The 1G biorefineries only have one fermentation process, where the A-molasses sugars are converted to the respective products. All the 1G2G scenarios, except for Scenario H have two fermentation processes, where the glucose from pretreatment-hydrolysis and the A-molasses sugars are utilized in the one process, while the xylose from the hemicellulose hydrolysate produced during pretreatment is utilized in the other. Irrespective of sugars utilized, the seed train and fermentation sections were similarly designed and simulated (indicated in Figure 12). Additional steps can potentially be required for 1G2G processes due to the concentration and detoxification of the hemicellulose hydrolysate.

It has previously been reported that 10% of the available feedstock is the appropriate portion to be sent to the seed train for microbial inoculum development (Humbird *et al.*, 2011); however, this portion was adjusted according to the microbial requirements of each individual process. This has been determined by conducting mass balance calculations in excel. The appropriate A-molasses portion (*SUGAR-1*), microbial culture (*MICRO*) and seed train medium (*MEDIUM*) are all mixed (*MIX-01*) before being pumped (*PUMP-01*) to the seed train reactors. Furthermore, the mixed stream is heated (or cooled) to the required seed train operating temperature (*HX-01*).

The 4 seed train fermenters were simulated as one large fermenter using the *RStoic* unit in Aspen Plus® (*SEEDTR*). The seed train reactors are operated in fed-batch mode, however the process was modelled in Aspen Plus® as a continuous process, due to limitations of software (Van Der Merwe, 2010). The compressor (*COMP*) sparging air into the fermentation tank at a pressure of 1.7 atm, is only present for microaerobic or aerobic processed (Batelle, 2001). Furthermore, CO_2 is produced during the fermentation process, which in the industry would have been vented into the atmosphere directly from the fermentation reactor. However, in Aspen Plus® this emission was simulated using a flash drum (*FLASH-01*), which follows the *RStoic* unit (Van Der Merwe, 2010). The flash drum was not accounted for in the economic analysis. The main fermentation process of each biorefinery scenario was simulated similar to the seed train.

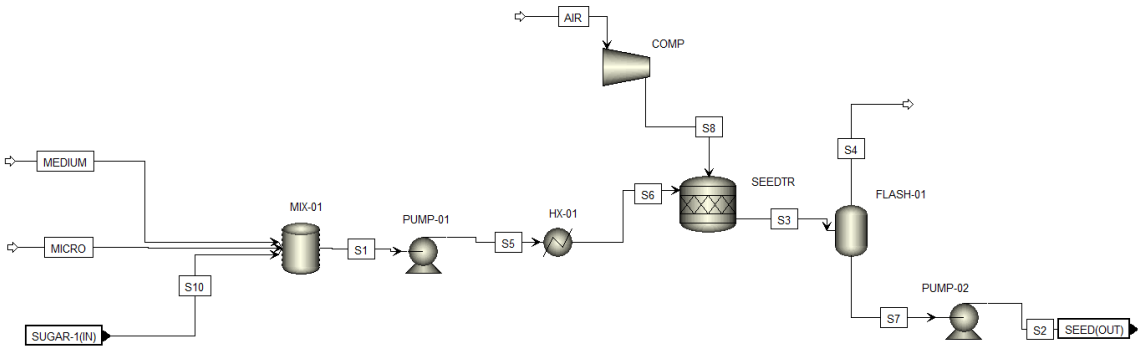

Figure 12: Section 200-2,1 flowsheet modelled in Aspen Plus®

The concentration of the hemicellulose hydrolysate is done using a feedforward triple effect evaporator (TEE), consisting of 3 flash drums (*FLASH-01*, *FLASH-02* & *FLASH-03*), with operating pressures of 1, 0.9 and 0.8 atm respectively. Furthermore, the TEE also consists of 3 condensing heat exchangers (*HX-01*, *HX-02* & *HX-03*). Heat is exchanged between *HX-01* & *FLASH-02* and between *HX-02* & *FLASH-03*. *HX-03*

uses cooling water utility and *FLASH-01* uses low pressure steam (LPS) at 130°C and 2.62 bar to achieve a 0.25 vapor fraction (Nieder-Heitmann, 2019).

Due to the presence of inhibitors in the hemicellulose hydrolysate, which affects microbial growth as well as metabolism, the concentrated hydrolysate is detoxified (*DETOX*) using 2.4% w/v activated carbon at 0.92 pH. Under these operating conditions almost all furfural (99%) and approximately 70% of acetic acid can be removed (Rodrigues, Felipe, Almeida e Silva, *et al.*, 2001). However, considered little is known about the pH of the feed stream, acetic acid removal of 65% was assumed to account for any variations in results due to difference in pH. Furfural removal is not affected by pH (Rodrigues *et al.*, 2001). The activated carbon detoxification process has merely been simulated as a separator block, however in the TEA the activated carbon columns as well as required activated carbon reagent stream has been accounted for.

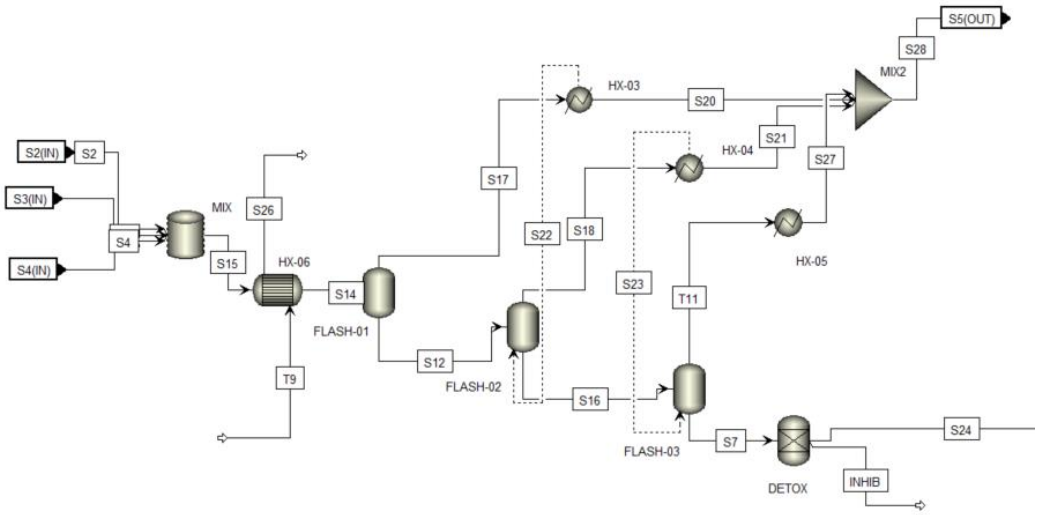

Figure 13: Concentration and detoxification of hemicellulose hydrolysate part of Section 200-2, flowsheet modelled in Aspen Plus®

3.1.4 2,3-Butanediol (Scenario A and B)

3.1.4.1 Scenario A – 2,3-Butanediol from 1G feedstock

The production of 2,3-Butanediol from A-molasses (1G feedstock) consisted of various steps which include dilution, sterilization and hydrolysis of A-molasses (*S200-1*), a seed train for the growth of *K. oxytoca* KMS005-73T (*S200-2,1*), fermentation (*S200-2,2*) and separation and purification (*S300*). Additional sections in the process include wastewater treatment (*S400*), the combined heat and power plant (*S500-1 & S500-2*) and other utilities (*S600*). In Figure 14 the basic flowsheet of Scenario is illustrated. A screenshot of the main flowsheet in Aspen Plus® is given in Appendix C.

Following dilution (to 250 g/L), sterilization and enzymatic hydrolysis of the A-molasses, 3.49 wt.% of the hydrolysis product stream is sent to the seed train, whilst the remainder is sent to fermentation for 2,3-BDO production. Both the seed train and fermentation reactors operate at 37°C (Jantama *et al.*, 2015). The nutrient medium is an AM1 medium with main constituents including $(NH_4)_2HPO_4$ (2.63 g/L) and $FeCl_3 \cdot 6H_2O$ (2.4 g/L) (Martinez, Grabar, Shanmugam, *et al.*, 2007), which have all been accounted for in

the techno-economic analysis (TEA). However, in Aspen Plus® this has merely been represented by NH_3, which is the only substance of the dissociated medium components directly being used for the growth of the microorganism *K. oxytoca* KMS005-73T. The stoichiometric reactions and fractional conversion used in the seed train and fermentation reactors can be found in Table 14, where the empirical formula of *K. oxytoca* was assumed as $CH_{1.750}O_{0.430}N_{0.220}$ (Popovic, 2019).

The fermentation broth produced in *S200-2* contains 117.4 g/L 2,3-BDO, with by-products reported as succinate, acetate and ethanol (Jantama *et al.*, 2015). It was mentioned by Jantama et al. (2015) that KOH was necessary for neutralisation of the broth. Therefore, it was assumed that neutralization of succinate and acetate took place by the addition of KOH and the final by-products formed were succinic acid and acetic acid, alongside ethanol. The appropriate amount of KOH required for this neutralization was determined in excel and only accounted for in the TEA.

The fermentation broth is sent to downstream processing for separation and purification of 2,3-BDO, with a recovery and purity of >90% and 98% respectively. The liquid devoid of 2,3-BDO is sent to wastewater treatment, whilst the solid biomass is separated from the fermentation broth and sent to the combined heat and power (CHP) plant for combustion.

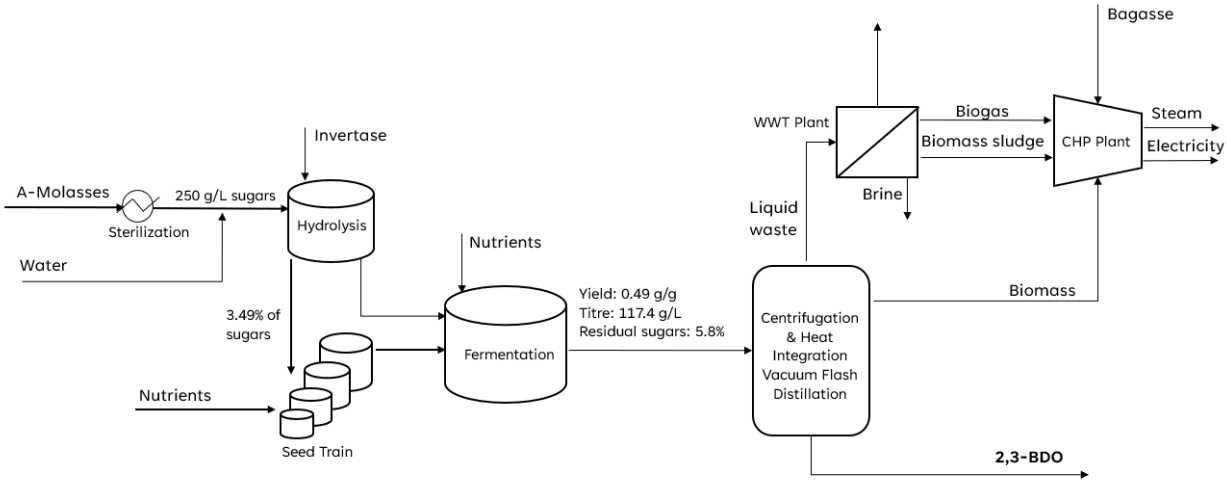

Figure 14: Scenario A Main Flowsheet

Table 14: Stoichiometric reactions used in the reactor units of Section 200-2, for Scenario A (Jantama et al., 2015; Koutinas, Yepez, Kopsahelis, et al., 2016; Nghiem, Kleff & Schwegmann, 2017; Patel & Pandya, 2015).

Stoichiometric Reaction	Fractional Conversion
S200-2: Seed Train	
$C_6H_{12}O_6 + 1.2482\ NH_3 \rightarrow 5.6737\ CH_{1.750}O_{0.430}N_{0.220} + 2.9078\ H_2O + 0.3262\ CO_2$	0.93
S200-3: 2,3- BDO Fermentation	
$C_6H_{12}O_6(Fructose) + 0.5\ O_2 \rightarrow C_4H_{10}O_2\ (BDO) + 2\ CO_2 + H_2O$	1
$C_6H_{12}O_6(Glucose) + 0.5\ O_2 \rightarrow C_4H_{10}O_2\ (BDO) + 2\ CO_2 + H_2O$	0.841
$C_6H_{12}O_6 + 1.2482\ NH_3 \rightarrow 5.6737\ CH_{1.750}O_{0.430}N_{0.220} + 2.9078\ H_2O + 0.3262\ CO_2$	0.082
By-Products	
$C_6H_{12}O_6 + 0.8571\ CO_2 \rightarrow 1.7142\ C_4H_6O_4(Succinic\ Acid) + 0.8571\ H_2O$	0.027
$C_6H_{12}O_6 \rightarrow 2\ C_2H_6O(Ethanol) + 2\ CO_2$	0.04
$C_6H_{12}O_6 + 2\ O_2 \rightarrow 2\ C_2H_4O_2(Acetic\ Acid) + 2\ CO_2 + 2H_2O$	0.121

3.1.4.2 Scenario B – 2,3-Butanediol from 1G2G feedstock

The production of 2,3-butanediol from 1G2G feedstock (A-molasses, bagasse, and brown leaves) consist of various steps which include SO_2 production (*S100-1*), pre-treatment and enzymatic hydrolysis (*S100-2*), dilution, sterilization, and hydrolysis of A-molasses (*S200-1*), fermentation using glucose/A-molasses (*S200-2*), fermentation using xylose (*S200-3*) and separation and purification (*S300*). Additional sections in the process include wastewater treatment (*S400*), the combined heat and power plant (*S500-1 & S500-2*) and other utilities (*S600*). In Figure 15 the basic flowsheet of Scenario B is illustrated. A screenshot of the main flowsheet in Aspen Plus® is given in Appendix C.

The 2G feedstock stream is divided, where a portion is sent to the CHP plant (so-called "bypass") and the other portion is sent to pre-treatment for sugar extraction. For the chosen pre-treatment process, SO_2 is required which is produced on site at the SO_2 production plant using sulphur and air as reagents. Following pre-treatment and enzymatic hydrolysis two main sugar streams are produced, the hemicellulose hydrolysate containing xylose and a glucose-rich stream. The majority of the glucose-rich stream is sent to *S200-2*, whilst a small portion is also sent to *S200-3* and the cellulase production plant. The entire hemicellulose hydrolysate stream is sent to *S200-3*. Two waste streams are produced in *S100-2*, the cellulignin solids, which is sent to the CHP plant and the combined liquid waste streams sent to wastewater treatment.

The 2,3-BDO fermentation section using glucose and A-molasses as feedstock consisted of two subdivisions, the seed train for *K. oxytoca* KMS005-73T growth (*S200-2-1*) and the fermentation section (*S200-2-2*). These sections have been designed similar to Scenario A. Similar to *S200-2*, the 2,3-BDO fermentation section, utilizing xylose consists of two subdivisions, the seed train for *S. cerevisiae* BD5X-TXmNP growth (*S200-3-1*) and the fermentation section (*S200-3-2*). Despite having xylose be the main sugar used for the 2,3-BDO fermentation in this section, a small continuous stream of glucose (<1 g/L) is still required during fermentation to increase production to a titre of 96.8 g/L (Kim *et al.*, 2017). Furthermore, glucose is also the monosaccharide used for microbial growth both in *S200-3-1* and *S200-3-2*. The combined stream to *S200-3* is concentrated to 220 g/L using a triple effect evaporator and detoxified prior to fermentation (Kim *et al.*, 2017).

The seed train and fermenter reactors of S200-3 operate at a temperature of 30 °C (Kim *et al.*, 2017). The empirical formula for *S. cerevisiae* has been assumed as $CH_{1.830}O_{0.560}N_{0.170}$ (Popovic, 2019). The seed train medium is called a YNB medium, which essentially contains ammonium sulphate for growth. Similar to what has previously been done, the medium has merely been represented by NH_3 in the simulation, whilst the entire medium was accounted for in the TEA. The fermentation medium has been specified as being a YP being, consisting of 10 g/L yeast extract and 20 g/L peptone (Kim *et al.*, 2017). However, due to the economic impact of these expensive substances, alternative nitrogen sources such as corn steep liquor (CSL) has instead been used for the growth of *S. cerevisiae* (Batista, Bataus, Campos, *et al.*, 2013; Taiwo, Madzimbamuto & Ojumu, 2018). The stoichiometric reactions and series fractional conversions used in the fed-batch fermentation reactors can be found in Table 15.

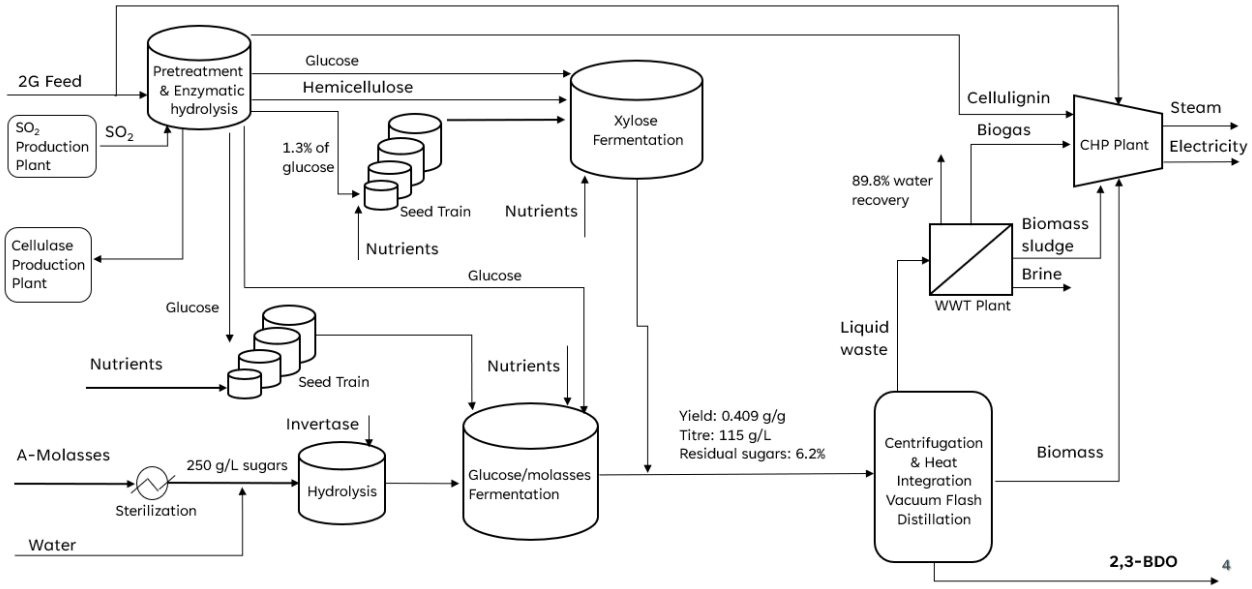

Figure 15: Scenario B Main Flowsheet

Table 15: : Stoichiometric reactions used in the reactor units of Section 200-3-1 and Section 200-3-2, for Scenario B (Kim et al., 2017).

Stoichiometric Reaction	Fractional Conversion
S. cerevisiae* BD5X-TXmNP *Seed Train	
$C_6H_{12}O_6 + 0.9714\ NH_3 \rightarrow 5.7139\ CH_{1.830}O_{0.560}N_{0.170} + 2.2289\ H_2O + 0.2862\ CO_2$	0.92
Fermentation	
$C_5H_{10}O_5 + 0.6\ O_2 \rightarrow 0.8\ C_4H_{10}O_2\ (BDO) + H_2O + 1.8\ CO_2$	0.91
$C_6H_{12}O_6 + 0.5\ O_2 \rightarrow C_4H_{10}O_2\ (BDO) + 2\ CO_2 + H_2O$	0.9
$C_6H_{12}O_6 + 0.9714\ NH_3 \rightarrow 5.7139\ CH_{1.830}O_{0.560}N_{0.170} + 2.2289\ H_2O + 0.2862\ CO_2$	0.83
By-Products	
$3\ C_5H_{10}0_5 \rightarrow 5\ C_2H_6O(Ethanol) + 5\ CO_2$	0.16
$3\ C_5H_{10}O_5 + 5\ H_2O \rightarrow 5\ C_3H_8O_3(Glycerol) + 2.5\ O_2$	0.13
$C_5H_{10}O_5 + 1.5\ O_2 \rightarrow 0.7\ C_4H_8O_2(Acetoin) + 2.2\ H_2O + 2.2\ CO_2$	0.1
$C_5H_{10}O_5 + H_2O \rightarrow C_5H_{12}O_5(Xylitol) + 0.5\ O_2$	0.04

3.1.4.3 Section 300: Separation and Purification of 2,3-BDO

The separation and purification sections of Scenario A and B have been designed and simulated similarly. For the separation and purification of 2,3-BDO a Heat-Integrated Vacuum Flash Distillation (HI-VFD) configuration was selected (Haider, Abdul, *et al.*, 2018). All units of the original HI-VFD configuration were retained, although some of these units were optimized for the individual scenarios and a number of units were additionally added to the configuration.

The fermentation broth from the fermentation section (*FERMBROT*) initially goes through a centrifuge (*CENTRF*) for the removal of the biomass/microorganisms (Dunn *et al.*, 2015). Due to the nature of the biomass particles, i.e., larger particles that will most likely drop out of suspension when left stationary, it was assumed that a very low liquid load of solids outlet of 0.01 (ratio) was achievable in the centrifuge. Thereafter the liquid stream is vacuum flashed (*FLASH-01*) at a temperature and pressure of 61°C and 0.2 atm (Haider, Abdul, *et al.*, 2018). Prior to the vacuum flash drum, the stream is heated through a series

of heat exchangers (*HX-01*, *HX-03*, *HX-04* & *HX-08*), part of the heat integration network of the system. The heat integration network was individually optimized for the scenarios.

The vapour stream from the flash drum is cooled (*HX-07*) to a temperature of approximately 38°C (lowest temperature the vapour can be cooled to by the cooling water utility), flashed to remove any non-condensable components (*FLASH-02*) and finally pumped by the vacuum pump (*VACUUMP*) at 1 atm (Khetni, 2018). The liquid stream from the flash drum is sent to a distillation column (*DISTILL*) with 12 stages, a reflux ratio of 0.04, a feed stream at stage 4 and a pressure of 0.2 atm (Haider, Abdul, *et al.*, 2018).

For optimal heat-integration purposes the condenser of the distillation column has been deconstructed. The distillate stream (*S26*) first goes through a compressor (*COMP-01*) with a pressure ratio of 1.5, increasing the temperature of the distillate stream, which is used in the heat integration network to heat the feed stream going to the vacuum flash drum (Haider, Abdul, *et al.*, 2018). Following heat integration, the pressure of the distillate stream is reduced back to 0.2 atm using a valve (*VALVE*) and condensed (*HX-05*) using cooling water, before being split according to the reflux ratio back to the first stage of the distillation column (*S15*). The second stream from *SPLIT-01* (*T3*) is used in the overall heat integration network, but eventually sent to the wastewater treatment plant.

The distillation column has been simulated as a *RadFrac* unit in Aspen Plus®, with a reboiler but no condenser. In the study by Haider et al. (2018), the separation and purification processes were designed by ensuring >90% recovery of 2,3-BDO. To ensure this recovery rate, the product flowrate together with the bottoms flowrate and product stage was adjusted to ensure the purity of 98% and recovery >90% was achieved (Haider, Abdul, *et al.*, 2018; Shao & Kumar, 2009). A design specification was used to vary the bottoms flowrate by specifying the purity of the product stream at 98%. The bottoms stream from the distillation column (*S16*) was combined with *S4* exiting the vacuum pump in *MIX-02*, prior to being sent to the wastewater treatment plant. Finally, the 2,3-BDO product from the distillation column (*T5*) is used in the overall heat integration network of the process prior to being cooled to 40°C (*HX-06*) for further distribution purposes.

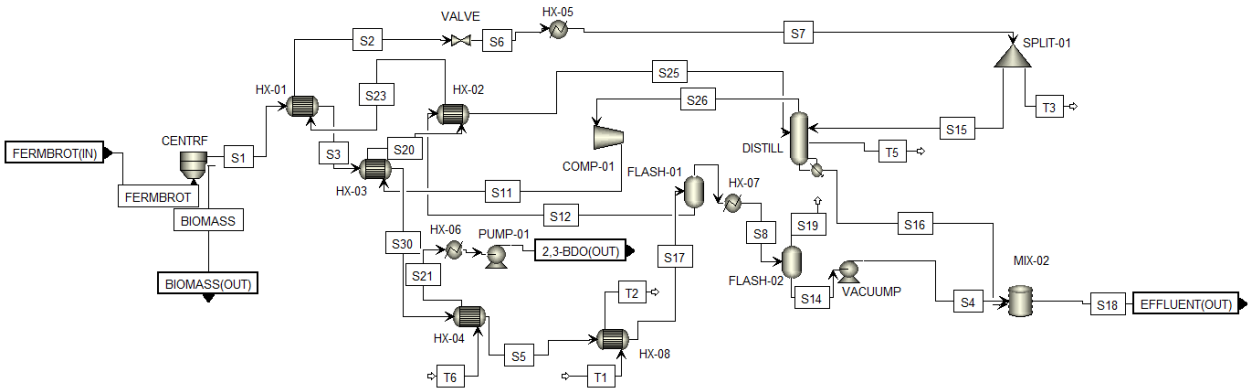

Figure 16: Scenario A and B, Section 300 flowsheet modelled in Aspen Plus®

3.1.5 1,3-Butadiene (Scenario C, D, E and F)

3.1.5.1 Scenario C - 1,3-Butadiene from 1G feedstock, with 2,3-Butanediol as intermediate product

The production of 1,3-butadiene from A-molasses (1G Feedstock) in Scenario C involves the fermentation to 2,3-BDO, after which the 2,3-BDO is catalytically upgraded to 1,3-butadiene. The 2,3-BDO fermentation is similar to the process developed and described for Scenario A. The only difference is the purity of 2,3-BDO being produced, which has been adjusted to 97.25% to coincide with the purity of the 2,3-BDO stream required to produce 1,3-butadiene (Tsukamoto *et al.*, 2016). Sections specific to the catalytic upgrading of 2,3-BDO to 1,3-BD include 1,3-BD Production (*S700*) and the thermal fluid heater (*S800*). In Figure 17 the basic flowsheet of Scenario C is illustrated. A screenshot of the main flowsheet in Aspen Plus® is given in Appendix C.

The 2,3-BDO purified in *S300* is sent to *S700* where 1,3-BD is produced and furthermore separated and purified, producing 1,3-BD at a purity of >99% (Song *et al.*, 2017a). The waste stream devoid of 1,3-BD produced in *S700* is sent to the wastewater treatment plant. Considering the catalytic upgrading of 2,3-BDO to 1,3-BD is a highly endothermic process, taking place at high temperatures, an additional utility was required, capable of maintaining these operating conditions. Molten salt is a thermal fluid with decomposition temperature >400°C, suitable as new heating utility (Reddy, 2011). Bagasse available from the sugar mill is separated and one portion is sent to the CHP plant for steam and electricity generation, and the other portion is sent to the thermal fluid heater (*S800*).

3.1.5.2 Scenario D – 1,3-butadiene from 1G2G feedstock, with 2,3-butanediol as intermediate product

The production of 1,3-Butadiene from 1G2G feedstock (A-molasses, bagasse, and brown leaves) in Scenario D involves the 2,3-BDO fermentation, after which the 2,3-BDO is catalytically upgraded to 1,3-butadiene. The 2,3-BDO fermentation is similar to the process developed and described for Scenario B. Similar to Scenario C, the 2,3-BDO intermediate product purity has been adjusted to 97.25% to coincide with the purity of the 2,3-BDO stream required to produce 1,3-butadiene (Tsukamoto *et al.*, 2016).). In Figure 18 the basic flowsheet of Scenario D is illustrated. A screenshot of the main flowsheet in Aspen Plus® is given in Appendix C.

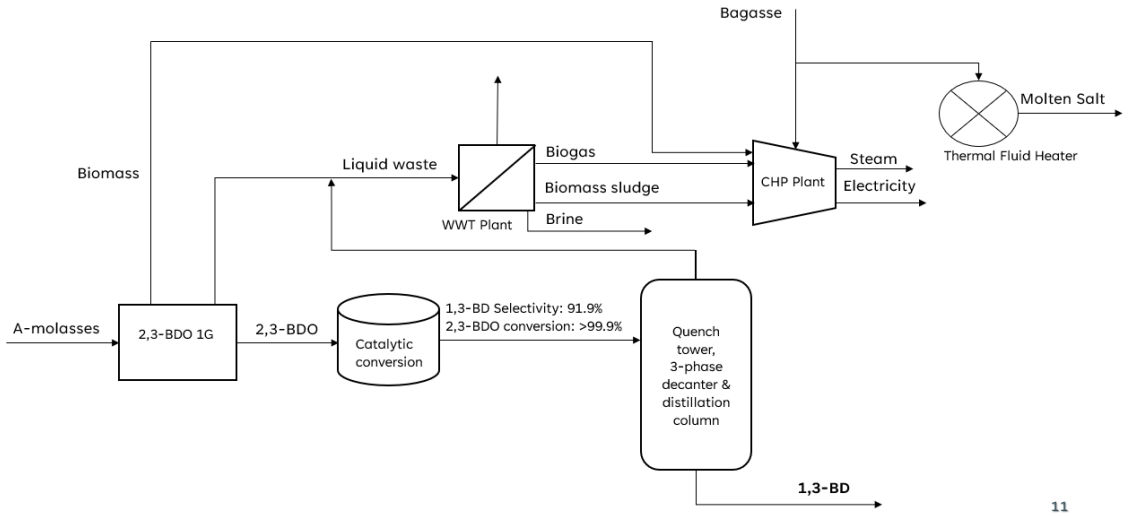

Figure 17: Scenario C Main Flowsheet

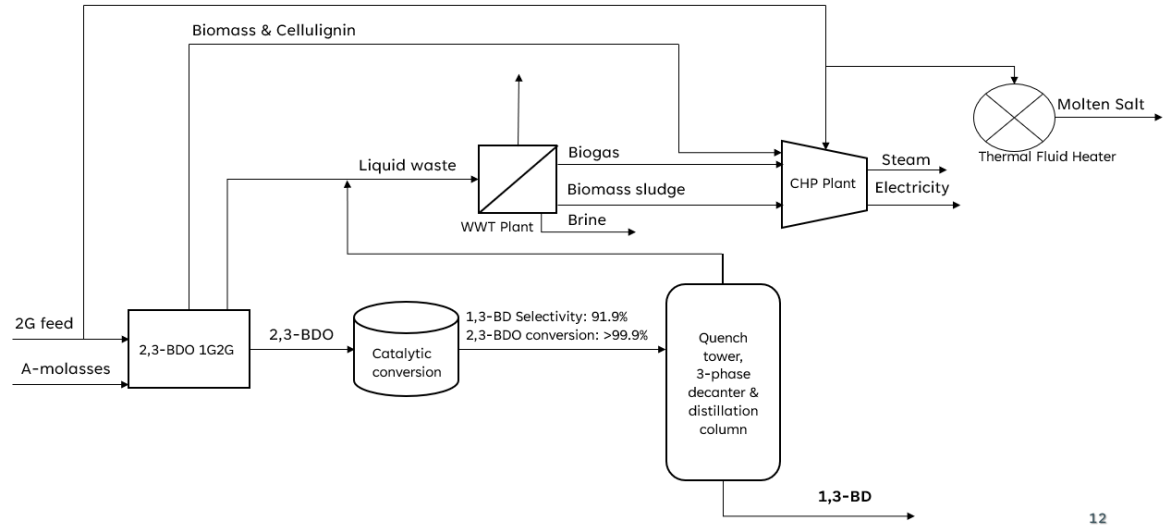

Figure 18: Scenario D Main Flowsheet

3.1.5.3 S700: 1,3-butadiene production from 2,3-butanediol

The 2,3-BDO stream from *S300* (*BDOPROD*) is heated to 401°C, prior to entering the catalytic reactor, by a number of heat exchangers optimizing energy transfer of available utilities. Initially high-pressure steam at 232°C and 28.6 bar is used to heat the stream to 222°C (*HX-01*), after which the stream exiting the catalytic reactor is used via heat integration to further heat this stream to 319°C (HX-02). The final heating to 401°C (*HX-03*), is done by using the thermal fluid, molten salt.

The dehydration of 2,3-BDO to 1,3-BD is conducted using an SiO_2-supported cesium dihydrogen phosphate catalyst at 401°C, achieving a 2,3-BDO conversion of >99.9% and 1,3-BD selectivity of 91.9%. The byproducts formed in the catalytic reactor (*CATREACT*) include methylethylketone (MEK), isobutylaldehyde (IBA), 3-butene-2-ol (3B2O), butene and 'others' (Tsukamoto *et al.*, 2016). It has been assumed that 'others' form part of butene being produced. The stoichiometric reactions with their corresponding series fractional conversions taking place in the catalytic reactor in Table 16. From

Table 16 it can be observed that one of the reactions uses hydrogen as reactant. However, it has not been reported that hydrogen is being fed to the process and therefore it has been assumed that the hydrogen is formed in the catalytic reactor, during the formation of coke (Trimm, 1999; Tsukamoto *et al.*, 2016).

Coking is a common phenomenon in catalytic reactions where a carbonaceous deposit is formed on the surface of the catalyst, producing hydrogen as a by-product (Trimm, 1999). In the simulation, a separation unit (*COKEREM*) has been added, where the coke component is removed from the stream exiting the catalytic reactor (*S1*). It is important to note that the coke will in fact have accumulated on the surface of the catalyst and will not be suspended in the stream exiting the catalytic reactor, as is the case in the Aspen Plus® simulation. Therefore, it was important to add the coke removal step to ensure that *S5* accurately represents the stream that would be leaving the catalytic reactor. The catalysts in each reactor were regenerated every five days using sparger air to burn off the coke formation. Catalyst regeneration by burning carbon deposits has previously been shown on silica-supported catalysts (Argyle & Bartholomew, 2015). Considering the regular regeneration of the catalyst it was assumed that the complete catalyst set only needed to be replaced once in the plant lifetime.

The dehydration of 2,3-BDO, the process taking place in the catalytic reactor (*CATREACT*), is a highly endothermic process (Song, 2018). To maintain the temperature of 401°C, molten salt produced in *Section 800*, is used as utility. The molten salt heating coil in the reactor (*CATREACT*) is represented by *HX-04* in Figure 19, where the heated molten salt (*T6*) from *S800*, is cooled from 555°C to 411°C (assuming a minimum temperature approach of 10°C). The heat released from *HX-04* is split (*SPLIT*), where a portion of the heat is used to heat the feed to the catalytic reactor by *HX-03* (*HX*) and another portion is used to maintain the temperature of *CATREACT (CATREAC)*. The split portions are controlled by design specifications, to ensure *S2* and *S1* are at a temperature of 401°C.

Following the catalytic reactor, the 1,3-BD needs to be separated and purified to finally obtain the saleable 1,3-BD product. The 1,3-BD separation and purification section was based on the process developed by Song, et al. (2017). The product stream from the catalytic reactor (*S5*), has a higher 1,3-BD purity compared to the downstream processing feed stream used in the study. Therefore, the design was altered to only use the specific units essential for the separation and purification of *T5* to a purity of >99% (Song, Yoon & Lee, 2017b). The essential units include a quench tower, 3-phase decanter, and distillation column.

Table 16: Stoichiometric reactions used in the catalytic reactor unit of Section 700, for Scenario C (Tsukamoto et al., 2016).

Stoichiometric Reaction	Fractional Conversion
Catalytic reactions	
$C_4H_{10}O_2\ (BDO) \rightarrow\ H_2O + C_4H_8O\ (3B2O)$	0.92
$C_4H_8O\ (3B2O) \rightarrow C_4H_6(1{,}3\_BD) + H_2O$	0.998
$C_4H_{10}O_2\ (BDO) \rightarrow\ H_2O + C_4H_8O\ (IBA)$	0.039
$C_4H_{10}O_2\ (BDO) \rightarrow\ H_2O + C_4H_8O\ (MEK)$	1
$C_4H_6 \rightarrow 4C\ (Coke) + 3H_2$	0.002
$MEK + H_2 \rightarrow C_4H_{10}O\ (methylpropanol)$	0.06
$C_4H_{10}O\ (methylpropanol) \rightarrow C_4H_8(butene) + H_2O$	1

The stream representing the product stream from the catalytic reactor (*S5*) is initially compressed to 1.37 bar (*COMP*), the required pressure of the quench tower. Thereafter the stream is cooled to 180°C, by means of heat integration, before entering the quench tower (*QUENCH*). The quench tower is simulated as a *RadFrac* unit with no condenser or reboiler, with 5 stages and a liquid pump-around loop. In the quench tower most of the water and MEK is condensed and exits at the bottom of the quench tower (*S4*), whilst most of the 1,3-BD exists as a vapor through the overhead stream (*S30*), at a temperature of 51°C. The temperature of the overhead stream is controlled by the liquid pump around loop. A portion of the bottoms stream exiting the quench tower (*S4*) is separated (*SPLIT*) into the portion (5%) of the bottoms stream sent to the wastewater treatment plant (*S15*) and the liquid pump-around stream being sent to the first stage of the quench tower (*S14*) (Song *et al.*, 2017b).

The butadiene-containing stream from the quench tower (*S30*), then goes to a 3-phase decanter (*DECANTER*), operating at a pressure of 3.43 bar (Song *et al.*, 2017b). The two liquid streams from the decanter (*S18* & *S19*) are both sent to the wastewater treatment plant, whilst the vaporous stream from the decanter (*S20*) is cooled (*HX-06*) to 44.4 °C prior to entering the final distillation column (*DISTILL*). The final distillation column (*DISTILL*) consists of 56 stages, has a distillate rate (*1,3-BD*), which ensures a 94% recovery of 1,3-BD and operates at a pressure of 3.43 bar (Song *et al.*, 2017b). The study did not specify a reflux ratio or optimal feed stage, and these were manually optimized to minimize the condenser and reboiler duty, whilst still ensuring a 1,3-BD purity of >99%.

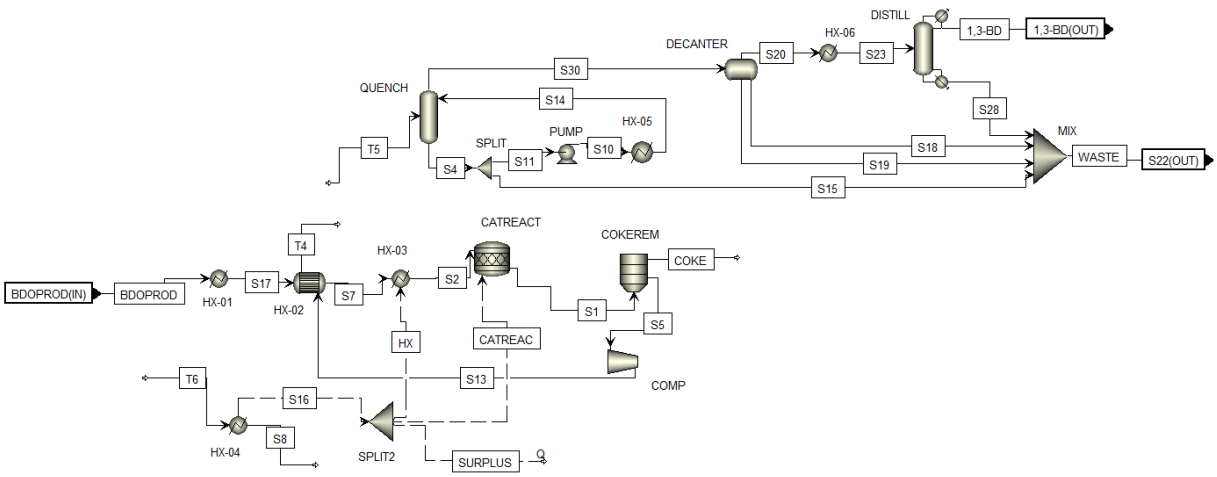

Figure 20: Scenario C and D, Section 700 flowsheet modelled in Aspen Plus®

3.1.5.4 Scenario E – 1,3-butadiene from 1G feedstock, with ethanol as intermediate product

The production of 1,3-butadiene from A-molasses (1G Feedstock) in Scenario E involves first the ethanol fermentation, whereafter ethanol is catalytically upgraded to 1,3-butadiene. The ethanol fermentation starts with an A-molasses dilution (200-220 g/L) and sterilization (*S200-1*) step after which ethanol fermentation takes place (*S200-2*) using the Melle-Boinot technique. Fermentation takes place at 30°C and uses a fermentation medium with nutrients such as urea, diammonium phosphate and ammonia (Moonsamy, 2021). Ethanol at a concentration of 100 g/L is produced in the fermentation process, along with glycerol, succinic acid and isoamyl-alcohol as by-products (Moonsamy, 2021; Ponce *et al.*, 2015). The stoichiometric reactions taking place in the fermenters, together with the series fractional

conversions can be found in Table 17. The empirical formula of *S. cerevisiae* has been assumed as $CH_{1.83}O_{0.56}N_{0.17}$ (Popovic, 2019). The ethanol fermentation process was based on the design by NREL and simulation by Moonsamy (2021), but adjusted to suit the specific biorefinery scenario as well as the conventions adopted in this study (Humbird *et al.*, 2011).

Table 17: Reactions taking place in the ethanol fermentation reactors and the corresponding fractional conversions (series reactions) specified in Aspen Plus®.

Stoichiometric Reaction	Fractional Conversion
S200-2: Ethanol Fermentation	
$C_{12}H_{22}O_{11}(Sucrose) + H_2O \rightarrow C_6H_{12}O_6(Glucose) + C_6H_{12}O_6(Fructose)$	1
$C_6H_{12}O_6(Glucose) \rightarrow 2\ C_2H_6O\ (Ethanol) + 2\ CO_2$	0.905
$C_6H_{12}O_6(Fructose) \rightarrow 2\ C_2H_6O\ (Ethanol) + 2\ CO_2$	0.905
$0.6\ C_6H_{12}O_6 + 0.5\ H_2O \rightarrow C_3H_8O_3\ (Glycerol) + 0.55\ CO_2$	0.28
$C_6H_{12}O_6 + 0.8571\ CO_2 \rightarrow 1.7142\ C_4H_6O_4\ (Succinic\ Acid) + 0.8571\ H_2O$	0.042
$5\ C_6H_{12}O_6 \rightarrow 4\ C_5H_{12}O\ (Isoamyl-alcohol) + 6\ H_2O + 10\ CO_2$	0.181
$C_6H_{12}O_6 + 0.971\ NH_3 \rightarrow 5.72\ CH_{1.83}O_{0.56}N_{0.17}\ (S.cerevis) + 2.23\ H_2O + 0.286\ CO_2$	0.255

The emissions from the fermenter in *S200-2*, the biomass separated from the fermentation broth in *S200-2* and the ethanol fermentation broth are all sent to ethanol separation and purification (*S300-1*). In *Section 300-1*, a purified ethanol stream at 92.5 wt.% is produced, which is sent for further catalytic upgrading. Furthermore, a solid-liquid stream from *S300* is sent to a pressure filter (*S300-2*) where a solid and liquid waste stream are produced, the former of which is set to the CHP plant for combustion and the latter of which is sent to the WWT plant. In Figure 21 the basic flowsheet of Scenario E is illustrated. A screenshot of the main flowsheet in Aspen Plus® is given in Appendix C.

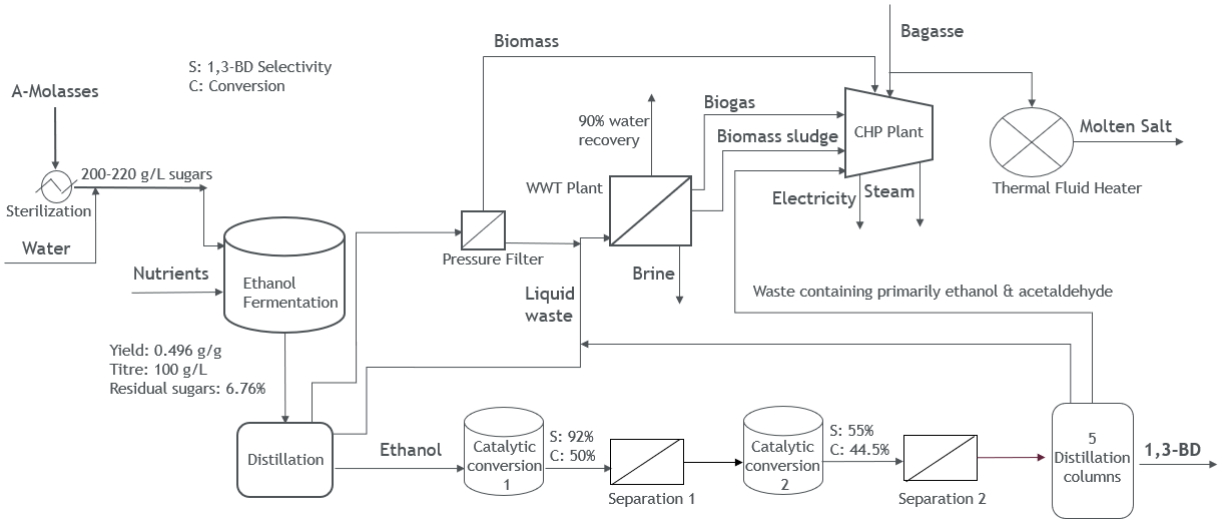

Figure 21: Scenario E Main Flowsheet

The purified ethanol from *S300-1*, is sent to the first catalytic upgrading step (*S700-1)*, after which the product of this section undergoes vapor-liquid separation in *S700-2.* The vapor stream is sent to the CHP plant and the liquid stream is sent to the second catalytic upgrading step (*S700-3*). The product from *S700-3* is sent to *S700-4*, where a vapour and liquid stream is produced, both of which are sent to the final 1,3-BD separation and purification step further downstream (*S700-5).* The purpose of *S700-4*, is to

adjust the vapour fraction of the feed to *S700-5*, where a set of distillations columns are used to produce the final 1,3-BD product at a purity of >98% (Burla *et al.*, 2012; Farzad, Mandegari & Görgens, 2017). The 1,3-BD production from ethanol is based on the process designed by Burla et al. (2012) and simulated by Farzad, et al. (2017), yet adjusted to suit the specific biorefinery scenario as well as the conventions adopted in this study.

The catalytic upgrading processes in both *S700-1* and *S700-3* are highly endothermic processes, taking place at high temperatures and require molten salt as heating utility. Bagasse is sent to the CHP plant for steam and electricity generation, and to the thermal fluid heater to produce molten salt.

3.1.5.5 Scenario F – 1,3-Butadiene from 1G2G feedstock, with Ethanol as intermediate product

The production of 1,3-butadiene from 1G2G feedstock in *Scenario F* involves fermentation to ethanol, whereafter ethanol is catalytically upgraded to 1,3-Butadiene, similar to *Scenario E*. The processing of A-molasses to ethanol i.e., *S200-1* and *S200-2*, is similar to what has been described for *Scenario E*. The second-generation feedstock however is processed separately to produce ethanol. The *2GFEED* stream is divided into three streams, one going to the thermal fluid heater (*S800*), another going to the CHP plant (*S500-1*) and finally the largest portion going to the pre-treatment (*S100-2*). The pre-treatment method used in *Scenario F* is an SO_2-catalysed steam pre-treatment process, where the SO_2 is produced on-site in *S100-1.*

In the pre-treatment section (*S100-2*), the hemicellulose hydrolysate and solid cellulignin portions are not separated from one another; this is because co-fermentation of xylose and glucose takes place in the 2G fermentation section (*S200-4*). Of the total stream produced during pre-treatment, a portion is sent to the 2G seed train (*S200-3*) for *S. cerevisiae* growth, whilst the remainder is sent to *S200-4* for separate hydrolysis and co-fermentation (SHcF). In this biorefinery scenario enzymatic hydrolysis does not take place directly after pretreatment, but instead takes place just before co-fermentation where xylose and glucose are both utilized to produce ethanol. The second-generation (2G) feedstock, separate hydrolysis and co-fermentation (SHcF) section is also based on a previously developed ethanol production process from 1G2G feedstock and adjusted accordingly (Moonsamy, 2021). The stoichiometric reactions and associated fractional conversions taking place in the 2G co-fermentation reactor is specified in Table 18.

Table 18: Stoichiometric reactions used in the fermentation reactor in Section 200-4, for Scenario F (Moonsamy, 2021).

Stoichiometric Reaction	Fractional Conversion
Ethanol Fermentation	
$C_6H_{12}O_6(Glucose) \rightarrow 2\ C_2H_6O\ (Ethanol) + 2\ CO_2$	0.905
$C_6H_{12}O_6(Fructose) \rightarrow 2\ C_2H_6O\ (Ethanol) + 2\ CO_2$	0.8
$C_{12}O_{22}H_{11} + H_2O \rightarrow\ C_6H_{12}O_6\ (Fructose) + C_6H_{12}O_6\ (Glucose)$	1
$3\ C_5H_{10}0_5\ (Xylose) \rightarrow 5\ C_2H_6O\ (Ethanol) + 5\ CO_2$	0.8
Microbial Growth	
$C_6H_{12}O_6 + 0.9712\ NH_3 \rightarrow 5.714\ CH_{1.83}O_{0.56}H_{0.17} + 2.229\ H_2O + 0.286\ CO_2$	0.085
$C_5H_{10}O_5 + 0.81\ NH_3 \rightarrow 4.76\ CH_{1.83}O_{0.56}H_{0.17} + 1.857\ H_2O + 0.238\ CO_2$	0.0425

The remainder of the production process is similar to what has been described for Scenario E. In Figure 22 the basic flowsheet of Scenario E is illustrated. A screenshot of the main flowsheet in Aspen Plus® is given in Appendix C.

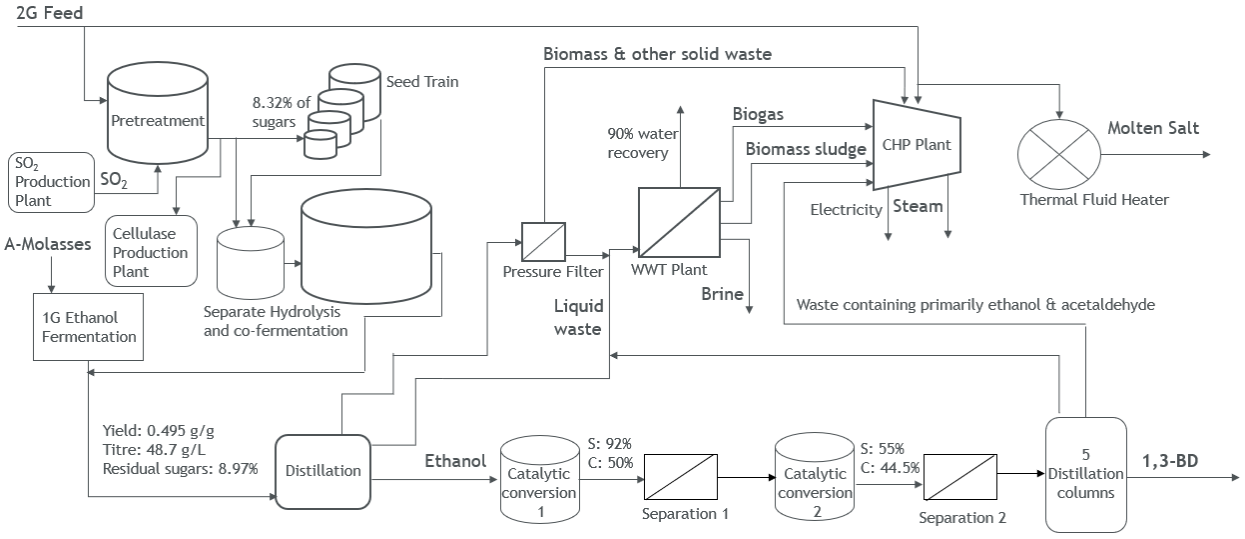

Figure 22: Scenario F Main Flowsheet

3.1.5.6 Section 300-1: Ethanol Separation and Purification

The ethanol separation and purification section, mainly consists of two distillation columns and a water scrubber. The fermentation broth and biomass solids from *S200-2* (*FERMBRTH* & *BIOMASS*), are mixed (*MIX-01*) with the bottoms stream of the water scrubber (*S6*), and pumped at a pressure of 4 atm, to the first distillation column (*DISTILL1*)(Moonsamy, 2021). The feed to *DISTILL1* (*S9*), initially passes through a number of heat exchangers (*HX-01*, *HX-05* & *HX-06*), as part of the heat integration network of the process, where other heated streams from within the process are used to heat the feed stream to approximately 100°C (Humbird *et al.*, 2011; Moonsamy, 2021).

The first distillation column operates at a pressure of 2 atm, contains 20 stages with the feed stage at 2 and the product stage drawn from stage 3, and finally a molar reflux ratio of 3 (Moonsamy, 2021). The product stream (*S13*) and distillate rate or overhead stream (*S11*) have both been determined by calculator blocks in Aspen Plus®, ensuring >99% ethanol recovery at a purity of 40% to *S13* and a complete recovery of CO_2 at a purity of 85%, to *S11* (Humbird *et al.*, 2011). The product stream is sent to the second distillation column (*DISTILL2*) for further purification, whilst the overhead stream, containing most of the CO_2, is sent to the water scrubber (*VENTSCRU*). Furthermore, the bottoms stream of *DISTILL1* (*S14*) is used as part of the heat integration network, prior to being sent to the pressure filter (*S300-2*) for solids-liquid separation.

The second and final distillation column operates at a pressure of 1.6 atm, consists of 41 stages, with a molar reflux ratio of 1 and a bottoms to feed ratio of 0.1 (Moonsamy, 2021). A portion of the overhead stream from *DISTILL2* (*S5*) is recycled back to the distillation column to achieve an overhead product purity of 92.5 wt% ethanol (Humbird *et al.*, 2011). The feed stream from DISTILL1 enters column 2 at

stage 14, whilst the recycle stream enters at stage 6. Furthermore, the split fraction in *SPLIT* was determined by means of a design specification in Aspen Plus®, where a final ethanol product stream, with a purity of 92.5% (*ETHANOL*), is produced. The final ethanol product is sent further downstream for catalytic upgrading to 1,3-BD, whilst the bottoms stream of *DISTILL2* (*S6*) is sent to the WWT plant (*S400*).

The feed to the water scrubber (vent scrubber) consists of the overhead stream from *DISTILL1* (*S11*), as well as the vented emissions from the ethanol fermenters in *S200-2* (*VENT*). The feed streams are mixed (*MIX-02*), compressed to 2.5 atm (*COMP*) and cooled to 35°C, by cooling water (*HX-03*) and chilled water (*HX-02*) prior to being sent to the vent scrubber. The amount of feed water to the scrubber (*H2O*), required to recover >99% ethanol at a purity of 1.8% to the scrubber bottoms (*S6*), is controlled by a design specification in Aspen Plus® (Humbird *et al.*, 2011).

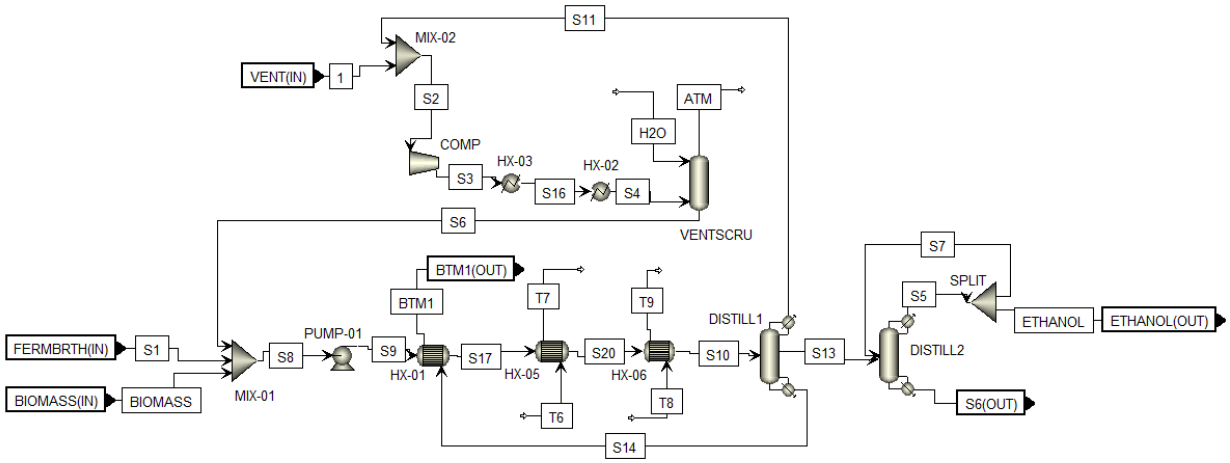

Figure 23: Scenario E & F, Section 300-1 flowsheet modelled in Aspen Plus®

3.1.5.7 Section 300-2: Pressure Filter

The purpose of the pressure filter is to separate the bottoms stream (*BTM1*) from DISTILL 1 in Figure 23 into the solids stream (*S8*), to the CHP plant, and the liquid stream (*S9*), to the WWT plant. In Aspen Plus®, the pressure filter has been simulated by first sending the stream *BTM1*, through a splitter, where 98.55% solids is separated to *S2* and 96.27% of the liquid stillage is separated to *S3* (Humbird *et al.*, 2011). The liquid stillage is then used in the heat integration network to be cooled prior to being pumped downstream. Furthermore, the solids stream (*S2*) is then dried (*FLASH*) using compressed (COMP) air at 9.5 atm (Moonsamy, 2021), to a final solids stream (*S8*), with a moisture content of 35% (Humbird *et al.*, 2011).

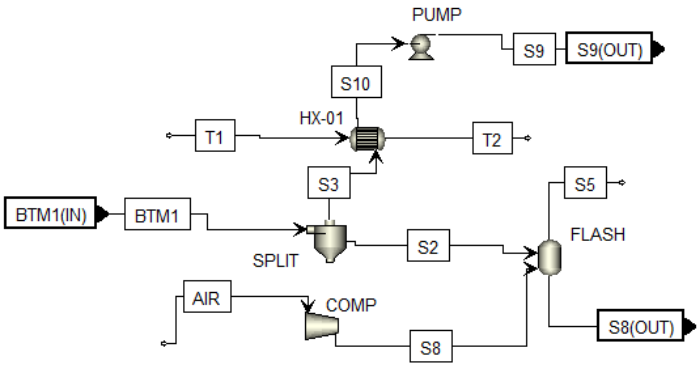

Figure 24: Scenario E & F, Section 300-2 flowsheet modelled in Aspen Plus®

3.1.5.8 Section 700-1: First Catalytic Upgrading Step

In the first catalytic upgrading step, ethanol is upgraded to acetaldehyde, whilst producing hydrogen as a by-product. The feed to the first set of catalytic reactors (*ETH*), is compressed to 3.4 atm (50 psi) (*COMP*) and heated to the optimal temperature of the first catalytic upgrading step, 312°C (595°F), using two heat exchangers. The first heat exchanger (*HX-01*) forms part of the heat integration network of the process, where the outlet of the first set of catalytic reactors (*CAT1*) are used to heat the feed stream (*S2*), and the second heat exchanger (*HX-02*) uses the thermal fluid, molten salt, as utility (Burla *et al.*, 2012).

The catalytic reactors are a set of three shell-and-tube, packed bed reactors, operating at optimal temperature and a pressure of 2.4 atm (35 psi). The catalyst used for the first catalytic upgrading step is a heterogeneous copper-chromite catalyst (Burla *et al.*, 2012). The stoichiometric reactions taking place in the reactor as well as parallel fractional conversions can be found in Table 19 (Farzad, Mandegari & Görgens, 2017). The three reactors have been simulated in Aspen Plus® as one *RStoic* unit, with molten salt as the heating utility. Furthermore, the stream exiting the catalytic reactor (S4) is used in the heat integration network and further cooled to 67°C (152°F) , prior to being sent to the first 1,3-BD separation step (*S700-2*).

Table 19: Reactions taking place in the first set of catalytic reactors and the corresponding fractional conversions (parallel reactions) specified in Aspen Plus® for Scenario E & F (Farzad, Mandegari & Görgens, 2017).

Stoichiometric Reaction	Fractional Conversion
S700-1: First Catalytic Upgrading Step	
$C_2H_6O\ (Ethanol) \rightarrow C_2H_4O\ (Acetaldehyde) + H_2$	0.46
$C_2H_6O \rightarrow CO + CH_4 + H_2$	0.00375
$C_2H_6O + H_2O \rightarrow CO_2 + CH_4 + 2\ H_2$	0.00375
$C_2H_6O + H_2O \rightarrow C_2H_4O_2(Acetic\ Acid) + 2\ H_2$	0.0125
$2\ C_2H_6O \rightarrow C_4H_{10}O\ (Diethyl - Ether) + H_2O$	0.0125
$C_2H_6O + C_2H_4O_2 \rightarrow C_4H_8O_2\ (Ethyl - Acetate) + H_2O$	0.0075

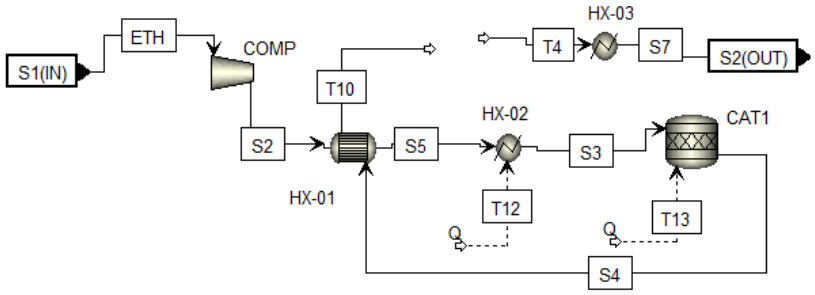

Figure 25: Scenario E & F, Section 700-1 flowsheet modelled in Aspen Plus®

3.1.5.9 Section 700-2: First 1,3-BD Separation Step

In the first 1,3-BD separation step, the aim is to separate the vaporous components (*S14*), which is sent to the CHP plant, from the liquid components (*S3*), to be used for further catalytic upgrading downstream. The process consists of two compressors, operating at 4 atm (60 psi) (*COMP-01*) and 10.5 atm (155 psi) (*COMP-02*) respectively, two heat exchangers, both operating at 42°C (108°F) (*HX-01* & *HX-02*), two pumps, both operating at 10.5 atm (155 psi) (*PUMP-01* & *PUMP-02*) and finally three flash drums at zero duty (*FLASH-01*, *FLASH-02* & *FLASH-03*)(Burla *et al.*, 2012).

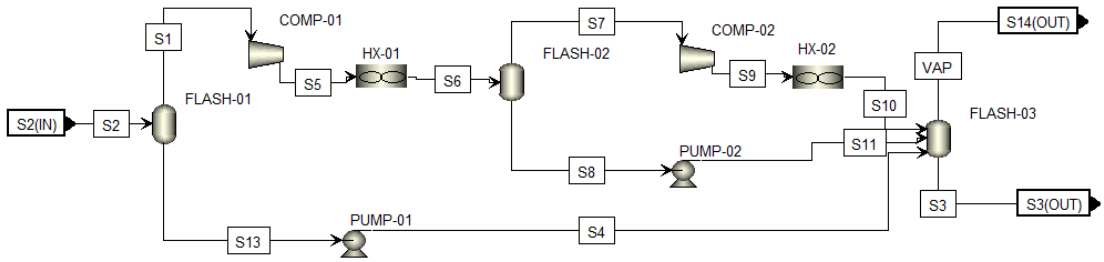

Figure 26: Scenario E & F, Section 700-2 flowsheet modelled in Aspen Plus®

3.1.5.10 Section 700-3: Second Catalytic Upgrading Step

In the second and final catalytic upgrading process, ethanol and acetaldehyde are converted to 1,3-butadiene. The feed to the second set of catalytic reactors consists of the separated liquid stream from *S700-2* (*S3*), a portion of the purified ethanol stream produced in *S300-1* (*MAKE-UP*), and the two recycled streams from the final 1,3-BD separation and purification section further downstream (*ETH* & *ACET*). The amount of ethanol make-up stream added to the second set of catalytic reactors, is controlled by a design specification, to ensure a molar ratio of 2.75:1 ethanol-to-acetaldehyde is achieved in the mixed feed stream (*S1*)(Burla *et al.*, 2012).

The mixed feed stream is heated by two heat exchangers part of the heat integration network of the process (*HX-01* &*HX-03*) and a final heat exchanger, using molten salt as heating utility, to a temperature of 350°C, prior to entering the set of catalytic reactors. Similar to the first set of catalytic reactors in *S700-1*, the catalytic reactors in this section are a set of three shell-and-tube, packed bed reactors, simulated in Aspen Plus® using an *RStoic* unit, with molten salt as the heating utility. The catalyst used for the second catalytic upgrading step is a heterogeneous tantala-silica catalyst, with optimal operating conditions of 6.4 bar and 350°C (Burla *et al.*, 2012). The stoichiometric reactions taking place in the catalytic reactors (*CAT2*), can be found in Table 20 (Farzad, Mandegari & Görgens, 2017). The catalyst in

each reactor were regenerated every five days by sparging with air. The deactivation of a catalyst caused by coke formation is easily reversed by burning the deposits with oxygen (Argyle & Bartholomew, 2015; Burla *et al.*, 2012).

Table 20: Reactions taking place in the second set of catalytic reactors and the corresponding fractional conversions (parallel reactions) specified in Aspen Plus® for Scenario E & F (Farzad, Mandegari & Görgens, 2017).

Stoichiometric Reaction	Fractional Conversion
S700-3: Second Catalytic Upgrading Step	
$C_2H_6O\ (Ethanol) + C_2H_4O\ (Acetaldehyde) \rightarrow C_4H_6\ (1,3-BD) + 2\ H_2O$	0.24475
$2\ C_2H_6O \rightarrow C_4H_{10}O\ (N-Butanol) + H_2O$	0.02225
$2\ C_2H_6O \rightarrow\ C_4H_{10}O\ (Diethyl-Ether) + H_2O$	0.089
$C_2H_6O \rightarrow C_2H_4(Ethylene) + H_2O$	0.0445
$2\ C_2H_6O\ \rightarrow C_4H_8\ (cis-2-butene) + 2\ H_2O$	0.02225
$C_2H_6O + C_2H_4O + C_2H_4 \rightarrow C_6H_{10}\ (1,5-Hexadiene) + 2\ H_2O$	0.02225
$2\ C_2H_4O\ \rightarrow C_4H_8O_2\ (Ethyl-Acetate)$	0.09

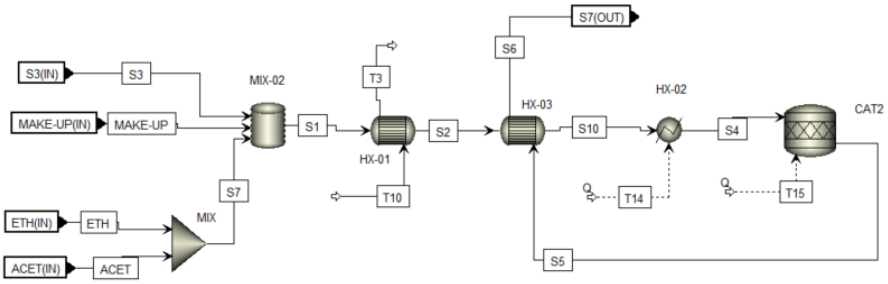

Figure 27: Scenario E & F, Section 700-3 flowsheet modelled in Aspen Plus®

3.1.5.11 Section 700-4: Second 1,3-BD Separation Step

In the second 1,3-BD separation step, the aim is to obtain a feed to the final 1,3-BD separation and purification section (*S700-5*), with a temperature of 93.3°C and a pressure of 8.6 bar. The process consists of two flash drums with zero duty (*FLASH-01* & *FLASH-02*), two pumps, both operating at 8.6 bar (*PUMP-01* & *PUMP-02*), two heat exchangers, both operating at 93.3°C (*HX-01* & *HX-02*) and finally a compressor operating at 9.2 bar (Burla *et al.*, 2012). Both the vapour and liquid streams (*VAP* & *LIQ*) produced in this section, are sent to *S700-5* as feed.

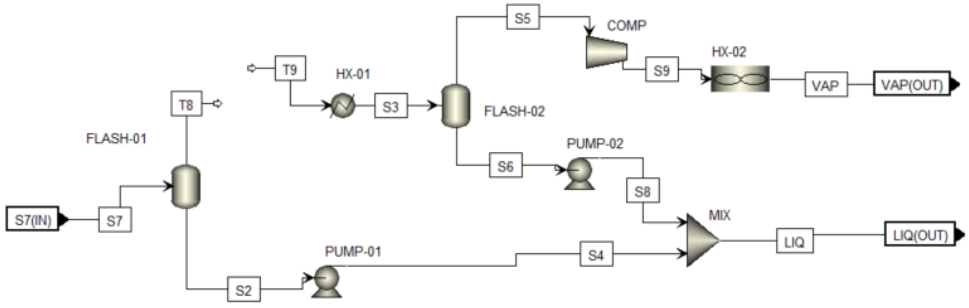

Figure 28: Scenario E & F, Section 700-4 flowsheet modelled in Aspen Plus®

3.1.5.12 Section 700-5: Final 1,3-BD Separation and Purification

The final 1,3-BD separation and purification section, consist of five distillation columns and one decanter, with the configuration evident in Figure 29. The number of stages, the feed stage of each column as well as pressure of the various columns were obtained from the simulation of Farzad, et al. (2017) as well as literature (Burla *et al.*, 2012). For the most part, the outcomes of each distillation column were obtained from Burla, et al. (2012); however, when there were inconsistencies or the outcomes were not clearly stated the simulation developed by Farzad, et al. (2017) was consulted. The design specifications, calculator blocks and parameters inserted for each of the 5 distillation columns in Aspen Plus®, will not be discussed in detail, instead a short list of the key outcomes will be given.

1. Distillation column 1: 1,3-Butadiene to the overhead stream at a 99.5% recovery at 92%wt purity.
2. Distillation column 2: 1,3-Butadiene to the bottoms stream at a >92% recovery at >96%wt purity.
3. Distillation column 4: 60% overall acetaldehyde recovery to the overhead stream.
4. Distillation column 5: Approx. 98% overall ethanol recovery to the overhead stream.

The various streams produced in the five distillation column, one decanter configuration, is the final 1,3-BD product stream at a purity >98% (*1,3-BD*), a predominantly acetaldehyde stream being recycled to S700-3 (*ACET*), a predominantly ethanol stream also being recycled to S700-3 (*ETH*) and two waste streams, one of which is sent to the CHP plant for combustion (*S16*) and the other sent to the wastewater treatment plant (*S17*).

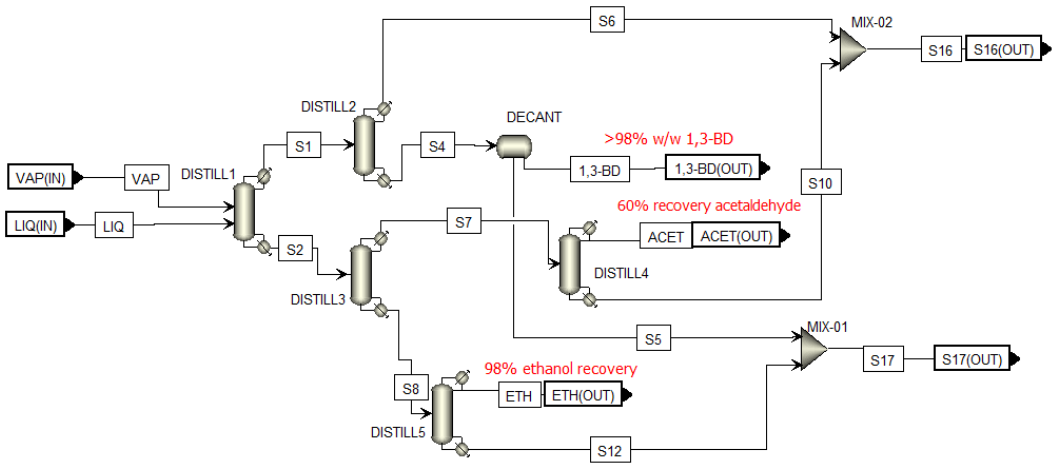

Figure 29: Scenario E & F, Section 700-5 flowsheet modelled in Aspen Plus®

3.1.6 Polyhydroxybutyrate (Scenario G and H)

3.1.6.1 Scenario G – Polyhydroxybutyrate from 1G feedstock

In Figure 30 the basic flowsheet of Scenario G is illustrated. A screenshot of the main flowsheet in Aspen Plus® is given in Appendix C. The production of polyhydroxybutyrate from A-molasses (1G feedstock) consisted of various steps, including the dilution, sterilization and hydrolysis of A-molasses (*S200-1,1*), sterilization of the fermentation medium (*S200-1,2*), seed train (*S200-2,1*), fermentation (*S200-2,2*), PHB separation and purification (*S300*) and utility sections used in all other scenarios such as the wastewater

treatment plant (*S400*) and other utilities (*S600*). In this scenario only the CEST section was simulated, where the available 15 t/h HPS (@360°C and 28.6 bar) from the existing sugar mill boiler, is used as feed to the CEST to produce MPS, LPS and electricity.

It is important to note that for this scenario a gas engine formed part of the other utilities (*S600*). Due to the low energy requirements of this scenario only additional electricity (and not steam) was required and the gas engine was included in the design, instead of a new CHP plant. The gas engine makes use of a portion of the biogas produced in the wastewater treatment plant (*S400*) to generate electricity. Similar to the remainder of the other utilities making up Section 600 in all scenarios, the gas engine was not simulated but merely accounted for in the techno-economic analysis. The remainder of the biogas and the biomass sludge produced in the wastewater treatment plant was emitted to the atmosphere and sent to municipal wastewater treatment respectively.

The seed train and fermentation reactors operate at a temperature of 37°C, with an aeration rate of 0.5 vvm, producing a fermentation broth containing 39.5 g/L biomass using *E.coli*, of which 80% is intracellular polyhydroxybutyrate (PHB), at a PHB productivity of 1 g/(L.h) (Kachrimanidou, Ioannidou, Ladakis, *et al.*, 2021; Liu *et al.*, 1998). The choice of microorganism employed for fermentation was majorly based on the ease of separation and purification from *E. coli*. The stoichiometric reactions used in the growth phase and synthesis phase reactors can be found in Table 21. It is important to note that both glucose and fructose are utilized equally for both cell growth, PHB and by-product formation. However, to simplify mass balancing and stoichiometric reactions it was assumed that only fructose was utilized for PHB production and only glucose was utilized for cell growth and by-product formation, keeping in mind that the residual sugars (70 g/L) at the end of fermentation consists of both fructose and glucose. The seed train and fermentation medium predominantly consist per L^{-1} of: $Na_2HPO_4 \cdot 12H_2O$ ***4.8 g***, KH_2PO_4 ***2.65 g***, $(NH_4)_2SO_4$ ***4 g*** and $MgSO_4 \cdot 7H_2O$ ***0.3 g*** (Liu *et al.*, 1998).

The fermentation broth produced in *S200-2* is sent to *S300* for separation and purification of PHB, where PHB is produced at a recovery of 97% and purity of >99% (Choi & Lee, 1999c; Nieder-Heitmann, 2019). The liquid waste stream produced during PHB separation and purification is sent to *S400* for wastewater treatment.

Table 21: Stoichiometric reactions and fractional conversions (series) used in the growth and synthesis phase reactors of PHB production from first-generation feedstock (Liu *et al.*, 1998; Nieder-Heitmann, 2019; Popovic, 2019).

Stoichiometric Reaction	Fractional Conversion
$C_6H_{12}O_6(Fructose) + 1.5\ O_2 \rightarrow C_4H_6O_2\ (PHB) + 2\ CO_2 + 3\ H_2O$	0.63
$C_6H_{12}O_6(Glucose) + 2\ O_2 \rightarrow 2\ C_2H_4O_2\ (Acetic\ Acid) + 2\ CO_2 + 2\ H_2O$	0.48
$C_6H_{12}O_6 + 0.8206\ NH_3 + 1.897\ O_2 \rightarrow 3.73\ CH_{1.740}O_{0.340}N_{0.220} + 3.9859\ H_2O + 2.2702\ CO_2$	0.31

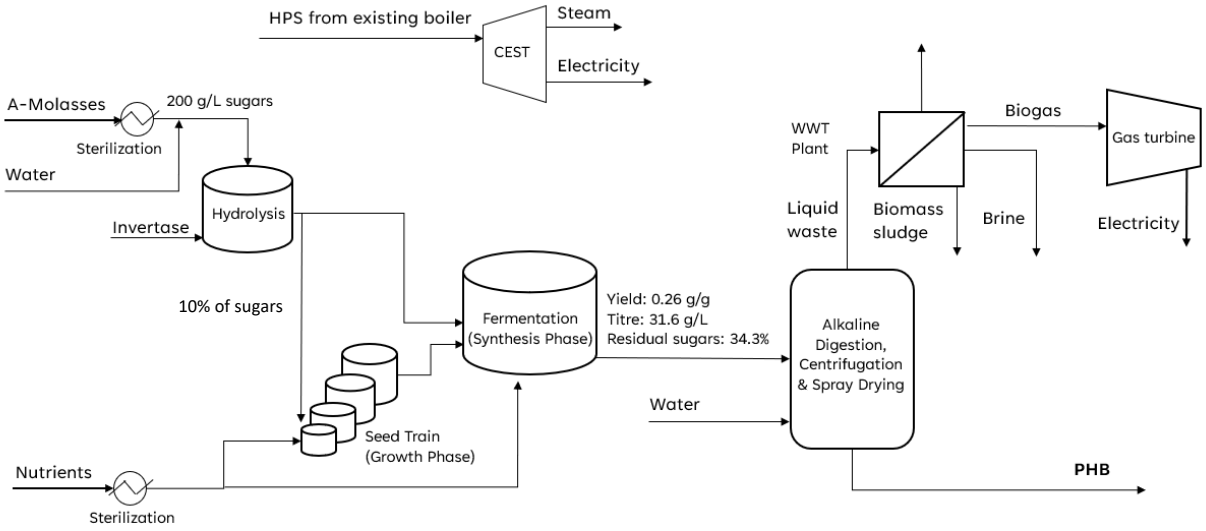

Figure 30: Scenario G Main Flowsheet

3.1.6.2 Scenario H – Polyhydroxybutyrate from 1G2G feedstock

The production of PHB from 1G2G feedstock consist of all sections described for *Scenario G*, with only two additional sections. The first additional section is dilute acid pre-treatment and enzymatic hydrolysis of the 2G feedstock (*S100-1*). The glucose-rich stream produced from these steps is mixed with the 1G feedstock, A-molasses and fermented together. The hemicellulose hydrolysate is sent to the WWT plant. Further processing to produce, separate and purify PHB (*S200-1*, *S200-2* and *S300*) are all similar to which has been described for *Scenario G*. The other additional section is the boiler section part of the CHP (*S500-1*). Furthermore, the gas engine, part of the *Scenario G* design has been omitted in the design of *Scenario H* because a new CHP plant was added to the process to produce the required electricity and steam. In Figure 31 the basic flowsheet of Scenario H is illustrated. A screenshot of the main flowsheet in Aspen Plus® is given in Appendix C.

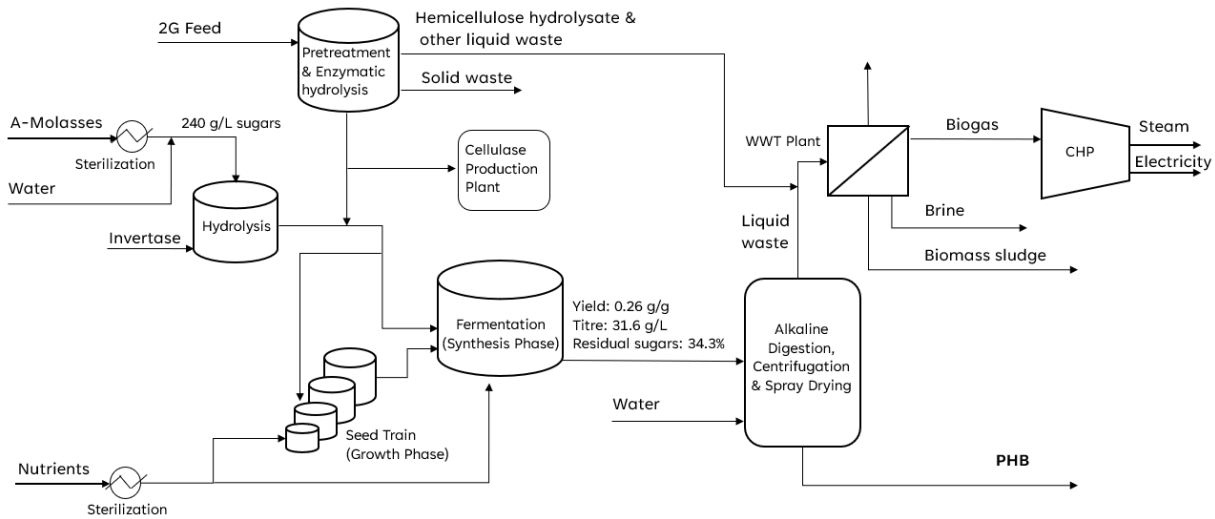

Figure 31: Scenario H Main Flowsheet

Dilute acid pretreatment was employed in this scenario, using a 0.65% sulphuric acid solution to modify the structure of the lignocellulosic material at a temperature of approx. 180°C and a pressure of approx. 10 bar (Nieder-Heitmann, 2019). The dilute acid solution is prepared and combined with the 2G feedstock in *MIX-01*, after which it is pumped to the pretreatment reactor (*PRETREAT*). Pretreatment takes place at a temperature and pressure of 178.1°C and 9.5 atm respectively. The stoichiometric reactions and associated fractional conversions can be found in Table 22. This pre-treatment method was chosen considering only glucose is used during fermentation and glucose formation is prioritized with dilute acid pre-treatment.

Table 22: Stoichiometric reactions and fractional conversions (parallel) used in pre-treatment reactor of Scenario H (Nieder-Heitmann, 2019).

Stoichiometric Reaction	Fractional Conversion
$Cellulose + H_2O \rightarrow Glucose$	0.043
$2\ Cellulose + H_2O \rightarrow Cellobiose$	0.003
$Cellulose + H_2O \rightarrow 3Acetic\ Acid$	0.219
$Cellulose \rightarrow HMF + 2\ H_2O$	0.003
$Xylan + \ H_2O \rightarrow Xylose$	0.731
$Xylan \rightarrow Furfural + 2H_2O$	0.08
$Arabinan + H_2O \rightarrow Arabinose$	0.812

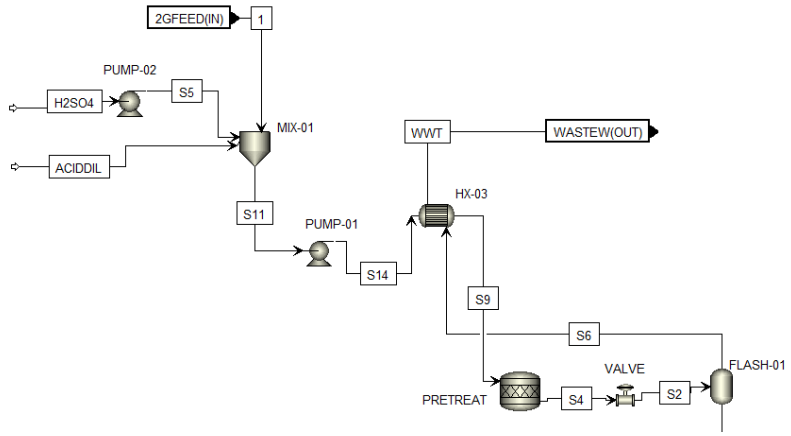

Figure 32: Scenario H, Section 100-1 flowsheet modelled in Aspen Plus®

3.1.6.3 Section 300: Polyhydroxybutyrate (PHB) Separation and Purification

A similar purification and separation process was developed and simulated for Scenario G and H. Initially the fermentation broth (*FERMBRTH*) is centrifuged (*CENTRF*) to separate a large portion of the fermentation broth (*S6*) from the *E. coli* cells containing the intracellular PHB. The stream containing the cells (*S7*) are then resuspended in recycled water (*DILUTW*) to a concentration of 50 g/L, required for alkaline digestion. During alkaline digestion the cells are mixed with 0.2 M NaOH to digest the non-PHB cellular components of the *E. coli* cells in a reactor operating at 37°C (*BLEND*) (Choi & Lee, 1999c). To separate the PHB granules from the aqueous component containing the digested cellular components, the solution is again centrifuged (*CENTRF2*), rinsed with recycled water (*RINSEW*) to remove all residual

sugars and NaOH from the solution containing the PHB granules and finally air dried (Lee, Choi, Han, *et al.*, 1999).

The PHB solution (*S19*) containing between 20-30% solids are sent to a spray dryer (*SPRAYDR*). According to literature, the solids content can range between 20% and 70%, although in Aspen Plus® the maximum limit of the *SPRAY* unit is 30% (Inc., 2005). The spray dryer (*SPRAYDR*) and dehumidified air amount was scaled and designed according to literature (Nieder-Heitmann, 2019). The air is dehumidified using *HX-02*, *FLASH-03* and *COMP*, similar to what has been described in *Section 100-1: SO2 Production* of *Scenario B*. Following a spray dryer, a cyclone usually follows to separate the dry PHB and vapour particles (Inc., 2005). In the simulation, due to limitations in Aspen Plus® a flash drum (*FLASH-02*) was added to represent the vaporization and separation that would have taken place.

3.1.7 Citric Acid (Scenario I and J)

3.1.7.1 Scenario I – Citric Acid from 1G feedstock

The production of citric acid from A-molasses consists of various steps which include dilution and sterilization of A-molasses and the fermentation medium (*S200-1,1*), separate dilution of the seed train medium (*S200-1,2*), a seed train for the growth of *A. niger* GCB-75 (*S200-2,1*), citric acid fermentation (*S200-2,2*) and separation and purification (*S300*). Additional sections in the process include wastewater treatment (*S400*), the combined heat and power plant (*S500-1 & S500-2*) and other utilities (*S600*). In Figure 34 the basic flowsheet of Scenario I is illustrated. A screenshot of the main flowsheet in Aspen Plus® is given in Appendix C.

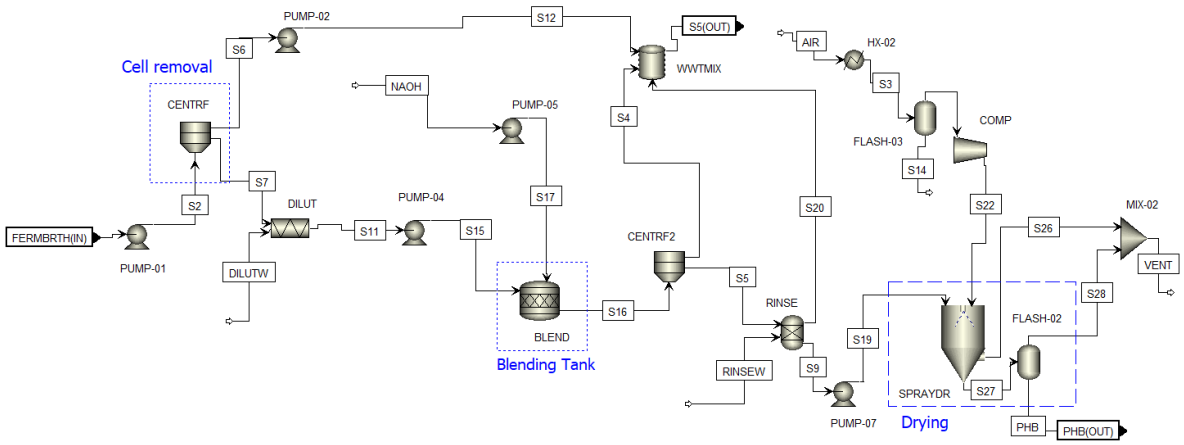

Figure 33: Scenario G & H, Section 300 flowsheet modelled in Aspen Plus®

Following dilution and sterilization to 150 g/L sugars the A-molasses is sent to *S200-2* for microbial growth in the seed train and citric acid fermentation (Ikram-Ul *et al.*, 2004). The fermentation medium primarily consists of NH_4NO_3 and after 6 hours of fermentation, $2X10^{-5}$ M of $MgSO4{\cdot}5H_2O$ is added, which aids in achieving a high citric acid titre of 113.6 g/L (Ikram-Ul *et al.*, 2004). However, due to limitations of the Aspen Plus® software this fermentation-aiding compound was added together with the rest of the fermentation medium. In the techno-economic analysis the correct amount used by the process was accounted for.

Both the seed train and fermentation reactors operate at a temperature of 30 °C , with an aeration rate of 0.5 vvm (Ikram-Ul *et al.*, 2004; Kachrimanidou *et al.*, 2021) Reactions taking place in the citric acid fermenters can be found in Table 23. Considering *A. niger* utilizes glucose at a slightly better rate compared to fructose in a glucose-fructose mixture, it was assumed that all glucose was consumed and all residual sugars consisted of fructose (Bizukojc & Ledakowicz, 2004). The fermentation broth is sent to *S300* for separation and purification of citric acid, with a recovery and purity of 84.9% and >99.8% respectively.

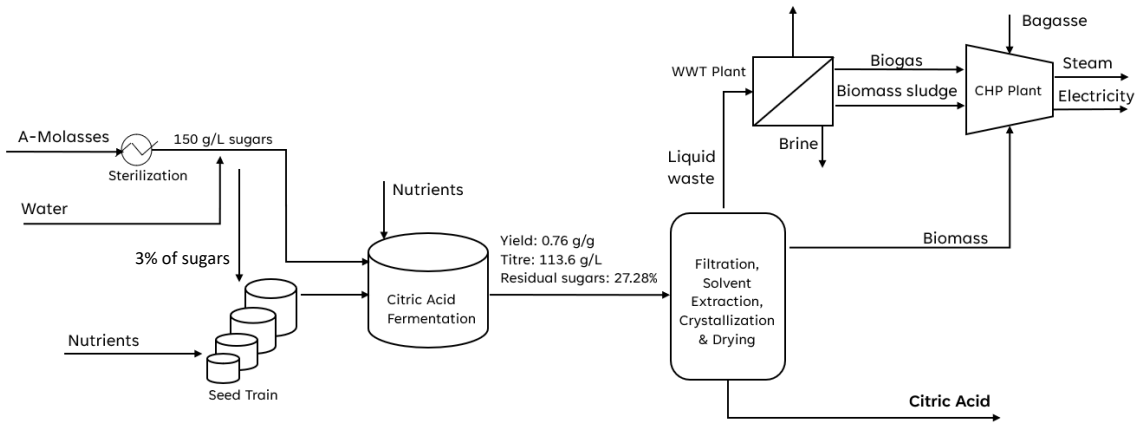

Figure 34: Scenario I Main Flowsheet

Table 23: Stoichiometric reactions occurring in series and corresponding fractional conversions used in the reactors of S200-2 and S200-3 for Scenario I (Ikram-Ul et al., 2004).

Stoichiometric Reaction	Fractional Conversion
Aspergillus niger Seed Train	
$C_{12}H_{22}O_{11}(Sucrose) + H_2O \rightarrow C_6H_{12}O_6(Glucose) + C_6H_{12}O_6(Fructose)$	1
$C_6H_{12}O_6 + 0.5636\ NH_3 + 0.0817\ O_2 \rightarrow 5.6364\ CH_{1.6}O_{0.55}N_{0.1} + 2.3364\ H_2O + 0.3635\ CO_2$	0.9576
Fermentation	
$C_{12}H_{22}O_{11}(Sucrose) + H_2O \rightarrow C_6H_{12}O_6(Glucose) + C_6H_{12}O_6\ (Fructose)$	1
$C_6H_{12}O_6(Glucose) + 1.5\ O_2 \rightarrow C_6H_8O_7 \cdot H_2O\ (Citric\ acid\ monohydrate) + H_2O$	0.8299
$C_6H_{12}O_6\ (Fructose) + 1.5\ O_2 \rightarrow C_6H_8O_7 \cdot H_2O\ (Citric\ acid\ monohydrate) + H_2O$	0.4738
$C_6H_{12}O_6 + 0.5636\ NH_3 + 0{,}0817\ O_2 \rightarrow 5.6364\ CH_{1.6}O_{0.55}N_{0.1} + 2.3364\ H_2O + 0.3635\ CO_2$	1

3.1.7.2 Scenario J – Citric Acid from 1G2G feedstock

The production of Citric Acid from integrated 1G2G feedstock consist of various steps including pretreatment and enzymatic hydrolysis (*S100*), dilution and sterilization of A-molasses and the fermentation mediums (*S200-1*), a seed train for the growth of *A. niger* GCB-75 (*S200-2,1*) for citric acid fermentation from glucose and A-molasses (*S200-2,2*), seed train of *Y. lipolytica* strain XYL+ for citric acid fermentation from xylose (*S200-4*), and separation and purification (*S300*). Additional sections in the process include wastewater treatment (*S400*), the combined heat and power plant (*S500-1 & S500-2*) and other utilities (*S600*). In Figure 35 the basic flowsheet of Scenario J is illustrated. A screenshot of the main flowsheet in Aspen Plus® is given in Appendix C.

The fermentation section where *A. niger* utilized glucose and A-molasses to produce citric acid was similarly designed and simulated to what has been described for *Scenario I*. A portion of the 2G feedstock

is sent to the CHP plant, whilst the remainder of 2G feedstock undergoes SO_2-catalysed steam pre-treatment and enzymatic hydrolysis to produce a hemicellulose hydrolysate to *S200-3*, a glucose-rich stream to *S200-2*, a cellulignin stream to the CHP plant and an effluent stream to the WWT plant.

The hemicellulose hydrolysate undergoes concentration using a triple effect evaporator and detoxification using activated carbon, prior to fermentation with *Y. lipolytica*. The seed train and fermentation occurring in *S200-3* takes place at 28°C, results in a titre of 79.4 g/L, with a growth medium consisting of per L^{-1}: NH_4Cl ***3 g***, KH_2PO_4 ***0.2 g***, $MgSO_4 \times 7H_2O$ ***1 g*** and yeast extract ***1 g*** (Ledesma-Amaro *et al.*, 2016). The yeast extract was however replaced with corn steep liquor, which is a much more cost-effective nutrient source. Similar to *S200-2*, the growth of *Y. lipolytica* strain XYL+ and the fermentation of citric acid in *S200-3* are aerobic processes, sparged with 0.5 vvm air (Kachrimanidou *et al.*, 2021). The seed train and fermentation reactions taking place in *S200-3*, can be found in Table 24. The only by-product produced was xylitol.

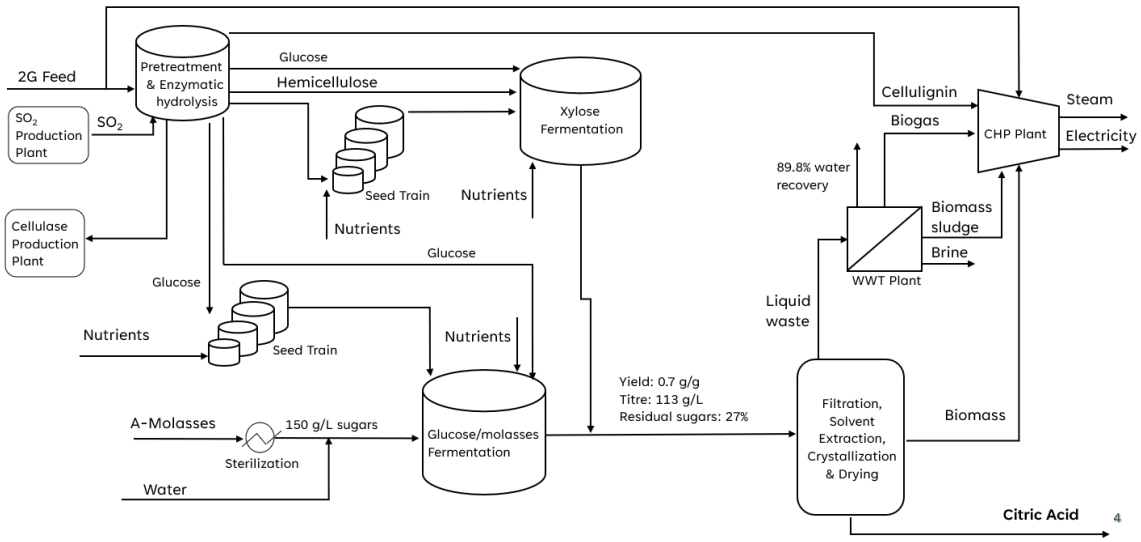

Figure 35: Scenario J Main Flowsheet

Table 24: Stoichiometric reactions occurring in series and corresponding fractional conversions used in the reactors of S200-3 for Scenario J (Ikram-Ul et al., 2004; Ledesma-Amaro et al., 2016).

Stoichiometric Reaction	Fractional Conversion
Yarrowia lipolytica strain XYL+ *Seed Train*	
$C_5H_{10}O_5 + 0.796\ NH_3 + 0.0828\ O_2 \rightarrow 4.68\ CH_{1.83}O_{0.56}N_{0.17} + 1.91\ H_2O + 0.3167\ CO_2$	0.91
Fermentation utilizing xylose	
$2\ C_5H_{10}O_5 + 5.5\ O_2 \rightarrow C_6H_8O_7 \cdot H_2O\ (Citric\ acid\ monohydrate) + 5\ H_2O + 4\ CO_2$	0.756
$C_5H_{10}O_5 + 0.796\ NH_3 + 0.0828\ O_2 \rightarrow 4.68\ CH_{1.83}O_{0.56}N_{0.17} + 1.91\ H_2O + 0.3167\ CO_2$	0.731
$2\ C_5H_{10}O_5 + 4.5\ O_2 \rightarrow C_5H_{12}O_5(Xylitol) + 4\ H_2O + 5\ CO_2$	1

3.1.7.3 Section 300: Separation and Purification of Citric Acid

The citric acid downstream processing section is made up of a number of steps including mycelium filtration, purification, evaporation, crystallization, centrifugation and finally drying to achieve anhydrous citric acid crystals at >99.8% purity (MacAringue *et al.*, 2020; Pasternack *et al.*, 1934). These steps are in

line with a current industrial citric acid production plant developed by VOGELBUSCH Biocommodities (Vogelbusch Biocommodities, 2020)

The fermentation broths produced from the citric acid production processes employing *A. niger* and *Y. lipolytica* respectively, are combined for separation and purification. The mycelium filter (*ROTVFIL*) removes the solid biomass and additionally acts as a pressure filter, ensuring traces of citric acid entrained in the mycelium is extracted for further recovery (De Beer, 2011; Özüdoğru, 2018). The mycelium filter is simulated in Aspen Plus® as a separator block instead of the appropriate rotary vacuum filter, due to limitations in Aspen Plus®. Considering that the citric acid product is a solid, it has been specified as such in the Aspen materials properties environment, however it only becomes a solid further downstream during crystallization. The rotary vacuum filter unit in Aspen Plus® does not recognize that it is in solution when being processed by the filter and separates the citric acid in solution with the solid biomass. The removed biomass is sent to the boiler for combustion.

The solution containing citric acid monohydrate (*S2*) is then pumped and heated by a combination of heat integration (HX-07) and LPS to 40°C prior to undergoing solvent extraction. For solvent extraction, 2 absorption columns are used, one for extraction and one for back extraction. The first of the two columns uses an amine solvent consisting of (w/v); 50% Isopar K, 47% Alamine®336 and 3% octanol to extract the citric acid monohydrate, after which water is used in the second column for back extraction of the product (Baniel, Vitner, Gonen, *et al.*, 2008; Özüdoğru, 2018). The amine solvent is fully recycled after back extraction (*BACKEXTR*) in the process, but to prevent impurity build-up a purge stream (*PRGE*) assumed to be 3% of the recycled solvent stream has been implemented. This translates to the make-up stream (*MAKEUP*) also only being 3% of the required solvent. Both absorption columns have been simulated as separation blocks to specify the required extraction but have been correctly cost in the TEA. The streams leaving the solvent extraction column (*SX*), is a waste stream containing most impurities and an extractant (EXT) stream consisting of 16% citric acid. The extractant stream undergoes back extraction with water, recovering all citric acid to *S3*.

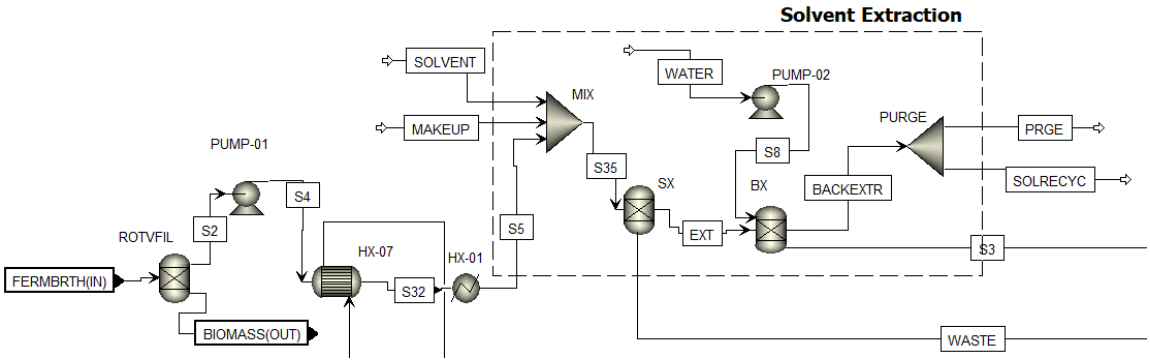

Figure 36: Scenario I & J, Section 300, Solvent Extraction flowsheet modelled in Aspen Plus®

The citric acid monohydrate and water mixture from solvent extraction (*S3*) is further concentrated using a triple effect evaporator (*FLASH-01*, *FLASH-02*, *FLASH-03*, *HX-02*, *HX-03* & *HX-04*) to obtain a solution (*S19*) containing 50% w/w citric acid (Baniel *et al.*, 2008). The triple effect evaporator was designed according to that developed by Nieder-Heitmann (2019) with a final evaporation pressure (pressure of

the subsequent crystallization step) of 0.8 atm (2.5 inches of mercury) (Pasternack *et al.*, 1934). Furthermore, the vapor fraction of the first evaporation step was adjusted by a design spec to ensure the effluent 50% w/w citric acid specification was met.

Anhydrous citric acid currently makes out the majority of the citric acid market, and can be produced from citric acid monohydrate during crystallization at temperatures above 36.5°C (Behera *et al.*, 2021). In the crystallizer (*CRYS-01* & *CRYS-02*) a pressure of 0.085 bar (8.5 kPa) and temperature of 52°C in a crystallizer ensures the formation of anhydrous citric acid crystals with a purity of >99% (Pasternack *et al.*, 1934). In Aspen Plus®, an *RStoic* unit (*CRYS-01*) is first used to convert the citric acid monohydrate to dissolved anhydrous citric acid, which is a process that would have taken place in the crystallizer but Aspen Plus® has limitations and does not allow the addition of this reaction in the crystallizer unit. In the crystallizer unit (*CRYS-02*) available in Aspen Plus® the vapor flowrate (*S14*) was controlled to ensure the appropriate operating temperature. In the vacuum crystallizer, 94% of the citric acid monohydrate could be converted to anhydrous citric acid crystals (Baniel *et al.*, 2008).

Following crystallization, the solid-liquid mixture (*S15*) is separated in a centrifuge (*CENTRF*) prior to the final drying step. According to Baniel, et al. (2008) the mother liquor needs to be recycled to extract the entrained citric acid; however, in this scenario the mother liquor (*MOTHERLQ*) contains no citric acid (due to similar limitations of the centrifuge as previously describe for the rotary vacuum filter) and it was instead directly sent to wastewater treatment.

Drying of the citric acid takes place using a fluidized bed dryer (*DRYER*), where hot air at approx. 130°C is the heating medium. According to De Beer (2011) the citric acid dryer has an electricity usage of 227 MJ/ton product produced and the inlet air is heated with a total of 1500 kg/ton product, saturated steam at 150°C. Considering steam at 150°C is not being produced in the CHP, the appropriate amount of MPS for the heating was determined and instead assigned as utility. These parameters were used to determine the air compressor duty and subsequently the air inlet flowrate. The drying unit itself was merely represented by a separator block, with anhydrous citric acid (>99.8%) as the final product. This was done because of a range of specifications required in the dryer block in Aspen Plus®, which was not essential to be obtained for an accurate costing of the dryer block.

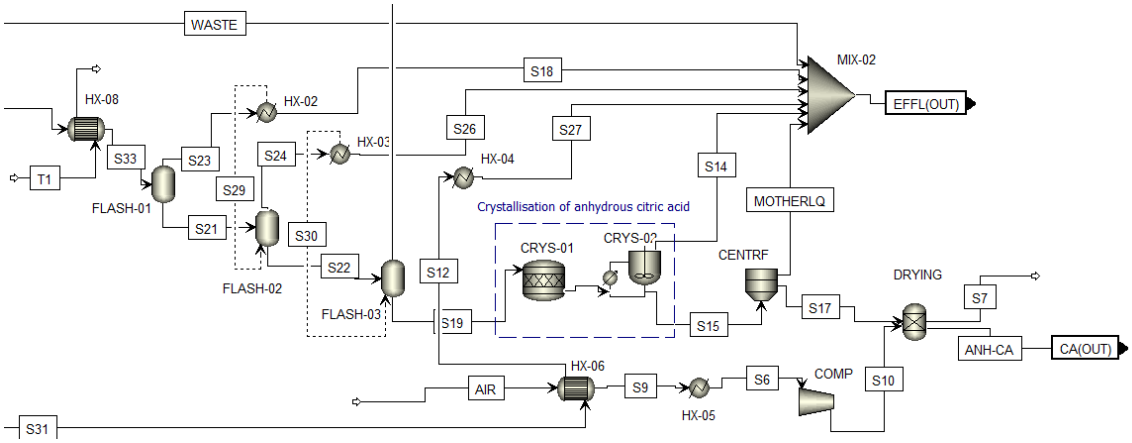

Figure 37: Scenario I & J, Section 300, Evaporation, Crystallization and Drying flowsheet modelled in Aspen Plus®

3.2 Economic Assessment

In this section the methodology followed to conduct a thorough techno-economic analysis will be discussed. The techno-economic analysis consists of three major sections, the capital expenditures (CAPEX), the operational expenditures (OPEX) and the discounted cash flow rate of return (DCFROR) analysis.

3.2.1 Capital Expenditures (CAPEX)

The main parameter to be determined for the capital expenditures is the Total Capital Investment (TCI). In Table 25 the breakdown of the TCI can be found. Determining the installed equipment cost (IEC) is the most demanding portion of the capital expenditures considering all the equipment required needs to be sized and/or scaled from reliable sources. In Appendix A, a detailed description is available describing where the cost of equipment was obtained. The installed equipment cost was calculated from the purchase cost using installation factors recommended by Humbird *et al*. (2011).

Table 25: Breakdown of all costs making up the Total Capital Investment (TCI) (Gorgens F; Mandegari, M A; Farzad, S; Daful, A G; Haigh, 2016; Humbird et al., 2011)

Category	Description
Total Direct Cost (TDC)	
Installed Equipment Cost	Purchase and Installation of all biorefinery equipment, determined through sizing and scaling
Warehouse	4% of ISBL*
Site Development	9% of ISBL*
Additional Piping	4.5% of ISBL*
Storage	5% of ISBL*
Total Indirect Cost (TIC)	
Prorateable costs	10% of TDC
Field Expenses	10% of TDC
Home Office and Construction	20% of TDC
Project Contingency	10% of TDC
Other Costs	10% of TDC This includes a number of costs such as start-up and commissioning costs, overtime pay during construction, taxes, permits etc.
Fixed Capital Investment (FCI)	TDC + TIC
Working Capital	5% of FCI
Total Capital Investment (TCI)	**FCI + Working Capital**

*ISBL: Installed Equipment Cost Inside Battery Limits, which excludes sections 400, 500, 600 & 800 (where applicable).

Important to note are a number of additional direct costs such as the initial refrigerant purchase cost, for all scenarios that required refrigerant for cooling. The refrigerant amount required was determined using an assumed storage tank holding time of 6 minutes (Burla et al., 2012). Furthermore, the cost of the catalyst and initial cost of the molten salt is required for scenarios C - E were also accounted for. For scenarios C and D, the catalyst amount was determined as 1 g of catalyst per 0.001 L/h 2,3-BDO flowrate (Tsukamoto et al., 2016). Due to a lack of information available regarding the cost of SiO2-supported

CsH_2PO_4, the cost of the catalyst in scenario C and D was assumed to be 100 $/kg, similar to another catalyst used to produce 1,3-BD from 2,3-BDO (Song, Yoon, et al., 2018). For scenarios E and F, the catalyst cost and amount required for each of the catalytic reactions was obtained from Burla, et al., 2012. For scenarios C - F, the amount of catalyst was increased for an additional catalytic reactor, which is regenerated whilst not being used to ensure continuous operation (Burla et al., 2012).

The total molten salt required for each scenario was determined similar to the refrigerant cost, by assuming a storage tank holding time of 6 minutes (Burla et al., 2012). Molten Salt has an approximate lifetime of 20 years, and it is assumed for the lifetime of this plant that the molten salt does not need to be replaced (Battisti, 2018). It was assumed that the initial melting of the molten salt formed part of indirect capital costs, start-up costs.

3.2.2 Operational Expenditures (OPEX)

The Total Production Cost (TPC) consist of two major components, the Fixed Operating Cost (FOC) and the Variable Operating Cost (VOC). An additional component of the OPEX is the annual capital charge, which for this thesis only includes activated carbon for detoxification which is not continually replaced, but instead only replaced every six months at a price of 1.2 $/kg (2013)(Nieder-Heitmann, 2019). FOC are costs that are deducted whether or not the plant operates at full capacity, or not whilst VOC are costs directly related to production and vary with capacity (Humbird *et al.*, 2011). Assumed FOC, consists of labour costs (salaries indicated in

Variable Operating Costs consist of raw material cost and waste disposal costs. Raw material costs includes both feedstock cost and chemicals costs. The individual price of each chemical can be found in Appendix B, whilst feedstock prices used has been summarized in Table 27. Chemical costs that were not obtained in the reference year of this study (2019) was adjusted using *Chemical Engineering Plant Cost Indices*. The price of A-molasses was calculated as the sum of the sugar (10.71 t/h and 303.0 $/t) and C-molasses (11.57 t/h and 145.7 $/t) revenue loss due to A-molasses extraction, divided by the A-molasses flowrate (OECD/FAO, 2019). The price of 2G feedstock was calculated as the sum of the cost of bagasse (37.1 t/h and 29.6 $/t) and brown leaves (23.5 t/h and 31.6 $/t), divided by the flowrate of the 2G feedstock (113.5 t/h) (Dogbe *et al.*, 2019). Waste for all biorefinery scenarios include ash from the combustor and brine produced in the wastewater treatment plant, which have been cost as 0.034 $/kg and 0.054 $/kg respectively (City of Cape Town, 2020; Özüdoğru, 2018). Other solid wastes pertaining to specific scenarios include gypsum and biomass sludge at 0.0765 $/kg (Özüdoğru, 2018).

Table 26), maintenance (3% of ISBL) and property insurance (0.7% of FCI)(Humbird *et al.*, 2011; Özüdoğru, 2018). The labour costs consist of all the salaries made out to employees. The amount of employees, except for the amount of machine operators, was based on suggestions by Humbird, et al. (2011) as well as Turton, et al. (2018). The amount of machine operators was calculated using Equation 3 obtained from Turton, et al. (2018), where N_{OL} refers to the number of operators, P refers to the number of processing steps involving the handling of solids and N_{np} refers to the number of nonparticulate processing steps. The FOC of each biorefinery scenario is given in Appendix E.

$$N_{OL} = \left(6.29 + 31.7P^2 + 0.23N_{np}\right)^{0.5} \quad 3$$

Variable Operating Costs consist of raw material cost and waste disposal costs. Raw material costs includes both feedstock cost and chemicals costs. The individual price of each chemical can be found in Appendix B, whilst feedstock prices used has been summarized in Table 27. Chemical costs that were not obtained in the reference year of this study (2019) was adjusted using *Chemical Engineering Plant Cost Indices*. The price of A-molasses was calculated as the sum of the sugar (10.71 t/h and 303.0 $/t) and C-molasses (11.57 t/h and 145.7 $/t) revenue loss due to A-molasses extraction, divided by the A-molasses flowrate (OECD/FAO, 2019). The price of 2G feedstock was calculated as the sum of the cost of bagasse (37.1 t/h and 29.6 $/t) and brown leaves (23.5 t/h and 31.6 $/t), divided by the flowrate of the 2G feedstock (113.5 t/h) (Dogbe *et al.*, 2019). Waste for all biorefinery scenarios include ash from the combustor and brine produced in the wastewater treatment plant, which have been cost as 0.034 $/kg and 0.054 $/kg respectively (City of Cape Town, 2020; Özüdoğru, 2018). Other solid wastes pertaining to specific scenarios include gypsum and biomass sludge at 0.0765 $/kg (Özüdoğru, 2018).

Table 26: Breakdown of labour costs, a components of the Fixed Operating Costs (FOC) (Gorgens F; Mandegari, M A; Farzad, S; Daful, A G; Haigh, 2016)

Job Title in South Africa	***2019 Salary ($/year)***
Process Manager	43730
Process Engineer	27183
Maintenance Engineer	27040
Machine Setter	19283
Chemical Engineer	22277
Chemical Lab Technician	16143
Chem Lab Technician (Enzyme)*	16143
Foreman	22917
Machine Operators	16088
Machine Operators – Enzyme*	16088
Laborer	13984
Helpdesk Operator	16994

*Only applicable to 1G2G scenarios

Table 27: Summary of feedstock prices.

Feedstock	**Price (2019) ($/kg)**	**Scenarios applicability**
A-molasses	0.1939	All
Bagasse	0.0296[a]	All 1G
2G Feedstock[b]	0.0162	All 1G2G

[a](Dogbe *et al.*, 2019). [b]Bagasse and Brown Leaves, # (Davis *et al.*, 2018)

3.2.3 Discounted Cash Flow Rate of Return (DCFROR)

A discounted cash flow rate of return analysis was used to determine the economic parameter, minimum selling price, when the NPV is zero. In Table 28 all economic parameters used for the analysis is summarized.

Table 28: Economic Parameters used in the DCFROR analysis

Economic Parameter	Value	Unit
Operating Hours	5000*	h/y
Equity	100	%
Land Cost	0	
Working Capital	5	% of FCI
Depreciation Period	5	years (20% per year)
Salvage Value	0	
Start-Up Duration	1	year
Variable Cost Incurred During Startup	75	%
% Spend In Year -2	10	%
% Spend In Year -1	60	%
% Spend In Year 0	30	%
Income Tax Rate	28	%
IRR	20	%
Revenues During Startup	50	%
Annual Depreciation	20	%

*Due to seasonality of sugar cane

3.3 Environmental Assessment

3.3.1 GHG Calculations

The environmental impact of each biorefinery scenario was assessed using the RSB GHG Calculator Tool (Roundtable on Sustainable Biomaterials (RSB), 2022). The calculator tool provides a template where various operations of the biorefinery scenario can be specified. Based on the various inputs, the calculator tool gives an estimate on the biorefinery greenhouse gas emissions. Although in the calculator tool, every aspect of the biorefinery scenario cannot be accounted for, it provides an adequate estimation. Furthermore, all the biorefineries scenarios in this paper were assessed similarly, from which sufficient comparisons can be made and insights can be obtained as to the environmental impact of producing a range of biochemical products at a biorefinery.

4 RESULTS AND DISCUSSION

This section will discuss the results obtained from designing, simulating, conducting techno-economic analyses and an environmental assessment for each of the ten biorefinery scenarios investigated in this study. The results will include the material and energy balances, capital costs, operational costs and other economic parameters as well as the GHG emissions determined for each biorefinery scenario. Furthermore, results obtained from conducting a sensitivity analysis will also be discussed as well as how all results obtained compare to what has already been published in literature. The results and discussion sections will consist of two main categories. First the results pertaining to a specific biochemical will be discussed and thereafter all ten scenarios will be compared.

For each of the biorefinery scenarios a diagram was constructed to illustrate the sugar, product and by-product flows between the main production process sections. The main production process sections include all sections relating to product formation and purification, these sections will furthermore be referred to as the inside battery limits (ISBL) sections. The utilities are not part of the ISBL sections. The utility consumption and production, installed equipment cost contributions and raw material cost contributions of each process section (incl. utilities) have also been indicated on each of the constructed diagrams. The raw material cost consists of both the feedstock cost and chemical costs. Energy flows are indicated by arrows, arrows entering the top of each section represent utilities consumed whilst arrows leaving a specific section represent utilities produced. Utilities of negligently small quantities were omitted. The installed equipment cost contribution and raw material cost contribution of each section is represented by rectangular blocks, size depending on the contribution.

4.1 2,3-Butanediol Biorefinery Scenarios

4.1.1 Material and Energy Balances of the 2,3-BDO Scenarios

Figure 38 illustrates the sugar, product and by-product flows, utility usage, installed equipment cost and raw material cost of Scenario A. The fermentation broth contains 11.74% 2,3-BDO, and small amounts of residual sugars. Following separation and purification of the fermentation broth in *S300*, purified 2,3-BDO (98 wt%) at 45.5 kt/y or 9100 kg/h is produced. The overall yield of 2,3-BDO from A-molasses (total flowrate) in Scenario A is 0.37 g/g_{feed}. The combustors of *S500-1&2* is supplied with 2.75 t/h bagasse to produce a portion of the electricity and heating utilities required by the biorefinery. This amounts to 9.03% of the total bagasse available from the sugar mill.

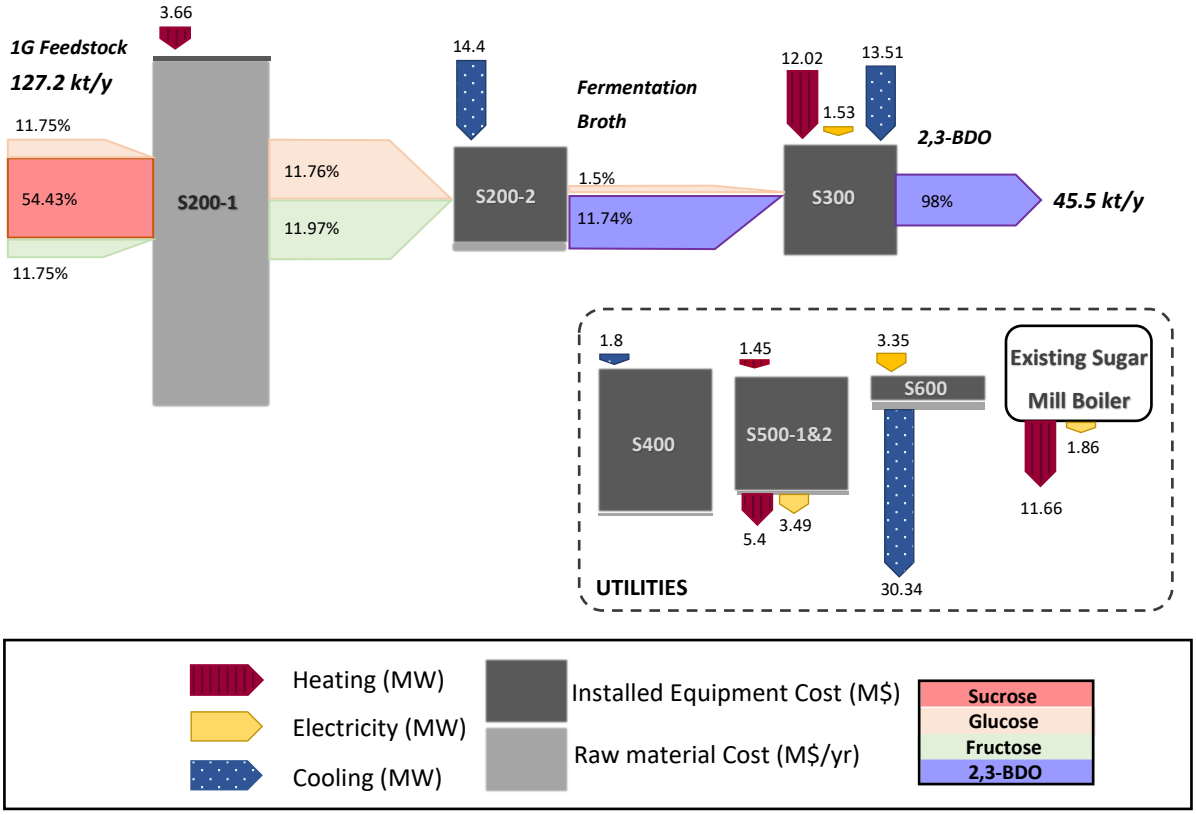

Figure 38: The distribution of Utility usage, Installed Equipment Cost and Raw Material Cost, between the main process sections of Scenario A.

Similarly, Figure 39 illustrates the sugar, product and by-product flows, utility usage, installed equipment cost and raw material cost of Scenario B. The overall fermentation yield obtained is 0.43 $g/g_{total\ sugars}$, resulting in a fermentation broth containing 11.57% 2,3-BDO and small quantities of residual sugars. Following separation and purification of the fermentation broth in *S300*, 2,3-BDO at a purity of 98% is produced at 68 kt/y or 13600 kg/h. The overall yield of Scenario B from 1G2G feedstock is 0.2 g/g_{feed}. The 1G2G feedstock flowrate includes the total A-molasses flowrate and flowrate of the 2G portion to the biorefinery. Scenario B has a bypass ratio of 33%.

Table 29 contains the most important material balance information for the 2,3-BDO scenarios. The overall yield of Scenario B is considerably lower at 0.20 g/g_{feed} compared to Scenario A at 0.37 g/g_{feed}, despite the fermentation yields being comparable (0.45 $g/g_{total\ sugars}$ and 0.43 $g/g_{total\ sugars}$). The benefits of utilizing 1G feedstock with readily available sugars is evident. The pretreatment processes are optimized to ensure sugar extraction; however sugar losses are inevitable. This includes sugars losses attributed to processes such as washing of solids; as well as effectual sugar losses due to unhydrolyzed xylan and cellulose.

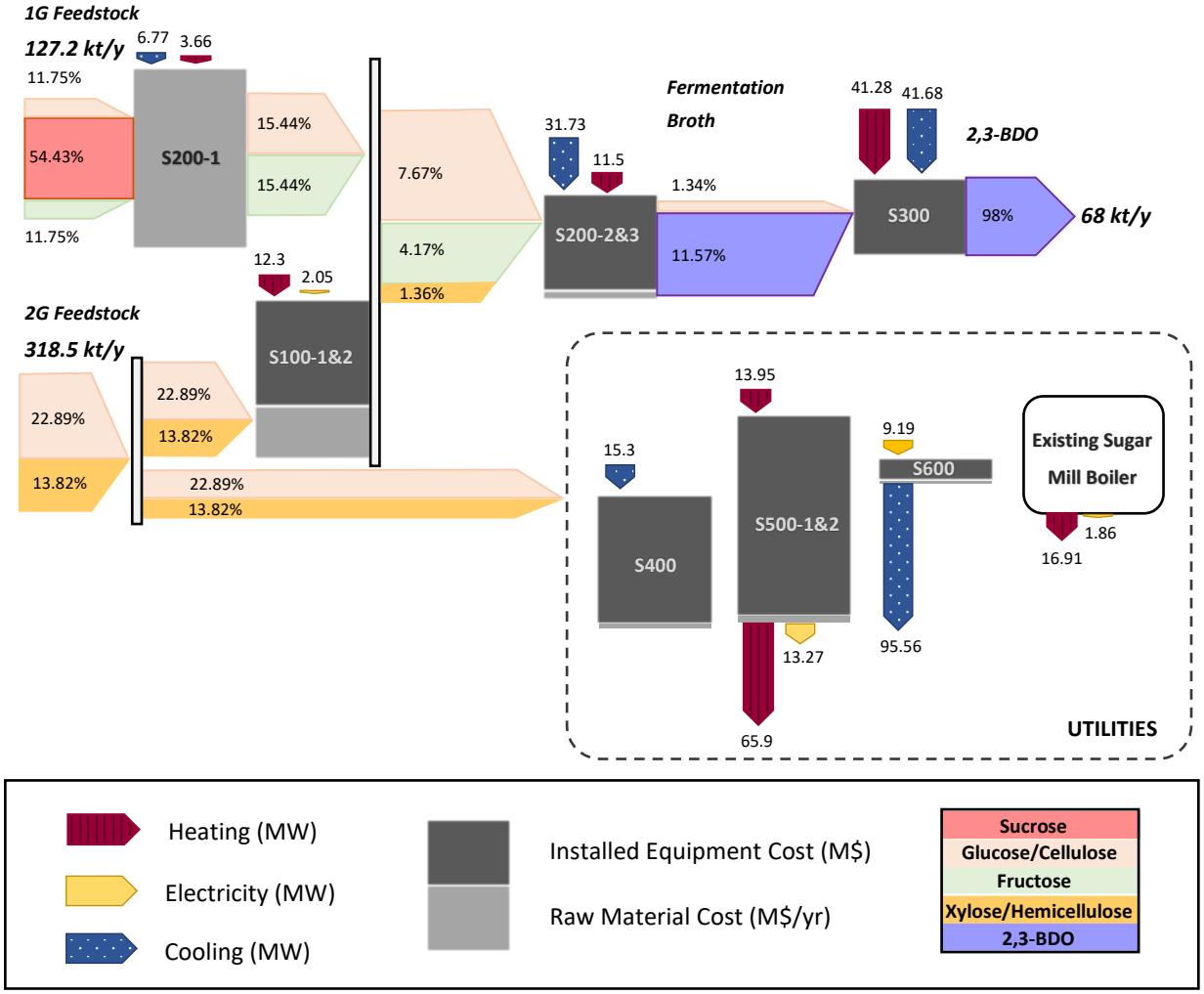

Figure 39: The distribution of Utility usage, Installed Equipment Cost and Raw Material Cost, between the main process sections of Scenario B.

The market size of 2,3-BDO is estimated as 14 million tons per year (Dowe, 2021; Zhang, 2021). The production rates for one typically sized sugar mill according to Scenario A and B would only contribute 0.33% and 0.49%, respectively, to the 2,3-BDO market. This illustrates the market entry potential of these scenarios, considering that <5% increase in the market volume will not result in issues associated with oversupply (Nieder-Heitmann, 2019). It is important to note that this does not necessarily represent the bio-based 2,3-BDO, only the total 2,3-BDO market volume. This should however not affect the aforementioned results, considering 2,3-BDO is a drop-in chemical and that bio-based 2,3-BDO is a direct substitute of the fossil-based 2,3-BDO, given it is cost-equivalent (Directorate-General Energy, 2015).

Table 29: Summary of main material balance information for 2,3-BDO Scenarios.

SCENARIO	PRODUCTION RATE (kt/y)	PURITY (%)	OVERALL YIELD (g/g_{feed})	% BAGASSE* OR 2G FEED# TO CHP (BYPASS RATIO)	% OF MARKET SHARE
A	45.5	98	0.37	9.03	0.33
B	68.0	98	0.20	33.00	0.49

*Applies to 1G Scenarios, #Applies to 1G2G Scenarios

Figure 40 compares the utility requirements of Scenario A and B in relation to their respective capacities. Evidently, Scenario B requires significantly more cooling, heating, and electricity per kg 2,3-BDO produced. In Table 30 and Table 31 the major heating and cooling consuming equipment of Scenario A and B are listed. Considering three of the entries in Table 31 are associated with pretreatment, enzymatic hydrolysis (*S100-1&2*) and xylose fermentation (*S200-3*), the higher utility consumption per kg is most likely due to the additional processes associated with the 2G feedstock. It also shows that the cost of producing 2,3 BDO from 2G feedstock compared with 1G feedstock is significantly higher.

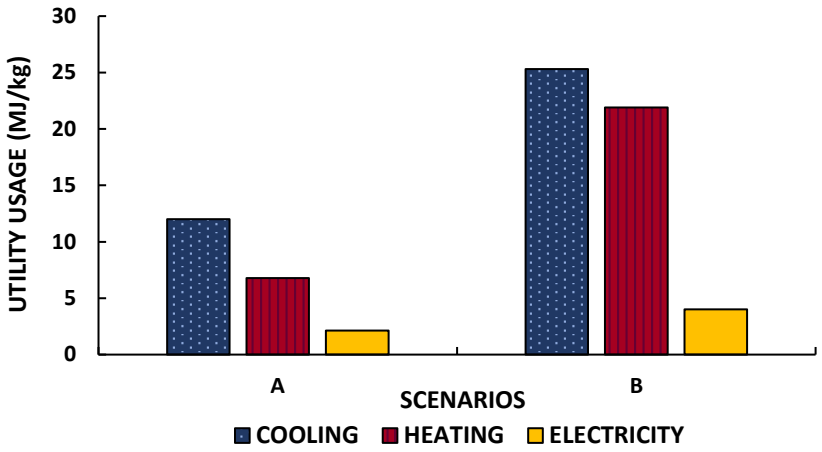

Figure 40: Utility usage per kg product produced for the 2,3-BDO Scenarios.

Table 30: Main heating and cooling utility consuming equipment of Scenario A.

PROCESS SECTION	EQUIPMENT	HEATING (MW)	COOLING (MW)
S200-2	Fermenter	-	12.24
S300	Heat Exchanger *(HX-07 [a])*	-	7.28
S300	Heat Exchanger *(HX-05 [a])*	-	6.00
S300	Distillation Column	8.22	-
S300	Flash Drum	3.80	-
S200-1	Heat exchanger	3.66	-

[a]In Figure 16

Table 31: Main heating and cooling utility consuming equipment of Scenario B.

PROCESS SECTION	EQUIPMENT	HEATING (MW)	COOLING (MW)
S300	Heat Exchanger *(HX-05 [a])*	-	34.4
S200-2	Fermenter	-	15.82
S400	Heat Exchanger *(HX-01 [b])*	-	14.68
S200-3	Heat Exchanger *(HX-05 [c])*	-	9.64
S300	Distillation Column	38.05	-
S100-2	Pretreatment Reactor	12.33	-
S200-3	Flash Drum *(FLASH-01 [c])*	11.50	-

[a]In Figure 16. [b]In Figure 3 [c]In Figure 13.

The existing sugar mill CHP plant (boiler) provides 68% and 35% of the total heating and electricity requirements for Scenario A. For Scenario B it provides 20% and 12% of the total heating and electricity requirements. The remaining heating and electricity requirements of the scenarios are provided by the new CHP plant constructed as part of the biorefinery expansion to the sugar mill.

The process sections requiring the largest amount of cooling for both Scenario A and B are *S200-2(&3)* and *S300*. The latter also has the highest heating requirements for both scenarios, indicating that the separation and purification of 2,3-BDO is the most energy intensive process steps in a 2,3-BDO biorefinery annexed to an existing sugar mill. This furthermore highlights the importance of choosing a microorganism and accompanying fermentation process that results in not only a high yield, but also a high titre, in order to simplify and reduce the energy intensity of the 2,3-BDO separation and purification process. The electricity requirements are concentrated at *S600*, which accounts for 62.4% and 60.65% for Scenario A and B respectively. Section 600 contains the cooling water tower and attached chilled water package, which consume 0.0837 kW and 0.1429 kW electricity per kW cooling water and chilled water produced, respectively (Petersen *et al.*, 2021).

Figure 41 indicates the total utility usage of each process section per kg 2,3-BDO produced. The utility usage of *S300* per kg is significantly higher for Scenario B at 22.42 MJ/kg compared to Scenario A at only 10.71 MJ/kg, despite being similarly designed for the two scenarios. Rigorous heat integration was implemented in the separation and purification section of Scenario A and B, not only within the separation and purification units, as described in literature, but also using appropriate streams elsewhere in the process (Haider, Abdul, *et al.*, 2018). The heat integration network of each scenario was individually optimized considering the processes are not identical, Scenario B has additional sections i.e., pretreatment and xylose fermentation. For Scenario A the implementation of a heat integration network reduced the heating and cooling requirements by 68.4% and 55% respectively, whilst for Scenario B they were only reduced by 31.93% and 30.08% respectively. Apart from *S300*, most of the other process sections also have higher utility requirements per kg product produced for Scenario B. This can most likely also be attributed to the higher heat integration network efficiency of Scenario A. Heat integration was merely conducted by hand and to obtain more accurate energy flow results, a pinch point analysis could be conducted in the future.

Section 200-3 is the second most energy intensive section of Scenario B, requiring 6.6 MJ/kg combined heating, cooling, and electricity. The large energy requirements can be ascribed to the concentration of the hemicellulose hydrolysate from 44.44 g/L to 220 g/L xylose, prior to fermentation. The triple effect evaporator responsible for this concentration process accounts for 11.55% of the total energy requirements of Scenario B. The triple effect evaporator requires both cooling water and LPS. The LPS requirements of the triple effect evaporator amounts to 0.44 kg_{LPS}/kg_{2GFeed}. The energy intensity of processing the hemicellulose hydrolysate to be suitable for fermentation quickly outweighs the benefits i.e., higher production rates obtained by utilizing hemicellulose hydrolysate for fermentation. Potentially, a biorefinery scenario such as Scenario B could benefit more from directly sending the hemicellulose hydrolysate to the wastewater treatment plant where biogas and biomass sludge (useful for electricity and steam generation) can be produced during anaerobic and aerobic digestion. However, further research will be required to confirm a positive economic impact following the aforementioned adjustment.

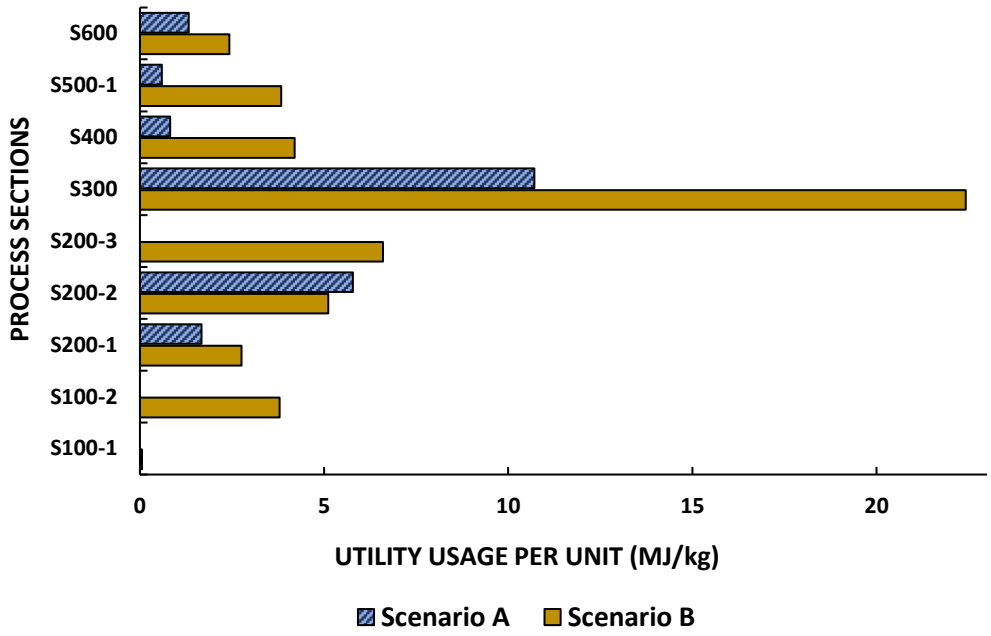

Figure 41: Total utility usage per kg product produced for the various process sections of Scenario A and B.

4.1.2 Capital Expenditure (CAPEX) of 2,3-BDO Scenarios

Table 32 contains the main capital expenditures of the 2,3-BDO scenarios. The full set of capital expenditures are available in Appendix D. The total capital investment per kg product produced for Scenario B, is approximately 1.6 times higher compared to Scenario A. Economies of scale benefits are therefore not realized by Scenario B. One of the reasons for this observation is attributed to the additional equipment costs associated with extra processes required for pretreating 2G feedstock in Scenario B. This is evident from Figure 42, which illustrates the process section installed equipment cost (IEC) per kg product produced for the 2,3-BDO scenarios. Pretreatment and enzymatic hydrolysis contributes significantly to the total IEC of Scenario B. More specifically, the enzymatic hydrolysis equipment, consisting of continuous enzymatic vessels and batch enzymatic hydrolysis reactors, accounting for 60% of the IEC of *S100-2*. This is a major disadvantage associated with utilizing 2G feedstock in a biorefinery.

The process section installed equipment cost (IEC) per kg product produced for the 2,3-BDO scenarios, is illustrated in Figure 42. The IEC of *S500* and *S400* are the main contributors for both scenarios. The high contribution of the WWT plant and the CHP plant to capital expenditures has similarly been found by NREL (Humbird *et al.*, 2011). The high capital cost associated with *S400* is on account of the three specialized units required to produce the process water, biogas, and biomass sludge. These units include the anaerobic biodigester, aerobic digester, and reverse osmosis unit. Of the three units, the anaerobic digester and associated equipment such as a biogas blower and biogas energy flare, account for 56% of the WWT plant installed equipment cost.

Table 32: Main Capital Expenditures of the 2,3-BDO Scenarios.

CAPITAL EXPENDITURES		**A**	**B**
TOTAL INSTALLED EQUIPMENT COST (M$)		67.45	161.87
ISBL: INSTALLED COST INSIDE BATTERY LIMITS (M$)		28.83	72.03
TOTAL DIRECT COST (TDC) (M$)		73.94	178.08
TOTAL INDIRECT COST (M$)		44.36	106.85
FIXED CAPITAL INVESTMENT (FCI) (M$)		118.30	284.93
TOTAL CAPITAL INVESTMENT (TCI) (M$)		**124.20**	**299.18**
TOTAL CAPITAL INVESTMENT$_{per\ unit}$	$/kg per year	**2.73**	**4.40**

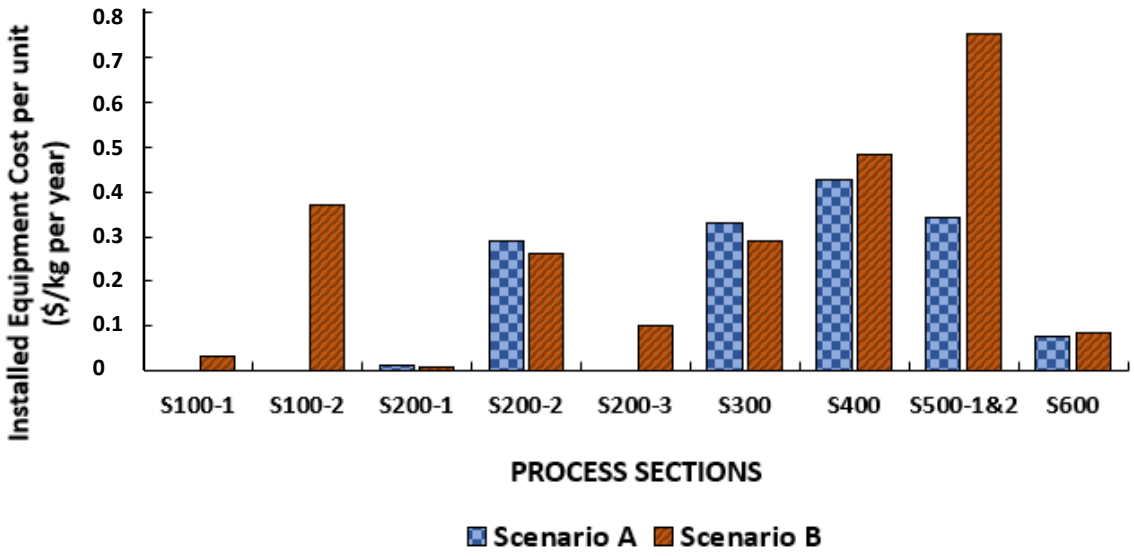

Figure 42: Installed equipment cost per kg product produced per section, for the 2,3-BDO Scenarios.

The high capital costs associated with higher heating and electricity requirements per kg also becomes evident in Figure 42. Scenario B requires a significantly larger CHP, owing to the additional utility requirements. The same however does not go for the cooling tower and chilled water tower. Despite the 100.77% higher cooling utility requirements per kg of Scenario B, the IEC of the cooling tower and chilled water package is comparable for the two scenarios.

Mailaram et al., (2022) similarly found that the anaerobic digester of the WWT plant, the CHP plant and the enzymatic hydrolysis reactors were the most capital-intensive equipment at 24%, 22% and 10% of the total installed equipment cost of a 2,3-BDO biorefinery utilizing brewers' spent grain. Furthermore, the high cost contribution of a boiler to the capital costs has previously been reported in literature (Farzad, Mandegari & Görgens, 2017; Nieder-Heitmann, 2019).

4.1.3 Operational Expenditure (OPEX) of 2,3-BDO Scenarios

A summary of the main contributors to the operational expenditure are presented in Table 33. A breakdown of the fixed operating costs of each individual scenario can be found in Appendix E. Evident from Table 33 is the slight economies of scale benefits (in terms of OPEX) being realized by Scenario B, with a TPC per kg 3.4% lower compared to that of Scenario A.

Table 33: Operational Expenditures of the 2,3-BDO Scenarios.

OPERATIONAL COST COMPONENT	COST (M$/year)	
	A	B
Fixed Operating Cost	**2.40**	**5.40**
*Feedstock Cost**	*26.05*	*30.28*
Chemical Cost	*23.30*	*35.15*
Waste Disposal Cost	*1.95*	*6.34*
Total Variable Operating Cost	**51.30**	**71.77**
Annual Capital Charge	-	*0.02*
Total Production Cost (TPC)	**53.71**	**77.19**
TPC per unit ($/kg per year)	**1.18**	**1.14**

*Includes all bagasse and brown leaves from harvesting residues, even portion sent to CHP plant is regarded as feedstock cost

Figure 43 illustrates the fixed operational costs and variable operating costs as a function of production capacities of the 2,3-BDO scenarios. The variable operating costs have been indicated as the components, i.e., feedstock cost, chemical cost, and waste disposal cost. The negligible annual capital charge of 0.02 M$/year of the activated carbon for hemicellulose hydrolysate detoxification, has been omitted from Figure 43.

The main operational costs for both scenarios are the feedstock and chemical costs. The procurement of feedstock generally dominates the operational costs of biorefineries, despite using cost-effective by-products and wastes from industrial processes (Moncada, Gursel, Worrell, *et al.*, 2018). The dominating cost however differs for the scenarios. For Scenario A, feedstock cost dominates whilst for Scenario B, chemical costs dominate. Comparing the feedstock costs, it is clear that, per kg 2,3-BDO produced, Scenario A pays $ 0.127 more for feedstock compared to Scenario B resulting in a lower total production cost per kg 2,3-BDO, for Scenario B. This highlights the economic benefits of utilizing integrated first- and second-generation feedstock as opposed to only utilizing first generation feedstock. These benefits however need to be weighed against the additional capital and other operating costs associated with a 1G2G biorefinery.

For both Scenario A and B, invertase accounts for the majority of the chemical costs, at 93% and 62% respectively. Where possible, microorganisms should be chosen that can either naturally hydrolyze sucrose or directly utilize sucrose for product formation, thereby greatly reducing variable operating costs.

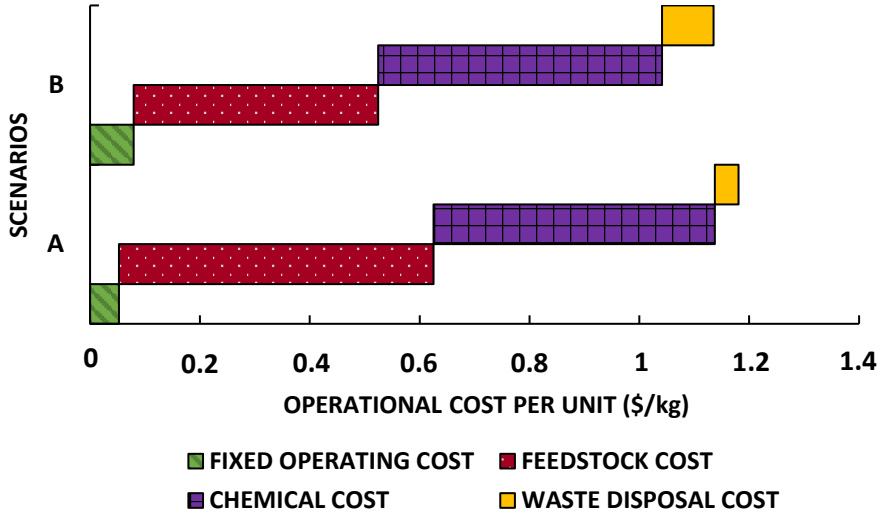

Figure 43: Operational cost components per kg product produced for the 2,3-BDO Scenarios.

4.1.4 Economic parameters of 2,3-BDO Scenarios

The main economic parameter, the minimum selling price, determined for Scenario A and B have been determined as 1.91 $/kg and 2.28 $/kg, respectively. The market price of petrochemically produced 2,3-BDO has been reported as 1.6 $/t (2016) (Maina, Stylianou, *et al.*, 2019). Compared to this market price neither Scenario A nor B are profitable, with MSPs 19% and 42.5% higher. However, bio-based chemicals that do not dominate their respective markets – like bio-based 2,3-BDO – generally have higher selling prices compared to their fossil-based counterparts (Directorate-General Energy, 2015). The market price of bio-based 2,3-BDO has however not been readily reported on, potentially due to 2,3-BDO itself not being sold in as large volumes as its derivatives such as MEK or 1,3-BD. A number of 2,3-BDO techno-economic analyses have reported that the bio-based 2,3-BDO market price is similar to the bio-based 1,4-BDO market price, 3.23 $/kg (2013) (Tan, Snowden-Swan, Abhijit Dutta, *et al.*, 2017; Zang, Shah & Wan, 2020). A similar approach was therefore adopted in this study and the 1,4-BDO price was adjusted for 2019 using Chemical Engineering Plant Cost Indices, giving 2.63 $/kg as the assumed bio-based 2,3-BDO market price. With regards to this assumed market price, both Scenario A and B are profitable biorefinery scenarios, with MSPs below the assumed market price.

4.1.5 Sensitivity analyses of the 2,3-BDO scenarios

The results of the sensitivity analyses conducted for Scenario A and B respectively can be found in Figure 44 and Figure 45. Parameters investigated are the fixed operating cost (FOC), invertase price, feedstock cost/price, fixed capital investment (FCI), total production cost (TPC) and operating hours per year of the plant. Furthermore, it is assumed that a change in any of the aforementioned parameters larger than 30% is unlikely, therefore 30% was chosen as the limits for the sensitivity analyses.

Figure 44 and Figure 45 additionally indicates the assumed market price for bio-based 2,3-BDO as well as the market price for fossil-based 2,3-BDO. Scenario A will remain profitable for a 30% change in all parameters except for the operating hours, at the assumed market price of 2.63 $/kg for bio-based 2,3-BDO. Only if the operating hours were to decrease by 25% to 3750 hours per year, will Scenario A become

unprofitable. On the other hand, if the operating hours were to increase by 20%, to 6000 hours per year, then Scenario A would become competitive with the current petrochemically produced 2,3-BDO.

Similarly, Scenario B will remain profitable for a 30% change in all parameters except for the operating hours. Only if the operating hours were to decrease by 13% to 4350 hours per year, will Scenario B become unprofitable. Contrary to Scenario A however, none of the parameters can be adjusted by 30% in order for Scenario B to become competitive with fossil-based 2,3-BDO. Both Scenario A and B are robust scenarios i.e., remains profitable despite substantial changes in costing parameters, Scenario A however would be a better investment.

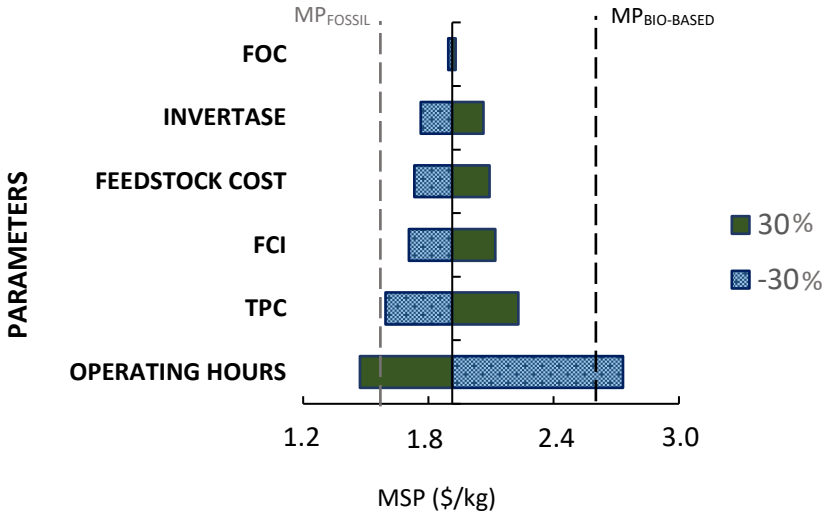

Figure 44: Sensitivity Analysis Results for Scenario A

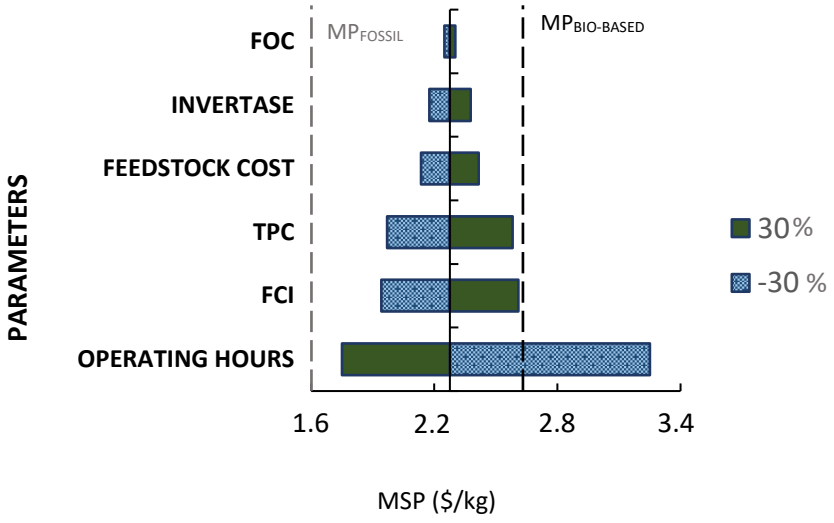

Figure 45: Sensitivity Analysis Results for Scenario B

4.1.6 Techno-economic comparison of 2,3-BDO scenarios to other bio-based processes

Table 34 contains the yields and main economic parameters obtained by techno-economic studies on 2,3-BDO production using different feed materials. Koutinas *et al*. (2016) utilized sugarcane molasses and obtained a yield and TCI per kg of 2.36-4.26 M$/kg per year, which is comparable to that of Scenario A of

2.73 $/kg per year. The biorefinery developed by Koutinas *et al*. (2016) purchases all utilities and does not produce any of these on-site. The cost of utility procurement was reported as 0.4 $/kg$_{2,3\text{-BDO}}$, which is almost 35% of the total production cost of Scenario A. This, in all likelihood, resulted in the higher MSP obtained, compared to Scenario A.

The biorefineries developed by Mailaram *et al*. (2022) and Zan *et al*. (2020) use lignocellulosic materials which also require pretreatment and enzymatic hydrolysis to extract the fermentable sugars, similar to Scenario B. The yields of the fermentation processes are evidently more comparable with that of Scenario B. The MSP determined by Mailaram *et al*. (2022) is 1.8 times higher than that of Scenario B, which was traced back to a different method used to determine capital costs. Mailaram *et al*. (2022) found that direct capital costs, excluding installed equipment cost, contributed as much as 50.6% to the total capital investment. This highlights the importance of having a universal method of conducting TEAs, which includes assumptions made and economic parameters used to obtain comparable results.

The MSP of Scenario B is 1.3 times higher than that obtained by Zan *et al*. (2020). However, Zang *et al*. (2020) worked with operating hours per year of 8140, which is 62.8% higher than the operating hours being worked with in this study. The sensitivity analysis results of Scenario B, displayed in Figure 45, reveals that the MSP of Scenario B would be lower than 1.70 $/kg, when working with operating hours per year of 8140. The better performance of Scenario B is therefore most likely due to the 66.7% higher overall yield.

Table 34: Techno-economic analysis study outcomes obtained for 2,3-BDO from literature

Nr.	Feedstock	MSP (*@IRR*)	Overall	TCI per unit	TPC per unit	Reference
		$/kg	g/g$_{\text{total feed}}$	M$/kg per y	M$/kg	
1	Sugarcane molasses	3.48-4[a](*@10%*)	0.33	2.36-4.26	-	(Koutinas *et al.*, 2016)
2	Brewers' spent grain	4.02(*@15%*)	0.16	6.00	1.74	(Mailaram *et al.*, 2022)
3	Switchgrass	1.70 (*@15%*)	0.12	3.05	2.25	(Zang *et al.*, 2020)
4	A-molasses	1.91 (*@20%*)	0.37	2.73	1.18	This study
5	1G2G feedstock	2.28 (*@20%*)	0.20	4.40	1.14	This study

[a]At the various TCI per unit also indicated for entry 1.

4.2 1,3-Butadiene Biorefinery Scenarios

4.2.1 Material and Energy Balances of the 1,3-BD Scenarios

Figure 46 illustrates the sugar, product and by-product flows, utility usage, installed equipment cost and raw material cost of Scenario C. The intermediate product, 2,3-BDO, is purified in *S300* to 97.25%. The final 1,3-BD product has a purity of >99% and is produced at 22.95 kt/y or 4590 kg/h, which translates to an overall yield from A-molasses of 0.18 g/g$_{\text{feed}}$. A total of 9.18 t/h bagasse is supplied to *S500* and *S800,* which amounts to 30.1% of the total bagasse available from the sugar mill.

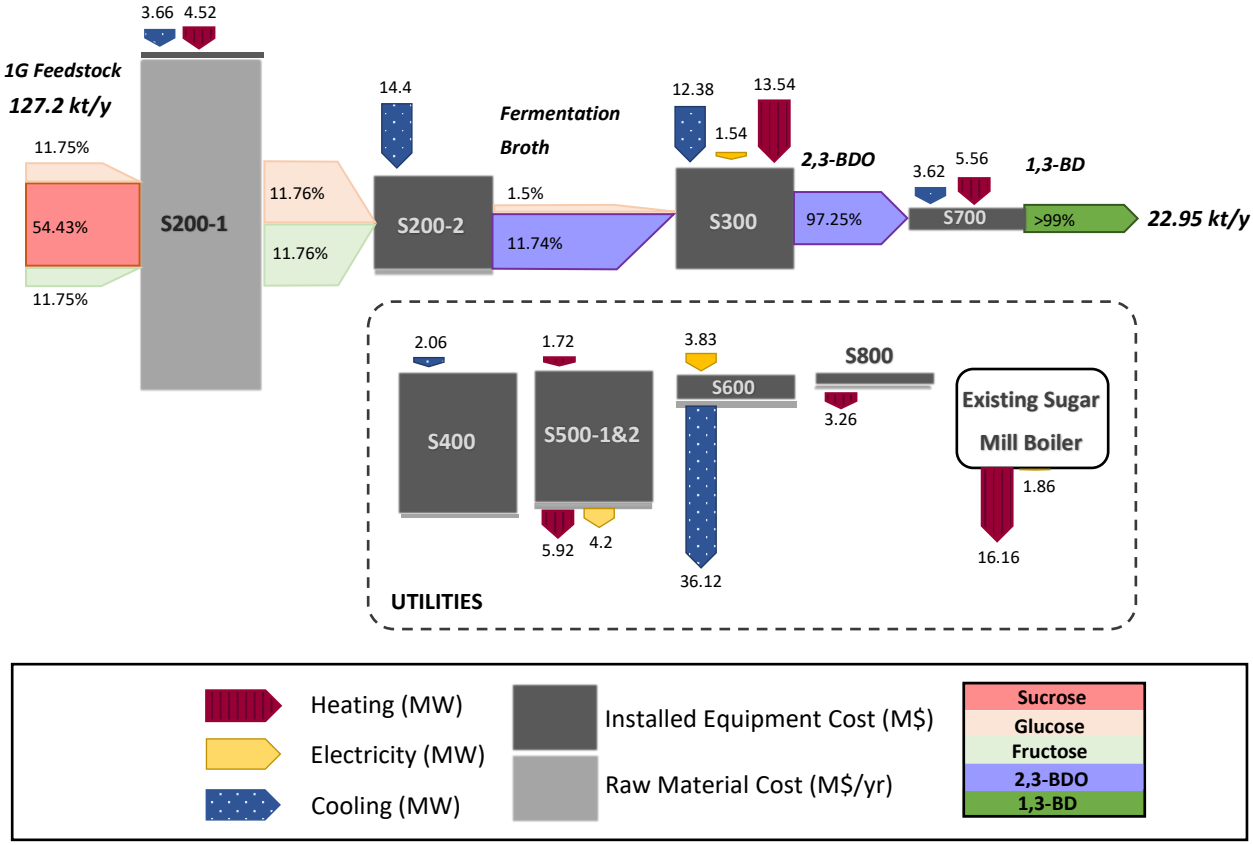

Figure 46: The distribution of Utility usage, Installed Equipment Cost and Raw Material Cost, between the main process sections of Scenario C.

Figure 47 illustrates the sugar, product and by-product flows, utility usage, installed equipment cost and raw material cost of Scenario D. The overall 2,3-BDO fermentation yield achieved from glucose, fructose and xylose is 0.43 g/g_{feed}. The intermediate product, 2,3-BDO, is purified in *S300* to 97.25%. The final 1,3-BD product has a purity of >99% and is produced at 34 kt/y or 6800 kg/h. The overall yield of Scenario D from the 1G2G feedstock is 0.11 g/g_{feed}. Scenario D has a bypass ratio of 39%.

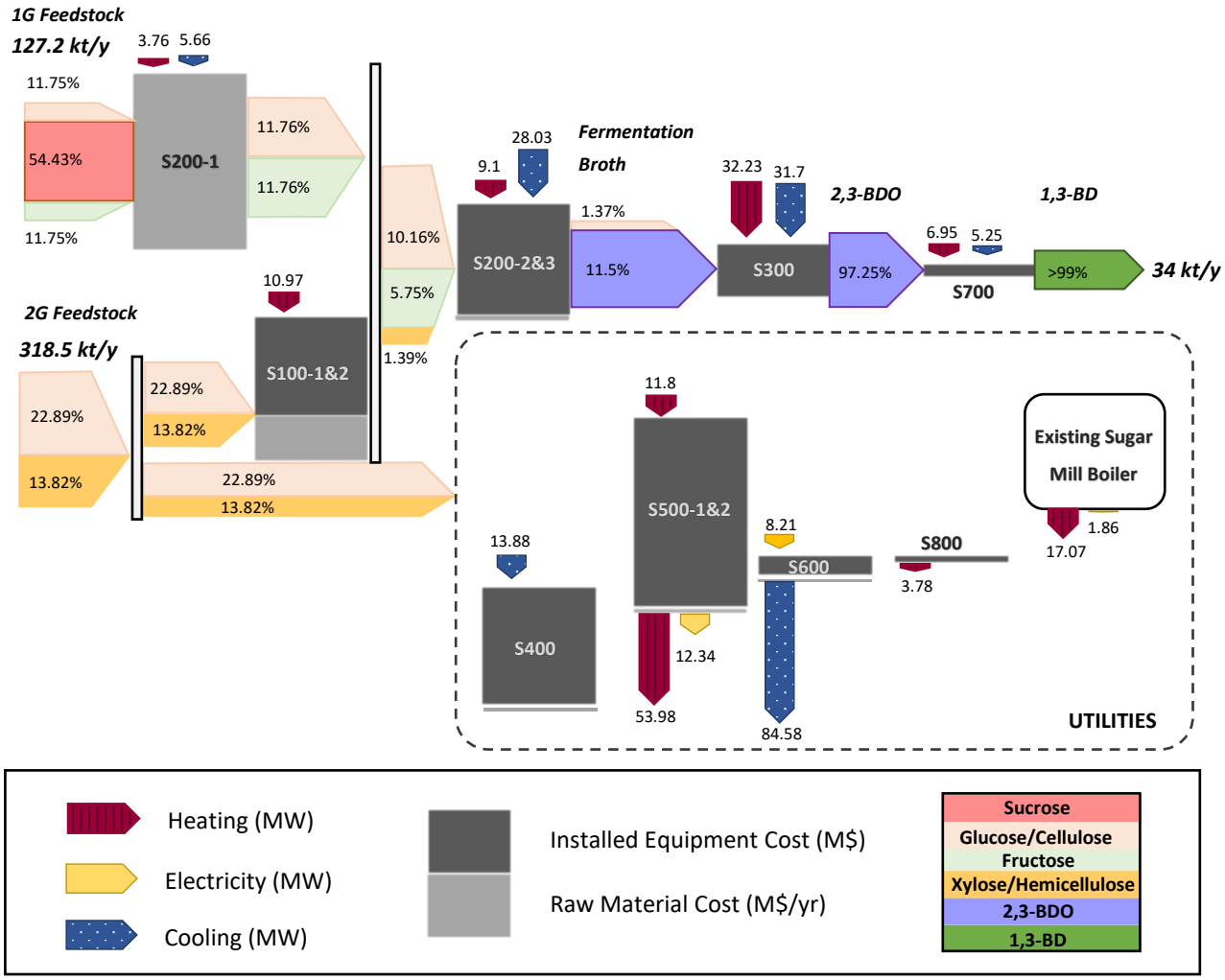

Figure 47: The distribution of Utility usage, Installed Equipment Cost and Raw Material Cost, between the main process sections of Scenario D.

Figure 48 illustrates the sugar, product and by-product flows, utility usage, installed equipment cost and raw material cost of Scenario E. The fermentation broth contains 9.96% ethanol and minor quantities of residual sugars. The 1,3-BD final product is obtained at a purity of >99% and production rate of 13.77 kt/y or 2754 kg/h. The overall yield of Scenario E from A-molasses is 0.11 g/g_{feed}. A total of 11.19 t/h bagasse is supplied to *S500* and *S800,* which amounts to 36.7% of the total bagasse available from the sugar mill.

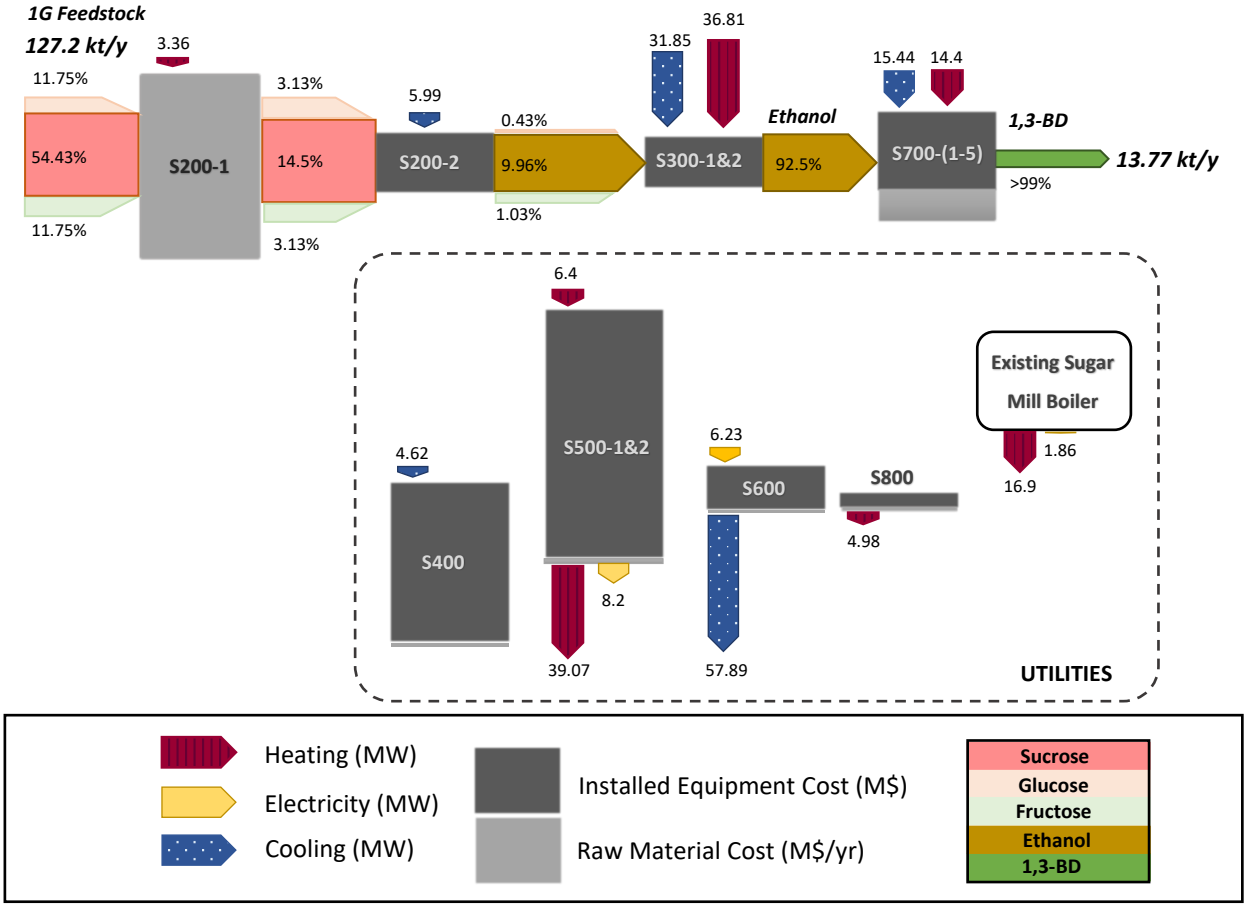

Figure 48: The distribution of Utility usage, Installed Equipment Cost and Raw Material Cost, between the main process sections of Scenario E.

Figure 49 illustrates the sugar, product and by-product flows, utility usage, installed equipment cost and raw material cost of Scenario F. The final 1,3-BD product is obtained at purity of >99% and a production rate of 23.02 kt/y or 4603 kg/h. The overall yield of the process from 1G2G feedstock is 0.07 g/g_{feed}. The bypass ratio of Scenario F is 34%.

In Table 35 the most important material balance information has been summarized for the four 1,3-BD scenarios. The overall yields of Scenario C and D, representing the 1,3-BD production scenarios via the BDO pathway, have yields approximately 1.6 times that of Scenario E and F respectively. This subsequently resulted in higher production rates for Scenario C and D at 22.95 kt/y and 34 kt/y respectively, compared to Scenario E and F at 13.77 kt/y and 23.02 kt/y, respectively. Producing 1,3-BD via the ethanol pathway is evidently less efficient compared to producing 1,3-BD via the 2,3-BDO pathway, based on overall product yields. Furthermore, the overall yields achieved by the 1G2G scenarios (0.11 g/g_{feed} and 0.07 g/g_{feed}) are significantly lower compared to the yields achieved by their 1G counterparts (0.18 g/g_{feed} and 0.11 g/g_{feed}).

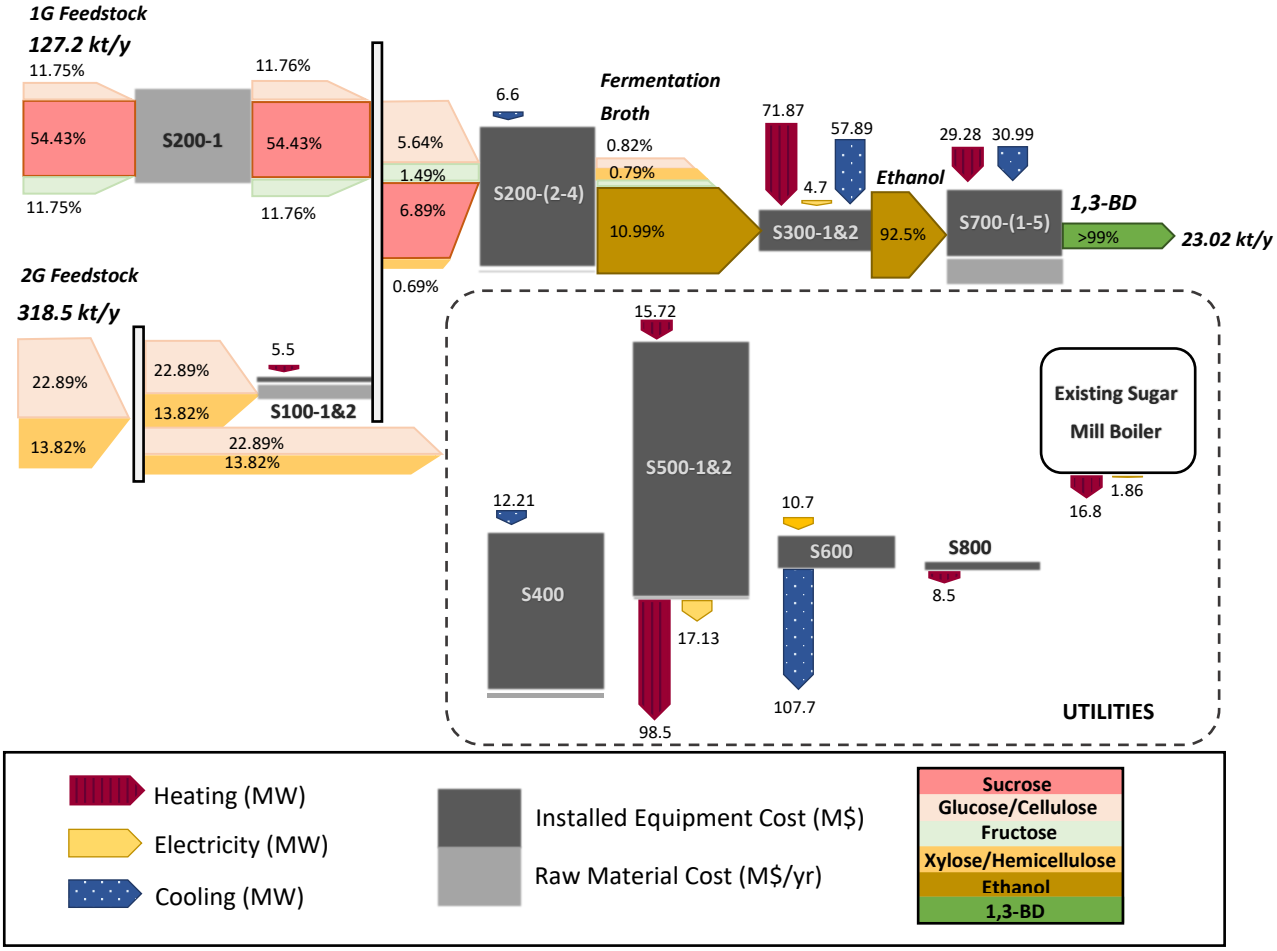

Figure 49: The distribution of Utility usage, Installed Equipment Cost and Raw Material Cost, between the main process sections of Scenario F.

Table 35: Summary of main material balance information for 1,3-BD Scenarios

SCENARIO	PRODUCTION RATE (kt/y)	PURITY (%)	OVERALL YIELD (g/g_{feed})	% BAGASSE OR 2G FEED TO CHP (BYPASS RATIO)	% OF MARKET SHARE
C	22.95	>99	0.18	30.1	0.15
D	34.00	>99	0.11	39.0	0.23
E	13.77	>99	0.11	36.7	0.09
F	23.02	>99	0.07	31.2	0.15

The market volume of 1,3-BD is approximately 15 million tons per year (Brencio *et al.*, 2022; Haque *et al.*, 2021). All of the scenarios have production rates that will contribute <5% to the total 1,3-BD globally produced per year.

Figure 50 presents the utility usage per kg 1,3-BD produced for the various 1,3-BD scenarios. Scenario C is the least energy intensive scenario followed by Scenario D, Scenario E and finally F. Butadiene production via the ethanol pathway is evidently more energy intensive compared to the production of 1,3-BD via the BDO pathway, irrespective of whether 1G or integrated 1G2G feedstock is utilized. In Table 36, Table 37, Table 38 and Table 39 the major heating and cooling consuming pieces of equipment of Scenario C, D, E and F are respectively listed together with their energy requirements.

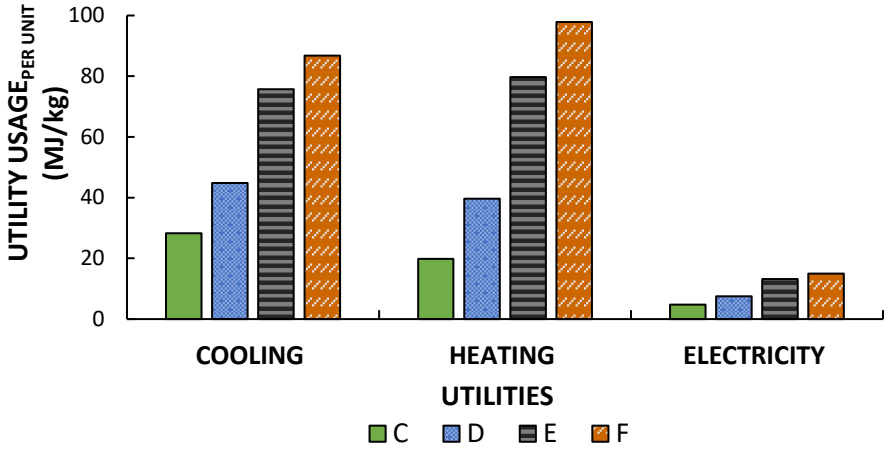

Figure 50: Utility usage per kg product produced for all 1,3-BD Scenarios.

Table 36: Main heating and cooling utility consuming equipment of Scenario C

PROCESS SECTION	EQUIPMENT	HEATING (MW)	COOLING (MW)
S200-2	Fermenter	-	12.24
S300	Heat Exchanger *(HX-07 [a])*	-	7.21
S300	Heat Exchanger *(HX-05 [a])*	-	5.16
S300	Distillation Column	7.29	-
S300	Flash Drum	6.24	-
S200-1	Heat Exchanger	3.66	-

[a] *In Figure 16.*

Table 37: Main heating and cooling utility consuming equipment of Scenario D

PROCESS SECTION	EQUIPMENT	HEATING (MW)	COOLING (MW)
S300	Heat Exchanger *(HX-05 [a])*	-	24.46
S200-2	Fermenter	-	14.96
S400	Heat Exchanger *(HX-01 [b])*	-	13.31
S300	Distillation Column	28.23	-
S100-2	Steam Pretreatment	10.97	-

[a] *In Figure 16.* [b] *In Figure 3*

Table 38: Main heating and cooling utility consuming equipment of Scenario E

PROCESS SECTION	EQUIPMENT	HEATING (MW)	COOLING (MW)
S300-1	Distillation Column 2	23.16	31.46
S300-1	Distillation Column 1	13.66	-

Table 39: Main heating and cooling utility consuming equipment of Scenario F

PROCESS SECTION	EQUIPMENT	HEATING (MW)	COOLING (MW)
S300-1	Distillation Column 2	43.11	56.98
S300-1	Distillation Column 1	25.28	-

From the existing sugar mill boiler, the biorefinery in Scenario C receives 63.78% of its total heating requirements and 30.97% of its total electricity requirements. The remainder of the electricity requirement and 23.34% of the total heating requirements are supplied by *S500*. The final 12.86% heating required is supplied by *S800*, where molten salt at 411°C is produced. The biorefinery in Scenario D

receives 22.8% of the total heating requirements and 13.2% of the total electricity requirements from the existing sugar mill boiler, respectively, whilst the remaining electricity required and 72.14% of the total heating required, is supplied by *S500*. The final 5% of heat is supplied by *S800*.

The existing sugar mill boiler supplies the biorefinery in Scenario E with 27.7% of the total heating requirements and 18.5% of the total electricity requirements. The remaining electricity required and 64.08% of the remaining heating required are supplied by *S500-1&2*. The final 8.2% heat is supplied by *S800*. Finally, Scenario F receives 13.6% and 9.8% of the total heating and electricity requirements from the existing sugar mill boiler. The remaining electricity and 79.5% of the heating requirements are supplied by *S500,* and the final 6.9% heat is supplied by *S800*.

Section 200-2(&3) and Section 300 account for the majority of the cooling utilities of Scenario C and D, with *S300* also accounting for the majority of the heating utilities. The separation and purification of 2,3-BDO is therefore the most energy intensive process step of a 1,3-BD biorefinery, having 2,3-BDO as intermediate product. Similarly, for a 1,3-BD biorefinery with ethanol as intermediate product, the most energy intensive process step is the separation and purification of the intermediate product, ethanol. For Scenario E the cooling and heating requirements are concentrated at *S300-1&2,* accounting for 55% and 60.4% respectively, whilst for Scenario F *S300-1&2* accounts for 53.75% and 58% of the total cooling and heating requirements of the biorefinery, respectively. For both scenario E and F the second most energy intensive process section is *S700*, where ethanol-to-1,3-BD conversion takes place.

The electricity requirements of the four 1,3-BD biorefinery scenarios are concentrated at *S600,* which accounts for 63.2%, 57.7%, 61.6% and 56.3% of the total electricity requirements of Scenario C, D, E and F, respectively. Scenario C does not require refrigeration cooling and *S600* mainly consist of the cooling tower and chilled water tower, whilst for scenario D, E and F the refrigeration cooling system is also contained in S600. The refrigerant system requires 0.714 kW electricity to produce 1 kW of refrigerant, whilst the cooling water and chilled water systems respectively only require 0.084 kW and 0.14 kW per 1 kW cooling utility produced.

In Figure 51 the specific cooling and heating utilities required by each of the 1,3-BD scenarios is presented. The largest utility required for all 1,3-BD scenarios is cooling water. Scenario D is the only 1,3-BD scenario that requires large amounts of HPS. This could explain a 7.8% higher bypass ratio for Scenario D compared with Scenario F, despite the heating and electricity requirements of Scenario F being 65.58% and 39% higher. When HPS is extracted, less electricity is generated in the CEST, compared to when MPS or LPS are extracted. This translates to more HHPS being required for an HPS-intensive process compared to a processes that instead requires more MPS and LPS, to also meet the electricity demand. Greater production of HHPS in the boiler translates then to a larger required bypass ratio.

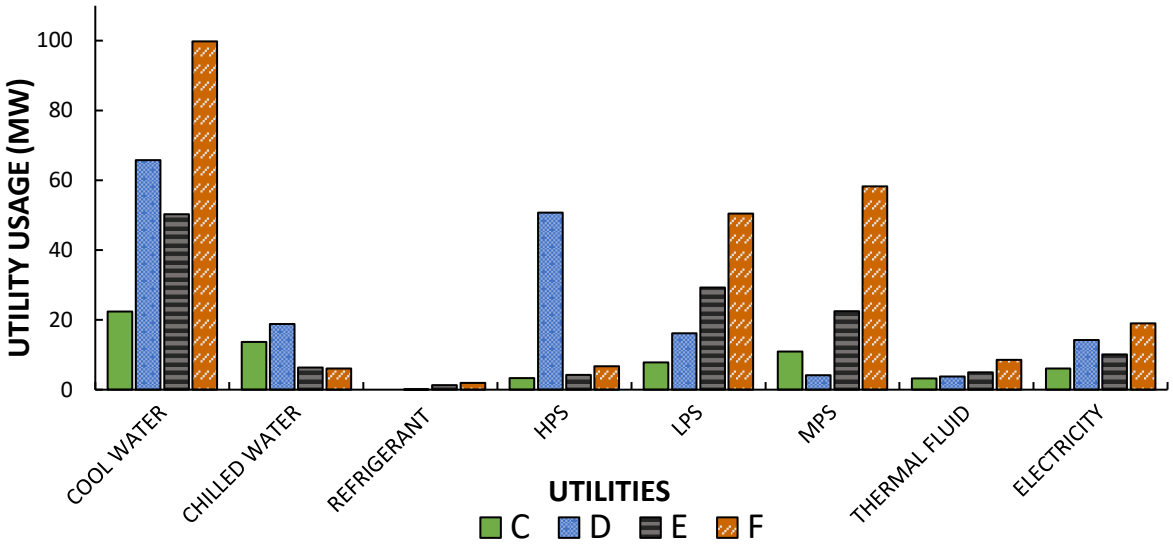

Figure 51: Specific cooling, heating, and electricity usage of all 1,3-BD Scenarios.

From Figure 51 it can be seen that the amounts of thermal fluid required by the scenarios are very low in comparison to the combined remaining heating utilities required, and it is deduced that the amount of bagasse or 2G feedstock sent to S800 does not have a significant impact on the bypass ratio. In addition to the high HPS requirements of Scenario D, another potential explanation for the higher required bypass ratio, is the difference in combustor feed composition to the CHP plant for each scenario, as further discussed below.

The composition of the feed stream to the CHP plant, referred to as the combustor feed stream, has been presented in Table 40 for each scenario. The total flowrate of the combustor feed stream is the highest for Scenario D, with the largest component being bagasse, whilst scenario F has the second largest flowrate, but the highest composition is the waste produced during the production process. The heat obtained from combusting the wastes produced within Scenario F clearly surpassed the larger amount of 2G feed fed to the combustor of Scenario D. Evidently the bypass ratio is not only dependent on the utility demands of a specific scenario but is also highly influenced by the amount of waste produced within a process. The less waste produced, the greater the bypass to meet the required energy needs.

Table 40: Stream Information to CHP Plant of each 1,3-BD Scenario

STREAM COMPONENT	UNIT	SCENARIO			
		C	D	E	F
Total flowrate	t/h	7.26	43.18	10.85	32.86
Bagasse	%	72.00	38.88	49.26	30.53
Brown leaves	%	-	10.33	-	8.11
Biogas	%	21.50	16.33	11.87	11.66
Biomass Sludge	%	3.42	1.35	2.59	1.89
Waste[a]	%	3.05	33.12	36.30	47.80

[a]Produced from within the biorefinery, including components like cellulignin, biomass, residual sugars etc.

Scenario C and D require notably larger quantities of chilled water compared to Scenario E and F. The chilled water utility is primarily utilized to maintain the fermentation reactor temperatures for all 1,3-BD

scenarios. This then translates to the 2,3-BDO fermentation being a more exothermic process compared to the ethanol fermentation, which is confirmed by comparing the heat of formation of each substance, which is -544.8 kJ/mol for 2,3-BDO and -276 kJ/mol for ethanol (Afeefy, Liebman & Stein, n.d.).

4.2.2 Capital Expenditure (CAPEX) of 1,3-BD Scenarios

In Table 41 the capital expenditures are detailed for all 1,3-BD production scenarios. A comprehensive list of capital expenditure components are given in Appendix D. The total installed equipment costs of Scenario E and F respectively, are larger than Scenario C and D. However, the opposite is true of the total installed equipment cost inside the battery limits (ISBL). For the ISBL, the installed equipment cost of Scenario C and D are 24% and 21.4% higher compared to Scenario E and F respectively. This signifies the high capital cost associated with the production of utilities for Scenarios E and F. This implies that producing 1,3-BD via the ethanol pathway will have lower capital costs than via the BDO pathway, but only at a biorefinery that does not produce its own utilities i.e., not energy self-sufficient. This is however not indicative of the economic feasibility of such a scenario considering operational costs will greatly increase due to the purchase of utilities.

Scenarios E and D have similar yields of 0.11 g/g_{feed}. However Scenario E has a 29% higher total capital investment per kg of production. This indicates that for processes operating at similar efficiencies, producing 1,3-BD via the BDO pathway at an energy self-sufficient biorefinery annexed to a sugar mill, requires lower capital costs per kg 1,3-BD, than via the ethanol pathway.

Table 41: Main Capital Expenditures of 1,3-BD Scenarios

CAPITAL EXPENDITURES		**C**	**D**	**E**	**F**
TOTAL INSTALLED EQUIPMENT COST (M$)		76.5	163.0	89.1	169.0
ISBL: INSTALLED COST INSIDE BATTERY LIMITS (M$)		32.1	74.3	26.1	62.1
TOTAL DIRECT COST (TDC) (M$)		86.4	184.0	96.0	186.0
TOTAL INDIRECT COST (M$)		51.9	110.0	57.6	111.8
FIXED CAPITAL INVESTMENT (FCI) (M$)		138.0	294.0	154.0	298.1
TOTAL CAPITAL INVESTMENT (TCI) (M$)		**145**	**308**	**161**	**313**
TOTAL CAPITAL INVESTMENT$_{per\ unit}$	$/kg per year	**6.33**	**9.07**	**11.71**	**13.6**

In Figure 52 the installed equipment cost per kg, of each process section has been illustrated for the 1,3-BD scenarios. The IEC per kg of S500 is the highest for Scenario F, followed by Scenario E, D and finally C. This correlates with the utility usage per kg of the 1,3-BD scenarios, illustrated in Figure 50. Furthermore, *S600* IEC per kg is comparable for Scenario E and F and comparable for Scenario C and D respectively. The aforementioned results illustrate that the heating and electricity requirements of a process has a large impact on capital expenditures, whilst the cooling requirements have a minimal affect.

The higher capital intensiveness associated with the ethanol pathway is most likely due to the high IEC per kg of the catalytic conversion process. This could potentially be due to the catalytic conversion of ethanol to 1,3-BD being a two-step process. The one-step catalytic conversion of ethanol to 1,3-BD has

also been readily researched, however lower yields are achievable compared to the two-step process (Burla *et al.*, 2012). The catalytic conversion of 2,3-BDO to 1,3-BD is a one-step process.

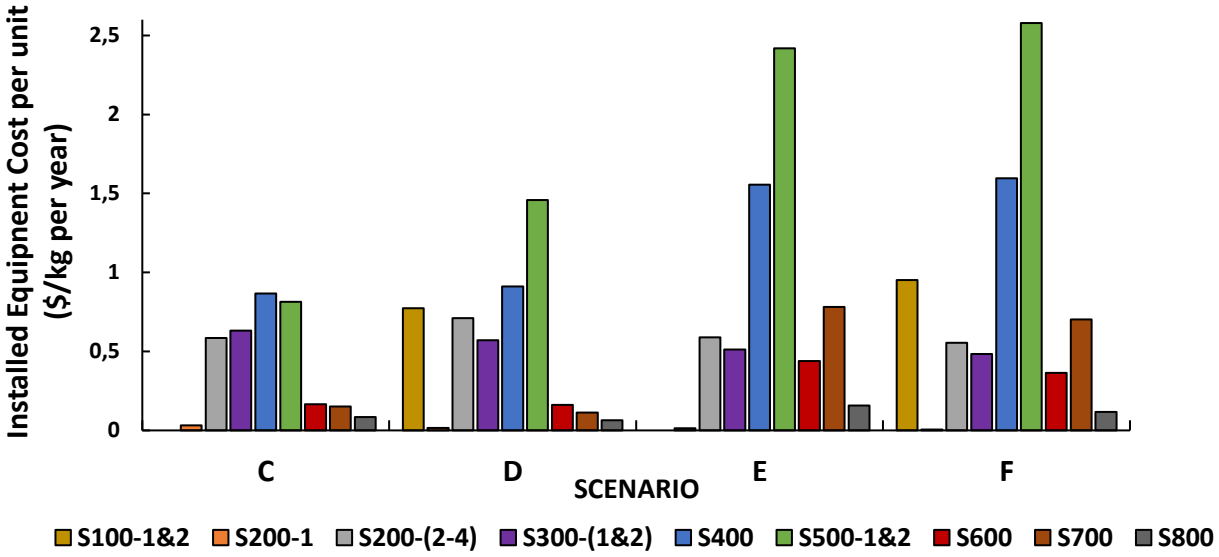

Figure 52: Installed equipment cost per kg product produced per section, for all 1,3-BD Scenarios.

4.2.3 Operational Expenditure (OPEX) of 1,3-BD Scenarios

In Table 42 the operational expenditures of the various 1,3-BD scenarios have been specified. The fixed operating components of each scenario is given in Appendix E. For both pathways economies of scale benefits (in terms of OPEX) have been realized, with Scenario D and F having 7.5% and 16.4% lower TPC values per kg 1,3-BD produced compared to Scenario A and E, respectively.

Figure 53 illustrates the production cost components per kg 1,3-BD produced. The total variable operating cost was represented by its components, i.e., feedstock cost, chemical costs, and waste disposal cost. Raw material costs (feedstock and chemicals costs) is the dominating operational cost for all scenarios, this is similar to what has been reported in literature (Moncada *et al.*, 2018). For Scenario E and F the feedstock cost accounts for the majority of the production cost, whilst for Scenario C and D both the chemical costs and feedstock cost contribute significantly. This is primarily due to the invertase cost dominating the chemical costs of Scenario C and D. Operational cost benefits are evidently associated with employing a microorganism which can naturally hydrolyze sucrose, as is the case for Scenario E and F.

The absolute feedstock costs of Scenario C and E (27.00 and 26.41 M$/year) and of Scenario D and F (30.28 and 30.26 M$/year) are comparable, as specified in Table 42. However the feedstock costs per kg 1,3-BD are significantly higher for Scenario E and F, due to the lower yields and subsequent production rates of these scenarios. This results in a higher production cost per kg 1,3-BD for Scenario E and F compared to Scenario C and D respectively, despite the significant chemical cost reductions resulting from the avoidable invertase cost. This indicates that yield should not be compromised by prioritizing a microorganism that can naturally hydrolyze sucrose.

Table 42: Operational Expenditures of 1,3-BD Scenarios

OPERATIONAL COST COMPONENT	COST (M$/year)			
	C	D	E	F
Fixed Operating Cost	**2.69**	**5.20**	**2.62**	**4.77**
*Feedstock Cost**	*27.00*	*30.28*	*26.41*	*30.26*
Chemical Cost	*23.33*	*33.63*	*5.25*	*9.68*
Waste Disposal Cost	*2.07*	*5.92*	*2.60*	*6.75*
Total Variable Operating Cost	**52.41**	**69.83**	**34.25**	**46.70**
Annual Capital Charge	-	0.01	-	-
Total Production Cost (TPC)	**55.10**	**75.04**	**36.87**	**51.89**
TPC per unit ($/kg per year)	**2.40**	**2.22**	**2.69**	**2.25**

*Includes all bagasse and brown leaves from harvesting residues, even portion sent to CHP plant is regarded as feedstock cost

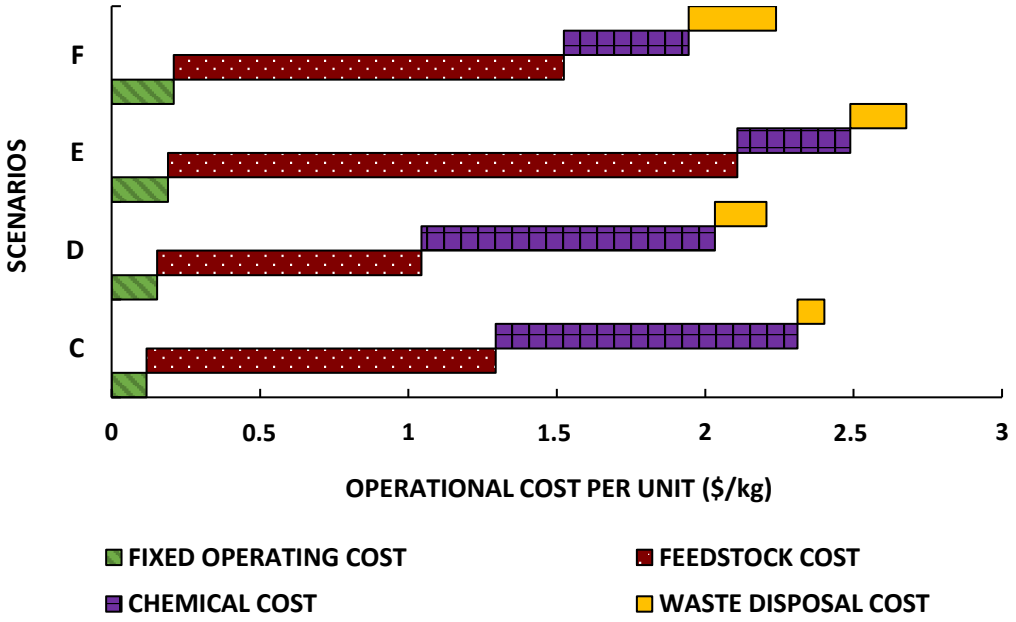

Figure 53: Operational cost components per kg product produced for 1,3-BD Scenarios.

4.2.4 Economic parameters of 1,3-BD Scenarios

The MSPs of the 1,3-BD scenarios have been determined as 4.08 $/kg, 4.55 $/kg, 5.71 $/kg and 5.72 $/kg for Scenario C, D, E and F respectively. According to the writer a distinct bio-based 1,3-BD market is yet to be established and therefore all market prices found from literature represent the fossil-based market price. The market price of 1,3-BD has been obtained from a number of sources as 1.05 $/kg (2019), 0.8 $/kg (2017), 1.53 €/kg (average from previous 10 years) and 0.9 €/kg (2014) translating to 1.56 $/kg and 0.92 $/kg at an assumed exchange rate of 1.02 euros to dollars (Cabrera Camacho *et al.*, 2020; Farzad, Mandegari & Görgens, 2017; Fernandez, 2020; Moncada *et al.*, 2018). For this study a 1,3-BD market price of 1.05 $/kg was assumed appropriate because it was obtained for the specific reference year. All 1,3-BD scenarios have a higher MSP than the fossil-based market price, irrespective of what source is used. This conveys that all the 1,3-BD biorefinery scenarios developed in this study are unprofitable compared to the fossil-based production of 1,3-BD.

The results found in this study confirm that producing bio-based 1,3-BD is more costly than producing fossil-based 1,3-BD, which, in all likelihood, is the reason why a distinct bio-based market has not yet been established. The results also indicates that a large green premium exists for 1,3-BD, at an average of approx. 4 $/kg for the four 1,3-BD scenarios investigated in this study. Farzad, et al. (2017) similarly found a high 1,3-BD green premium of 2.14 $/t.

The MSP values determined for the 1,3-BD scenarios via the BDO pathway are lower compared to the ethanol pathway. This concludes that, from an economic perspective, producing 1,3-BD via the BDO pathway is a better investment. More specifically, producing 1,3-BD via the BDO pathway, at a biorefinery annexed to an existing sugar mill, utilizing 1G feedstock available from the sugar mill, is the best investment option. The key to improving the economics of Scenario E and F could lie in improving the catalytic conversions (50% and 44.5%) and selectivities (92% and 55%) which will lead to higher production rates that can counteract the high capital costs associated with catalytic conversion of ethanol to 1,3-BD.

Furthermore, the MSPs of Scenarios E and F are comparable, whilst the MSP of Scenario D is higher than its counterpart, Scenario C. These results indicate that producing 1,3-BD via the ethanol pathway from both 1G and 1G2G feedstock available at a sugar mill, will be a similarly-attractive investment. These results are beneficial considering 1,3-BD production at a biorefinery can be scaled up by combining 2G feedstock with 1G feedstock, while providing similar returns on investment, albeit with a larger capital cost investment. The feasibility of the biorefinery is however subject to the profitability of the scenarios.

Scenario E has a 13.9% lower TCI per kg compared to Scenario F yet has an 18.76% higher TPC per kg, which explains the comparable minimum selling price determined for the scenarios. The higher TPC per kg of Scenario E has previously been established to be attributed to the higher feedstock cost per kg 1,3-BD produced, which is a reoccurring observation made for the 1G scenarios investigated in this study.

4.2.5 Sensitivity analyses of the 1,3-BD scenarios

The results of the sensitivity analyses conducted for each 1,3-BD scenario, can be found in Figures 54-57. Parameters investigated for all scenarios are the fixed operating cost (FOC), feedstock cost/price, fixed capital investment (FCI), total production cost (TPC) and operating hours per year of the plant. Evidently, the assumed market price of 1,3-BD at 1.05 $/kg was not added to Figure 54-57, considering it is notably lower than any MSP values determined during the sensitivity analyses of Scenario C, D, E and F and it would have been redundant to do so. For Scenarios C and D, an additional parameter, the invertase price was investigated and for Scenario E and F, the production rate was additionally included. The production rate was not investigated for Scenarios C and D, because the fermentation yield of approximately 0.45 $g/g_{total\ sugars}$ is 90% of the theoretical yield, in addition to the selectivity and conversion of the catalytic process being >91.9% and >99.9% respectively, little room is available for improvement to the overall yield (Tsukamoto *et al.*, 2016).

A 30% change in operating hours had the largest impact on the MSP, whilst changes in the fixed operating cost had the smallest impact. Specifically for Scenario E and F, a 30% change in production rate, which

would materialize following a change in overall yield, has a similar effect on the MSP to the operating hours. The overall yield of Scenario E and F can only be improved by adjusting the catalyst selectivity and conversion, considering the ethanol fermentation yield is already close to the theoretical yield of 0.51 $g/g_{consumed\ sugars}$ (Moncada *et al.*, 2018). Comparing the effect that a 30% change in TCI and TPC have on the MSP of each scenario, it is evident that for Scenario C, E and F, a change in TPC has a larger effect on the MSP. As for Scenario D, a change in TCI has a larger effect on the MSP, which could potentially be due to Scenario D having the lowest TPC per kg of all the 1,3-BD scenarios.

Nevertheless, changing any of the abovementioned parameters by 30% does not bring the MSP values of any of the 1,3-BD scenarios close the market price of 1.05 $/kg. Scenario C with operating hours of 6500 per year comes closest to the fossil-based market price at 3.14 $/kg, which is still 200% higher. By increasing the operating hours per year of Scenario C to the maximum hours per year of 8760, the MSP is still 120% higher than the market price. This means that a number of parameters will need to drastically change for the MSP to reach the market price, which is highly unlikely. Similar results were obtained by Moncada, et al., (2018) and Farzad, et al. (2017), where the former obtained MSP values which were approximately 380% higher than the market price used of 0.9 €/kg and a 100% increase in production rate still resulted in an MSP 330% higher than the assumed market price. For the latter, a 267.5% higher MSP was determined than the market price used in the study of 0.8 $/kg, and increasing the operating hours from 6480 h to 7920 h still resulted in an MSP which is 155.6% higher than the market price (Farzad, Mandegari & Görgens, 2017).

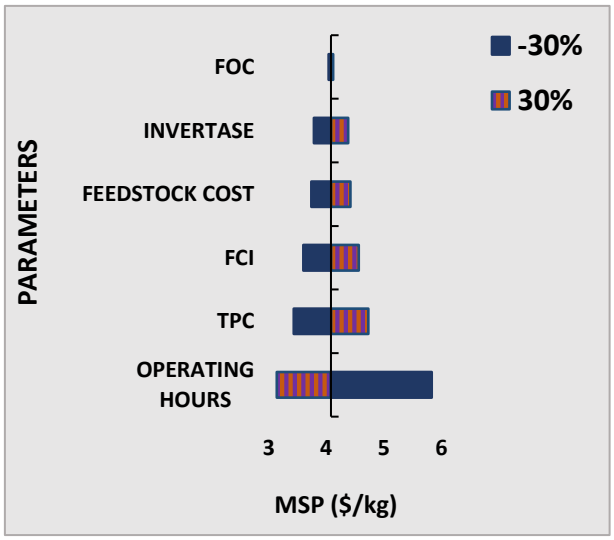

Figure 54: Sensitivity Analysis Results for Scenario C

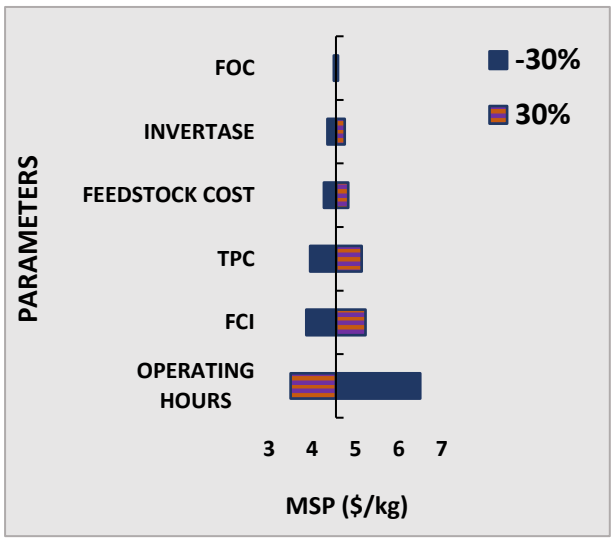

Figure 55: Sensitivity Analysis Results for Scenario D

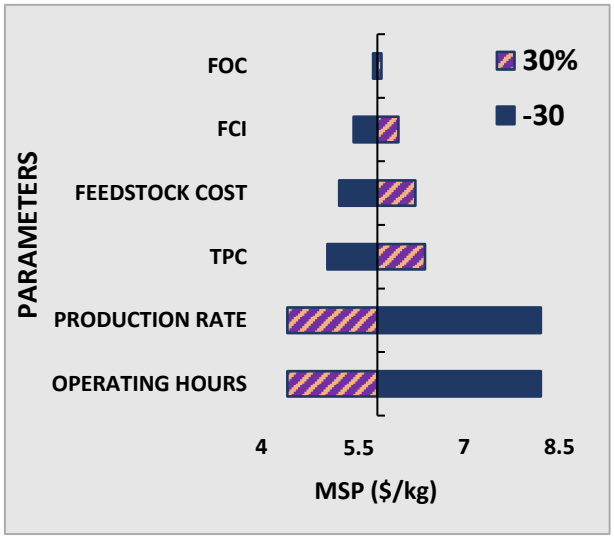

Figure 56: Sensitivity Analysis Results for Scenario E

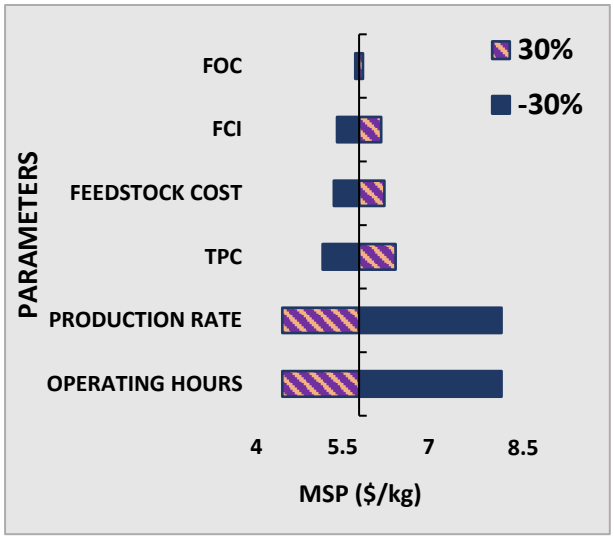

Figure 57: Sensitivity Analysis Results for Scenario F

4.2.6 Techno-economic comparison of 1,3-BD scenarios to other bio-based processes

In Table 43 various techno-economic analysis study results found in literature, were specified. The various studies investigated the economic feasibility of producing 1,3-BD from a range of different feedstock.

A study omitted from Table 43 tested the economic feasibility of producing 1,3-BD from purchased 2,3-BDO. Instead of determining a minimum selling price of 1,3-BD for which the process will be economically feasible, they determined what minimum price of 2,3-BDO is required to obtain a profitable process. The minimum 2,3-BDO price was determined to be 0.991-1.3 $/kg (Song, Yoon, *et al.*, 2018). This validates the high MSPs obtained for Scenario C and D. From the results obtained for Scenario A and B, it is known that the production of 2,3-BDO costs 1.914 - 2.27 $/kg, which is higher than the minimum 2,3-BDO price stipulated by Song, et al., (2018).

The overall yields of the remaining entries in Table 43 are all similar to the yields obtained for the 1,3-BD scenarios in this study. Furthermore, the MSPs of the entries in Table 43 are all lower than the MSPs determined for Scenario C, D, E and F, which could be due to a number of factors. Factors can include, but are not limited to, this study having a higher desired IRR of 20%; the feedstock cost of A-molasses being higher, especially in comparison with Farzad *et al*., (2017) and more cost-effective pretreatment and enzymatic hydrolysis options being available for sugar extraction from corn stover, and poplar wood could be one factor.

Table 43: Techno-economic analysis study outcomes obtained for 1,3-BD from literature

Nr.	Feedstock (*Flowrate*)	MSP (*@IRR*)	Overall Yield	TCI per unit	TPC per unit	Reference
	(*kt/y*)	$/kg	g/g	M$/kg per y	M$/kg	
1	C6 sugars (*200*)	4.46[a] (*@10%*)	0.12	5.42	4.07	(Moncada *et al.*, 2018)
2	2G feedstock[b] (*337*)	2.94 (*@12%*)	0.09	13.25	0.72	(Farzad, Mandegari & Görgens, 2017)
3	Corn Stover (*657*)	1.32 (*@10%*)	0.15	-	-	(Phillips, Jones, Meyer, *et al.*, 2022)
4	Poplar Wood (*2000 tpd*)[c]	1.15 (-)	0.15	-	-	(Cheali, Posada, Gernaey, *et al.*, 2016)
5	A-molasses	4.08 (*@20%*)	0.18	6.33	2.40	This study
6	A-molasses	4.55 (*@20%*)	0.11	9.07	2.22	This study
7	1G2G feedstock	5.71 (*@20%*)	0.11	11.71	2.69	This study
8	1G2G feedstock	5.72 (*@20%*)	0.07	13.60	2.25	This study

[a]Converted to US dollar using an assumed exchange rate of 1.02 € to US$. [b]Sugarcane bagasse and Brown leaves, similar to what has been used in this study. [c]No information was found regarding the operating hours per year.

4.3 Polyhydroxybutyrate Biorefinery Scenarios

4.3.1 Material and Energy Balances of the PHB Scenarios

Figure 58 illustrates the sugar, product and by-product flows, utility usage, installed equipment cost and raw material cost of Scenario G. The PHB fermentation yield achieved from glucose and fructose in *S200-2* is 0.155 $g/g_{total\ sugars}$. The fermentation broth consists – in almost equal parts – of PHB, glucose, fructose, and acetic acid. The fermentation process resulted in 34% unconverted sugars. The intracellularly produced PHB is separated and purified in *S300* to a purity of >99%. The final PHB product is produced at a production rate of 15.37 kt/y or 3074 kg/h. The overall yield of Scenario G from A-molasses is 0.12 $g/g_{total\ sugars}$.

Scenario G overall has low utility requirements and subsequently has no need for a new CHP plant: All of the steam required is obtained from the existing sugar mill boiler. In the CEST (*S500*), the HPS from the sugar mill is used to produce the MPS, LPS and electricity required by the process. The electricity produced in the CEST unit of Scenario G is however insufficient and a gas engine was designed to produce the remainder of the electricity required. The gas engine only required 10% of the biogas produced in the WWT plant. The remaining, unused portion of the biogas, which primarily consist of greenhouse gases such as CH_4 and CO_2, is flared thereby only releasing CO_2 into the atmosphere which has a lower environmental impact compared to CH_4. Alternatively, biogas can be bottled and sold, however this option was not considered in this study.

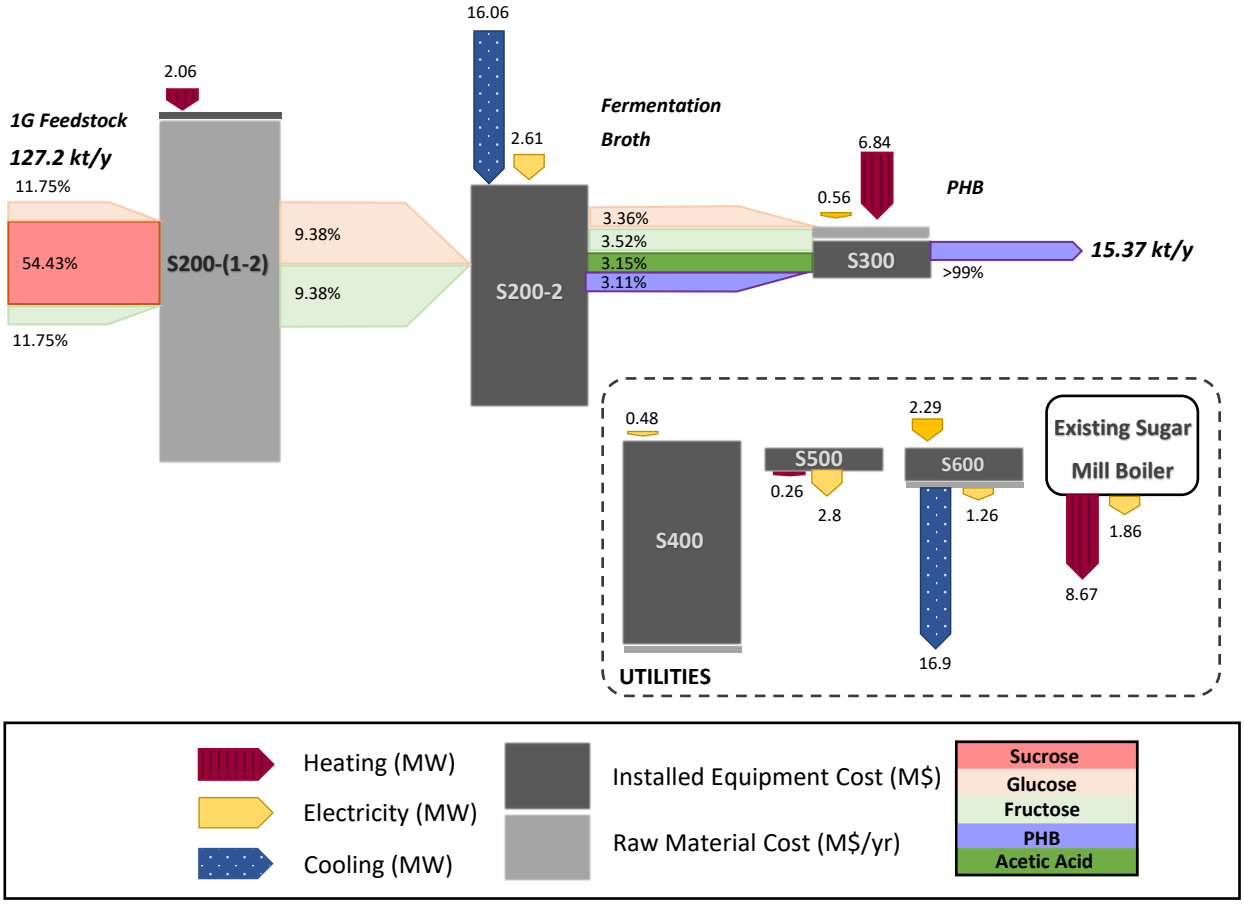

Figure 58: The distribution of Utility usage, Installed Equipment Cost and Raw Material Cost, between the main process sections of Scenario G.

Figure 59 illustrates the sugar, product and by-product flows, utility usage, installed equipment cost and raw material cost of Scenario H. The PHB fermentation yield achieved from glucose and fructose in *S200-2* is 0.155 g/$g_{total\ sugars}$. Xylose from the hemicellulose hydrolysate is not utilized for fermentation. The fermentation broth contains equal amounts of PHB and acetic acid and almost twice the amount of glucose than PHB, indicating an inefficient fermentation process. PHB at a purity of >99% is produced in *S300* at a production rate of 23.36 kt/y or 4671 kg/h. The overall yield of Scenario H from 1G2G feedstock is 0.05 g/g_{feed}. The bypass ratio of Scenario H is 0%. Due to the low utility requirements of Scenario H, the biogas produced in *S400* is sufficient for combustion in the CHP plant. Only 45% of the biogas is used, whilst the remainder is flared. The existing sugar mill boiler supplies Scenario H with 50.25% and 15% of the total heating and electricity requirements and the remaining electricity and heating required are produced in *S500*.

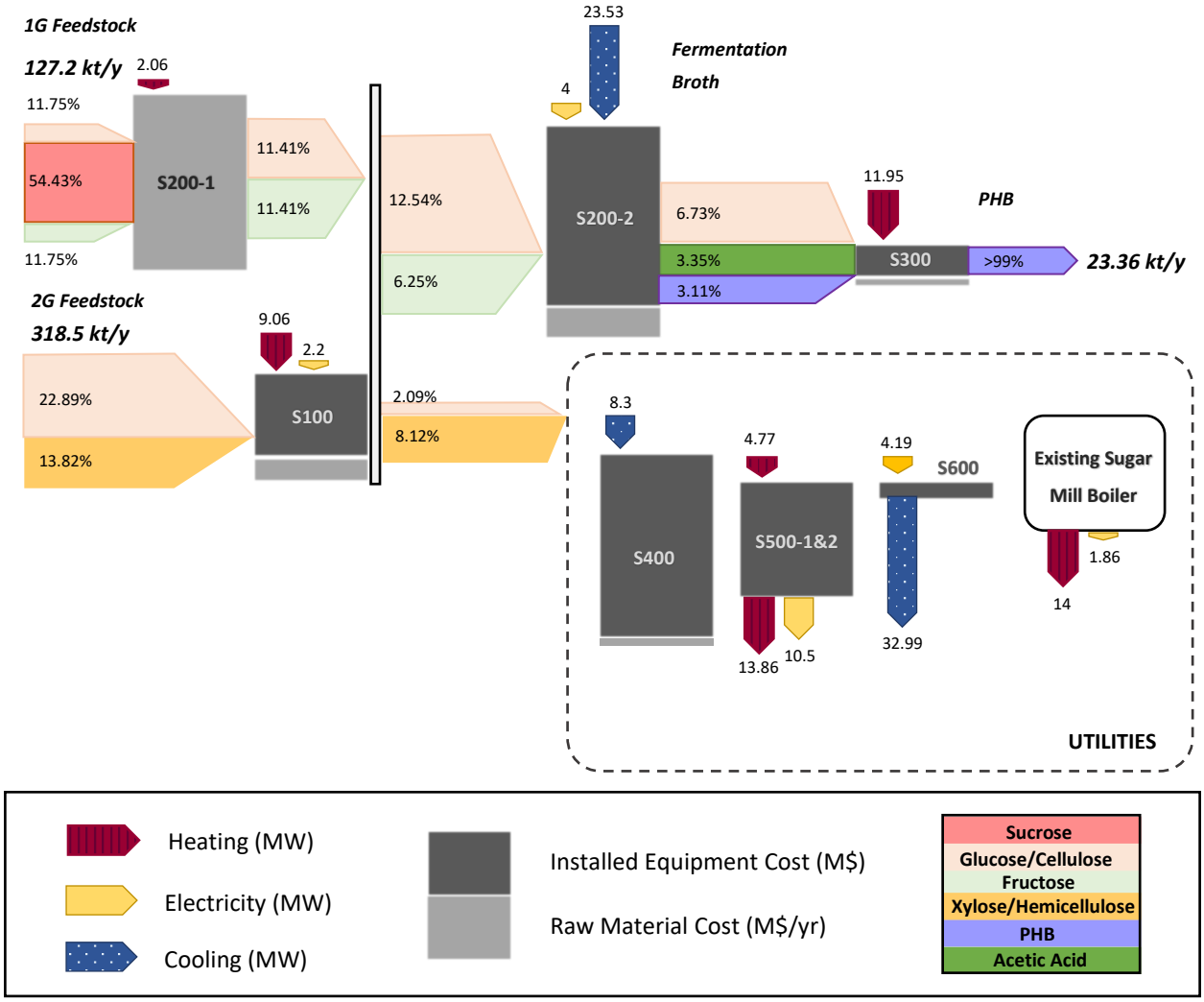

Figure 59: The distribution of Utility usage, Installed Equipment Cost and Raw Material Cost, between the main process sections of Scenario H.

A summary of the main material balance information of the PHB scenarios is represented in Table 44. The overall yield of Scenario H is almost 60% lower compared to Scenario G. This is indicative of the lower efficiency of a 1G2G biorefinery and furthermore the significantly low efficiency experienced when a 1G2G biorefinery does not utilize the hemicellulose hydrolysate.

The current PHB market volume is approximately 40 kt/y (Price *et al.*, 2020a; Saratale *et al.*, 2021). The yearly production rates of Scenario G and H are 38.4% and 58.4% of the global PHB yearly production, indicating the maximum amounts that can be produced by one typically-sized sugar mill. This is highly unrealistic for implementation to the PHB market, considering it will lead to a substantial oversupply. However, similar to what has previously been done in literature, Scenario G and H could instead be considered for introduction into the larger bioplastics market of 4 million tons per year, where their contribution will have little to no effect on the global production volumes (Nieder-Heitmann, 2019). The feasibility of introduction into the bioplastics market will depend on how the production cost of PHB in Scenario G and H compare to the production costs of bioplastics.

Table 44: Summary of main material balance information for the PHB Scenarios

SCENARIO	PRODUCTION RATE (kt/y)	PURITY (%)	OVERALL YIELD (g/g_{feed})	% BAGASSE* OR 2G FEED# TO CHP (BYPASS RATIO)	% OF MARKET SHARE
G	15.37	>99	0.12	0	38.4
H	23.36	>99	0.05	0	58.4

*Applies to 1G Scenarios, #Applies to 1G2G Scenarios

To compare the utility usage of each process in relation to the respective capacities, Figure 60 is presented. Per kg product produced, Scenario G requires 28%, 105% and 37% less cooling, heating and electricity compared to Scenario H. The main cooling, heating and electricity consuming equipment of Scenario G and H have respectively been tabulated in Table 45 and

Table *46*. Considering two of the entries in

Table *46* are associated with pretreatment, enzymatic hydrolysis (*S100*) and the CHP plant (*S500*), the higher utility consumption per kg is most likely due to the additional processes required for Scenario H.

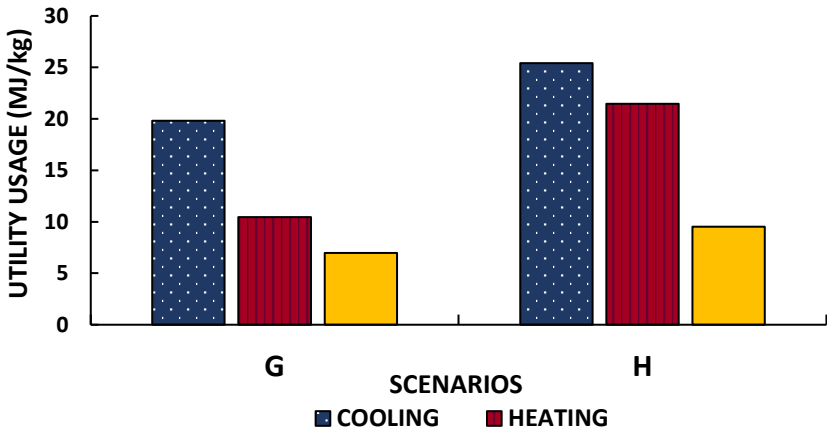

Figure 60: Utility usage per kg product produced for the PHB Scenarios

The cooling requirements are highly concentrated at *S200-2* for both Scenario G and H. The heating requirements of Scenario G are concentrated at *S300* and for Scenario H, S300 and S100 both account for the majority of the heating requirements. The main electricity consuming sections for both Scenario G and H are *S200-2* and *S600*.

Table 45: Main heating and cooling utility consuming equipment of Scenario G

PROCESS SECTION	EQUIPMENT	COOLING (MW)	HEATING (MW)	ELECTRICITY (MW)
S200-2	Fermenter	12.42	-	-
S200-2	Heat Exchanger	1.83	-	-
S300	Spray Dryer	-	5.83	-
S200-1	Heat Exchanger	-	2.06	-
S300	Alkaline Digester	-	1.01	-
S200-2	Compressors	-	-	2.56
S600	Chilled Water Package	-	-	1.79

Table 46: Main heating and cooling utility consuming equipment of Scenario H

PROCESS SECTION	EQUIPMENT	COOLING (MW)	HEATING (MW)	ELECTRICITY (MW)
S200-2	Fermenter	18.66	-	-
S400	Heat Exchanger	7.08	-	-
S300	Spray Dryer	-	10.22	-
S100	Pretreatment	-	8.23	-
S500-1	Heat Exchanger	-	3.42	-
S200-2	Compressor	-	-	3.88
S600	Chilled Water Package	-	-	3.19

Figure 61 compares the total utility usage per kg of the various process section comprising Scenario G and H. Section 200-2 is the most energy intensive section for both scenarios. From Table 45 and

Table *46* it is evident that the two main equipment responsible for the energy intensity of S200-2 are the fermenters, which require chilled water, and the compressors that require electricity. The compressors in S200-2 are responsible for air sparging at 0.5 vvm, considering PHB fermentation is aerobic. The high cooling requirements and electricity requirements associated with an aerobic fermentation process is readily known (Davis *et al.*, 2018).

The utility consumption of S100 is significant, especially considering the section utility consumption per kg of Scenario G (excl. S200-2). The processing of 2G feedstock contributes 15.4% to the total utility requirements of Scenario H, highlighting the benefits of utilizing 1G feedstock which requires little to no processing prior to fermentation.

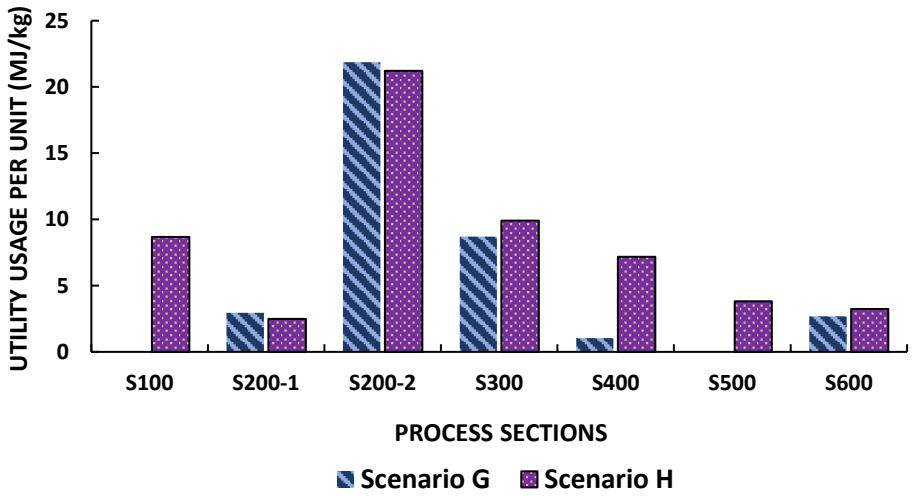

Figure 61: Utility usage per kg product produced of the various process sections making out the PHB Scenario

4.3.2 Capital Expenditure (CAPEX) of PHB Scenarios

In Table 47 the capital expenditures of the PHB scenarios are specified. The full set of capital expenditures are available in Appendix D. The total capital investment per kg product PHB produced of Scenario H is 1.3 times the TCI per kg of Scenario G. Economies of scale benefits are therefore not realized for Scenario

H. A potential factor could be that the hemicellulose from pretreatment is not utilized for product formation, which would have resulted in higher production rates. However, as observed with other products in this paper, the processing of hemicellulose hydrolysate is an energy intensive process which could potentially outweigh the production increase benefits.

Table 47: Main Capital Expenditures of the PHB Scenarios

CAPITAL EXPENDITURES		**G**	**H**
TOTAL INSTALLED EQUIPMENT COST (M$)		80.71	161.56
ISBL: INSTALLED COST INSIDE BATTERY LIMITS (M$)		40.72	78.43
TOTAL DIRECT COST (TDC) (M$)		89.87	179.20
TOTAL INDIRECT COST (M$)		53.92	107.53
FIXED CAPITAL INVESTMENT (FCI) (M$)		143.80	286.73
TOTAL CAPITAL INVESTMENT (TCI) (M$)		**150.99**	**301.07**
TOTAL CAPITAL INVESTMENT$_{\text{per unit}}$	$/kg per year	**9.82**	**12.89**

All installed equipment costs are higher, per section, for Scenario H, except for *S600* containing all other utilities apart from the WWT plant and the CHP plant. The higher cost of *S600* can be ascribed to the capital cost of the gas engine, which is present in Scenario G and not in H. The gas engine installed equipment cost is 39.1% of the total *S600* installed equipment cost for Scenario G.

Figure 62 illustrates the IEC per kg of the various process sections comprising Scenario G and H. Sections 200-2 and 400 account for the highest capital cost for both PHB scenarios. The high capital costs of a WWT plant is readily known (Humbird *et al.*, 2011). The high capital cost associated with PHB production (*S200-2*) can be attributed to the aerobic nature of the fermentation process. Smaller fermenters are required for aerobic fermentation compared to microaerobic or anaerobic fermentation, to properly maintain the required oxygen levels. This leads to the requirements of large quantities of fermenters, increasing the capital cost significantly due to economy of scale penalties. The high capital costs associated with PHB fermentation as well as aerobic fermentation in general has similarly been found in literature (Davis *et al.*, 2018; Kachrimanidou *et al.*, 2021).

From Figure 62 it is evident that the higher TCI per kg of Scenario H can be attributed to the higher utility usage per kg PHB, translating to a larger CHP plant per kg PHB, as well as the requirement of pretreatment and enzymatic hydrolysis. The IEC per kg of *S600* is higher for Scenario G due to the capital cost of the gas engine being accounted for on this section. The capital cost of the gas engine is however not significant in comparison to other utility generating equipment.

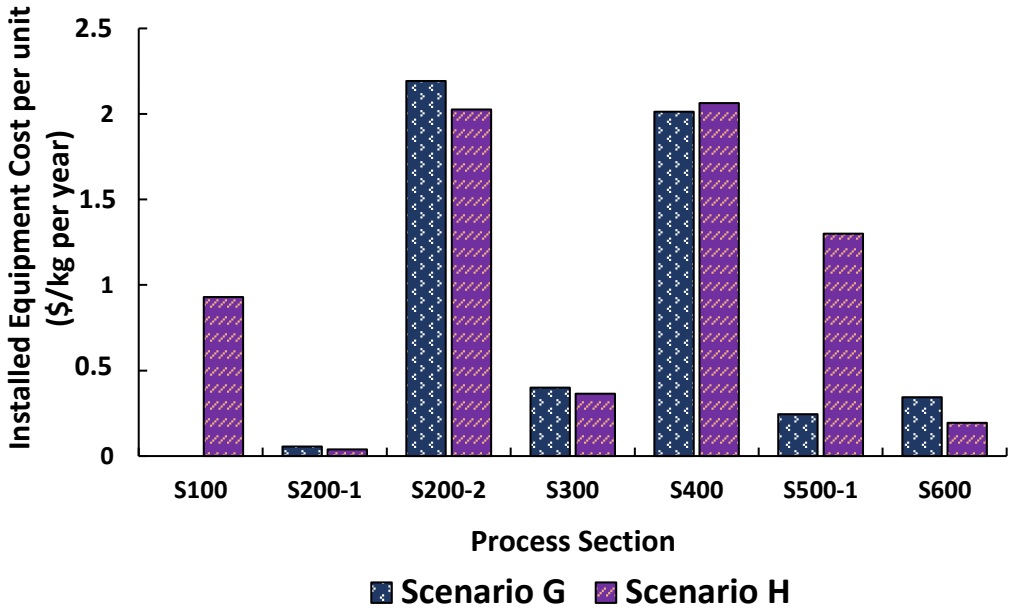

Figure 62: Installed equipment cost per kg product produced per section, for the PHB Scenarios.

4.3.3 Operational Expenditure (OPEX) of PHB Scenarios

Table 48 is a summary of the main operational expenditures of the PHB scenarios. A breakdown of the fixed operating costs of each individual scenario can be found in the Appendix E. For Scenario H economies of scale benefits (in terms of OPEX) have been realized, having a TPC per kg which is 7.7% lower compared to that of Scenario G.

Figure 63 illustrates the production cost components per kg PHB produced for Scenario G and H. The total variable operating cost was represented by its components, i.e., feedstock cost, chemical costs, and waste disposal cost. The feedstock and chemical cost are the main production cost constituent for both scenarios, with the latter being the larger of the two. The chemical costs for both scenarios consist mainly of invertase, specifically 71.8% and 61.19% for Scenario G and H respectively. The second largest chemical cost component for both scenarios is the NaH_2PO_4 component of the fermentation medium, contributing 10% and 13% respectively.

Table 48: Operational Expenditures of the PHB Scenarios

OPERATIONAL COST COMPONENT	**COST (M$/year)**	
	G	**H**
Fixed Operating Cost	**2.92**	**5.60**
*Feedstock Cost**	*25.64*	*30.28*
Chemical Cost	*30.23*	*35.47*
Waste Disposal Cost	*5.37*	*18.75*
Total Variable Operating Cost	**61.24**	**84.50**
Total Production Cost (TPC)	**64.17**	**90.10**
TPC per unit ($/kg per year)	**4.18**	**3.86**

*Includes all bagasse and brown leaves from harvesting residues, even portion sent to CHP plant is regarded as feedstock cost

The waste disposal cost of Scenario H is significantly higher compared to Scenario G. It is known that a 1G2G biorefinery will produce larger quantities of solid wastes compared to a 1G process due to the cellulignin being produced during pretreatment. However, this waste is not sufficiently utilized in Scenario H, as has been done for the other 1G2G processes investigated in this study. This is due to biogas from WWT being sufficient feedstock to the CHP plant, most likely attributed to the large quantities of sugars from the unused hemicellulose hydrolysate as well as the residual sugars from fermentation being sent to the WWT plant. Nevertheless, the reduction in production cost will be far outweighed by the capital costs of a larger CHP plant if the solids wastes were instead used for combustion.

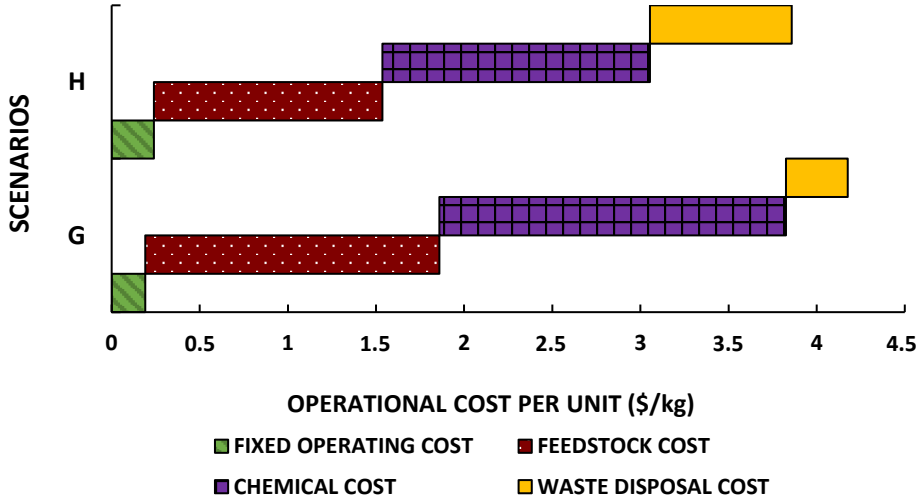

Figure 63: Operational cost components per kg product produced for the PHB Scenarios.

4.3.4 Economic parameters of PHB Scenarios

The MSPs of the PHB scenarios have been determined as 6.81 $/kg and 7.23 $/kg for Scenario G and H respectively. The market price of PHB has been obtained from a number of sources, which vary vastly in reported price. The prices obtained ranged from as low as 4.4 $/kg (2008) to as high as 11.42 $/kg (2016), with an intermediate (Int) price of 6.5 $/kg (2015) (Directorate-General Energy, 2015; Nieder-Heitmann, 2019). Furthermore, large fluctuations in the PHB price have been observed over the past 20 years, with PHB Industrial S/A Company selling PHB at 12.5-15 $/kg in 2003, which greatly reduced to 3.12-3.75 $/kg in 2010 (Posada, Naranjo, López, *et al.*, 2011). Considering PHB, and PHAs in general, are niche materials, a higher market price is definitely to be expected. Furthermore, a higher selling price can be justified for PHB with a high purity (>99%) because it can be used for biomedical applications (Khanna & Srivastava, 2005). Considering the average of the aforementioned market prices (adjusted for 2019) is approximately 7.6 $/kg, this has been assumed an appropriate reference market price. With regards to the assumed market price, both Scenario G and H are profitable. However, a low confidence level is associated considering the MSPs determined for the respective scenarios are only 11.6% and 5% lower than the assumed market price.

Previously mentioned is the potential of introducing PHB into the bio-plastics market, due to the small current market size of PHB. The market price of the most common bioplastic, polylactic acid (PLA) is

however as low as 2.2 $/kg (2015) (Directorate-General Energy, 2015). The high MSP of Scenario G and H convey that the production cost of PHB from 1G or 1G2G feedstock available at a sugar mill, still prohibits entry into the bioplastic market.

Table 49: Minimum selling price (MSP) determined for each of the PHB Scenarios

Scenario	MSP ($/kg)
G	6.81
H	7.23
Min. Market Price	4.40
Max. Market price	11.42

4.3.5 Sensitivity analyses of the PHB scenarios

The results of sensitivity analyses conducted for Scenario G and H respectively is presented in Figure 64 and Figure 65. On Figure 64 and Figure 65, the assumed average market price for PHB has also been indicated. Scenario G will remain profitable for a 30% increase FOC, invertase cost, feedstock cost and fixed capital investment (FCI), however the scenario becomes unprofitable for a 30% increase in TPC and 30% reduction in production rate and operating hours. Scenario H on the other hand will only remain profitable for a 30% increase in FOC and invertase cost. A 30% increase in feedstock cost, FCI and TPC and a 30% decrease in operating hours and production rate will result in an unprofitable Scenario H. It can be concluded that Scenario G is the more robust investment option.

A 30% increase in the operating hours and production rate, results in an MSP of 5.2 $/kg and 5.56 $/kg for Scenario G and H respectively. These represent the realistic, lowest MSP attainable for the two PHB scenarios. These MSPs are however still 2.4-2.5 times the market price of PLA. With the PHB biorefinery scenarios developed in this study, introduction of PHB into the bioplastic market is therefore not currently realistic.

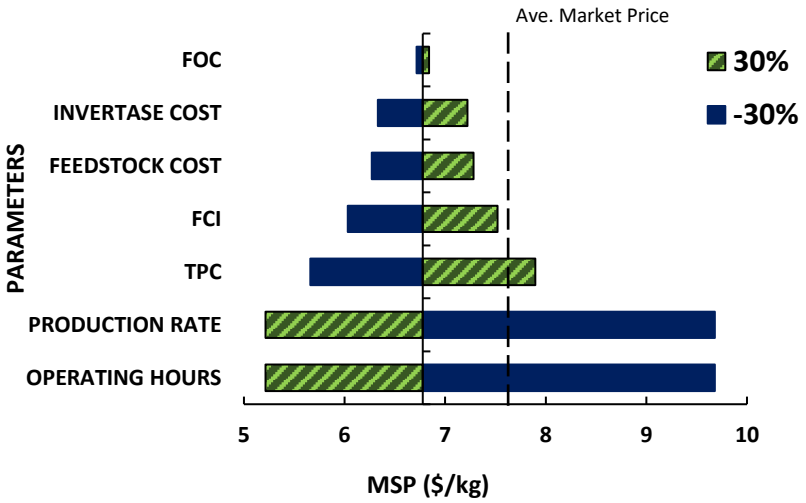

Figure 64: Sensitivity Analysis Results for Scenario G

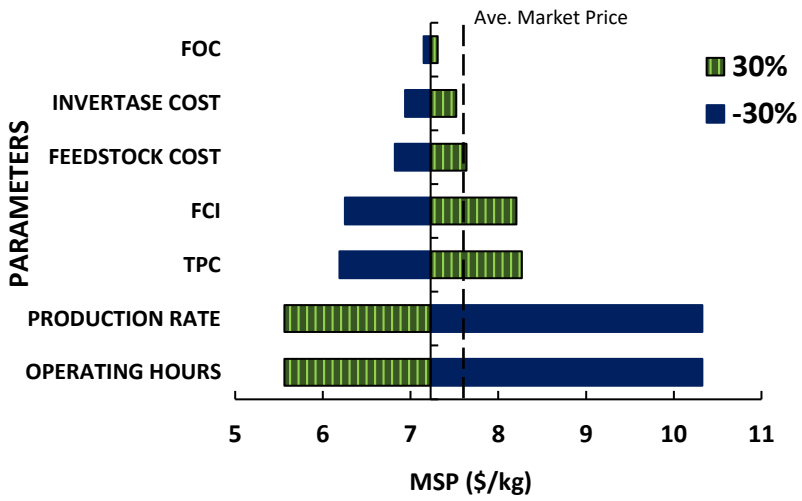

Figure 65: Sensitivity Analysis Results for Scenario H

4.3.6 Techno-economic comparison of PHB scenarios to other bio-based processes

In Table 50 various PHB biorefinery techno-economic analysis study results found in literature, were specified. The yields indicated in Table 50 are all comparable to the overall yield of Scenario H. The low yield of PHB from lignocellulosic material is a major shortcoming. Further research should focus on developing more efficient PHB production processes from these cost-effective materials, which will most likely need to involve genetic manipulation of PHB producing microorganisms.

None of the entries in Table 50 determined a minimum selling price as the main economic parameter. Nieder-Heitmann, (2019) used a PHB market price of 11.42 $/kg to determine the IRR. Considering scenario G and H achieved a 20% IRR at a selling price of 6.81 $/kg and 7.23 $/kg respectively, implies that producing PHB at a biorefinery utilizing 1G or 1G2G feedstock is more profitable compare to a biorefinery utilizing only 2G feedstock. The potential reasons differ for 1G and 1G2G feedstock. The higher yield obtained for 1G feedstock is in all likelihood the reason for the better economics of Scenario G. Scenario H has a comparable yield to the process of Nieder-Heitmann, (2019), which means that the better economics of Scenario H could potentially be attributed to the higher capacity and subsequent economies of scale benefits associated with combined 1G and 2G feedstock.

Three entries in Table 50 (entry 3, 4 and 5) developed processes where PHB was not the sole product being produced. The processes developed by Moncada, El-Halwagi & Cardona, (2013) and Moncada, Matallana & Cardona, (2013), produced PHB alongside ethanol and electricity, whilst Kachrimanidou *et al*., (2021) co-produced PHB, crude phenolic compounds (CPE) and protein isolate (PI). All these studies reported better economics than what has been obtained in this study, only producing PHB. The co-generation of PHB at a biorefinery could therefore be the key to improving the economics. Furthermore, considering the small market size of PHB, the sole production of PHB at a biorefinery at the production rate of Scenario G and H is not currently feasible.

Table 50: Techno-economic analysis study outcomes obtained for PHB from literature

Nr.	Feedstock	MSP (*@IRR*)	Overall Yield	TCI per unit	TPC per unit	Reference
		$/kg	g/g	M$/kg per y	M$/kg	
1	2G Feedstock[d]	(*34.7%*)	0.050	18.44	2.06	(Nieder-Heitmann, 2019)
2	Crude Glycerol	(*@16%*)	0.025	-	2.18[e]	(Posada *et al.*, 2011)
3[b]	Sugarcane Bagasse	-	0.094[a]	-	2.12[e]	(Moncada, El-Halwagi & Cardona, 2013)
4[b]	SFM[c] and crude glycerol	- (@10%)	0.030	20.60	8.20	(Kachrimanidou *et al.*, 2021)
5[b]	Sugarcane Bagasse	-	0.044[a]	-	3.33[e]	(Moncada, Matallana & Cardona, 2013)
6	A-molasses	6.81 (*20%*)	0.120	9.82	4.18	This study
7	1G2G Feedstock	7.23 (*20%*)	0.05	12.89	3.86	This study

[a]g PHB/ g total sugars [b]Co-generation processes [c]Sunflower meal [d]Sugarcane bagasse and Brown leaves, similar to what has been used in this study. [e]Total Production cost includes depreciation of capital.

4.4 Citric Acid Biorefinery Scenarios

4.4.1 Material and Energy Balances of the Citric Acid Scenarios

Figure 66 illustrates the sugar, product and by-product flows, utility usage, installed equipment cost and raw material cost of Scenario I. The fermentation broth produced, contains 12.18% citric acid, and 4.29% residual sugars. Following separation and purification of the fermentation broth in *S300*, citric acid is produced at a production rate of 65.21 kt/y or 13042 kg/h, with a purity of >99%. The overall yield of Scenario I from A-molasses is 0.51 g/g_{feed}. The combustors of *S500-1&2* is supplied with 10.09 t/h bagasse to produce the remaining electricity and heating utilities. This amounts to 33% of the total bagasse available from the sugar mill.

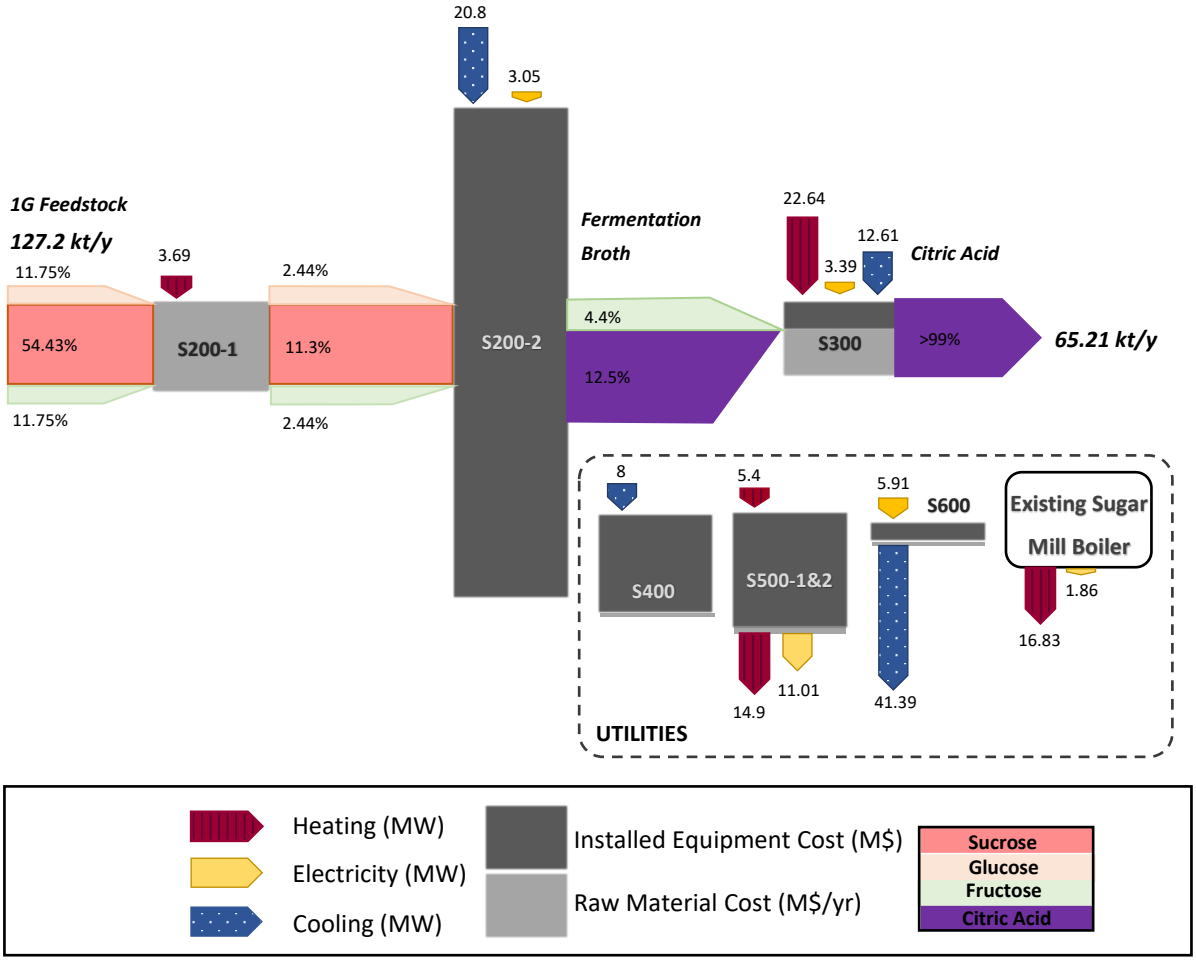

Figure 66: The distribution of Utility usage, Installed Equipment Cost and Raw Material Cost, between the main process sections of Scenario I.

Figure 67 illustrates the sugar, product and by-product flows, utility usage, installed equipment cost and raw material cost of Scenario J. The overall fermentation yield of Scenario J is 0.72 $g/g_{total\ sugars}$. Following separation and purification of the fermentation broth in *S300*, citric acid is produced at 95.76 kt/y or 19151 kg/h. The overall yield of Scenario J from 1G2G feedstock is 0.289 g/g_{feed}.

The cooling utility requirements of Scenario J is the highest, with heating and electricity following. The existing sugar mill CHP plant provides 22% and 6.47% of the total heating and electricity requirements. The remainder of the heating and electricity is supplied by S500. The bypass ratio of Scenario J is 36%.

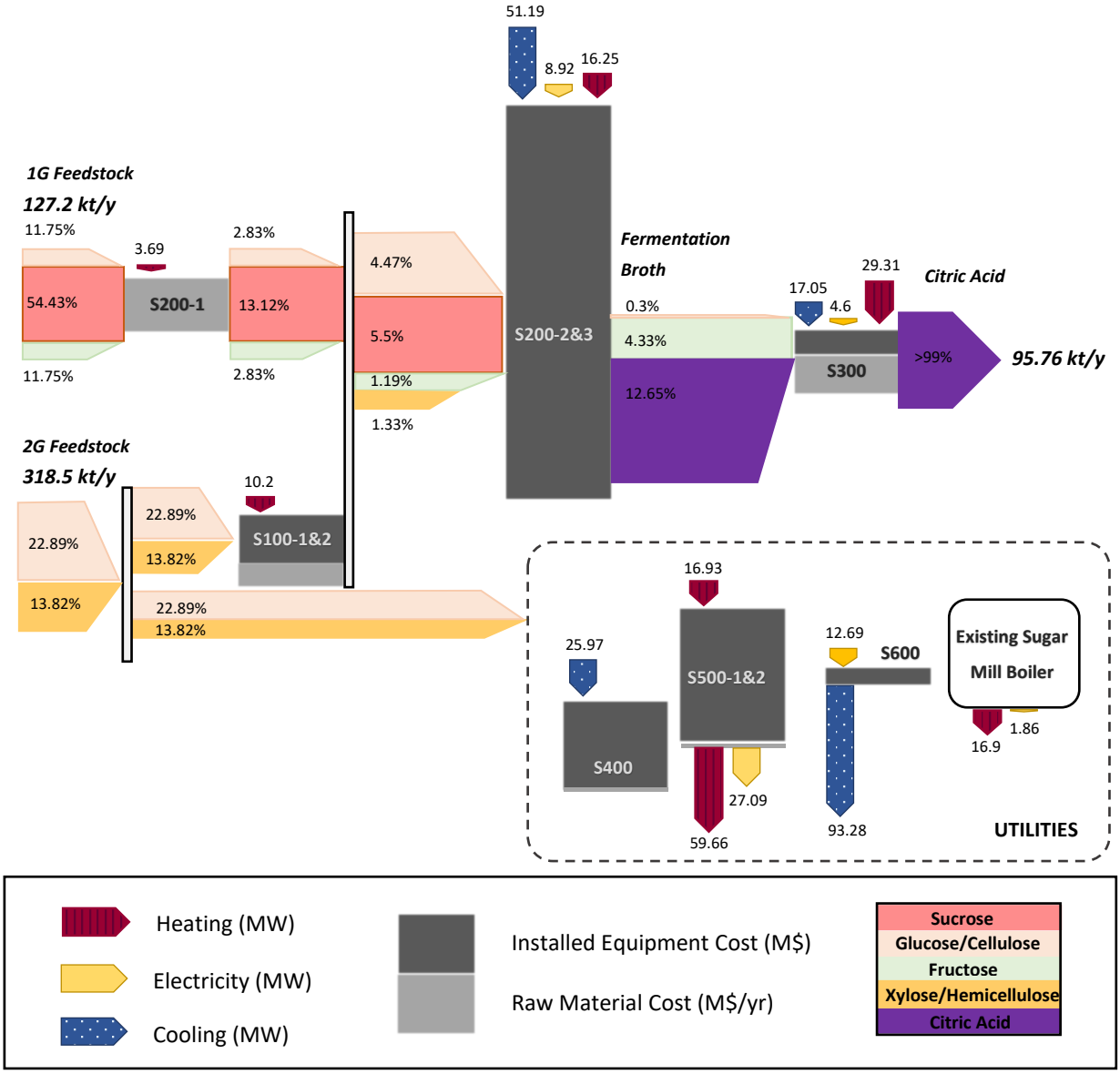

Figure 67: The distribution of Utility usage, Installed Equipment Cost and Raw Material Cost, between the main process sections of Scenario J.

Table 51 contains the most important material balance information for the citric acid scenarios. Promising citric acid yields of 0.51 g/g_{feed} and 0.29 g/g_{feed}, achieved for Scenario I and J resulted in high production rates for both processes of 65.12 kt/y and 95.76 kt/y.

Table 51: Summary of main material balance information for Citric Acid Scenarios

SCENARIO	PRODUCTION RATE (kt/y)	PURITY (%)	OVERALL YIELD (g/g_{feed})	% BAGASSE* OR 2G FEED# TO CHP (BYPASS RATIO)	% OF MARKET SHARE
I	65.12	>99	0.51	33	3.26
J	95.76	>99	0.29	36	4.79

*Applies to 1G Scenarios, #Applies to 1G2G Scenarios

The citric acid production rates achieved for Scenario I and J, are respectively 3.26% and 4.79% of the current global market volume of citric acid. The citric acid market size is approximately 2 million tons per year, of which 99% is being produced via fermentation making it the represented bio-based market

(Bastos & Ribeiro, 2020; Ciriminna *et al.*, 2017; Mores *et al.*, 2021). The introduction of Scenario I and J into the citric acid market is therefore realistic. By contributing <5% to the global market volume, with introduction, the market will in all likelihood remain stable, causing minor to no fluctuations in the market price of citric acid (Nieder-Heitmann, 2019).

Figure 68 illustrates the utility requirements of Scenario I and J in relation to their respective capacities. Scenario J requires, per kg citric acid, 53%, 64% and 53% more cooling, heating, and electricity respectively. Table 52 and Table 53 contain the major utility consuming equipment of Scenario I and J respectively. Two entries in Table 53 are associated with the processing of 2G feedstock i.e., pretreatment and EH (*S100-1&2*) and the xylose utilizing fermentation section (*S200-3*). This indicates that the higher energy requirements per kg citric acid could potentially be ascribed to the sections only pertaining to the 1G2G scenario.

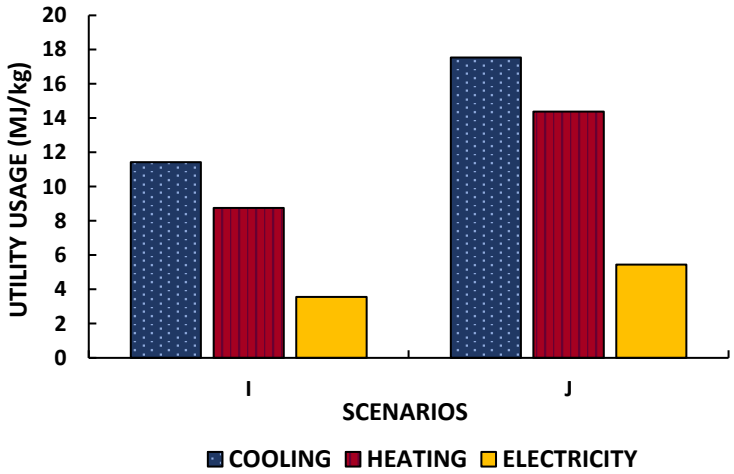

Figure 68: Utility usage per kg product produced for the Citric Acid Scenarios.

The existing sugar mill CHP plant provides 53% and 14.45% of the total heating and electricity requirements to the biorefinery of Scenario I. For scenario J the existing sugar mill CHP plant provides 22% and 6.47% of the total heating and electricity requirements. The remainder of the heating and electricity is supplied by S500 of the respective scenarios.

The process section of Scenario I that requires the largest amount of cooling is *S200-2*, followed closely by *S300*. The latter also has the highest heating requirements. The separation and purification of citric acid is overall the most energy intensive process step of Scenario I. However, for Scenario J, the most energy intensive process section is *S200-2&3,* where citric acid formation takes place. The electricity requirements for both Scenario I and J are concentrated at *S600*.

Table 52: Main heating and cooling utility consuming equipment of Scenario I

PROCESS SECTION	EQUIPMENT	COOLING (MW)	HEATING (MW)	ELECTRICITY (MW)
S200-2	Fermenter	20.54	-	-
S300	Heat Exchanger *(HX-04 [b])*	12.61	-	-
S400	Heat Exchanger *(HX-01 [a])*	7.8	-	-
S300	Flash Drum	-	11.14	-
S300	Heat Exchanger *(HX-05 [b])*	-	10.57	-
S500-1	Heat Exchanger *(HX-05 [c])*	-	4.3	-
S200-1	Heat Exchanger	-	3.58	-
S600	Chilled Water Package	-	-	5.89
S200-2	Compressor	-	-	2.91
S300	Crystallizer	-	-	2.38

[a]*In Figure 3.* [b]*In Figure 37.* [c]*In Figure 4.*

Table 53: Main heating and cooling utility consuming equipment of Scenario J

PROCESS SECTION	EQUIPMENT	COOLING (MW)	HEATING (MW)	ELECTRICITY (MW)
S200-2	Fermenter	26.57	-	-
S400	Heat Exchanger *(HX-01 [a])*	25.97	-	-
S300	Heat Exchanger *(HX-04 [b])*	17.05	-	-
S200-3	Flash Drum	-	16.25	-
S300	Drying	-	14.55	-
S300	Flash Drum	-	14.22	-
S500-1	Heat Exchanger *(HX-05 [c])*	-	13.39	-
S100-1&2	Pretreatment	-	10.28	-
S600	Chilled Water Package	-	-	11.55
S200-2,2	Compressor	-	-	7.41
S300	Crystallizer	-	-	3.19

[a]*In Figure 3.* [b]*In Figure 37.* [c]*In Figure 4.*

Figure 69 compares the total utility usage per kg of the various process section comprising Scenario I and J. When only considering the process sections present in Scenarios I and J, all utility producing sections i.e., *S400*, *S500* and *S600* require, per kg, more utilities for Scenario J. The more utilities these aforementioned sections need to produce per kg citric acid, the more utilities they consume per kg citric acid. Furthermore, the utility usage per kg of sections *200-1*, *S200-2* and *S300* are either comparable or less for Scenario J, indicating economies of scale benefits realized.

The utility consumption of *S200-3* constitutes 18.63% of the total utility consumption of Scenario J. This is mainly attributed to the cooling water and LPS required in a triple effect evaporator to concentrate the hemicellulose hydrolysate from 35 g/L to approximately 150 g/L, prior to fermentation. The triple effect evaporator accounts for 70.65% of the utility consumption of *S200-3*, indicating the high energy demand associated with concentration of solutions. Combining the hemicellulose hydrolysate with the glucose from pretreatment and A-molasses for co-fermentation of xylose, glucose and fructose will in all likelihood result in energy reductions, considering the hemicellulose hydrolysate requires concentration whilst the glucose/A-molasses mixture requires dilution. However, to the knowledge of the writer, microorganisms capable of producing citric acid through co-fermentation with comparable yields to that of utilizing only hexose sugars is yet to be identified.

The most energy intensive section for both scenarios is *S300*, where separation and purification takes place. Large amounts of utilities are required to concentrate (triple effect evaporator), crystallize, and finally dry the citric acid monohydrate. These combined operations account for 25.27% of Scenario J's utility consumption. Section 200-2 is the second most energy intensive section, attributed to the chilled water and electricity required for the aerobic citric acid fermentation.

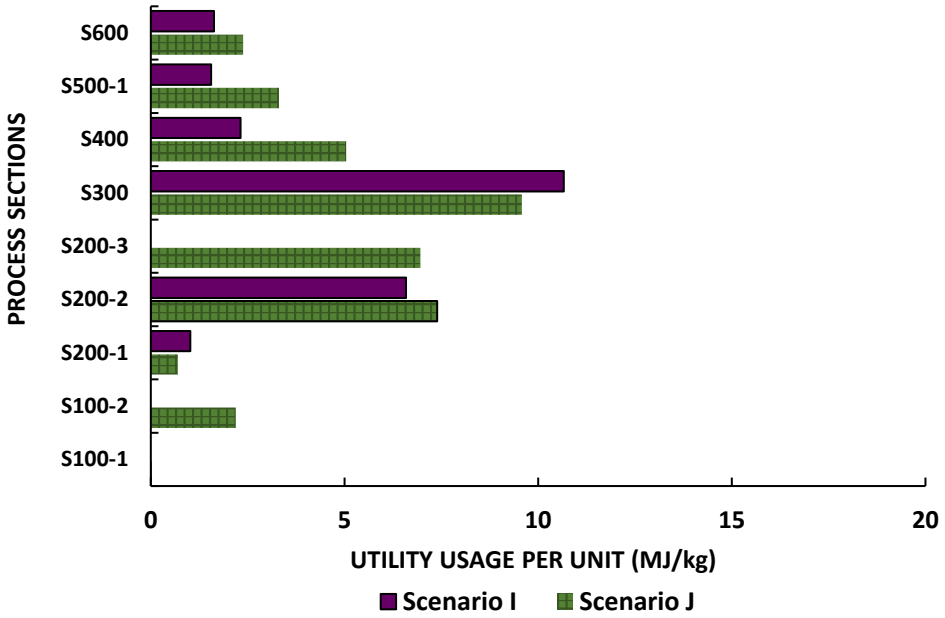

Figure 69: Total utility usage per kg product produced for the various process sections of Scenario I and J.

4.4.2 Capital Expenditure (CAPEX) of Citric Acid Scenarios

In Table 54 the capital expenditures of the citric acid biorefinery scenarios are presented. The full set of capital expenditures are available in Appendix D. The total capital investment per kg citric acid produced of Scenario J is 1.08 times that of Scenario I, indicating that economies of scale benefits (in terms of CAPEX) have not been realized by Scenario J.

The IEC per kg of the various process sections comprising Scenario I and J have been illustrated in Figure 70. For Sections 200-2, 300 and 400, the IEC per kg citric acid is comparable or lower for Scenario J compared to Scenario I, indicating where the economies of scale benefits were realized. Furthermore, the pretreatment and enzymatic hydrolysis section (*S100-1*) as well as xylose fermentation section (*S200-3*) have very low contributions to the total IEC per kg of Scenario J, especially compared to the IEC per kg of *S200-2&3*. This is in contrast to what has been observed for the other products investigated in this study. The cost implications associated with the processing of 2G feedstock are considerable lessened as the efficiency of the 1G2G process increases, i.e., the process has a higher yield. Scenario J has the highest overall yield of all the 1G2G scenarios investigated in this study.

Table 54: Capital Expenditures of the Citric Acid Scenarios

CAPITAL EXPENDITURES		**I**	**J**
TOTAL INSTALLED EQUIPMENT COST (M$)		213.72	340.90
ISBL: INSTALLED COST INSIDE BATTERY LIMITS (M$)		147.79	227.00
TOTAL DIRECT COST (TDC) (M$)		246.97	392.00
TOTAL INDIRECT COST (M$)		148.18	235.20
FIXED CAPITAL INVESTMENT (FCI) (M$)		395.15	627.20
TOTAL CAPITAL INVESTMENT (TCI) (M$)		**414.91**	**658.60**
TOTAL CAPITAL INVESTMENT$_{\text{per unit}}$	$/kg per year	**6.36**	**6.88**

Section 200-2, where citric acid fermentation from glucose and fructose takes place, accounts for the majority of IEC for both citric acid scenarios. The high capital costs of this section is attributed to citric acid fermentation being an aerobic process. Similar has been found in this study for aerobic PHB fermentation. This corresponds to results reported in literature, where the citric acid fermenters and associated compressors accounted for 50% of the total equipment cost of a biorefinery (Wang *et al.*, 2020). The smaller fermenters required for aerobic fermentation as well as the long fermentation time of 144 hours resulted in the requirement of 18 and 21 aerobic fermenters required for Scenario I and J respectively. A potential strategy to reduce the capital costs could be to find a microorganism that can ferment citric acid at a higher productivity, without compromising yield. Another solution could be to contact multiple bioreactor suppliers to compare maximum aerobic bioreactor sizes. Technological developments could potentially have occurred in the industry to address this issue, which is yet to be reported on in literature.

In contrast to what has been found in literature however was that the separation and purification of citric acid accounts for up to 40% of the IEC (Mores *et al.*, 2021). This could merely be due to the capital costs of *S200-2* completely surpassing the remainder of the process sections, minimizing their contribution.

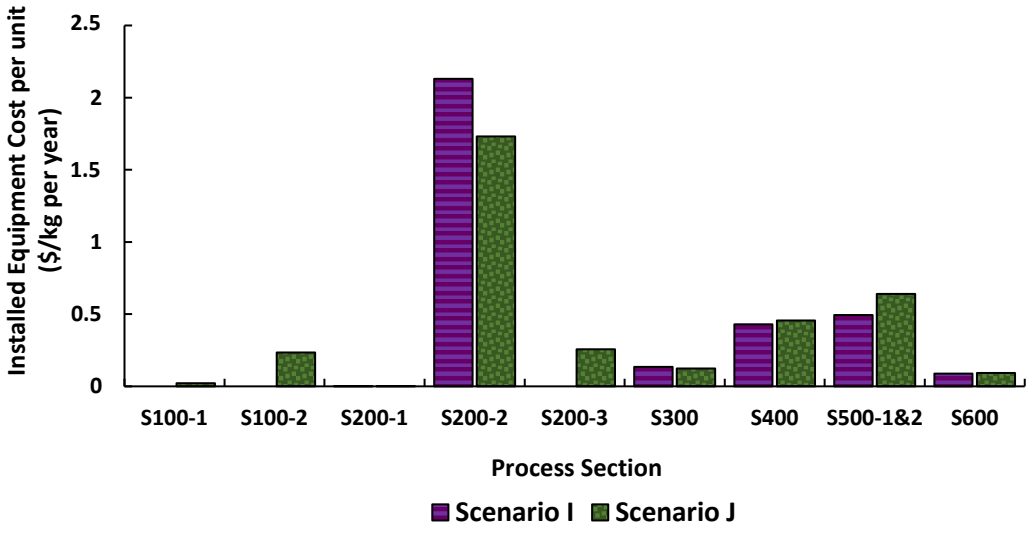

Figure 70: Installed equipment cost per kg product produced per section, for the Citric Acid Scenarios.

4.4.3 Operational Expenditure (OPEX) of Citric Acid Scenarios

A summary of the main operational expenditures of the citric acid scenarios is presented in Table 55. A breakdown of the fixed operating costs of each individual scenario can be found in the Appendix E. Similar to the CAPEX of the citric acid scenarios, economies of scale benefits in terms of OPEX have not been realized for Scenario J, with a TPC per kg 3.6% higher than that of Scenario I.

Table 55: Operational Expenditures of the Citric Acid Scenarios

OPERATIONAL COST COMPONENT	**COST (M$/year)**	
	I	**J**
Fixed Operating Cost	**7.94**	**12.20**
*Feedstock Cost**	*27.41*	*30.28*
Chemical Cost	*15.06*	*30.50*
Waste Disposal Cost	*3.76*	*9.05*
Total Variable Operating Cost	**45.95**	**69.81**
Annual Capital Charge	-	*0.03*
Total Production Cost (TPC)	**53.90**	**82.04**
TPC per unit ($/kg per year)	**0.83**	**0.86**

*Includes all bagasse and brown leaves from harvesting residues, even portion sent to CHP plant is regarded as feedstock cost

Figure 71 illustrates the production cost components per kg citric acid produced for Scenario G and H. The variable operating costs is represented as its components which includes the feedstock cost, the chemicals costs, and waste disposal costs.

The main operational costs for both Scenario I and J are the feedstock and chemicals costs. Similar to what has been observed for the other product biorefineries investigated in this study, the feedstock cost per kg product is lower for the 1G2G process compared to the 1G process. The feedstock cost of Scenario I dominates at 51% of the TPC. For Scenario J however, the contribution is almost equally distributed between the feedstock cost and chemicals cost. The largest chemical cost for both scenarios is the cost of the amine solvent used for solvent extraction, making out 87.11% and 63.08% of the total chemical cost of the respective scenarios. This comes despite most of the amine solvent being recycled and the amine solvent cost part of the chemicals costs only being the make-up stream of 3% accounting for leakages, highlighting the importance of recycling the solvent. The large contribution of the amine solvent to the variable operating cost of a biorefinery has previously been reported (Özüdoğru, 2018).

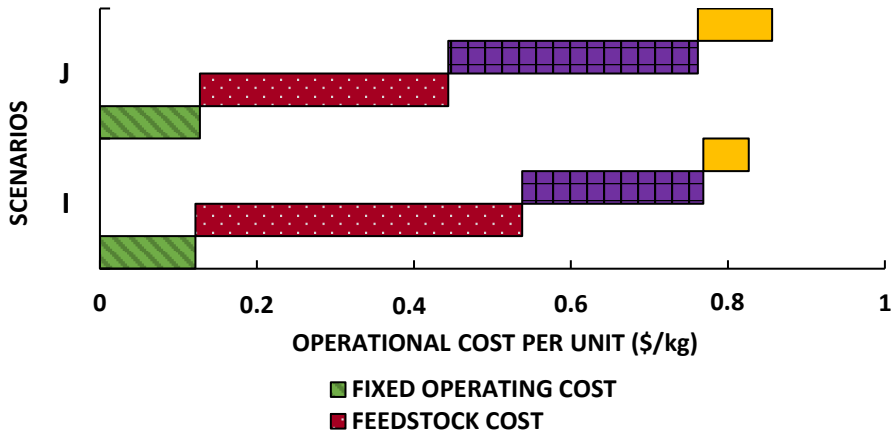

Figure 71: Operational cost components per kg product produced for the Citric Acid Scenarios.

4.4.4 Economic parameters of Citric Acid Scenarios

The MSPs of Scenario I and J have been determined as 2.44 $/kg and 2.6 $/kg respectively. The market price of citric acid has been reported on by an number of studies as 0.7 $/kg (2015), 0.8 $/kg (2018) and 0.62-1.1 $/kg (2020) (Becker, Kohlheb, Hunger, *et al.*, 2020; Behera *et al.*, 2021; Wang *et al.*, 2020). In this study an average citric acid market price of 0.8 $/kg was assumed. At this market price, both Scenario I and J are deemed unprofitable, with minimum selling prices 3-4 times the assumed market price.

4.4.5 Sensitivity analyses of the citric acid scenarios

The results of sensitivity analyses conducted for Scenarios I and J respectively can be found in Figure 72 and Figure 73. Although changes in the productivity (fermentation time) does in fact results in changes to the TCI, both parameters were included in the sensitivity analysis to compare the effect of fermentation time to the effect that other parameters have. The fermentation time of the citric acid biorefineries have a greater effect on the MSP compared to all operational costs. This confirms that for more profitable citric acid biorefinery scenarios, capital costs will need to be reduced by reducing fermentation time.

A 30% increase in operating hours, which results in the lowest realistic MSP, does not lead to an MSP close to the assumed market price for citric acid. The industrial citric acid fermentation is already a well-established process. Most of the citric acid currently being produced is from corn or starch as feedstock. The cost-effectiveness of these substrates cannot alone be the reason for the low market price exhibited for citric acid, as confirmed by the little effect feedstock cost had on the MSP in the sensitivity analyses. Nevertheless, improved yields, cheaper pretreatment methods, higher productivities etc. or a combination thereof could be the reasons why citric acid from corn and starch has been commercially established and citric acid from A-molasses and/or bagasse is too expensive for market introduction.

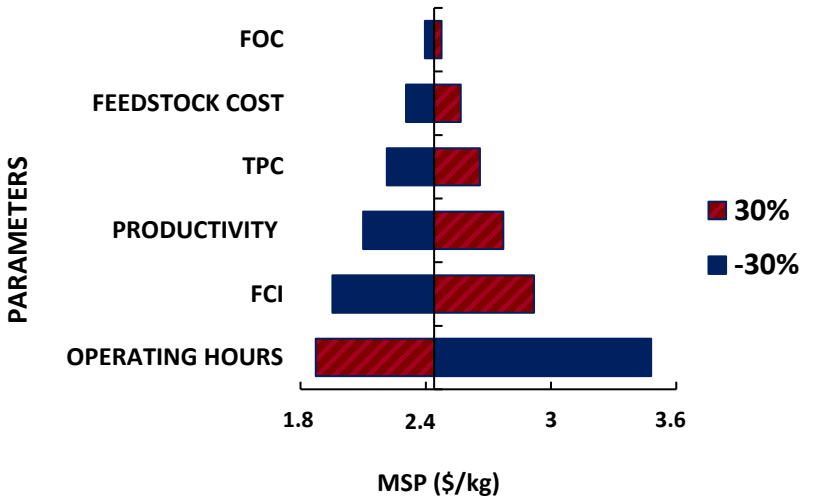

Figure 72: Sensitivity Analysis Results for Scenario I

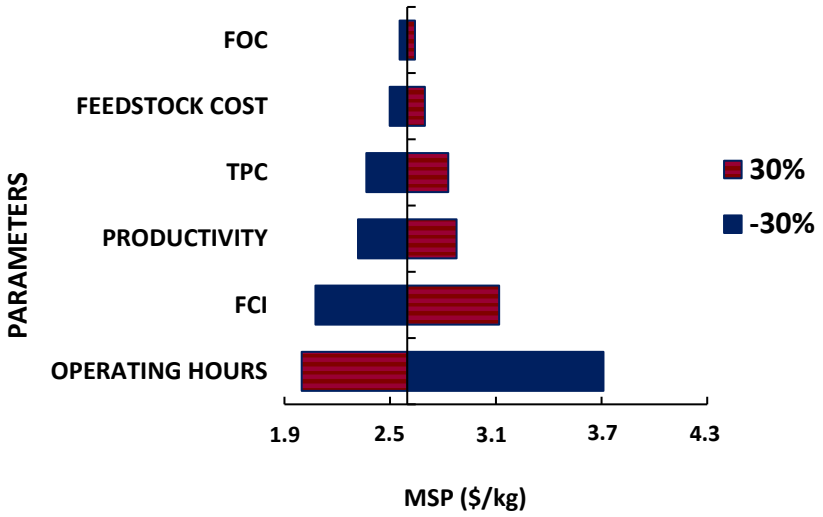

Figure 73: Sensitivity Analysis Results for Scenario J

4.4.6 Techno-economic comparison of Citric Acid scenarios to other bio-based processes

To investigate how the citric acid biorefineries designed and developed in this study compare to other citric acid processes obtained from literature, Table 56 is presented. In Table 56 the yields and main economic results of various techno-economic studies conducted on citric acid, are listed.

De Beer, (2011) utilized A-molasses and reported a yield similar to what has been achieved for Scenario I. However, all other yields in Table 56 are substantially higher than Scenario I and J. Considering the high fermentation yields of Scenario I and J, the low overall yields are attributed to the pretreatment efficiency as well as the separation and purification recovery of 84%. They key to more economic processes could therefore lie in the improvement of 2G processing by instead using simultaneous saccharification and purification to minimize sugar losses and/or improving the recovery achieved in the separation and purification of citric acid.

The TPC per kg reported for the various entries in Table 56 is comparable to the TPC per kg determined for Scenario I and J. The TIC per kg of the entries however differ vastly with each other and with that of

Scenario I and J. Wang *et al*., (2020) and Özüdoğru, (2018) obtained TCIs per kg on the lower end whilst De Beer, (2011) obtained TCIs (entry 1 and 4) on the higher end, with Scenario I and J in the middle. It is unsure what the reason is for the vastly different installed equipment cost estimations of the various studies. Despite the low TCI per kg obtained by Wang *et al*., (2020), it was reported that the citric acid fermenters and compressors accounted for 50% of the IEC similar to this paper, whilst Özüdoğru, (2018) found that the citric acid fermenters only accounted for 1.6% of the IEC. Entries 1 and 4 were investigated in the same paper by De Beer, (2011), which could potentially indicate an overestimation of equipment cost by the study. It is suggested that in the future, industrial quotes be obtained for main process units such as fermenters to further increase the reliability of the techno-economic analysis results.

Table 56: Techno-economic analysis study outcomes obtained for Citric Acid from literature

Nr.	Feedstock	MSP (*@IRR*)	Overall	TCI per unit	TPC per unit	Reference
		$/kg	$g/g_{total\ feed}$	$/kg per y	$/kg	
1	A-molasses	- (*@12%*)	0.36	14.90	3.25	(De Beer, 2011)
2	Corn	0.73 (*@15%*)	0.65	0.64	1.07	(Wang *et al.*, 2020)
3	2G feedstock[a]	- (*@13%*)	0.54	2.97	0.61	(Özüdoğru, 2018)
4	Starch	- (*@12%*)	0.83	13.87	2.89	(De Beer, 2011)
5	A-molasses	2.44 (*20%*)	0.51	6.36	0.83	This study
6	1G2G feedstock	2.60 (*20%*)	0.29	6.88	0.86	This study

[a] Sugarcane bagasse and Brown leaves, similar to what has been used in this study

4.5 Environmental assessment

Although the economic performance of the various biorefinery scenarios designed in this study is the main focus, it is also important to investigate the environmental impact of a biorefinery. The production of biochemicals cannot just be assumed as sustainable because they are produced from renewable feedstock. Biochemical production also includes the use of various unsustainable methods and chemicals (Ögmundarson, Sukumara, Herrgård, *et al.*, 2020). This comes in addition to CO_2 emissions within the process. Examples include emissions from fermentation and emissions from combustion.

It is important to note that all the processes minimize waste production by combusting the solid waste produced within the system. Furthermore, the processes all have a WWT plant that produces purified water from liquid wastes produced within the biorefinery, which is subsequently recycled to the various water consuming biorefinery processes. In Table 57 the total water usage per kg product produced for each of the scenarios have been indicated, in addition to the amount of fresh water that needs to be purchased. Albeit a small amount, Scenario G and H have the largest fresh water requirements of the ten scenarios. These scenarios also have the largest total water usage, due to the water required to resuspend the *E.coli* cells to 50 g/L prior to alkaline digestion (Choi & Lee, 1999c). Evidently, the WWT plant included in the design greatly reduces water consumption, and for most of the Scenarios (B, C, D, E, F and J) no additional fresh water needs to be purchased. Reduced water consumption is important for

the environmental sustainability of a process, especially considering the water crisis across the globe and specifically in South Africa.

Table 57: Water usage of each scenario

SCENARIO	A	B	C	D	E	F	G	H	I	J
TOTAL WATER USAGE ($kg_{water}/kg_{product}$)	7.22	9.95	14.51	15.31	29.81	42.25	53.69	68.87	10.30	12.87
FRESH WATER REQUIRED ($kg_{water}/kg_{product}$) ($x10^{-3}$)	0.01	0	0	0	0	0	1.39	1.00	0.11	0

Comprehensive life-cycle analyses are outside the scope of this project. Instead, the environmental impact of each individual biorefinery scenario was determined by calculating the greenhouse-gas emissions (g CO_2/ kg dry product) using the RSB GHG Calculator Tool. The GHG emission results obtained for each scenario has been indicated in Figure 74, in addition to the MSP determined for each. The relationship between economics and environmental sustainability is not a set, prescribed relationship. Sometimes technological developments can lead to economic and environmental improvements, whilst other times the environmental impact of a process will need to increase in order to improve the economics (Ögmundarson *et al.*, 2020). The results obtained from the GHG Calculator Tool for each biorefinery scenario, is given in Appendix F.

In the RSB GHG Calculator tool, two main processes are distinguished. Process 1 encompasses the feedstock production process i.e., the sugar mill emissions associated with producing A-molasses, bagasse and brown leaves. Process 2 encompasses the biochemical production process, which includes all emissions from the biorefinery and its associated facilities. Between Process 1 and Process 2, the latter accounts for the largest portion of CO_2 emissions. The CO_2 emissions of Process 2 mainly consist of the emissions from combustion as well as the CO_2 emissions associated with the manufacturing process of chemicals procured, albeit not very sensitive to either.

In Figure 74, the 1G processes and 1G2G processes were separated considering the 1G2G processes operate at larger capacities, which means chemical usage and emissions from the CHP plant will in all likelihood be higher. Evidently there is no correlation between the MSPs and the CO_2 emissions of the processes. Apart from Scenario G and H, the CO_2 emissions are comparable between the 1G and 1G2G scenarios respectively, whilst the MSPs differ vastly. This could be due to the design of all the processes being similar. All the scenarios contain fermentation processes that have CO_2 emissions as well as a CHP plant which releases flue gas containing CO_2. Although the amounts might differ slightly, the CO_2 emissions are comparable due to similar technologies being employed. Furthermore, the majority of chemicals being used in the scenarios are associated with the growth medium. Although the growth medium compositions might differ slightly, all basically consist of a nitrogen source and minor amounts of other chemicals that aid fermentation.

Scenario G and H have, in comparison to the respective feedstock scenarios, significantly high GHG emissions. Because the utility requirements of both these scenarios are low, only portions of the biogas produced in the respective WWT plants is used in the gas engine or CHP plant. For Scenario G, a CHP plant is not required, only a gas engine which utilizes 10% of the produced biogas. For Scenario H, only

45% of the biogas produced is used for combustion. For both these scenarios the remaining, unused biogas is flared, releasing large quantities of CO_2 into the atmosphere. A potential solution to reduce these emissions could be to instead bottle the biogas and sell it. Another potential solution could be to co-produce PHB at the biorefinery. If co-products are chosen which are slightly more energy intensive compared to PHB, all the biogas will most likely be utilized for combustion. Co-generation of electricity has readily been shown to negatively affect economics and therefore biochemicals as co-products should instead be considered. Furthermore, considering the Zero Routine Flaring by 2030 program, which was signed by over 55 countries, the use of biogas might become compulsory (Zardoya, Lucena, Bengoetxea, *et al.*, 2022).

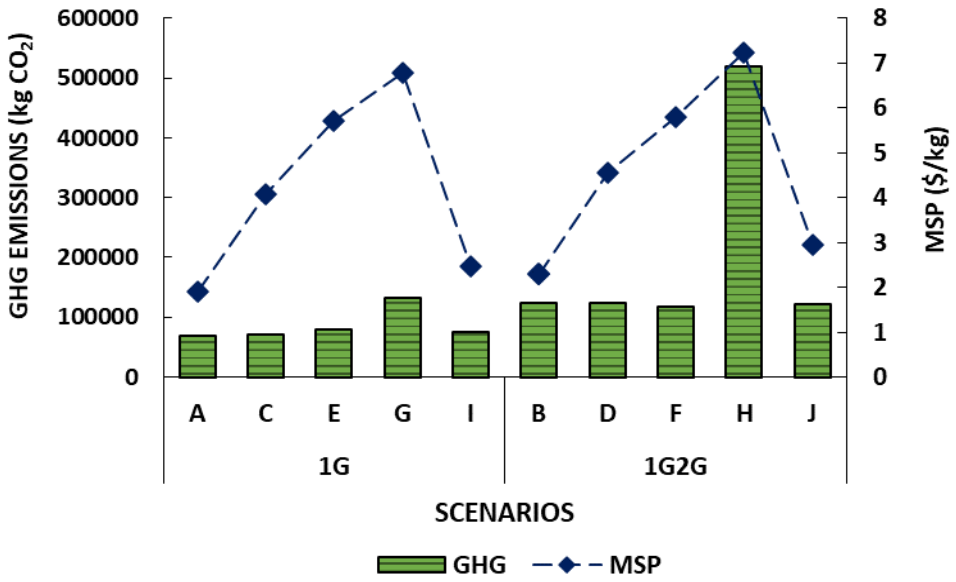

Figure 74: Greenhouse gas emissions versus the minimum selling price determined for each biorefinery scenario

4.6 Comparison of most profitable scenarios of each products

In this section, the most promising biorefinery scenario for each of the four products investigated in this study will be compared. For each of the four products, the most promising scenario, from an economic perspective, relates to the scenario with the lowest minimum selling price. From previous results discussed, the most promising scenario for each product is:

- 2,3-Butanediol:
  - Scenario A, utilizing 1G feedstock.
- 1,3-Butadiene:
  - Scenario C, utilizing 1G feedstock, via the BDO pathway.
- Polyhydroxybutyrate:
  - Scenario G, utilizing 1G feedstock.
- Citric Acid:
  - Scenario I, utilizing 1G feedstock.

Evidently, utilizing 1G feedstock at a biorefinery annexed to a sugar mill is overall a more economic option compared to utilizing integrated 1G2G feedstock. Although the use of integrated 1G2G feedstock leads to an increased capacity, in most cases the increased capacity did not outweigh the costs associated with additional sections such as pretreatment and enzymatic hydrolysis. It has been reported in literature that the technological readiness level of processes utilizing 2G feedstock hinders their commercialization and is also why building block biochemicals are mostly produced from 1G feedstock (Ögmundarson *et al.*, 2020). Future research should therefore focus on developing more efficient and more economical technologies for the extraction of sugars from 2G feedstock.

The important material balance information and economic parameters of Scenario A, C, G, and I is given in Table 58. The highest yield and production rate is achieved by Scenario I, followed by Scenario A, Scenario C, and finally Scenario G. However, the lowest MSP was obtained for Scenario A, followed by I, C and finally G. This indicates that the yield and subsequent production rate does have a large influence on the MSP, however, is not the sole decisive factor. Considering the TPC of Scenario A and Scenario I are comparable, the lower MPS of Scenario A can only be attributed to the major difference in TCI of the two scenarios.

Scenario I has a significantly high total capital investment cost compared to the remaining entries in Table 58. As previously established, this high capital cost is a result of the combined high capital costs associated with an aerobic fermentation process and the high fermentation time of 144 hours required. The higher capital cost of an aerobic fermentation process is corroborated by Scenario G having the second highest capital cost. Scenario A and C operate under anaerobic conditions. The lower capital cost of scenario G compared to I is due to a shorter fermentation time required of 31.5 hours as well as the lack of CHP plant.

Scenario I is the only entry in Table 58 that does not require invertase for sucrose hydrolysis. This indicates that using microorganisms that can naturally hydrolyze sucrose could be beneficial in reducing operational expenditures for a specific process, however it does not ensure a low production cost. Furthermore, hydrolysis of sucrose inside the fermentation tank could very likely be a contributing factor to the long fermentation time required for Scenario I.

From Table 58, it is evident that the high MSP of PHB is attributed foremost to the low yield achieved, together with a 16-20% higher total production cost mainly attributed to the high cost contribution of NH_2PO_4 part of the fermentation medium. It is readily known that fermentation efficiency is a decisive factor affecting the profitability of a process (Maina, Prabhu, Vivek, *et al.*, 2022).

Table 58: Important material balance and economic information of Scenario A, C, G, and I

Scenarios	Production Rate (kt/y)	Yield (g/g_{feed})	TCI (M$)	TPC (M$/y)	MSP ($/kg)
A	45.50	0.37	124	53.7	1.91
C	22.95	0.18	145	55.1	4.08
G	15.37	0.12	151	64.2	6.81
I	65.21	0.51	415	53.9	2.44

As a final comparison of Scenarios A, C, G, and I, Table 59 is presented. In Table 59 the profitability as well as environmental impact of the scenarios are indicated. It is important to note that profitability is solely dependent on the market price of a specific product and not on the MSP in comparison with the other products. Scenario A and Scenario G have MSPs 27.27% and 10.82% lower than their respectively market prices deeming them profitable. Scenario C and I are unprofitable due to substantially higher MSPs than their market prices.

The scenarios have been ranked in Table 59 according to the greenhouse gas emissions previously discussed. A ranking of 1 corresponds to the lowest emissions, whilst a ranking of 4 corresponds to the highest emissions. Furthermore, the profitable scenarios have also been ranked in accordance with their robustness. Robustness was determined by inspecting the sensitivity analysis of each. Scenario A was awarded the most robust scenarios, considering most process parameters can be changed by 30% and the process will remain profitable, whereas for Scenario G, a 30% change in TPC and operating hours will cause the process to become unprofitable. Overall, Scenario A is the most favorable biorefinery scenario.

Table 59: Profitability and environmental ranking of Scenario A, C, G, and I

Scenarios	Profitable?	Difference to market price (%)	Greenhouse gas emissions ranking	Robustness ranking
A	Yes	27.27	1	1
C	No	288.66	3	-
G	Yes	10.82	4	2
I	No	209.58	2	-

5 CONCLUSIONS

In this study the economic feasibility of individually producing four biochemicals at a biorefinery annexed to an existing South African sugar mill, was considered. The biochemicals investigated are 2,3-Butanediol, 1,3-Butadiene, Polyhydroxybutyrate and citric acid. For each of the four biochemicals, biorefinery scenarios were developed that use either first-generation feedstock only or integrated first-and second-generation feedstock, available at a sugar mill. The first- and second-generation feedstock considered in this study include A-molasses (1G) and bagasse and brown leaves from harvesting residues (2G).

A thorough literature review was conducted on the bio-based production of the aforementioned biochemicals. From the literature review findings, the most optimal production processes were designed and developed by simulating each, using Aspen Plus® software. The economic feasibility of each of these biorefinery scenarios was assessed by conducting detailed techno-economic analyses, using Microsoft Excel. The main economic indicator determined for each scenario is the minimum selling price (MSP). A basic environmental assessment was additionally conducted, using the RSB GHG Calculator tool.

Two biorefinery scenarios were developed for 2,3-BDO, PHB and citric acid, utilizing either 1G or integrated 1G2G feedstock. For 1,3-BD however, four scenarios were developed as two main production pathways exist for bio-based 1,3-BD. The first pathway produces 1,3-BD from ethanol as intermediate product and the second from 2,3-BDO as intermediate. Each of the pathways were then considered from either 1G or 1G2G feedstock.

The 2,3-BDO and PHB biorefinery scenarios were all deemed profitable, with regards to the respective market prices of 2.63 $/kg and 7.6 $/kg. On the other hand the 1,3-BD and citric acid scenarios were all deemed unprofitable, with market prices of 1.05 $/kg and 0.8 $/kg. The MSPs determined for the various biochemicals are 1.91 - 2.28 $/kg, 4.08 - 5.72 $/kg, 6.81 - 7.23 $/kg, and 2.44 - 2.6 $/kg for 2,3-BDO, 1,3-BD, PHB and citric acid respectively. The difference in MSPs can overall be attributed to the yields of the various processes. However, the yield is not the only decisive factor.

The yields achieved for citric acid were significantly higher compared to that of 2,3-BDO, however the MSPs are higher. The higher MSPs determined for citric can be attributed to the exceptionally high capital costs associated with aerobic fermentation. Similarly, the high MSP of PHB is attributed to the low yields achieved, in combination with the high equipment cost of aerobic fermenters and air sparging compressors.

It was found that producing 1,3-BD via the BDO pathway was more economical compared to the ethanol pathway. Lower yields were achieved for the latter, due to inefficient selectivities and conversion available for catalysts responsible for ethanol to 1,3-BD conversion. Ethanol to 1,3-BD conversion consist of two upgrading steps, whilst BDO to 1,3-BD only has one. The capital cost associated with the two-step process furthermore impacted the economics.

Lower MSP values were determined for most of the 1G utilizing scenarios of the various chemicals. The inferior economics of 1G2G biorefinery scenarios can be attributed to the significant utility and capital cost contributions associated with 2G feedstock processing. This processing includes pretreatment,

enzymatic hydrolysis, and xylose utilization during fermentation. Higher utility usage, especially heating and electricity, leads to a larger CHP plant, which was the dominating capital cost for most scenarios. Furthermore, enzymatic hydrolysis equipment is another major contributor to capital cost. The high utility consumption associated with xylose fermentation is primarily due to the concentration of the hemicellulose hydrolysate prior to fermentation. The 1,3-BD production via the ethanol pathway is the only process that exhibited similar economics for the 1G and 1G2G versions. This was also the only 1G2G scenario where xylose and glucose were co-fermented, eliminating the need for concentration.

All the biorefinery scenarios minimize waste production by combusting solid waste and treating liquid waste in the WWT plant. In the WWT plant purified water is produced, which is then recycled back to the process and used for dilution etc. Reduced water consumption is important for the environmental sustainability of a process, especially considering the water crisis across the globe and specifically in South Africa.

The PHB scenarios were the only scenarios with notable GHG emissions. The low utility requirements meant that most of the biogas produced in the wastewater treatment plant was flared, thereby releasing large quantities of CO_2 into the atmosphere.

6 RECOMMENDATIONS

Further research could focus on developing microorganisms that can co-ferment xylose and glucose to produce biochemicals. Considerable utility reductions and subsequent capital cost reductions are observed when the concentration of hemicellulose hydrolysate is eliminated by combining it with the glucose stream from pre-treatment and A-molasses. Furthermore, if co-fermentation is not an option, the economic impact of sending the hemicellulose hydrolysate directly to the WWT plant for biogas and biomass sludge production, instead of using it for fermentation, could be investigated.

Where possible, microorganisms employed for fermentation should be chosen that can either naturally hydrolyze sucrose or directly utilize sucrose for product formation, thereby greatly reducing variable operating costs. This could also potentially be achieved through genetic engineering experimental work. From the OPEX results obtained for the 1,3-BD scenarios it was observed that the cost of invertase had a signifcant impact on the total production cost, however the fermentation yield had a larger impact, which indicates that yield should not be compromised to prioritize a microorganism that can naturally hydrolyze sucrose.

Further research could also focus on improving the heat integration networks of the various scenarios investigated in this study, by using the pinch point analysis method. As observed with Scenario A and B, considerable energy reductions are accompanied by an efficient heat integration network. Specifically for the 1G2G scenarios, energy reductions translate to higher poduction rates which could potentially allow for some of the scenarios to realize economy of scale benefits, which have not been realized with the current heat integration networks.

Exceptionally high capital costs were observed for aerobic fermenters and associated air sparging compressors. A number of industrial quotes could be obtained to verify the estimated costs used in this study.

To improve the economics of producing PHB at a biorefinery, co-generation scenarios could be investigated from 1G and 1G2G feedstock. When co-products are chosen that are slightly more energy intensive compared to PHB, the environmental sustainability will also improve considering all the biogas will be utilized for combustion instead of emitting it to the atmosphere. Alternatively, the biogas can be bottled and sold to prospective buyers.

From the sensitivity analyses conducted for all the scenarios investigated in this study, it is clear that the amount of operating hours has the largest impact on the MSP. Further research could therefore investigate the economic impact of increasing the operating hours of each scenario, by also taking the additional costs of alternative biomass procurement into account, which will be required in the periods outside the sugarcane harvesting season.

7 REFERENCES

Abdullah-Al-Mahin, Sharifuzzaman, A.B.M., Faruk, M.O., Kader, M.A., Alam, J., Begum, R. & Harun-Or-Rashid. 2012a. Improved Citric Acid Production by Radiation Mutant Aspergillus niger Using Sugarcane Bagasse Extract. *Biotechnology*. 11(1):44–49.

Abdullah-Al-Mahin, Sharifuzzaman, A.B.M., Faruk, M.O., Kader, M.A., Alam, J., Begum, R. & Harun-Or-Rashid. 2012b.

Adlakha, N. & Yazdani, S.S. 2015. Efficient production of (R,R)-2,3-butanediol from cellulosic hydrolysate using Paenibacillus polymyxa ICGEB2008. *Journal of Industrial Microbiology and Biotechnology*. 42(1):21–28.

Afeefy, H.Y., Liebman, J.F. & Stein, S.E. n.d. Condensed phase thermochemistry data - 2,3-BDO. in *NIST Chemistry WebBook, NIST Standard Reference Database Number 69* N.I. of S. and T. P.J. Linstrom and W.G. Mallard (ed.). Gaithersburg MD N.I. of S. and T. P.J. Linstrom and W.G. Mallard (ed.). [Online], Available: https://webbook.nist.gov/cgi/cbook.cgi?ID=C513859&Mask=1EFF.

Afeefy, H.Y., Liebman, J.F. & Stein, S.E. n.d. Condensed phase thermochemistry data - Ethanol. in *NIST Chemistry WebBook, NIST Standard Reference Database Number 69,* N.I. of S. and T. P.J. Linstrom and W.G. Mallard (ed.). Gaithersburg MD, 20899 N.I. of S. and T. P.J. Linstrom and W.G. Mallard (ed.). [Online], Available: https://webbook.nist.gov/cgi/cbook.cgi?ID=C64175&Mask=2#Thermo-Condensed.

Alekseev, K. V., Dubina, M. V. & Komov, V.P. 2015. Metabolic characteristics of citric acid synthesis by the fungus Aspergillus niger. *Applied Biochemistry and Microbiology*. 51(9):857–865.

Alibaba. 2022a. *Ferric Chloride Price*. [Online], Available: https://www.alibaba.com/product-detail/Ferric-Chloride-Chloride-Best-Quality-Promotional_1600223626002.html?spm=a2700.7724857.0.0.54661568VeSZe6&s=p [2022, July 08].

Alibaba. 2022b. *Industrial/Food Grade nah2po4 price sodium phosphate*. [Online], Available: https://www.alibaba.com/product-detail/Industrial-Food-Grade-nah2po4-price-sodium_60776134218.html [2022, July 08].

Alibaba. 2022c. *Sodium Citrate*. [Online], Available: https://www.alibaba.com/product-detail/Sodium-Citrate-Sodium-Citrate-6132-04_1600108990781.html?spm=a2700.7724857.0.0.67c819cadaMfuE&s=p [2022, July 08].

Alokika, Anu, Kumar, A., Kumar, V. & Singh, B. 2021. Cellulosic and hemicellulosic fractions of sugarcane bagasse: Potential, challenges and future perspective. *International Journal of Biological Macromolecules*. 169:564–582.

Anastassiadis, S. & Rehm, H.J. 2006. Citric acid production from glucose by yeast Candida oleophila ATCC 20177 under batch, continuous and repeated batch cultivation. *Electronic Journal of Biotechnology*. 9(1):26–39.

de Andrade, R.R., Maugeri Filho, F., Maciel Filho, R. & da Costa, A.C. 2013. Kinetics of ethanol production from sugarcane bagasse enzymatic hydrolysate concentrated with molasses under cell recycle. *Bioresource Technology*. 130:351–359.

Anu, Kumar, A., Rapoport, A., Kunze, G., Kumar, S., Singh, D. & Singh, B. 2020. Multifarious pretreatment strategies for the lignocellulosic substrates for the generation of renewable and sustainable biofuels: A review. *Renewable Energy*. 160:1228–1252.

Araújo, E.M.R., Coelho, F.E.B., Balarini, J.C., Miranda, T.L.S. & Salum, A. 2017. Solvent Extraction of Citric Acid with Different Organic Phases. *Advances in Chemical Engineering and Science*. 07(03):304–324.

Argyle, M.D. & Bartholomew, C.H. 2015. Heterogeneous catalyst deactivation and regeneration: A review. *Catalysts*. 5(1):145–269.

Ashby, M.F. 2013. Material Profiles. in *Materials and the Environment* Second ed. Amsterdam: Elsevier Inc. 99–117.

Atlić, A., Koller, M., Scherzer, D., Kutschera, C., Grillo-Fernandes, E., Horvat, P., Chiellini, E. & Braunegg, G. 2011. Continuous production of poly([R]-3-hydroxybutyrate) by Cupriavidus necator in a multistage bioreactor cascade. *Applied Microbiology and Biotechnology*. 91(2):295–304.

Ayodele, B.V., Alsaffar, M.A. & Mustapa, S.I. 2020. An overview of integration opportunities for sustainable bioethanol production from first- and second-generation sugar-based feedstocks. *Journal of Cleaner Production*. 245.

Baerdemaeker, T. De, Feyen, M., Mu, U., Yilmaz, B., Xiao, F., Zhang, W., Yokoi, T., Bao, X., et al. 2015. Bimetallic Zn and Hf on Silica Catalysts for the Conversion of Ethanol to 1,3-Butadiene. *ACS Catalysis*. 5:3393–3397.

De Baerdemaeker, T., Feyen, M., Müller, U., Yilmaz, B., Xiao, F.S., Zhang, W., Yokoi, T., Bao, X., et al. 2015. Bimetallic Zn and Hf on silica catalysts for the conversion of ethanol to 1,3-butadiene. *ACS Catalysis*. 5(6):3393–3397.

Bakhiet, S.E.A. & Al-Mokhtar, E.A.I. 2015. Production of citric acid by Aspergillus niger using sugarcane molasses as substrate. *Jordan Journal of Biological Sciences*. 8(3):211–215.

Baniel, A., Vitner, A., Gonen, D. & Heidel, D. 2008. *Patent No. US 7411090 B2*. United States.

Bankar, A. & Dr Geetha, N. 2018a. Fungal Citric acid production using waste materials : A mini-review. *Journal of Microbiology and Biotechnology and Food Sciences*. 8(2):821–828.

Bankar, A. & Dr Geetha, N. 2018b. Fungal Citric acid production using waste materials : A mini-review. *Journal of Microbiology and Biotechnology and Food Sciences*. (October).

Basso Carlos, L., Basso Olitta, T. & Rocha Nitsche, S. 2011. Ethanol Production in Brazil: The Industrial Process and Its Impact on Yeast Fermentation. *Biofuel Production-Recent Developments and Prospects*. 1530.

Bastos, R.G. & Ribeiro, H.C. 2020. Citric Acid Production by the Solid-State Cultivation Consortium of Aspergillus Niger and Trichoderma Reesei from Sugarcane Bagasse. *The Open Biotechnology Journal*. 14(1):32–41.

Batelle. 2001. Air Sparging Guidance Document. *Naval Facilities Engineering Service Center*. 1–118.

Batista, K.A., Bataus, L.A.M., Campos, I.T.N. & Fernandes, K.F. 2013. Development of culture medium using extruded bean as a nitrogen source for yeast growth. *Journal of Microbiological Methods*. 92(3):310–315.

Baylon, R.A.L., Sun, J. & Wang, Y. 2016. Conversion of ethanol to 1,3-butadiene over Na doped ZnxZryOz mixed metal oxides. *Catalysis Today*. 259(Part 2):446–452.

Becker, M.Y., Kohlheb, N., Hunger, S., Eschrich, S., Müller, R. & Aurich, A. 2020. Early-stage sustainability assessment of biotechnological processes: A case study of citric acid production. *Engineering in Life Sciences*. 20(3–4):90–103.

De Beer, A. 2011. Modelling and Simulation Based Assessment in Sustainable Bioprocess Development. *University of Cape Town.*

Behera, B.C., Mishra, R. & Mohapatra, S. 2021. Microbial citric acid: Production, properties, application, and future perspectives. *Food Frontiers*. (January):62–76.

Benjamin, Y., García-Aparicio, M.P. & Görgens, J.F. 2014. Impact of cultivar selection and process

optimization on ethanol yield from different varieties of sugarcane. *Biotechnology for Biofuels*. 7(1):1–17.

Bharti, S.N. & Swetha, G. 2016. Need for Bioplastics and Role of Biopolymer PHB: A Short Review. *Journal of Petroleum & Environmental Biotechnology*. 7(2).

Das Bhowmik, S.S., Brinin, A.K., Williams, B. & Mundree, S.G. 2016. Sugarcane biotechnology: Tapping unlimited potential. *Sugarcane-based Biofuels and Bioproducts*. (April):23–52.

Biocycle. 2012. *Sustainable polymer from sugarcane-Biocycle(R)-*. [Online], Available: https://fapesp.br/eventos/2012/07/Biopolymers/ROBERTO.pdf [2022, March 20].

Birajdar, S.D., Rajagopalan, S., Sawant, J.S. & Padmanabhan, S. 2015. Continuous predispersed solvent extraction process for the downstream separation of 2,3-butanediol from fermentation broth. *Separation and Purification Technology*. 151:115–123.

Bizukojc, M. & Ledakowicz, S. 2004. The kinetics of simultaneous glucose and fructose uptake and product formation by Aspergillus niger in citric acid fermentation. *Process Biochemistry*. 39(12):2261–2268.

Bozorg, A., Vossoughi, M., Kazemi, A. & Alemzadeh, I. 2015. Optimal medium composition to enhance poly-β-hydroxybutyrate production by Ralstonia eutropha using cane molasses as sole carbon source. *Applied Food Biotechnology*. 2(3):39–47.

Bratu, M.G., Stoica, A. & Buruleanu, L. 2008. a Study on the Behavior of a Commercial Invertase in Different Action Conditions . IX(June):109–112.

Breeze, P. 2014. Chapter 5 - Piston Engine-Based Power Plants. in *Power Generation Technologies* Elsevier Ltd. 93–110. [Online], Available: https://www.sciencedirect.com/science/article/pii/B9780080983301000053.

Brencio, C., Maruzzi, M., Manzolini, G. & Gallucci, F. 2022. Butadiene production in membrane reactors: A techno-economic analysis. *International Journal of Hydrogen Energy*. 47(50):21375–21390.

Bu, J., Wang, Y.T., Deng, M.C. & Zhu, M.J. 2021. Enhanced enzymatic hydrolysis and hydrogen production of sugarcane bagasse pretreated by peroxyformic acid. *Bioresource Technology*. 326(December 2020):124751.

Burla, J., Fehnel, R., Louie, P. & Terpeluk, P. 2012. Two-step Production of 1,3-Butadiene from Ethanol. *Senior Design Reports (CBE)*. 190. [Online], Available: http://repository.upenn.edu/cbe_sdr/42.

Cabrera Camacho, C.E., Alonso-Fariñas, B., Villanueva Perales, A.L., Vidal-Barrero, F. & Ollero, P. 2020. Techno-economic and Life-Cycle Assessment of One-Step Production of 1,3-Butadiene from Bioethanol Using Reaction Data under Industrial Operating Conditions. *ACS Sustainable Chemistry and Engineering*. 8(27):10201–10211.

Cai, D., Zhu, Q., Chen, C., Hu, S., Qin, P., Wang, B. & Tan, T. 2018. Fermentation–pervaporation–catalysis integration process for bio-butadiene production using sweet sorghum juice as feedstock. *Journal of the Taiwan Institute of Chemical Engineers*. 82:137–143.

Carrasco, C., Baudel, H.M., Sendelius, J., Modig, T., Roslander, C., Galbe, M., Hahn-Hagerdal, B., Zacchi, G., et al. 2010a. SO2-catalyzed steam pretreatment and fermentation of enzymatically hydrolyzed sugarcane bagasse. 46:64–73.

Carrasco, C., Baudel, H.M., Sendelius, J., Modig, T., Roslander, C., Galbe, M., Hahn-Hagerdal, B., Zacchi, G., et al. 2010b. SO2-catalyzed steam pretreatment and fermentation of enzymatically hydrolyzed sugarcane bagasse. (August 2019).

Carsanba, E., Papanikolaou, S., Fickers, P. & Erten, H. 2019. Screening various Yarrowia lipolytica strains for citric acid production. *Yeast*. 36(5):319–327.

Cavallo, E., Nobile, M., Cerrutti, P. & Foresti, M.L. 2020. Exploring the production of citric acid with

Yarrowia lipolytica using corn wet milling products as alternative low-cost fermentation media. *Biochemical Engineering Journal*. 155(December 2019):107463.

Celińska, E. & Grajek, W. 2009. Biotechnological production of 2,3-butanediol-Current state and prospects. *Biotechnology Advances*. 27(6):715–725.

Cha, J.W., Jang, S.H., Kim, Y.J., Chang, Y.K. & Jeong, K.J. 2020. Engineering of Klebsiella oxytoca for production of 2,3-butanediol using mixed sugars derived from lignocellulosic hydrolysates. *GCB Bioenergy*. 12(4):275–286.

Chaijamrus, S. & Udpuay, N. 2008. Production and Characterization of Polyhydroxybutyrate from Molasses and Corn Steep Liquor produced by Bacillus megaterium ATCC 6748. *Agricultural Engineering International: CIGR Journal*. X:1–12.

Chandel, A.K., da Silva, S.S. & Singh, O. V. 2011. Detoxification of Lignocellulosic Hydrolysates for Improved Bioethanol Production. *Biofuel Production-Recent Developments and Prospects*.

Cheali, P., Posada, J.A., Gernaey, K. V. & Sin, G. 2016. Economic risk analysis and critical comparison of optimal biorefinery concepts. *Biofuels, Bioproducts and Biorefining*. [Online], Available: https://onlinelibrary-wiley-com.ez.sun.ac.za/doi/10.1002/bbb.1654.

Cheong, J.L., Shao, Y., Tan, S.J.R., Li, X., Zhang, Y. & Lee, S.S. 2016. Highly Active and Selective Zr/MCF Catalyst for Production of 1,3-Butadiene from Ethanol in a Dual Fixed Bed Reactor System. *ACS Sustainable Chemistry and Engineering*. 4(9):4887–4894.

Choi, J. Il & Lee, S.Y. 1999a. Efficient and economical recovery of poly(3-hydroxybutyrate) from recombinant Escherichia coli by simple digestion with chemicals. *Biotechnology and Bioengineering*. 62(5):546–553.

Choi, J. & Lee, S.Y. 1999b. Factors affecting the economics of polyhydroxyalkanoate production by bacterial fermentation. *Applied Microbiology and Biotechnology*. 51(1):13–21.

Choi, J. & Lee, S.Y. 1999c. Efficient and economical recovery of poly(3-hydroxybutyrate) from recombinant Escherichia coli by simple digestion with chemicals. *Biotechnol Bioeng*. 543–553.

Choi, J. Il, Lee, S.Y. & Han, K. 1998. Cloning of the Alcaligenes latus polyhydroxyalkanoate biosynthesis genes and use of these genes for enhanced production of poly(3-hydroxybutyrate) in Escherichia coli. *Applied and Environmental Microbiology*. 64(12):4897–4903.

Choi, M., Kim, S., Kim, J., Park, Y. & Seo, J. 2016. Molecular cloning and expression of Enterobacter aerogenes ␣ -acetolactate decarboxylase in pyruvate decarboxylase-deficient Saccharomyces cerevisiae for efficient 2 , 3-butanediol production. 51:170–176.

Church, A.L., Sun, N., Yan, J., Karp, E., Tan, E., McNamara, I., Freeman, C., Liu, J., et al. 2021. *Separations Consortium 2,3-Butanediol (BDO) Separations*. [Online], Available: https://www.energy.gov/sites/default/files/2021-04/beto-18-peer-review-2021-bioproduct-church.pdf [2022, March 30].

Ciriminna, R., Meneguzzo, F., Delisi, R. & Pagliaro, M. 2017. Citric acid: Emerging applications of key biotechnology industrial product. *Chemistry Central Journal*. 11(1):1–9.

City of Cape Town. 2020. WATER AND WASTE SERVICES - WATER & SANITATION - SANITATION CONSUMPTIVE TARIFFS : LEVEL 3 WATER AND WASTE SERVICES - WATER & SANITATION - SANITATION CONSUMPTIVE TARIFFS : (May):1–8.

Clifton-García, B., González-Reynoso, O., Robledo-Ortiz, J.R., Villafaña-Rojas, J. & González-García, Y. 2020. Forest soil bacteria able to produce homo and copolymers of polyhydroxyalkanoates from several pure and waste carbon sources. *Letters in Applied Microbiology*. 70(4):300–309.

Cortivo, P.R.D., Machado, J., Hickert, L.R., Rossi, D.M. & Ayub, M.A.Z. 2019. Production of 2,3-butanediol

by Klebsiella pneumoniae BLh-1 and Pantoea agglomerans BL1 cultivated in acid and enzymatic hydrolysates of soybean hull. *Biotechnology Progress*. 35(3):1–8.

Dagle, V.L., Flake, M.D., Lemmon, T.L., Lopez, J.S., Kovarik, L. & Dagle, R.A. 2018. Effect of the SiO2 support on the catalytic performance of Ag/ZrO2/SiO2 catalysts for the single-bed production of butadiene from ethanol. *Applied Catalysis B: Environmental*. 236(May):576–587.

Dai, J., Zhang, Y. & Xiu, Z. 2011. Salting-out Extraction of 2 , 3-Butanediol from Jerusalem artichoke-based Fermentation Broth *. *Chinese Journal of Chemical Engineering*. 19(4):682–686.

Dai, W., Zhang, S., Yu, Z., Yan, T., Wu, G., Guan, N. & Li, L. 2017. Zeolite Structural Confinement Effects Enhance One-Pot Catalytic Conversion of Ethanol to Butadiene. *ACS Catalysis*. 7(5):3703–3706.

Davis, R., Grundl, N., Tao, L., Biddy, M.J., Tan, E.C.D., Beckham, G.T., Humbird, D., Thompson, D.N., et al. 2018. Process Design and Economics for the Conversion of Lignocellulosic Biomass to Hydrocarbon Fuels and Coproducts: 2018 Biochemical Design Case Update: Biochemical Deconstruction and Conversion of Biomass to Fuels and Products via Integrated Biorefinery Path. *Renewable Energy*. (November):147. [Online], Available: www.nrel.gov/publications.

Delgado Dobladez, J.A., Águeda Maté, V.I., Uribe Santos, D.L., Torrellas, S.Á. & Larriba, M. 2019. Citric Acid Purification by Simulated Moving Bed Adsorption with Methanol as Desorbent. *Separation Science and Technology (Philadelphia)*. 54(6):930–942.

Dezam, A.P.G., Vasconcellos, V.M., Lacava, P.T. & Farinas, C.S. 2017. Microbial production of organic acids by endophytic fungi. *Biocatalysis and Agricultural Biotechnology*. 11(August):282–287.

Dheskali, E. V. 2017. Techno-economic evaluation of biorefineries. (February).

Dhillon, G.S., Brar, S.K., Verma, M. & Tyagi, R.D. 2011. Recent Advances in Citric Acid Bio-production and Recovery. *Food and Bioprocess Technology*. 4(4):505–529.

Dias, M.O.D.S., Cavalett, O. & Filho, R.M. 2016. Integrated first- and second-generation processes for bioethanol production from sugarcane.

Dias, M.O.S., Junqueira, T.L., Filho, R.M., Maciel, M.R.W., Rossell, C.E.V. & Atala, D.I.P. 2009. Optimization of bioethanol distillation process evaluation of different configurations of the fermentation process. *Computer Aided Chemical Engineering*. 27(C):1893–1898.

Directorate-General Energy. 2015. From the Sugar Platform to biofuels and biochemicals.

Dogbe, E.S. 2020. Exergy, techno-economic and exergoeconomic analyses for improving energy efficiency of a typical sugar mill and designing integrated biorefineries. Stellenbosch University.

Dogbe, E.S., Mandegari, M. & Görgens, J.F. 2019a. Assessment of the thermodynamic performance improvement of a typical sugar mill through the integration of waste-heat recovery technologies. *Applied Thermal Engineering*. 158(February):113768.

Dogbe, E.S., Mandegari, M. & Görgens, J.F. 2019b. Assessment of the thermodynamic performance improvement of a typical sugar mill through the integration of waste-heat recovery technologies. *Applied Thermal Engineering*. 158(April):113768.

Dogbe, E.S., Mandegari, M. & Görgens, J.F. 2020. Revitalizing the sugarcane industry by adding value to A-molasses in biorefineries. *Biofuels, Bioproducts and Biorefining*. 14(5):1089–1104.

Dowe, N. 2021. *BETO 2021 Peer Review: Bench Scale Integration WBS 2.4.1.100*. [Online], Available: https://www.nrel.gov/docs/fy21osti/79309.pdf [2021, March 30].

Duan, H., Yamada, Y. & Sato, S. 2016. Future prospect of the production of 1,3-butadiene from butanediols. *Chemistry Letters*. 45(9):1036–1047.

Van Duc Long, N., Hong, J., Nhien, L.C. & Lee, M. 2018. Novel hybrid-blower-and-evaporator-assisted

distillation for separation and purification in biorefineries. 123(August 2017):195–203.

Dunn, J.B., Adom, F., Sather, N., Han, J. & Snyder, S. 2015. Life-cycle Analysis of Bioproducts and Their Conventional Counterparts in GREET ™. *Argoone National Laboratory*. 95.

Ensinas, A. V., Codina, V., Marechal, F., Albarelli, J. & Silva, M.A. 2013. Thermo-economic optimization of integrated first and second generation sugarcane ethanol plant. *Chemical Engineering Transactions*. 35:523–528.

enzymes.bio. 2022. *Invertase Enzyme For Sale*. [Online], Available: https://enzymes.bio/invertase-enzyme-for-sale/#:~:text=Our food-grade invertase powder,enzyme pricing and order page. [2022, July 07].

Erian, A.M., Gibisch, M. & Pflügl, S. 2018. Engineered E. coli W enables efficient 2,3-butanediol production from glucose and sugar beet molasses using defined minimal medium as economic basis. 1–17.

Farzad, S., Mandegari, M.A. & Görgens, J.F. 2017. Integrated techno-economic and environmental analysis of butadiene production from biomass. *Bioresource Technology*. 239:37–48.

Farzad, S., Mandegari, M.A., Guo, M., Haigh, K.F., Shah, N. & Görgens, J.F. 2017. Multi-product biorefineries from lignocelluloses: A pathway to revitalisation of the sugar industry? *Biotechnology for Biofuels*. 10(1):1–24.

Favaro, L., Basaglia, M., Casella, S. & Food, A. 2019. Improving polyhydroxyalkanoate production from inexpensive carbon sources by genetic approaches: a review. *Biofuels, Bioproducts and Biorefining*. 208–227.

Fernandez, L. 2020. *Global price of butadiene 2017-2022*. [Online], Available: https://www.statista.com/statistics/1171063/price-butadiene-forecast-globally/ [2022, July 08].

Fernandez, L. 2022. *Price of sulfur in the United States from 2014 to 2021*. [Online], Available: https://www.statista.com/statistics/1031180/us-sulfur-price/ [2022, July 08].

Förster, A., Aurich, A., Mauersberger, S. & Barth, G. 2007. Citric acid production from sucrose using a recombinant strain of the yeast Yarrowia lipolytica. *Applied Microbiology and Biotechnology*. 75(6):1409–1417.

Fu, C., Li, Z., Sun, Z. & Xie, S. 2020. A review of salting-out effect and sugaring-out effect: driving forces for novel liquid-liquid extraction of biofuels and biochemicals. *Frontiers of Chemical Science and Engineering*.

García-Torreiro, M., Lu-Chau, T.A. & Lema, J.M. 2016. Effect of nitrogen and/or oxygen concentration on poly(3-hydroxybutyrate) accumulation by Halomonas boliviensis. *Bioprocess and Biosystems Engineering*. 39(9):1365–1374.

Ge, Y., Li, K., Li, L., Gao, C., Zhang, L., Ma, C. & Xu, P. 2016. Contracted but effective: Production of enantiopure 2,3-butanediol by thermophilic and GRAS: Bacillus licheniformis. *Green Chemistry*. 18(17):4693–4703.

Getachew, A. & Woldesenbet, F. 2016. Production of biodegradable plastic by polyhydroxybutyrate (PHB) accumulating bacteria using low cost agricultural waste material. *BMC Research Notes*. 9(1):1–9.

Gorgens F; Mandegari, M A; Farzad, S; Daful, A G; Haigh, K.F. 2016. A BIOREFINERY APPROACH TO IMPROVE THE SUISTANABILITY OF THE SOUTH AFRICAN SUGAR. (January).

Guragain, Y.N. & Vadlani, P. V. 2017. 2,3-Butanediol production using Klebsiella oxytoca ATCC 8724: Evaluation of biomass derived sugars and fed-batch fermentation process. *Process Biochemistry*. 58(May):25–34.

Guragain, Y.N., Chitta, D., Karanjikar, M. & Vadlani, P. V. 2017. Appropriate lignocellulosic biomass processing strategies for efficient 2,3-butanediol production from biomass-derived sugars using

Bacillus licheniformis DSM 8785. *Food and Bioproducts Processing*. 104:147–158.

Haga, N. 2011. Combustion engine power plants - White paper.

Haider, J., Abdul, M., Hussain, A., Yasin, M. & Lee, M. 2018. Techno-economic analysis of various process schemes for the production of fuel grade 2,3-butanediol from fermentation broth. 140(April):93–107.

Haider, J., Harvianto, G.R., Qyyum, M.A. & Lee, M. 2018. Cost- and Energy-Efficient Butanol-Based Extraction-Assisted Distillation Designs for Purification of 2,3-Butanediol for Use as a Drop-in Fuel. *ACS Sustainable Chemistry and Engineering*. 6(11):14901–14910.

Hamann, M.L. 2020. Uncatalysed steam pretreatment regimes for bagasse and harvest residues in a sugarcane biorefinery. (March). [Online], Available: http://hdl.handle.net/10019.1/109744.

Haque, M.E., Gupta, T.K., Nazier, P. & Palanki, S. 2021. Techno-Economic Analysis of an Integrated Process Plant for the Production of 1,3-Butadiene from Natural Gas a. *Industrial and Engineering Chemistry Research*. 60(30):11187–11201.

Harrison, M.D. 2016. Sugarcane-derived animal feed. 281–310.

Harvianto, G.R., Haider, J., Hong, J., Long, N.V.D. & Shim, J.J. 2018a. Biotechnology for Biofuels Purification of 2,3-butanediol from fermentation broth : process development and techno-economic analysis. *Biotechnology for Biofuels*. 1–16.

Harvianto, G.R., Haider, J., Hong, J., Long, N.V.D. & Shim, J.J. 2018b. Biotechnology for Biofuels Purification of 2,3-butanediol from fermentation broth : process development and techno-economic analysis. *Biotechnology for Biofuels*. 1–16.

Häßler, T., Schieder, D., Pfaller, R., Faulstich, M. & Sieber, V. 2012. Enhanced fed-batch fermentation of 2,3-butanediol by Paenibacillus polymyxa DSM 365. *Bioresource Technology*. 124:237–244.

Hernández Rodríguez, T., Pörtner, R. & Frahm, B. 2013. Seed train optimization for suspension cell culture. *BMC Proceedings*. 7(S6):P9.

Huang, X., Men, Y., Wang, J., An, W. & Wang, Y. 2017. Highly active and selective binary MgO-SiO2 catalysts for the production of 1,3-butadiene from ethanol. *Catalysis Science and Technology*. 7(1):168–180.

Humbird, D., Davis, R., Tao, L., Kinchin, C., Hsu, D., Aden, A., Schoen, P., Lukas, J., et al. 2011. Process design and economics for conversion of lignocellulosic biomass to ethanol. *NREL technical report NREL/TP-5100-51400*. 303(May 2011):275–3000. [Online], Available: http://www.nrel.gov/docs/fy11osti/51400.pdf%5Cnpapers2://publication/uuid/49A5007E-9A58-4E2B-AB4E-4A4428F6EA66.

Huu Phong, T., Minh Khuong, D., Hop, D. Van & Thuoc, D. Van. 2017. DIFFERENT FRUCTOSE FEEDING STRATEGIES FOR POLY(3-HYDROXYBUTYRATE) PRODUCTION BY Yangia sp. ND199. *Journal of Science and Technology*. 55(2).

Ikram-Ul, H., Ali, S., Qadeer, M.A. & Iqbal, J. 2004. Citric acid production by selected mutants of Aspergillus niger from cane molasses. *Bioresource Technology*. 93(2):125–130.

Inc., B. 2005. Spray Dry Manual. 1–24.

INTRATEC. 2007a. *Potassium Hydroxide Prices*. [Online], Available: https://www.intratec.us/chemical-markets/potassium-hydroxide-price [2022, July 08].

INTRATEC. 2007b. *Calcium Carbonate Prices*. [Online], Available: https://www.intratec.us/chemical-markets/calcium-carbonate-price [2022, July 08].

INTRATEC. 2007c. *Ammonium Sulphate*. [Online], Available: https://www.intratec.us/chemical-

markets/ammonium-sulfate-price [2022, July 08].

INTRATEC. 2007d. *Ammonium Nitrate Prices*. [Online], Available: https://www.intratec.us/chemical-markets/ammonium-nitrate-price [2022, July 08].

Jantama, K., Polyiam, P., Khunnonkwao, P., Chan, S., Sangproo, M., Khor, K. & Suvarnakuta, S. 2015. Efficient reduction of the formation of by-products and improvement of production yield of 2 ,3-butanediol by a combined deletion of alcohol dehydrogenase , acetate kinase-phosphotransacetylase , and lactate dehydrogenase genes in metabolically enginee. 30:16–26.

Jenkins, S. 2020. *2019 CHEMICAL ENGINEERING PLANT COST INDEX ANNUAL AVERAGE*. [Online], Available: https://www.chemengonline.com/2019-chemical-engineering-plant-cost-index-annual-average/.

Ji, X.J., Nie, Z.K., Huang, H., Ren, L.J., Peng, C. & Ouyang, P.K. 2011. Elimination of carbon catabolite repression in Klebsiella oxytoca for efficient 2,3-butanediol production from glucose-xylose mixtures. *Applied Microbiology and Biotechnology*. 89(4):1119–1125.

Jiang, L.Q., Fang, Z., Zhao, Z.L., He, F. & Li, H. Bin. 2015. 2,3-butanediol and acetoin production from enzymatic hydrolysate of ionic liquid-pretreated cellulose by Paenibacillus polymyxa. *BioResources*. 10(1):1318–1329.

Jianlong, W., Xianghua, W. & Ding, Z. 2000. Production of citric acid from molasses integrated with in-situ product separation by ion-exchange resin adsorption. *Bioresource Technology*. 75(3):231–234.

Jones, M.D. 2014. Catalytic transformation of ethanol into 1,3-butadiene. *Chemistry Central Journal*. 8(1):1–5.

Jurchescu, I.M., Hamann, J., Zhou, X., Ortmann, T., Kuenz, A., Prüße, U. & Lang, S. 2013. Enhanced 2,3-butanediol production in fed-batch cultures of free and immobilized Bacillus licheniformis DSM 8785. *Applied Microbiology and Biotechnology*. 97(15):6715–6723.

Kachrimanidou, V., Ioannidou, S.M., Ladakis, D., Papapostolou, H., Kopsahelis, N., Koutinas, A.A. & Kookos, I.K. 2021. Techno-economic evaluation and life-cycle assessment of poly(3-hydroxybutyrate) production within a biorefinery concept using sunflower-based biodiesel industry by-products. *Bioresource Technology*. 326(January):124711.

Kanjanachumpol, P., Kulpreecha, S., Tolieng, V. & Thongchul, N. 2013. Enhancing polyhydroxybutyrate production from high cell density fed-batch fermentation of Bacillus megaterium BA-019. *Bioprocess and Biosystems Engineering*. 36(10):1463–1474.

Kaur, L., Khajuria, R., Parihar, L. & Dimpal Singh, G. 2017. Polyhydroxyalkanoates: Biosynthesis to commercial production- A review. *Journal of Microbiology, Biotechnology and Food Sciences*. 6(4):1098–1106.

Khan, Z., Dwivedi, A.K., Engineering, C. & College, U.E. 2013. Fermentation of Biomass for Production of Ethanol : A Review Abstract : 2 . Potential of Biomass. *Universal Journal of Environmental Research and Technology*. 3(1):1–13.

Khanna, S. & Srivastava, A.K. 2005. Recent advances in microbial polyhydroxyalkanoates. *Process Biochemistry*. 40(2):607–619.

Khetni, M. 2018. Design, construction and evaluation of vacuum evaporation system for the concentration of aqueous whey protein solutions. (March):164.

Kim, K.H., Lee, H. & Lee, C.Y. 2015. Pretreatment of Sugarcane Molasses and Citric Acid Production by Candida zeylanoides. *Microbiology and Biotechnology Letters*. 43:164–168.

Kim, S.-K., Park, D.-H., Song, S.H., Wee, Y.-J. & Jeong, G.-T. 2013. Effect of fermentation inhibitors in the presence and absence of activated charcoal on the growth of Saccharomyces cerevisiae. 659–666.

Kim, S.J., Sim, H.J., Kim, J.W., Lee, Y.G., Park, Y.C. & Seo, J.H. 2017. Enhanced production of 2,3-butanediol from xylose by combinatorial engineering of xylose metabolic pathway and cofactor regeneration in pyruvate decarboxylase-deficient Saccharomyces cerevisiae. *Bioresource Technology*. 245:1551–1557.

King, M.J., Davenport, W.G. & Moats, M.S. 2013. Sulphur Burning. in *Sulphuric Acid Manufacture* 2nd ed. 19–29.

Koekemoer, T. 2018. Lactic acid production from sugarcane bagasse and harvesting residues. (March).

Koller, M. 2018. A Review on Established and Emerging Fermentation Schemes for Microbial Production of Polyhydroxyalkanoate (PHA) Biopolyesters. *Fermentation*.

Koller, M., Niebelschütz, H. & Braunegg, G. 2013. Strategies for recovery and purification of poly[(R)-3-hydroxyalkanoates] (PHA) biopolyesters from surrounding biomass. *Engineering in Life Sciences*. 13(6):549–562.

Konzock, O., Zaghen, S. & Norbeck, J. 2021. Tolerance of Yarrowia lipolytica to inhibitors commonly found in lignocellulosic hydrolysates. *BMC Microbiology*. 21(1):1–10.

Koutinas, A.A., Yepez, B., Kopsahelis, N., Freire, D.M.G., de Castro, A.M., Papanikolaou, S. & Kookos, I.K. 2016. Techno-economic evaluation of a complete bioprocess for 2,3-butanediol production from renewable resources. *Bioresource Technology*. 204(October):55–64.

Kuenz, A., Jäger, M., Niemi, H., Kallioinen, M., Mänttäri, M. & Prüße, U. 2020. Conversion of Xylose from Birch Hemicellulose Hydrolysate to 2,3-Butanediol with Bacillus vallismortis. *Fermentation*. 6(3):86.

Kuznetsov, A., Kumar, G., Ardagh, M.A., Tsapatsis, M., Zhang, Q. & Dauenhauer, P.J. 2020. On the Economics and Process Design of Renewable Butadiene from Biomass-Derived Furfural. *ACS Sustainable Chemistry and Engineering*. 8(8):3273–3282.

Kyriienko, P.I., Larina, O. V., Balakin, D.Y., Stetsuk, A.O., Nychiporuk, Y.M., Soloviev, S.O. & Orlyk, S.M. 2021. 1,3-Butadiene production from aqueous ethanol over ZnO/MgO-SiO2 catalysts: Insight into H2O effect on catalytic performance. *Applied Catalysis A: General*. 616(March):118081.

Laluce, C., Leite, G.R., Zavitoski, B.Z., Zamai, T.T. & Ventura, R. 2016. *Fermentation of sugarcane juice and molasses for ethanol production*.

LanzaTech. 2018. *CCU-Now: fuels and chemicals from waste*. [Online], Available: https://ec.europa.eu/energy/sites/default/files/documents/25_sean_simpson-lanzatech.pdf [2022, April 06].

Larina, O. V, Remezovskyi, I.M., Kyriienko, P.I., Soloviev, S.O. & Orlyk, S.M. 2019. 1,3-Butadiene production from ethanol-water mixtures over Zn-La-Zr-Si oxide catalyst. *Reaction Kinetics, Mechanisms and Catalysis*. 903–915.

Ledesma-Amaro, R., Lazar, Z., Rakicka, M., Guo, Z., Fouchard, F., Coq, A.M.C. Le & Nicaud, J.M. 2016. Metabolic engineering of Yarrowia lipolytica to produce chemicals and fuels from xylose. *Metabolic Engineering*. 38:115–124.

Lee, S.Y. & Choi, J. Il. 1998. Effect of fermentation performance on the economics of poly(3-hydroxybutyrate) production by Alcaligenes latus. *Polymer Degradation and Stability*. 59(1–3):387–393.

Lee, Y.G. & Seo, J.H. 2019. Production of 2,3-butanediol from glucose and cassava hydrolysates by metabolically engineered industrial polyploid Saccharomyces cerevisiae. *Biotechnology for Biofuels*. 12(1):1–12.

Lee, S.Y., Choi, J. Il, Han, K. & Song, J.Y. 1999. Removal of endotoxin during purification of poly(3-hydroxybutyrate) from gram-negative bacteria. *Applied and Environmental Microbiology*.

65(6):2762–2764.

Leibbrandt, N.H. 2010. TECHNO - ECONOMIC STUDY FOR SUGARCANE BAGASSE TO LIQUID BIOFUELS IN SOUTH AFRICA : A COMPARISON BETWEEN BIOLOGICAL AND THERMOCHEMICAL PROCESS ROUTES. (March).

Li, Y. & Wu, Y. 2016. Separating 2,3-butanediol from fermentation broth using n-butylaldehyde.

Li, H., Pang, J., Jaegers, N.R., Kovarik, L., Engelhard, M., Savoy, A.W., Hu, J., Sun, J., et al. 2020. Conversion of ethanol to 1,3–butadiene over Ag–ZrO2/SiO2 catalysts: The role of surface interfaces. *Journal of Energy Chemistry*. 54:7–15.

Li, L., Li, K., Wang, K., Chen, C., Gao, C., Ma, C. & Xu, P. 2014. Efficient production of 2,3-butanediol from corn stover hydrolysate by using a thermophilic Bacillus licheniformis strain. *Bioresource Technology*. 170:256–261.

Li, L., Chen, C., Li, K., Wang, Y., Gao, C., Ma, C. & Xu, P. 2014. Efficient simultaneous saccharification and fermentation of inulin to 2,3-butanediol by thermophilic Bacillus licheniformis ATCC 14580. *Applied and Environmental Microbiology*. 80(20):6458–6464.

Li, Q.Z., Jiang, X.L., Feng, X.J., Wang, J.M., Sun, C., Zhang, H.B., Xian, M. & Liu, H.Z. 2015. Recovery processes of organic acids from fermentation broths in the biomass-based industry. *Journal of Microbiology and Biotechnology*. 26(1):1–8.

Li, Y., Wu, Y., Zhu, J., Liu, J. & Shen, Y. 2016. Separating 2,3-butanediol from fermentation broth using n-butylaldehyde. *Journal of Saudi Chemical Society*.

Liu, F., Li, W., Ridgway, D., Gu, T. & Shen, Z. 1998. Production of poly-β-hydroxybutyrate on molasses by recombinant Escherichia coli. *Biotechnology Letters*. 20(4):345–348.

Luyben, W.L. 2017. Estimating refrigeration costs at cryogenic temperatures. *Computers and Chemical Engineering*. 103:144–150.

MacAringue, E.G.J., Li, S., Li, M., Gong, J. & Tang, W. 2020. Crystallization behavior of citric acid based on solution speciation and growth kinetics. *CrystEngComm*. 22(47):8189–8196.

Mailaram, S., Narisetty, V., Ranade, V. V., Kumar, V. & Maity, S.K. 2022. Techno-Economic Analysis for the Production of 2,3-Butanediol from Brewers' Spent Grain Using Pinch Technology. *Industrial and Engineering Chemistry Research*. 61(5):2195–2205.

Maina, S., Mallouchos, A., Nychas, G.E., Freire, D.M.G., Castro, M. De, Papanikolaou, S., Kookos, I.K. & Koutinas, A. 2019. Bioprocess development for (2R, 3R)-butanediol and acetoin production using very high polarity cane sugar and sugarcane molasses by a Bacillus amyloliquefaciens strain. (January).

Maina, S., Stylianou, E., Vogiatzi, E., Vlysidis, A., Mallouchos, A., Nychas, G.J.E., de Castro, A.M., Dheskali, E., et al. 2019. Improvement on bioprocess economics for 2,3-butanediol production from very high polarity cane sugar via optimisation of bioreactor operation. *Bioresource Technology*. 274(October 2018):343–352.

Maina, S., Prabhu, A.A., Vivek, N., Vlysidis, A., Koutinas, A. & Kumar, V. 2022. Prospects on bio-based 2,3-butanediol and acetoin production: Recent progress and advances. *Biotechnology Advances*. 54(June 2021).

Makhetha, M. 2016. Fractionation of Lignocellulosic Biomass for Production of Materials and Chemicals by. *Masters' Thesis, Stellenbosch University*. (March).

Makshina, E. V., Dusselier, M., Janssens, W., Degrève, J., Jacobs, P.A. & Sels, B.F. 2014. Review of old chemistry and new catalytic advances in the on-purpose synthesis of butadiene. *Chemical Society Reviews*. 43(22):7917–7953.

Mandegari, M., Farzad, S. & Görgens, J.F. 2018. A new insight into sugarcane biorefineries with fossil fuel co-combustion: Techno-economic analysis and life cycle assessment. *Energy Conversion and Management*. 165(October 2017):76–91.

Mandegari, M.A., Farzad, S. & Görgens, J.F. 2017. Economic and environmental assessment of cellulosic ethanol production scenarios annexed to a typical sugar mill. *Bioresource Technology*. 224:314–326.

Mantingh, J. & Kiss, A.A. 2021. Enhanced process for energy efficient extraction of 1,3-butadiene from a crude C4 cut. *Separation and Purification Technology*. 267(February):118656.

Marciniak, P. & Możejko-Ciesielska, J. 2021. What is new in the field of industrial wastes conversion into polyhydroxyalkanoates by bacteria? *Polymers*. 13(11).

Martín, C., Galbe, M., Nilvebrant, N.O. & Jönsson, L.J. 2002. Comparison of the fermentability of enzymatic hydrolyzates of sugarcane bagasse pretreated by steam explosion using different impregnating agents. *Applied Biochemistry and Biotechnology - Part A Enzyme Engineering and Biotechnology*. 98–100:699–716.

Martinez., A., Grabar, T.B., Shanmugam, K.T., Yomano, L.P., York, S.W. & Ingram, L.O. 2007. Low salt medium for lactate and ethanol production by recombinant Escherichia coli B. 107:397–404.

McAdam, B., Fournet, M.B., McDonald, P. & Mojicevic, M. 2020. Production of polyhydroxybutyrate (PHB) and factors impacting its chemical and mechanical characteristics. *Polymers*. 12(12):1–20.

Van Der Merwe, A.B. 2010. Evaluation of Different Process Designs for Biobutanol Production from Sugarcane Molasses. (March).

Michelin. 2019. *Michelin, IFP Energies nouvelle, ad Axens give a new dimension to the Biobutterfly project*. [Online], Available: https://www.michelin.com/en/press-releases/michelin-ifp-energies-nouvelles-and-axens-give-a-new-dimension-to-the-biobutterfly-project/ [2022, April 06].

Miyazawa, T., Tanabe, Y., Nakamura, I., Shinke, Y., Hiza, M., Choe, Y.K. & Fujitani, T. 2020. Fundamental roles of ZnO and ZrO2in the conversion of ethanol to 1,3-butadiene over ZnO-ZrO2/SiO2. *Catalysis Science and Technology*. 10(22):7531–7541.

Moeller, L., Zehnsdorf, A., Aurich, A., Barth, G., Bley, T. & Strehlitz, B. 2013. Citric acid production from sucrose by recombinant Yarrowia lipolytica using semicontinuous fermentation. *Engineering in Life Sciences*. 13(2):163–171.

Mohammad, M. Bin, Brooks, G. & Akbar Rhamdhani, M. 2017. High temperature properties of molten nitrate salt for solar thermal energy storage application. *Minerals, Metals and Materials Series*. (9783319510903):531–539.

Moncada, J., El-Halwagi, M.M. & Cardona, C.A. 2013. Techno-economic analysis for a sugarcane biorefinery: Colombian case. *Bioresource Technology*. 135:533–543.

Moncada, J., Matallana, L.G. & Cardona, C.A. 2013. Selection of process pathways for biorefinery design using optimization tools: A colombian case for conversion of sugarcane bagasse to ethanol, poly-3-hydroxybutyrate (PHB), and energy. *Industrial and Engineering Chemistry Research*. 52(11):4132–4145.

Moncada, J., Gursel, I.V., Worrell, E. & Ramírez, A. 2018. Production of 1,3-butadiene and ε-caprolactam from C6 sugars: Techno-economic analysis. *Biofuels, Bioproducts and Biorefining*. 12(4):600–623.

Moonsamy, T.A. 2021. Techno-economic analysis and benchmarking of integrated first and second generation biorefinery scenarios annexed to a typical sugar mill for bioethanol production.

Mores, S., Vandenberghe, L.P. de S., Magalhães Júnior, A.I., de Carvalho, J.C., de Mello, A.F.M., Pandey, A. & Soccol, C.R. 2021. Citric acid bioproduction and downstream processing: Status, opportunities, and challenges. *Bioresource Technology*. 320(October 2020).

Naleli, K. 2016. Process Modelling In Production of Biobutanol from Lignocellulosic Biomass via ABE Fermentation. (March).

Narayanamurthy, G., Ramachandra, Y.L., Rai, S.P., Ganapathy, P.S.S., Kavitha, B.T. & Manohara, Y.N. 2008. Comparative studies on submerged, liquid surface and solid state fermentation for citric acid production by Aspergillus niger RCNM 17. *Asian Journal of Microbiology, Biotechnology and Environmental Sciences*. 10(2):361–364.

Nghiem, N.P., Kleff, S. & Schwegmann, S. 2017. Succinic acid: Technology development and commercialization. *Fermentation*. 3(2):1–14.

Nieder-Heitmann, M. 2019. Techno-economic and life cycle analyses for comparison of biorefinery scenarios for the production of succinic acid, itaconic acid and polyhydroxybutyrate (PHB) from sugarcane lignocelluloses. (April).

NIH. 2019. NIH Guidelines for Research Involving Recombinant or Synthetic Nucleic Acid Molecules. *NIH Guidelines*. 2(April):1–7. [Online], Available: https://osp.od.nih.gov/wp-content/uploads/nih_guidelines.pdf.

O'Hair, J., Jin, Q., Yu, D., Poe, N., Li, H., Thapa, S., Zhou, S. & Huang, H. 2020. Thermophilic and Alkaliphilic Bacillus licheniformis YNP5-TSU as an Ideal Candidate for 2,3-Butanediol Production. *ACS Sustainable Chemistry and Engineering*. 8(30):11244–11252.

O'Hara, I.M. 2016. *Sugarcane-Based Biofuels and Bioproducts. Chapter 1: The sugarcane industry, biofuel, and bioproduct perspectives.*

OECD/FAO. 2019. *OECD-FAO Agricultural Outlook 2019-2028. Special Focus: Latin America*. [Online], Available: https://doi.org/10.1787/agr_outlook-2018-en%0Ahttp://www.oecd-ilibrary.org/content/book/agr_outlook-2012-en.

Ögmundarson, Ó., Sukumara, S., Herrgård, M.J. & Fantke, P. 2020. Combining Environmental and Economic Performance for Bioprocess Optimization. *Trends in Biotechnology*. 38(11):1203–1214.

Okonkwo, C.C. 2017. Process development and metabolic engineering to enhance 2 , 3- butanediol production by Paenibacillus polymyxa DSM 365.

Oliveira, F.M.V., Pinheiro, I.O., Souto-Maior, A.M., Martin, C., Gonçalves, A.R. & Rocha, G.J.M. 2013. Industrial-scale steam explosion pretreatment of sugarcane straw for enzymatic hydrolysis of cellulose for production of second generation ethanol and value-added products. *Bioresource Technology*. 130:168–173.

Ourique, L.J., Rocha, C.C., Gomes, R.C.D., Rossi, D.M. & Ayub, M.A.Z. 2020. Bioreactor production of 2,3-butanediol by Pantoea agglomerans using soybean hull acid hydrolysate as substrate. *Bioprocess and Biosystems Engineering*. 43(9):1689–1701.

Özüdoğru, H.M.R. 2018. Techno-economic Analysis of Xylitol, Citric Acid and Glutamic Acid Biorefinery Scenarios Utilizing Sugarcane Lignocellulose. (March).

Pagliano, G., Galletti, P., Samorì, C., Zaghini, A. & Torri, C. 2021. Recovery of Polyhydroxyalkanoates From Single and Mixed Microbial Cultures: A Review. *Frontiers in Bioengineering and Biotechnology*. 9(February):1–28.

Park, J.M., Song, H., Lee, H.J. & Seung, D. 2013. In silico aided metabolic engineering of Klebsiella oxytoca and fermentation optimization for enhanced 2,3-butanediol production. *Journal of Industrial Microbiology and Biotechnology*. 40(9):1057–1066.

Park, J.M., Rathnasingh, C. & Song, H. 2015. Enhanced production of (R,R)-2,3-butanediol by metabolically engineered Klebsiella oxytoca. *Journal of Industrial Microbiology and Biotechnology*. 42(10):1419–1425.

Pasternack, R., Mead, F.L. & Davenport, J.L. 1934. *Patent No. US 1965429*. United States.

Patel, R. & Pandya, H.N. 2015. Production of acetic acid from molasses by fermentation process. *Ijariie Journal*. 1(2):58–60. [Online], Available: https://www.academia.edu/12652526/Production_of_acetic_acid_from_molasses_by_fermentation_process?auto=download.

Petersen, A.M. 2012. Comparisons of the technical, financial risk and life cycle assessments of various processing options of sugercane bagasse to biofuels in {South} {Africa}. (March). [Online], Available: http://scholar.sun.ac.za/handle/10019.1/20156.

Petersen, A.M., Brown, L.J., Xavier, F. & Johann, C. 2021. Flowsheet Analysis of Valourising Mixed Lignocellulose and Plastic Wastes via Fast Pyrolysis at a Paper Mill. *Waste and Biomass Valorization*. 12(2):1025–1038.

Phillips, S.D., Jones, S.B., Meyer, P.A. & Snowden-Swan, L.J. 2022. Techno-economic analysis of cellulosic ethanol conversion to fuel and chemicals. *Biofuels, Bioproducts and Biorefining*. 16(3):640–652.

Pillai, J. & Desai, R. 2018. Dehumidification strategies and their applicability based on climate and building typology. *ASHRAE and IBPSA-USA Building Simulation Conference*. 759–766.

Pomalaza, G., Capron, M., Ordomsky, V. & Dumeignil, F. 2016. Recent breakthroughs in the conversion of ethanol to butadiene. *Catalysts*. 6(12).

Pomalaza, G., Vofo, G., Capron, M. & Dumeignil, F. 2018. ZnTa-TUD-1 as an easily prepared, highly efficient catalyst for the selective conversion of ethanol to 1,3-butadiene. *Green Chemistry*. 20(14):3203–3209.

Pomalaza, G., Arango Ponton, P., Capron, M. & Dumeignil, F. 2020a. Ethanol-to-butadiene: The reaction and its catalysts. *Catalysis Science and Technology*. 10(15):4860–4911.

Pomalaza, G., Arango Ponton, P., Capron, M. & Dumeignil, F. 2020b. Ethanol-to-butadiene: The reaction and its catalysts. *Catalysis Science and Technology*. 10(15):4860–4911.

Ponce, G.H.S.F., Miranda, J.C.C., Maciel Filho, R., De Andrade, R.R. & Wolf, M.R.M. 2015. Simulation, analysis and optimization of sugar concentration in an in situ gas stripping fermentation process for bioethanol production. *Chemical Engineering Transactions*. 43:319–324.

Popovic, M. 2019. Thermodynamic properties of microorganisms : determination and analysis of enthalpy , entropy , and Gibbs free energy of biomass , cells and colonies of 32 microorganism species. *Heliyon*. 5(December 2018):e01950.

Posada, J.A., Naranjo, J.M., López, J.A., Higuita, J.C. & Cardona, C.A. 2011. Design and analysis of poly-3-hydroxybutyrate production processes from crude glycerol. *Process Biochemistry*. 46(1):310–317.

Price, S., Kuzhiumparambil, U., Pernice, M. & Ralph, P.J. 2020a. Cyanobacterial polyhydroxybutyrate for sustainable bioplastic production: Critical review and perspectives. *Journal of Environmental Chemical Engineering*. 8(4):104007.

Price, S., Kuzhiumparambil, U., Pernice, M. & Ralph, P.J. 2020b. Cyanobacterial polyhydroxybutyrate for sustainable bioplastic production: Critical review and perspectives. *Journal of Environmental Chemical Engineering*. 8(4):104007.

Priya, A., Dureja, P., Rathi, R. & Lal, B. 2021. Comparative assessment of separation techniques for downstream processing of 2,3-Butanediol. 292(February).

Rackemann, D.W., Zhang, Z. & Doherty, W.O.S. 2016. Conversion of sugarcane carbohydrates into platform chemicals. *Sugarcane-based Biofuels and Bioproducts*. 207–236.

Rameshwari, R. & Meenakshisundaram, M. 2014. A Review on Downstream Processing of Bacterial Thermoplastic- Polyhydroxyalkanoate. *International Journal of Pure and Applied Bioscience*.

2(2):68–80.

Reddick, J. & Kruger, R. 2019. GreenCape 2019 Market Intelligence report. *Greencape*. 21.

Reddy, R.G. 2011. Molten salts: Thermal energy storage and heat transfer media. *Journal of Phase Equilibria and Diffusion*. 32(4):269–270.

Rodrigues, R.C.L.B., Felipe, M.G.A., Almeida e Silva, J.B., Vitolo, M. & Gomez, P. V. 2001. The influence of pH, temperature and hydrolyzate concentration on the removal of volatile and nonvolatile compounds from sugarcane bagasse hemicellulosic hydrolyzate treated with activated charcoal before or after vacuum evaporation. *Brazilian Journal of Chemical Engineering*. [Online], Available: https://www-scielo-br.ez.sun.ac.za/j/bjce/a/xctwtvnvzG6zGp9QbDbwzMH/?lang=en#.

Rosales-Calderon, O. & Arantes, V. 2019. *A review on commercial-scale high-value products that can be produced alongside cellulosic ethanol*. Vol. 12. BioMed Central.

Roundtable on Sustainable Biomaterials (RSB). 2022. *GHG Calculator*. [Online], Available: https://rsb.org/services-products/ghg-calculator/ [2021, December 02].

Roy, P. & Sardar, A. 2015. SO2 Emission Control and Finding a Way Out to Produce Sulphuric Acid from Industrial SO2 Emission. *Journal of Chemical Engineering & Process Technology*. 06(02).

Sabapathy, P.C., Devaraj, S., Anburajan, P., Parvez, A., Kathirvel, P. & Qi, X. 2021. Active polyhydroxybutyrate (PHB)/sugarcane bagasse fiber-based anti-microbial green composite: material characterization and degradation studies. *Applied Nanoscience (Switzerland)*. (0123456789).

Sabra, W., Quitmann, H., Zeng, A.-P., Dai, J.-Y. & Xiu, Z.-L. 2011. Microbial Production of 2,3-Butanediol. in *Comprehensive Biotechnology* Second Edi ed. 87–97.

Samrot, A. V, Samanvitha, S.K., Shobana, N., Renitta, E.R., Kumar, P.S., Kumar, S.S., Abirami, S., Dhiva, S., et al. 2021. The Synthesis , Characterization and Applications of Polyhydroxyalkanoates (PHAs) and PHA - Based Nanoparticles. 1–29.

Samsudin, I. Bin, Zhang, H., Jaenicke, S. & Chuah, G. 2020. Recent Advances in Catalysts for the Conversion of Ethanol to Butadiene. 4199–4214.

Bin Samsudin, I., Zhang, H., Jaenicke, S. & Chuah, G.K. 2020. Recent Advances in Catalysts for the Conversion of Ethanol to Butadiene. *Chemistry - An Asian Journal*. 15(24):4199–4214.

Saratale, R.G., Cho, S.K., Saratale, G.D., Ghodake, G.S., Bharagava, R.N., Kim, D.S., Nair, S. & Shin, H.S. 2021. Efficient bioconversion of sugarcane bagasse into polyhydroxybutyrate (PHB) by Lysinibacillus sp. and its characterization. *Bioresource Technology*. 324(January):124673.

Shao, P. & Kumar, A. 2009. Recovery of 2 , 3-butanediol from water by a solvent extraction and pervaporation separation scheme ☪. 329:160–168.

Show, P.L., Oladele, K.O., Siew, Q.Y., Aziz Zakry, F.A., Lan, J.C.W. & Ling, T.C. 2015. Overview of citric acid production from Aspergillus niger. *Frontiers in Life Science*. 8(3):271–283.

Shrivastav, A., Lee, J., Kim, H.Y. & Kim, Y.R. 2013. Recent insights in the removal of klebseilla pathogenicity factors for the industrial production of 2,3-butanediol. *Journal of Microbiology and Biotechnology*. 23(7):885–896.

Sikora, B., Kubik, C., Kalinowska, H., Gromek, E., Białkowska, A., Jędrzejczak-Krzepkowska, M., Schüett, F. & Turkiewicz, M. 2016. Application of byproducts from food processing for production of 2,3-butanediol using Bacillus amyloliquefaciens TUL 308. *Preparative Biochemistry and Biotechnology*. 46(6):610–619.

Silva, L.F., Taciro, M.K., Michelin Ramos, M.E., Carter, J.M., Pradella, J.G.C. & Gomez, J.G.C. 2004. Poly-3-hydroxybutyrate (P3HB) production by bacteria from xylose, glucose and sugarcane bagasse

hydrolysate. *Journal of Industrial Microbiology and Biotechnology*. 31(6):245–254.

Silveira, M.H.L., Chandel, A.K., Vanelli, B.A., Sacilotto, K.S. & Cardoso, E.B. 2018. Production of hemicellulosic sugars from sugarcane bagasse via steam explosion employing industrially feasible conditions: Pilot scale study. *Bioresource Technology Reports*. 3(August):138–146.

Singh, A. & Yakhmi, J. 2017. *Polyhydroxyalkanoates: Biodegradable Plastics and Their Applications*. Springer, Cham.

Soccol, C.R., Vandenberghe, L.P.S., Rodrigues, C. & Pandey, A. 2006. New perspectives for citric acid production and application. *Food Technology and Biotechnology*. 44(2):141–149.

Song, D.S. 2018. *Patent No. US 9884800 B2*. United States.

Song, C.W., Rathnasingh, C., Park, J.M., Lee, J. & Song, H. 2018. Isolation and evaluation of Bacillus strains for industrial production of 2,3-butanediol. *Journal of Microbiology and Biotechnology*. 28(3):409–417.

Song, C.W., Park, J.M., Chung, S.C. & Song, H. 2019a. Microbial production of 2,3-butanediol for industrial applications. *Journal of Industrial Microbiology & Biotechnology*. 46(11):1583–1601.

Song, C.W., Park, J.M., Chung, S.C. & Song, H. 2019b. Microbial production of 2,3-butanediol for industrial applications. *Journal of Industrial Microbiology & Biotechnology*. 46(11):1583–1601.

Song, D., Yoon, Y.G. & Lee, C.J. 2017a. Conceptual design for the recovery of 1,3-Butadiene and methyl ethyl ketone via a 2,3-Butanediol-dehydration process. *Chemical Engineering Research and Design*. 123:268–276.

Song, D., Yoon, Y.G. & Lee, C.J. 2017b. Conceptual design for the recovery of 1,3-Butadiene and methyl ethyl ketone via a 2,3-Butanediol-dehydration process. *Chemical Engineering Research and Design*. 123:268–276.

Song, D., Yoon, Y.G. & Lee, C.J. 2018. Techno-economic evaluation of the 2,3-butanediol dehydration process using a hydroxyapatite-alumina catalyst. *Korean Journal of Chemical Engineering*. 35(12):2348–2354.

Song, D., Yoon, Y.-G., Seo, S.-K. & Lee, C.-L. 2019. Improvement of 1,3-Butadiene Separation in 2,3-Butanediol Dehydration Using Extractive Distillation. *Processes*.

Sorrels, J.L. & Walton, T.G. 2017. Cost Estimation: Concepts and Methodology. *Epa Air Pollution Control Cost Manual*. 1–45.

de Sousa Dias, M.M., Koller, M., Puppi, D., Morelli, A., Chiellini, F. & Braunegg, G. 2017. Fed-batch synthesis of poly(3-hydroxybutyrate) and poly(3-hydroxybutyrate-co-4-hydroxybutyrate) from sucrose and 4-hydroxybutyrate precursors by burkholderia sacchari strain DSM 17165. *Bioengineering*. 4(2).

Srivastava, R.K., Jozewicz, W. & Singer, C. 2001. SO2 Scrubbing Technologies :A Review. 20(4):219–228.

Sun, D., Li, Y., Yang, C., Su, Y., Yamada, Y. & Sato, S. 2020. Production of 1,3-butadiene from biomass-derived C4 alcohols. *Fuel Processing Technology*. 197(May 2019).

Sun, L., Gong, M., Lv, X., Huang, Z., Gu, Y., Li, J., Du, G. & Liu, L. 2020. Current advance in biological production of short-chain organic acid. *Applied Microbiology and Biotechnology*. 104(21):9109–9124.

Taiwo, A.E., Madzimbamuto, T.N. & Ojumu, T.V. 2018. Optimization of corn steep liquor dosage and other fermentation parameters for ethanol production by saccharomyces cerevisiae type 1 and anchor instant yeast. *Energies*. 11(7):1–20.

Tan, D., Xue, Y.S., Aibaidula, G. & Chen, G.Q. 2011. Unsterile and continuous production of

polyhydroxybutyrate by Halomonas TD01. *Bioresource Technology*. 102(17):8130–8136.

Tan, E.C.D., Snowden-Swan, L.J., Abhijit Dutta, M.T., Jones, S., Ramasamy, K.K., Gray, M., Dagel, R., Padmaperuma, A., et al. 2017. Comparative techno-economic analysis and process design for indirect liquefication pathways to distillate-range fuels via biomass-derived oxygenated intermediates upgrading. *Biofuels, Bioproducts and Biorefining*.

Tan, M.J., Chen, X., Wang, Y.K., Liu, G.L. & Chi, Z.M. 2016. Enhanced citric acid production by a yeast Yarrowia lipolytica over-expressing a pyruvate carboxylase gene. *Bioprocess and Biosystems Engineering*. 39(8):1289–1296.

Tao, L., Aden, A., Elander, R.T., Pallapolu, V.R., Lee, Y.Y., Garlock, R.J., Balan, V., Dale, B.E., et al. 2011. Process and technoeconomic analysis of leading pretreatment technologies for lignocellulosic ethanol production using switchgrass. *Bioresource Technology*. 102(24):11105–11114.

The Engineering Toolbox. 2022. *Ammonia- Thermophysical Properties*. [Online], Available: https://www.engineeringtoolbox.com/ammonia-d_1413.html [2022, July 09].

Tinôco, D., Borschiver, S., Coutinho, P.L. & Freire, D.M.G. 2021. Technological development of the bio-based 2,3-butanediol process. *Biofuels, Bioproducts and Biorefining*. 15(2):357–376.

Trimm, D.L. 1999. Catalysts for the control of coking during steam reforming. *Catalysis Today*. 49(1–3):3–10.

Tripathi, N., Palanki, S., Xu, Q. & Nigam, K.D.P. 2019. Production of 1,3-Butadiene and Associated Coproducts Ethylene and Propylene from Lignin. *Industrial and Engineering Chemistry Research*. 58(35):16182–16189.

Tsukamoto, D., Sakami, S., Ito, M., Yamada, K. & Yonehara, T. 2016. Production of bio-based 1,3-butadiene by highly selective dehydration of 2,3-butanediol over SiO2-supported cesium dihydrogen phosphate catalyst. *Chemistry Letters*. 45(7):831–833.

Turton, R.; Shaeiwitz, J.A.; Bhattacharyya, D.; Whiting, W.B. 2018. *Analysis, Synthesis And Design of Chemical Processes*. 5th ed.

United States Department of Labor US. 2020. *U.S BUREAU OF LABOR STATISTICS*. [Online], Available: https://www.bls.gov/help/hlpforma.htm#WM.

Valappil, S.P., Misra, S.K., Boccaccini, A.R., Keshavarz, T., Bucke, C. & Roy, I. 2007. Large-scale production and efficient recovery of PHB with desirable material properties, from the newly characterised Bacillus cereus SPV. *Journal of Biotechnology*. 132(3):251–258.

Vogelbusch Biocommodities. 2020. *Citric Acid Process Technology*. [Online], Available: https://www.vogelbusch-biocommodities.com/assets/1-Technology/Brochures/VBC-CitricAcid-Technology-EN-WEB.pdf [2022, April 25].

Wallace, J. 2013. Enzymatic hydrolysis of steam pretreated bagasse: Enzyme preparations for efficient cellulose conversion and evaluation of physicochemical changes during hydrolysis. *Master's Thesis, Stellenbosch University*. (March).

Wang, F. & Lee, S.Y. 1997a. Production of poly(3-hydroxybutyrate) by fed-batch culture of filamentation-suppressed recombinant Escherichia coli. *Applied and Environmental Microbiology*. 63(12):4765–4769.

Wang, F. & Lee, S.Y. 1997b. Poly(3-hydroxybutyrate) production with high productivity and high polymer content by a fed-batch culture of Alcaligenes latus under nitrogen limitation. *Applied and Environmental Microbiology*. 63(9):3703–3706.

Wang, B., Li, H., Zhu, L., Tan, F., Li, Y., Zhang, L., Ding, Z. & Shi, G. 2017. High-efficient production of citric acid by Aspergillus niger from high concentration of substrate based on the staged-addition

glucoamylase strategy. *Bioprocess and Biosystems Engineering*. 40(6):891–899.

Wang, B., Tan, F., Yu, F., Li, H. & Zhang, M. 2021. Efficient biorefinery of whole cassava for citrate production using Aspergillus niger mutated by atmospheric and room temperature plasma and enhanced co-saccharification strategy. *Journal of the Science of Food and Agriculture*. (January).

Wang, J., Cui, Z., Li, Y., Cao, L. & Lu, Z. 2020. Techno-economic analysis and environmental impact assessment of citric acid production through different recovery methods. *Journal of Cleaner Production*. 249.

Wang, X.X., Hu, H.Y., Liu, D.H. & Song, Y.Q. 2016. The implementation of high fermentative 2,3-butanediol production from xylose by simultaneous additions of yeast extract, Na2EDTA, and acetic acid. *New Biotechnology*. 33(1):16–22.

Van der Westhuizen, W.A. 2013. A Techno-Economic Evaluation of Integrating First and Second Generation Bioethanol Production From Sugarcane in Sub-Saharan Africa. (December).

Wu, J., Peng, Q., Arlt, W. & Minceva, M. 2009. Model-based design of a pilot-scale simulated moving bed for purification of citric acid from fermentation broth. *Journal of Chromatography A*. 1216(50):8793–8805.

Xie, S., Zhang, Y., Zhou, Y., Wang, Z., Yi, C. & Qiu, X. 2017. Salting-out of bio-based 2,3-butanediol from aqueous solutions. *Journal of Chemical Technology and Biotechnology*. 92(1):122–132.

Yadvika, Santosh, Sreekrishnan, T.R., Kohli, S. & Rana, V. 2004. Enhancement of biogas production from solid substrates using different techniques - A review. *Bioresource Technology*. 95(1):1–10.

Yamada, R., Nishikawa, R., Wakita, K. & Ogino, H. 2018. Rapid and stable production of 2,3-butanediol by an engineered Saccharomyces cerevisiae strain in a continuous airlift bioreactor. *Journal of Industrial Microbiology and Biotechnology*. 45(5):305–311.

Yu, B., Zhang, X., Sun, W., Xi, X., Zhao, N., Huang, Z., Ying, Z., Liu, L., et al. 2018. Continuous citric acid production in repeated-fed batch fermentation by Aspergillus niger immobilized on a new porous foam. *Journal of Biotechnology*. 276–277(December 2017):1–9.

Zang, G., Shah, A. & Wan, C. 2020. Techno-economic analysis of co-production of 2,3-butanediol, furfural, and technical lignin via biomass processing based on deep eutectic solvent pretreatment. *Biofuels, Bioproducts and Biorefining*. 14(2):326–343.

Zardoya, A.R., Lucena, I.L., Bengoetxea, I.O. & Orosa, J.A. 2022. Research on an internal combustion engine with an injected pre-chamber to operate with low methane number fuels for future gas flaring reduction. *Energy*. 253.

Zhang, M. 2021. *BETO 2021 Peer Review Targeted Microbial Development*. [Online], Available: https://www.energy.gov/sites/default/files/2021-04/beto-07-peer-review-2021-convlignin-zhang.pdf [2021, April 18].

Zhang, Z., Harrison, M.D. & O'Hara, I.M. 2016. Production of fermentable sugars from sugarcane bagasse. in *Sugarcane-based Biofuels and Bioproducts* 1st ed. Ian M. O'Hara and Sagadevan G. Mundree (ed.). John Wiley and Sons, Inc Ian M. O'Hara and Sagadevan G. Mundree (ed.). 87–110.

Zhou, P.P., Meng, J. & Bao, J. 2017. Fermentative production of high titer citric acid from corn stover feedstock after dry dilute acid pretreatment and biodetoxification. *Bioresource Technology*. 224:563–572.

APPENDICES

APPENDIX A – INSTALLED EQUIPMENT COST

Table 60: Installed equipment cost determination of each piece of equipment.

SCENARIO	EQUIPMENT	DESCRIPTION	SOURCE
All	Pumps	Sizing and Costing obtained from Aspen Plus® Economic Analyzer	-
All	Heat Exchangers	Sizing and Costing obtained from Aspen Plus® Economic Analyzer	-
All	Compressors used for air sparging	Sizing and Costing obtained from Aspen Plus® Economic Analyzer	-
All	Flash Drums	Sizing and Costing obtained from Aspen Plus® Economic Analyzer	-
All	Anaerobic Digester	Sized, Cost, and designed according to NREL	(Humbird *et al.*, 2011)
All	Aerobic Digester	Sized, Cost, and designed according to NREL	(Humbird *et al.*, 2011)
All	Reverse Osmosis	Sized, Cost, and designed according to NREL	(Humbird *et al.*, 2011)
All	New Combined Heat and Power Plant	Sized, Cost, and designed according to NREL	(Humbird *et al.*, 2011)
All	Cooling Water tower and chilled water	Sized, Cost, and designed according to NREL	(Humbird *et al.*, 2011)
All	Process Water Storage	Sized, Cost, and designed according to NREL	(Humbird *et al.*, 2011)
A, B, C, D, G, H	Sucrose Hydrolysis Reactor and Agitators	Sized using residence time of 6 hours, working volume of 80% and assumed volume of one reactor of 3785.4 kiloliters (1 000 000 gallons). Installed equipment cost was determined by scaling from NREL, using a scaling factor of 1 and installation factor of 1.5 (reactors and agitators).	(Bratu *et al.*, 2008; Humbird *et al.*, 2011)
All	Seed Train Reactors and Agitators (only for largest 2 reactors)	Sized using residence time of 9 hours, working volume of 80% and assumed only 4 reactors required in seed train. Installed equipment cost was determined by scaling from NREL, using a scaling factor and installation factor of 0.7 and 1.8 (seed train reactors 1-3), 0.7 and 2 (seed train reactor 4) and 0.5 and 1.5 (agitators).	(Dheskali, 2017; Humbird *et al.*, 2011)
A, B, C & D	2,3-BDO Fermenters and Agitators (using A-molasses/glucose)	Sized using residence time of 126 hours, working volume of 80% and assumed volume of one anaerobic reactor of 3785.4 kiloliters (1 000 000 US gallons). Installed equipment cost was determined by scaling from NREL, using a scaling factor of 1 and installation factor of 1.5 (reactors and agitators).	(Humbird *et al.*, 2011; Jantama *et al.*, 2015)

B & D	2,3-BDO Fermenters and Agitators (using xylose)	Sized using residence time of 168 hours, working volume of 80% and assumed volume of one anaerobic reactor of 3785.4 kiloliters (1 000 000 US gallons). Installed equipment cost was determined by scaling from NREL, using a scaling factor of 1 and installation factor of 1.5 (reactors and agitators).	(Humbird *et al.*, 2011)
B, D, J	Activated Carbon Detoxification Column	Sized, Cost, and designed according to Özüdoğru, 2018.	(Özüdoğru, 2018)
B, D, I, J	Triple Effect Evaporator	Sizing and Costing obtained from Aspen Plus® Economic Analyzer for each individual flash drum and heat exchanger making out the triple effect evaporator.	-
A, B, C, D, E, F	Distillation columns	Sizing and Costing obtained from Aspen Plus® Economic Analyzer	-
All	Centrifuge	Sizing and Costing obtained from Aspen Plus® Economic Analyzer	-
A, B, C, D	Compressor part of 2,3-BDO separation and purification	Costing of a centrifugal compressor determined using cost equations.	(Turton, R.; Shaeiwitz, J.A.; Bhattacharyya, D.; Whiting, 2018)
B, D, F, J	Sulphur Furnace	The cost of a reformer furnace determined using cost equations. Sulphur furnace is slightly out of bounds for reformer furnace, but it was the best estimate obtained.	(Turton, R.; Shaeiwitz, J.A.; Bhattacharyya, D.; Whiting, 2018)
B, D, F, J	Steam Pretreatment Reactor	Sizing and Costing obtained from Aspen Plus® Economic Analyzer	-
B, D, J	Sulphur Dioxide Scrubber	Installed equipment cost was determined by scaling from NREL, using a scaling factor and installation factor of 0.6 and 2.4 (scrubber) and 0.8 and 2.3 (scrubber bottoms pump).	(Humbird *et al.*, 2011)
B, D, H, J	Washing of cellulignin	Sizing and Costing obtained from Aspen Plus® Economic Analyzer	-

B, D, F, H, J	Enzymatic Hydrolysis and additional Enzymatic Hydrolysis Equipment	Sized using residence time of 24 hours, working volume of 100% and assumed volume of one reactor of 946.4 kiloliters (250 000 US gallons) (continuous vessels) and a residence time of 96 hours, working volume of 95% and assumed volume of one reactor of 3596.1 kiloliters (950 000 US gallons) (batch vessels). Installed equipment cost was determined by scaling from NREL, using a scaling factor and installation factor of 0.7 and 2 (continuous vessels), 1 and 1.5 (batch vessels), 0.8 and 2.3 (pump between continuous and batch vessels), 0.5 and 1.7 (mixer) and 1 and 1.5 (agitators).	(Humbird *et al.*, 2011)
B, D, F, H & J	Cellulase Production Plant	Sized, Cost, and designed according to NREL	(Davis *et al.*, 2018)
C, D, E, F	Thermal Fluid Heater	Sized, Cost, and designed according to NREL. Similarly designed to combustor, part of new combined heat and power plant (CHP).	(Humbird *et al.*, 2011)
C & D	Catalytic Reactor	Sized, Cost, and designed according to Burla, et al., (2012). The study described the catalytic upgrade of ethanol to 1,3-BD; however, it was assumed that the catalytic reactor design would be similar for the catalytic upgrade of 2,3-BDO to 1,3-BD and therefore the cost could be determined by scaling using the volumetric flowrate of the liquid entering the catalytic process as well as a scaling factor of 0.7 and installation factor of 2.	(Burla *et al.*, 2012)
C & D	Quench Tower	Sizing and Costing obtained from Aspen Plus® Economic Analyzer	-
C & D	Decanter	Sizing and Costing obtained from Aspen Plus® Economic Analyzer	-
B, D, E, F, G, H, J	Refrigerant Production unit	Sized, Cost, and designed according to process for Ammonia refrigerant designed by Luyben (2017). The capital cost was scaled from 1 MW, which is the size of the original process. Cooling water usage and compressor electricity usage was additional accounted for.	(Luyben, 2017)

E, F	Ethanol Fermenters and agitators (using A-molasses)	Sized using residence time of 48 hours, working volume of 80% and assumed volume of one anaerobic reactor of 1 000 000 US gallons. Installed equipment cost was determined by scaling from NREL, using a scaling factor of 1 and installation factor of 1.5 (reactors and agitators).	(Humbird *et al.*, 2011; Moonsamy, 2021)
F	Ethanol Fermenters and agitators (part of separate hydrolysis ad co-fermentation)	Sized using residence time of 24 hours, working volume of 80% and assumed volume of one anaerobic reactor of 3785.4 kiloliters (1 000 000 US gallons). Installed equipment cost was determined by scaling from NREL, using a scaling factor of 1 and installation factor of 1.5 (reactors and agitators).	(Humbird *et al.*, 2011; Moonsamy, 2021)
E, F	Vent Scrubber & Bottoms Pump	Installed equipment cost was determined by scaling from NREL, using a scaling factor and installation factor of 0.6 and 2.4 (scrubber) and 0.8 and 2.3 (scrubber bottoms pump).	(Humbird *et al.*, 2011)
E, F	Pressure Filter and additions	Installed equipment cost was determined by scaling from NREL, using a scaling factor and installation factor of 0.8 and 1.7 (pressure filter, lignin wet cake conveyor and lignin wet cake screw), 0.6 and 1.6 (pressure filter drying compressor), 0.7 and 3.1 (drying air compressor receiver), 0.7 and 2 (Feed Tank) and 0.8 and 2.3 (Feed Pump).	(Humbird *et al.*, 2011)
E & F	Catalytic Reactors	Sized, Cost, and designed according to Burla, et al., (2012). The study described the catalytic upgrade of ethanol to 1,3-BD and therefore the cost could be determined by scaling using the volumetric flowrate of the liquid entering the catalytic process as well as a scaling factor of 0.7 and installation factor of 2.	(Burla *et al.*, 2012)
G & H	Alkaline digestion Blending Tank	Sizing and Costing obtained from Aspen Plus® Economic Analyzer	-
G & H	Spray Dryer	Sizing and Costing obtained from Aspen Plus® Economic Analyzer	-
G & H	PHB Fermenters and agitators	Sized using residence time of 31.5 hours, working volume of 80% and assumed volume of one aerobic reactor of 302.8 kiloliters (80 000 US gallons). Installed equipment cost was determined by scaling from NREL, using a scaling factor of 1 and installation factor of 1.5 (reactors and agitators).	(Davis *et al.*, 2018; Liu *et al.*, 1998)

G,	Gas Engine	$Gas\ Engine\ Capital\ Cost\ (2016\ USD) = 5474 \times Power\ (kW)^{0.8119} \times {}^{538}/_{525}$ Where, $Power\ (kW) = HHV\left(\frac{MJ}{kg}\right) \times Biogas\ Flowrate\left(\frac{kg}{h_{dry}}\right) \times efficiency\ \times 0.2778$ Where the efficiency was assumed as 30% and the HHV was obtained from Aspen Plus®	(Breeze, 2014)
H,	Dilute Acid Pretreatment Reactor	Sizing and Costing obtained from Aspen Plus® Economic Analyzer	-
I & J	Citric Acid Fermentation	Sized using residence time of 31.5 hours, working volume of 80% and assumed volume of one aerobic reactor of 302.8 kiloliters (80 000 US gallons). Installed equipment cost was determined by scaling from NREL, using a scaling factor of 1 and installation factor of 1.5 (reactors and agitators).	(Davis *et al.*, 2018; Ikram-Ul *et al.*, 2004)
I & J	Mycelium Filter	Costing of a disc and drum filter determined using cost equations.	(Turton, R.; Shaeiwitz, J.A.; Bhattacharyya, D.;
I & J	Solvent Extraction	Sized, Cost, and designed according to Özüdoğru, 2018.	(Özüdoğru, 2018)
I & J	Citric Acid Crystallizer and Dryer	Sized, Cost, and designed according to Özüdoğru, 2018.	(Özüdoğru, 2018)

APPENDIX B – CHEMICAL PRICES

CHEMICAL	DESCRIPTION	PRICE (2019) ($/kg)	SOURCE
Invertase	Food-grade Invertase used for sucrose hydrolysis	37.63	(enzymes.bio, 2022)
$(NH_4)_2HPO_4$	Fermentation medium component	0.4022	(Davis *et al.*, 2018)
$FeCl_3$	Fermentation medium component	0.34	(Alibaba, 2022a)
KOH	Fermentation medium component	1.1	(INTRATEC, 2007a)
Caustic	Required for aerobic digestion, scaled from NREL requirement (Humbird *et al.*, 2011)	0.1704	(Davis *et al.*, 2018)
NH_3	Required for anaerobic digestion	0.4646	(Davis *et al.*, 2018)
Boiler chemicals	Scaled from NREL requirement (Humbird *et al.*, 2011)	7.28	(Davis *et al.*, 2018)
Cooling tower chemicals	Scaled from NREL requirement (Humbird *et al.*, 2011)	4.3626	(Davis *et al.*, 2018)
Fresh process water	Make-up water	0.002	(Reddick & Kruger, 2019)
Sulphur	Used for SO_2 production	0.051	(Fernandez, 2022)
Refrigerant (Ammonia)	Cooling below that attainable by chilled water	0.4646	(Davis *et al.*, 2018)
Limestone	Required for limestone slurry part of SO_2 scrubbing	0.87	(INTRATEC, 2007b)
Cellulase Production Plant Operating Costs	Usage was scaled from NREL. The price of all chemicals required for cellulase production is combined and cost as one raw material.	2.22	(Humbird *et al.*, 2011)
Ammonium Sulphate	Fermentation medium component	0.21	(INTRATEC, 2007c)
Corn Steep Liquor	Fermentation medium component	0.0831	(Davis *et al.*, 2018)
Urea	Fermentation medium component	0.268	(Özüdoğru, 2018)
H_2SO_4	Fermentation medium component	0.1051	(Davis *et al.*, 2018)
NaH_2PO_4	Fermentation medium component	0.975	(Alibaba, 2022b)
KH_2PO_4	Fermentation medium component	1.054	(Özüdoğru, 2018)
$MgSO_4$	Fermentation medium component	0.1054	(Özüdoğru, 2018)

NaOH	Alkaline digestion to break down walls of *E. coli* to extract PHB	0.5829	(Davis *et al.*, 2018)
NH_4NO_3	Fermentation medium component	0.62	(INTRATEC, 2007d)
Trisodium Citrate	Fermentation medium component	0.6	(Alibaba, 2022c)
$MgSO_4.5H_2O$	Fermentation medium component	0.1054	(Özüdoğru, 2018)
Amine Solvent	Solvent used for solvent extraction. Only make-up stream of 3%.	3.05	(Özüdoğru, 2018)
NH_4Cl	Fermentation medium component	0.244	(Özüdoğru, 2018)
$MgSO_4 \cdot 7H_2O$	Fermentation medium component	0.1054	(Özüdoğru, 2018)

APPENDIX C – MATERIAL BALANCES AND MAIN ASPEN PLUS® FLOWSHEETS

Figure 75: Material Balances of Scenario A, Main Flowsheet

Material Balance - Scenario A															
Stream Name	**Units**	**2,3-BDO**	**A-MOLASS**	**B2**	**BIOGAS**	**BIOMASS**	**BMSLUDGE**	**EFFLUENT**	**FERMBROT**	**H2O**	**HHPS**	**S9**	**SEED**	**SUGAR-1**	**SUGAR-2**
Description															
From		S300			S400	S300	S400	S300	S200-2,2		S500-1	S200-1	S200-2,1	SPLIT	SPLIT
To			S200-1	S500-1	S500-1	S500-1	S500-1	S400	S300	S200-1	S500-2	SPLIT	S200-2,2	S200-2,1	S200-2,2
Stream Class		CONVEN	CONVEN	CONVEN	CONVEN	CONVEN	CONVEN	CONVEN	CONVEN	CONVEN	CONVEN	CONVEN	CONVEN	CONVEN	CONVEN
Total Stream															
Temperature	C	40,03	56,00	25,00	34,96	37,02	34,98	47,64	37,01	25,00	452,00	55,00	37,01	55,00	55,00
Pressure	bar	1,52	1,01	1,01	1,01	1,01	1,52	0,20	1,52	1,01	63,02	1,01	1,52	1,01	1,01
Mass Vapor Fraction		0,00	0,00	0,00	1,00	0,00	0,00	0,00	0,00	0,00	1,00	0,00	0,00	0,00	0,00
Mass Liquid Fraction		1,00	1,00	0,54	0,00	0,01	0,33	1,00	1,00	1,00	0,00	1,00	0,94	1,00	1,00
Mass Solid Fraction		0,00	0,00	0,46	0,00	0,99	0,67	0,00	0,00	0,00	0,00	0,00	0,06	0,00	0,00
Mass Enthalpy	cal/gm	-1444,80	-1961,86	-2643,59	-1839,88	-1026,52	-1722,21	-3527,44	-3458,37	-3789,48	-3025,60	-3248,85	-3334,56	-3248,85	-3248,85
Mass Entropy	cal/gm	-1,63	-1,83	-1,70	-0,33	-3,35	-2,26	-2,01	-2,04	-2,16	-0,65	-2,32	-2,52	-2,32	-2,32
Mass Density	gm/cc	0,98	1,22	1,09	0,00	0,88	1,12	0,75	1,00	1,00	0,02	1,04	1,02	1,04	1,04
Enthalpy Flow	cal/sec	-3652128,72	-13859967,19	-2021278,15	-735802,70	-62879,34	-114270,70	-11757975,48	-76263278,08	-65050951,52	-12931904,44	-78826629,10	-2774394,12	-2751049,39	-76075580,74
Average MW		91,10	66,03	31,62	27,19	23,70	41,00	19,97	20,25	18,02	18,02	22,85	20,67	22,85	22,85
Mass Flows	kg/hr	9100,00	25433,00	2752,55	1439,71	220,52	238,86	11999,82	79386,57	61798,30	15387,00	87346,66	2995,24	3048,40	84298,26
2,3-BDO	kg/hr	8900,18	0,00	0,00	0,00	0,26	0,00	282,75	9320,89	0,00	0,00	0,00	0,00	0,00	0,00
WATER	kg/hr	0,00	5613,06	1398,45	53,57	1,89	79,58	10654,68	68422,62	61798,30	15387,00	66798,16	2445,03	2331,26	64466,90
CO2	kg/hr	0,00	0,00	0,00	919,51	0,00	0,04	1,54	34,62	0,00	0,00	0,00	0,54	0,00	0,00
SUCCINAC	kg/hr	7,71	0,00	0,00	0,00	0,00	0,00	39,93	47,64	0,00	0,00	0,00	0,00	0,00	0,00
OXYGEN	kg/hr	0,00	0,00	0,00	0,00	0,00	0,00	0,00	0,00	0,00	0,00	0,00	0,00	0,00	0,00
ACETICAC	kg/hr	0,00	0,00	0,00	0,00	0,00	0,00	11,79	118,53	0,00	0,00	0,00	0,00	0,00	0,00
ETHANOL	kg/hr	0,00	0,00	0,00	0,00	0,00	0,00	9,38	31,18	0,00	0,00	0,00	0,00	0,00	0,00
NH3	kg/hr	0,00	0,00	0,00	0,01	0,00	0,00	0,89	1,19	0,00	0,00	0,00	0,70	0,00	0,00
GLUCOSE	kg/hr	192,11	2988,38	0,00	0,00	0,03	0,00	998,86	1191,01	0,00	0,00	10274,25	24,75	358,57	9915,68
FRUCTOSE	kg/hr	0,00	2988,38	0,00	0,00	0,00	0,00	0,00	0,00	0,00	0,00	10274,25	358,57	358,57	9915,68
SUCROSE	kg/hr	0,00	13843,18	0,00	0,00	0,00	0,00	0,00	0,00	0,00	0,00	0,00	0,00	0,00	0,00
K.OXYTOC	kg/hr	0,00	0,00	0,00	0,00	218,33	0,00	0,00	218,33	0,00	0,00	0,00	165,63	0,00	0,00
BMSLUDGE	kg/hr	0,00	0,00	0,00	0,00	0,00	159,24	0,00	0,00	0,00	0,00	0,00	0,00	0,00	0,00
PROPACID	kg/hr	0,00	0,00	0,00	0,00	0,00	0,00	0,00	0,00	0,00	0,00	0,00	0,00	0,00	0,00
BUTYACID	kg/hr	0,00	0,00	0,00	0,00	0,00	0,00	0,00	0,00	0,00	0,00	0,00	0,00	0,00	0,00
H2	kg/hr	0,00	0,00	0,00	0,00	0,00	0,00	0,00	0,00	0,00	0,00	0,00	0,00	0,00	0,00
CH4	kg/hr	0,00	0,00	0,00	466,62	0,00	0,00	0,00	0,00	0,00	0,00	0,00	0,00	0,00	0,00
N2	kg/hr	0,00	0,00	0,00	0,00	0,00	0,00	0,00	0,55	0,00	0,00	0,00	0,03	0,00	0,00
CELLULOS	kg/hr	0,00	0,00	551,18	0,00	0,00	0,00	0,00	0,00	0,00	0,00	0,00	0,00	0,00	0,00
MANNAN	kg/hr	0,00	0,00	2,14	0,00	0,00	0,00	0,00	0,00	0,00	0,00	0,00	0,00	0,00	0,00
GALACTAN	kg/hr	0,00	0,00	10,09	0,00	0,00	0,00	0,00	0,00	0,00	0,00	0,00	0,00	0,00	0,00
XYLAN	kg/hr	0,00	0,00	270,09	0,00	0,00	0,00	0,00	0,00	0,00	0,00	0,00	0,00	0,00	0,00
ARABINAN	kg/hr	0,00	0,00	22,33	0,00	0,00	0,00	0,00	0,00	0,00	0,00	0,00	0,00	0,00	0,00
LIGNIN	kg/hr	0,00	0,00	345,33	0,00	0,00	0,00	0,00	0,00	0,00	0,00	0,00	0,00	0,00	0,00
EXTRACT	kg/hr	0,00	0,00	101,55	0,00	0,00	0,00	0,00	0,00	0,00	0,00	0,00	0,00	0,00	0,00
ASH	kg/hr	0,00	0,00	51,39	0,00	0,00	0,00	0,00	0,00	0,00	0,00	0,00	0,00	0,00	0,00

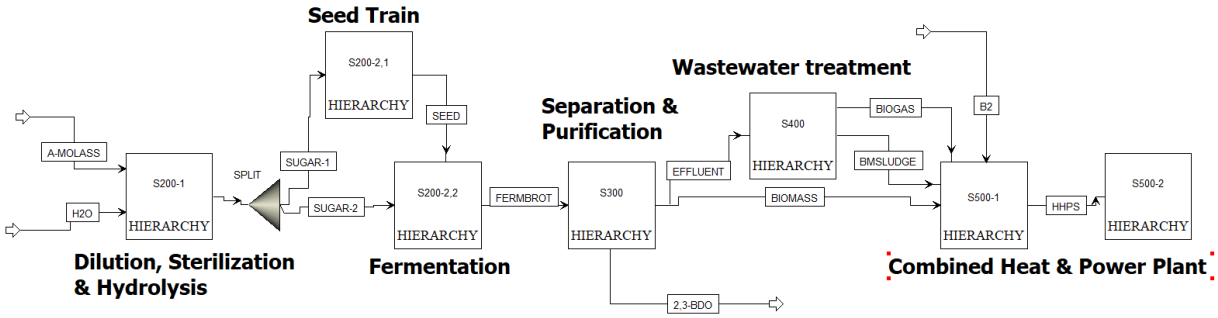

Figure 76: Scenario A, Main Flowsheet in Aspen Plus®

Table 61: Material Balances of Scenario B, Main Flowsheet

Material Balance - Scenario B														
Stream Name	**Units**	**2,3-BDO**	**2GFEED**	**A-MOLASS**	**AIR**	**BIOGAS**	**BYPASS**	**CELLIG**	**GLUCOSE**	**GLUCSEED**	**H2O**	**H2O1**	**HEMICELL**	**HHPS**
Description														
From		S300				S400	SPLIT	S100-2	S100-2	S100-2			S100-2	S500-1
To			SPLIT	S200-1	S100-1	S500-1	S500-1	S500-1	S200-2	S200-2	S100-2	S200-1	S200-3	S500-2
Stream Class		CONVEN	CONVEN	CONVEN	CONVEN	CONVEN	CONVEN	CONVEN	CONVEN	CONVEN	CONVEN	CONVEN	CONVEN	CONVEN
Total Stream														
Temperature	C	40,03	25,00	56,00	25,00	34,91	25,00	50,00	50,00	50,00	25,00	93,24	97,97	452,00
Pressure	bar	1,52	1,01	1,01	1,01	1,01	1,01	1,01	1,01	1,01	1,01	0,81	1,01	63,02
Mass Vapor Fraction		0,00	0,00	0,00	1,00	1,00	0,00	0,00	0,00	0,00	0,00	0,00	0,00	1,00
Mass Liquid Fraction		1,00	0,47	1,00	0,00	0,00	0,47	0,33	1,00	1,00	1,00	1,00	1,00	0,00
Mass Solid Fraction		0,00	0,53	0,00	0,00	0,00	0,53	0,67	0,00	0,00	0,00	0,00	0,00	0,00
Mass Enthalpy	cal/gm	-1443,99	-2424,11	-1961,86	-32,12	-1089,22	-2424,11	-1922,33	-3446,67	-3446,67	-3789,48	-3709,77	-3525,49	-3025,60
Mass Entropy	cal/gm-K	-1,64	-1,47	-1,83	0,03	-0,09	-1,47	-1,34	-2,00	-2,00	-2,16	-1,95	-2,07	-0,65
Mass Density	gm/cc	0,99	1,10	1,22	0,00	0,00	1,10	1,13	1,01	1,01	1,00	0,59	1,00	0,02
Enthalpy Flow	cal/sec	-5455079,08	-42894650,58	-13859967,19	-28548,72	-2540823,57	-14155234,69	-7667069,06	-45277376,10	-3150451,33	-49467082,16	-42250176,09	-63175270,91	-116419880,01
Average MW		90,93	35,71	66,03	28,60	28,56	35,71	47,33	20,87	20,87	18,02	18,09	19,57	18,02
Mass Flows	kg/hr	13600,00	63702,00	25433,00	3199,54	8397,75	21021,66	14358,33	47291,67	3290,61	46993,65	41000,00	64510,52	138521,96
O2	kg/hr	0,00	0,00	0,00	671,90	0,18	0,00	0,00	0,00	0,00	0,00	0,00	0,00	0,00
SO2	kg/hr	0,00	0,00	0,00	0,00	47,03	0,00	0,08	0,79	0,05	0,00	9,38	12,18	0,00
FES2	kg/hr	0,00	0,00	0,00	0,00	0,00	0,00	0,00	0,00	0,00	0,00	0,00	0,00	0,00
H2O	kg/hr	0,00	27626,01	5613,06	32,00	295,84	9116,58	4059,10	40108,03	2790,76	46993,65	40770,32	58632,05	138521,96
CELLULOS	kg/hr	0,00	14583,17	0,00	0,00	0,00	4812,45	422,02	0,00	0,00	0,00	0,00	0,00	0,00
MANNAN	kg/hr	0,00	56,13	0,00	0,00	0,00	18,52	37,61	0,00	0,00	0,00	0,00	0,00	0,00
GALACTAN	kg/hr	0,00	291,89	0,00	0,00	0,00	96,32	195,56	0,00	0,00	0,00	0,00	0,00	0,00
XYLAN	kg/hr	0,00	7808,00	0,00	0,00	0,00	2576,64	2009,98	0,00	0,00	0,00	0,00	0,00	0,00
ARABINAN	kg/hr	0,00	645,52	0,00	0,00	0,00	213,02	156,30	0,00	0,00	0,00	0,00	0,00	0,00
LIGNIN	kg/hr	0,00	8863,27	0,00	0,00	0,00	2924,88	5938,39	0,00	0,00	0,00	0,00	0,00	0,00
FURFURAL	kg/hr	0,24	0,00	0,00	0,00	0,00	0,00	0,43	4,27	0,30	0,00	14,37	65,86	0,00
ACETICAC	kg/hr	0,00	0,00	0,00	0,00	0,00	0,00	2,55	25,18	1,75	0,00	205,19	388,24	0,00
EXTRACT	kg/hr	97,63	2615,55	0,00	0,00	0,00	863,13	10,10	99,77	6,94	0,00	0,00	1538,47	0,00
CELLOBIO	kg/hr	5,78	0,00	0,00	0,00	0,00	0,00	8,25	81,51	5,67	0,00	0,00	0,00	0,00
ASH	kg/hr	0,00	1212,46	0,00	0,00	0,00	400,11	812,35	0,00	0,00	0,00	0,00	0,00	0,00
CO2	kg/hr	0,00	0,00	0,00	0,00	3217,20	0,00	0,00	0,00	0,00	0,00	0,14	0,00	0,00
2,3-BDO	kg/hr	13326,57	0,00	0,00	0,00	0,00	0,00	0,00	0,00	0,00	0,00	0,00	0,00	0,00
ETHANOL	kg/hr	0,00	0,00	0,00	0,00	0,00	0,00	0,00	0,00	0,00	0,00	0,00	0,00	0,00
GLYCEROL	kg/hr	23,87	0,00	0,00	0,00	0,00	0,00	0,00	0,00	0,00	0,00	0,00	0,00	0,00
XYLITOL	kg/hr	5,42	0,00	0,00	0,00	0,00	0,00	0,00	0,00	0,00	0,00	0,00	0,00	0,00
ACETOIN	kg/hr	0,03	0,00	0,00	0,00	0,02	0,00	0,00	0,00	0,00	0,00	0,00	0,00	0,00
SUCCINIC	kg/hr	3,81	0,00	0,00	0,00	0,00	0,00	0,00	0,00	0,00	0,00	0,00	0,00	0,00
FRUCTOSE	kg/hr	0,00	0,00	2988,38	0,00	0,00	0,00	0,00	0,00	0,00	0,00	0,00	0,00	0,00
SUCROSE	kg/hr	0,00	0,00	13843,18	0,00	0,00	0,00	0,00	0,00	0,00	0,00	0,00	0,00	0,00
FE2O3	kg/hr	0,00	0,00	0,00	0,00	0,00	0,00	0,00	0,00	0,00	0,00	0,00	0,00	0,00
SCEREVIS	kg/hr	0,00	0,00	0,00	0,00	0,00	0,00	0,00	0,00	0,00	0,00	0,00	0,00	0,00
KOXYTOCA	kg/hr	0,00	0,00	0,00	0,00	0,00	0,00	0,00	0,00	0,00	0,00	0,00	0,00	0,00
XYLOSE	kg/hr	22,60	0,00	0,00	0,00	0,00	0,00	20,39	201,43	14,02	0,00	0,00	3106,10	0,00
ARABINOS	kg/hr	17,99	0,00	0,00	0,00	0,00	0,00	1,81	17,87	1,24	0,00	0,03	275,54	0,00
GLUCOSE	kg/hr	96,06	0,00	2988,38	0,00	0,00	0,00	683,41	6752,83	469,87	0,00	0,00	492,04	0,00
NH3	kg/hr	0,00	0,00	0,00	0,00	0,93	0,00	0,00	0,00	0,00	0,00	0,52	0,00	0,00
PROPACID	kg/hr	0,00	0,00	0,00	0,00	0,01	0,00	0,00	0,00	0,00	0,00	0,00	0,00	0,00
BUTYRACI	kg/hr	0,00	0,00	0,00	0,00	0,00	0,00	0,00	0,00	0,00	0,00	0,00	0,00	0,00
CH4	kg/hr	0,00	0,00	0,00	0,00	1168,09	0,00	0,00	0,00	0,00	0,00	0,00	0,00	0,00
H2	kg/hr	0,00	0,00	0,00	0,00	0,00	0,00	0,00	0,00	0,00	0,00	0,00	0,00	0,00
BMSLUDGE	kg/hr	0,00	0,00	0,00	0,00	0,00	0,00	0,00	0,00	0,00	0,00	0,00	0,00	0,00
ISOVACID	kg/hr	0,00	0,00	0,00	0,00	0,00	0,00	0,00	0,00	0,00	0,00	0,00	0,00	0,00
C3H6O2	kg/hr	0,00	0,00	0,00	0,00	1,08	0,00	0,00	0,00	0,00	0,00	0,00	0,00	0,00
N2	kg/hr	0,00	0,00	0,00	2495,64	3667,36	0,00	0,00	0,00	0,00	0,00	0,05	0,05	0,00
S	kg/hr	0,00	0,00	0,00	0,00	0,00	0,00	0,00	0,00	0,00	0,00	0,00	0,00	0,00
NO2	kg/hr	0,00	0,00	0,00	0,00	0,00	0,00	0,00	0,00	0,00	0,00	0,00	0,00	0,00
CACO3	kg/hr	0,00	0,00	0,00	0,00	0,00	0,00	0,00	0,00	0,00	0,00	0,00	0,00	0,00
CASO3	kg/hr	0,00	0,00	0,00	0,00	0,00	0,00	0,00	0,00	0,00	0,00	0,00	0,00	0,00
CASO4	kg/hr	0,00	0,00	0,00	0,00	0,00	0,00	0,00	0,00	0,00	0,00	0,00	0,00	0,00

Material Balance - Scenario B														
Stream Name	**Units**	**KOXYTOCA**	**S1**	**S2**	**S3**	**S12**	**S17**	**SCEREVIS**	**SLUDGE**	**SO2**	**SULPHUR**	**WASTE**	**XFERM**	**XSEED**
Description														
From		S200-2	S200-3	S200-2	S300	SPLIT	S200-1	S200-3	S400	S100-1		S100-2	S100-2	S100-2
To		S500-1	S300	S300	S400	S100-2	S200-2	S500-1	S500-1	S100-2	S100-1	S400	S200-3	S200-3
Stream Class		CONVEN	CONVEN	CONVEN	CONVEN	CONVEN	CONVEN	CONVEN	CONVEN	CONVEN	CONVEN	CONVEN	CONVEN	CONVEN
Total Stream														
Temperature	C	36,77	30,02	36,77	60,12	25,00	55,00	30,02	34,93	190,00	25,00	94,89	50,00	50,00
Pressure	bar	1,01	1,01	1,01	0,20	1,01	1,01	1,01	1,52	1,01	1,01	1,01	1,01	1,01
Mass Vapor Fraction		0,00	0,00	0,00	0,00	0,00	0,00	0,00	0,00	1,00	0,00	0,41	0,00	0,00
Mass Liquid Fraction		0,01	1,00	1,00	1,00	0,47	1,00	0,01	0,33	0,00	1,00	0,59	1,00	1,00
Mass Solid Fraction		0,99	0,00	0,00	0,00	0,53	0,00	0,99	0,67	0,00	0,00	0,00	0,00	0,00
Mass Enthalpy	cal/gm	-1027,33	-3161,90	-3448,84	-3636,23	-2424,11	-3082,11	-1264,45	-1250,17	-365,72	1959,79	-3190,37	-3446,67	-3446,67
Mass Entropy	cal/gm-K	-3,35	-2,06	-2,04	-2,03	-1,47	-2,39	-4,16	-0,71	0,14	1,64	-1,29	-2,00	-2,00
Mass Density	gm/cc	1,10	1,04	1,00	0,04	1,10	1,06	1,10	1,12	0,00	2,13	0,00	1,01	1,01
Enthalpy Flow	cal/sec	-84980,42	-13478767,91	-101609865,34	-108849547,17	-28739415,89	-56974912,95	-40028,74	-239154,28	-392173,91	366483,65	-38992333,57	-5397867,09	-744652,13
Average MW		23,70	23,56	20,38	18,89	35,71	25,03	25,18	41,34	34,72	32,07	18,95	20,87	20,87
Mass Flows	kg/hr	297,79	15346,34	106063,26	107765,10	42680,34	66548,36	113,97	688,67	3860,39	673,21	43998,83	5638,01	777,78
O2	kg/hr	0,00	0,01	0,00	0,00	0,00	0,00	0,00	0,00	0,19	0,00	0,18	0,00	0,00
SO2	kg/hr	0,00	0,00	1,12	0,99	0,00	9,38	0,00	0,03	1345,00	0,00	67,05	0,09	0,01
FES2	kg/hr	0,00	0,00	0,00	0,00	0,00	0,00	0,00	0,00	0,00	0,00	0,00	0,00	0,00
H2O	kg/hr	2,53	11019,57	90862,19	101880,50	18509,43	45770,17	0,81	226,61	19,55	0,00	39053,45	4781,59	659,63
CELLULOS	kg/hr	0,00	0,00	0,00	0,00	9770,73	0,00	0,00	0,00	0,00	0,00	0,00	0,00	0,00
MANNAN	kg/hr	0,00	0,00	0,00	0,00	37,61	0,00	0,00	0,00	0,00	0,00	0,00	0,00	0,00
GALACTAN	kg/hr	0,00	0,00	0,00	0,00	195,56	0,00	0,00	0,00	0,00	0,00	0,00	0,00	0,00
XYLAN	kg/hr	0,00	0,00	0,00	0,00	5231,36	0,00	0,00	0,00	0,00	0,00	0,00	0,00	0,00
ARABINAN	kg/hr	0,00	0,00	0,00	0,00	432,50	0,00	0,00	0,00	0,00	0,00	0,00	0,00	0,00
LIGNIN	kg/hr	0,00	0,00	0,00	0,00	5938,39	0,00	0,00	0,00	0,00	0,00	0,00	0,00	0,00
FURFURAL	kg/hr	0,00	0,48	18,92	19,16	0,00	14,37	0,00	0,04	0,00	0,00	4,09	0,51	0,07
ACETICAC	kg/hr	0,01	42,85	391,11	433,96	0,00	205,19	0,00	0,00	0,00	0,00	63,78	3,00	0,41
EXTRACT	kg/hr	0,00	1551,89	106,71	1560,97	1752,42	0,00	0,11	2,23	0,00	0,00	77,63	11,89	1,64
CELLOBIO	kg/hr	0,00	11,06	87,18	92,45	0,00	0,00	0,00	0,01	0,00	0,00	0,00	9,72	1,34
ASH	kg/hr	0,00	0,00	0,00	0,00	812,35	0,00	0,00	0,00	0,00	0,00	0,00	0,00	0,00
CO2	kg/hr	0,00	6,24	46,17	10,18	0,00	0,14	0,00	0,07	0,00	0,00	868,62	0,00	0,00
2,3-BDO	kg/hr	0,35	1450,52	12597,21	721,15	0,00	0,00	0,11	0,00	0,00	0,00	0,00	0,00	0,00
ETHANOL	kg/hr	0,00	255,53	42,12	297,64	0,00	0,00	0,02	0,00	0,00	0,00	0,00	0,00	0,00
GLYCEROL	kg/hr	0,00	356,66	0,00	332,80	0,00	0,00	0,03	0,00	0,00	0,00	0,00	0,00	0,00
XYLITOL	kg/hr	0,00	92,14	0,00	86,71	0,00	0,00	0,01	0,12	0,00	0,00	0,00	0,00	0,00
ACETOIN	kg/hr	0,00	89,08	0,00	89,05	0,00	0,00	0,01	0,12	0,00	0,00	0,00	0,00	0,00
SUCCINIC	kg/hr	0,00	0,00	64,37	60,56	0,00	0,00	0,00	0,00	0,00	0,00	0,00	0,00	0,00
FRUCTOSE	kg/hr	0,00	0,00	0,00	0,00	0,00	10274,25	0,00	0,00	0,00	0,00	0,00	0,00	0,00
SUCROSE	kg/hr	0,00	0,00	0,00	0,00	0,00	0,00	0,00	0,00	0,00	0,00	0,00	0,00	0,00
FE2O3	kg/hr	0,00	0,00	0,00	0,00	0,00	0,00	0,00	0,00	0,00	0,00	0,00	0,00	0,00
SCEREVIS	kg/hr	0,00	0,00	0,00	0,00	0,00	0,00	112,84	0,00	0,00	0,00	0,00	0,00	0,00
KOXYTOCA	kg/hr	294,84	0,00	0,00	0,00	0,00	0,00	0,00	0,00	0,00	0,00	0,00	0,00	0,00
XYLOSE	kg/hr	0,01	168,44	215,44	361,28	0,00	0,00	0,01	0,00	0,00	0,00	156,74	24,01	3,31
ARABINOS	kg/hr	0,00	277,89	19,15	279,05	0,00	0,03	0,02	0,02	0,00	0,00	13,90	2,13	0,29
GLUCOSE	kg/hr	0,04	22,78	1609,27	1535,99	0,00	10274,25	0,00	0,00	0,00	0,00	24,83	805,06	111,06
NH3	kg/hr	0,00	1,07	1,58	2,65	0,00	0,52	0,00	0,03	0,00	0,00	0,00	0,00	0,00
PROPACID	kg/hr	0,00	0,00	0,00	0,00	0,00	0,00	0,00	0,06	0,00	0,00	0,00	0,00	0,00
BUTYRACI	kg/hr	0,00	0,00	0,00	0,00	0,00	0,00	0,00	0,00	0,00	0,00	0,00	0,00	0,00
CH4	kg/hr	0,00	0,00	0,00	0,00	0,00	0,00	0,00	0,00	0,00	0,00	0,00	0,00	0,00
H2	kg/hr	0,00	0,00	0,00	0,00	0,00	0,00	0,00	0,00	0,01	0,00	0,01	0,00	0,00
BMSLUDGE	kg/hr	0,00	0,00	0,00	0,00	0,00	0,00	0,00	459,11	0,00	0,00	0,00	0,00	0,00
ISOVACID	kg/hr	0,00	0,00	0,00	0,00	0,00	0,00	0,00	0,00	0,00	0,00	0,00	0,00	0,00
C3H6O2	kg/hr	0,00	0,00	0,00	0,00	0,00	0,00	0,00	0,22	0,00	0,00	0,00	0,00	0,00
N2	kg/hr	0,00	0,11	0,74	0,00	0,00	0,05	0,00	0,00	2495,64	0,00	3668,54	0,00	0,00
S	kg/hr	0,00	0,00	0,00	0,00	0,00	0,00	0,00	0,00	0,00	673,21	0,00	0,00	0,00
NO2	kg/hr	0,00	0,00	0,00	0,00	0,00	0,00	0,00	0,00	0,00	0,00	0,00	0,00	0,00
CACO3	kg/hr	0,00	0,00	0,00	0,00	0,00	0,00	0,00	0,00	0,00	0,00	0,00	0,00	0,00
CASO3	kg/hr	0,00	0,00	0,00	0,00	0,00	0,00	0,00	0,00	0,00	0,00	0,00	0,00	0,00
CASO4	kg/hr	0,00	0,00	0,00	0,00	0,00	0,00	0,00	0,00	0,00	0,00	0,00	0,00	0,00

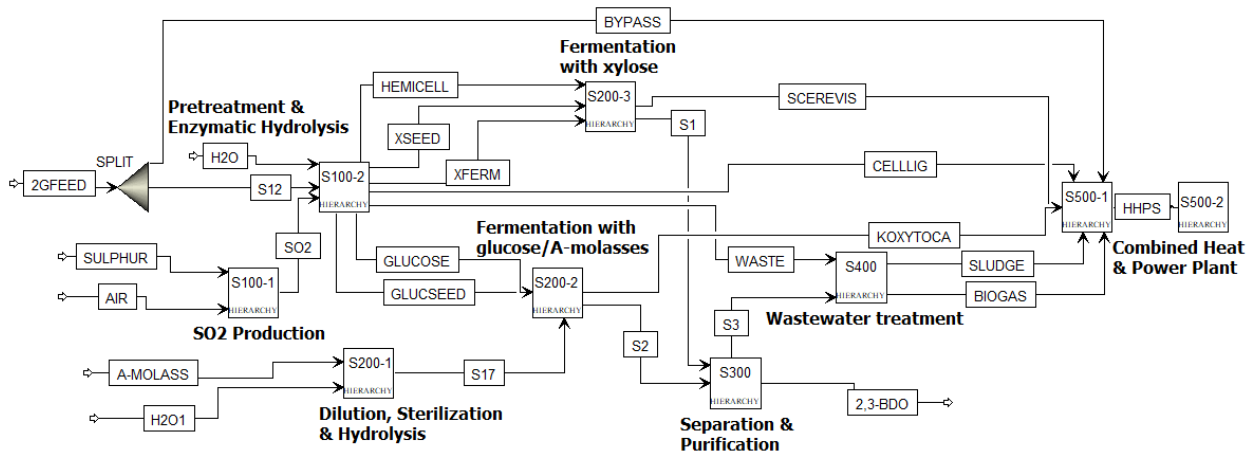

Figure 77: Scenario B, Main Flowsheet in Aspen Plus®

Table 62: Material Balances of Scenario C, Main Flowsheet

Material Balance - Scenario C																			
Stream Name	**Units**	**1,3-BD**	**A-MOLASS**	**B1**	**B2**	**BAGASSE**	**BDOPROD**	**BIOGAS**	**BIOMASS**	**BMSLUDGE**	**EFFLUENT**	**FERMBROT**	**H2O**	**HHPS**	**S19**	**S22**	**SEED**	**SUGAR-1**	**SUGAR-2**
Description																			
From		S700		SPLIT-02	SPLIT-02		S300	S400	S300	S400	S300	S200-2,2		S500-1	S200-1	S700	S200-2,1	SPLIT-01	SPLIT-01
To			S200-1	S800	S500-1	SPLIT-02	S700	S500-1	S500-1	S500-1	S400	S300	S200-1	S500-2	SPLIT-01	S400	S200-2,2	S200-2,1	S200-2,2
Stream Class		CONVEN	CONVEN	CONVEN	CONVEN	CONVEN	CONVEN	CONVEN	CONVEN	CONVEN	CONVEN	CONVEN	CONVEN	CONVEN	CONVEN	CONVEN	CONVEN	CONVEN	CONVEN
Total Stream																			
Temperature	C	27,48	56,00	25,00	25,00	25,00	122,73	34,95	37,02	34,97	52,10	37,01	25,00	452,01	55,00	67,03	37,01	55,00	55,00
Pressure	bar	3,43	1,01	1,01	1,01	1,01	1,52	1,01	1,01	1,52	0,20	1,52	1,01	63,02	1,01	1,37	1,52	1,01	1,01
Mass Vapor Fraction		0,00	0,00	0,00	0,00	0,00	0,00	1,00	0,00	0,00	0,00	0,00	0,00	1,00	0,00	0,00	0,00	0,00	0,00
Mass Liquid Fraction		1,00	1,00	0,54	0,54	0,54	1,00	0,00	0,01	0,33	1,00	1,00	1,00	0,00	1,00	1,00	0,94	1,00	1,00
Mass Solid Fraction		0,00	0,00	0,46	0,46	0,46	0,00	0,00	0,99	0,67	0,00	0,00	0,00	0,00	0,00	0,00	0,06	0,00	0,00
Mass Enthalpy	cal/gm	389,87	-1961,86	-2643,59	-2643,59	-2643,59	-1424,61	-1809,59	-1026,52	-1711,02	-3497,02	-3458,37	-3789,48	-3025,59	-3248,85	-3151,80	-3334,56	-3248,85	-3248,85
Mass Entropy	cal/gm-K	-0,94	-1,83	-1,70	-1,70	-1,70	-1,50	-0,34	-3,35	-2,26	-2,00	-2,04	-2,16	-0,65	-2,32	-1,85	-2,52	-2,32	-2,32
Mass Density	gm/cc	0,61	1,22	1,09	1,09	1,09	0,90	0,00	0,88	1,12	0,70	1,00	1,00	0,02	1,04	0,91	1,02	1,04	1,04
Average MW		54,10	66,03	31,62	31,62	31,62	87,80	26,97	23,70	41,23	20,15	20,25	18,02	18,02	22,85	20,73	20,67	22,85	22,85
Mass Flows	kg/hr	4590,00	25433,00	3950,00	5225,16	9175,16	9100,00	1563,74	220,52	248,23	12143,77	79386,57	61798,30	21736,48	87346,66	4503,05	2995,24	3048,40	84298,26
2,3-BDO	kg/hr	0,00	0,00	0,00	0,00	0,00	8773,68	0,00	0,26	0,00	463,29	9320,89	0,00	0,00	0,00	0,00	0,00	0,00	0,00
WATER	kg/hr	0,00	5613,06	2006,82	2654,68	4661,50	87,93	58,48	1,89	81,87	10651,03	68422,62	61798,30	21736,48	66798,16	3688,30	2445,03	2331,26	64466,90
CO2	kg/hr	0,00	0,00	0,00	0,00	0,00	0,00	971,59	0,00	0,04	1,18	34,62	0,00	0,00	0,00	0,00	0,54	0,00	0,00
SUCCINAC	kg/hr	0,00	0,00	0,00	0,00	0,00	8,95	0,00	0,00	0,00	38,68	47,64	0,00	0,00	0,00	0,45	0,00	0,00	0,00
OXYGEN	kg/hr	0,00	0,00	0,00	0,00	0,00	0,00	0,00	0,00	0,00	0,00	0,00	0,00	0,00	0,00	0,00	0,00	0,00	0,00
ACETICAC	kg/hr	0,00	0,00	0,00	0,00	0,00	6,00	0,00	0,00	0,00	11,79	118,53	0,00	0,00	0,00	4,07	0,00	0,00	0,00
ETHANOL	kg/hr	0,00	0,00	0,00	0,00	0,00	0,00	0,00	0,00	0,00	9,37	31,18	0,00	0,00	0,00	0,00	0,00	0,00	0,00
NH3	kg/hr	0,00	0,00	0,00	0,00	0,00	0,00	0,02	0,00	0,00	0,88	1,19	0,00	0,00	0,00	0,00	0,70	0,00	0,00
GLUCOSE	kg/hr	0,00	2988,38	0,00	0,00	0,00	223,44	0,00	0,03	0,00	967,54	1191,01	0,00	0,00	10274,25	11,17	24,75	358,57	9915,68
FRUCTOSE	kg/hr	0,00	2988,38	0,00	0,00	0,00	0,00	0,00	0,00	0,00	0,00	0,00	0,00	0,00	10274,25	0,00	358,57	358,57	9915,68
SUCROSE	kg/hr	0,00	13843,18	0,00	0,00	0,00	0,00	0,00	0,00	0,00	0,00	0,00	0,00	0,00	0,00	0,00	0,00	0,00	0,00
MICROORG	kg/hr	0,00	0,00	0,00	0,00	0,00	0,00	0,00	218,33	0,00	0,00	218,33	0,00	0,00	0,00	0,00	165,63	0,00	0,00
BMSLUDGE	kg/hr	0,00	0,00	0,00	0,00	0,00	0,00	0,00	0,00	165,49	0,00	0,00	0,00	0,00	0,00	0,00	0,00	0,00	0,00
PROPACID	kg/hr	0,00	0,00	0,00	0,00	0,00	0,00	0,00	0,00	0,00	0,00	0,00	0,00	0,00	0,00	0,00	0,00	0,00	0,00
BUTYACID	kg/hr	0,00	0,00	0,00	0,00	0,00	0,00	0,00	0,00	0,00	0,00	0,00	0,00	0,00	0,00	0,00	0,00	0,00	0,00
H2	kg/hr	0,01	0,00	0,00	0,00	0,00	0,00	0,00	0,00	0,00	0,00	0,00	0,00	0,00	0,00	0,00	0,00	0,00	0,00
CH4	kg/hr	0,00	0,00	0,00	0,00	0,00	0,00	519,91	0,00	0,00	0,00	0,00	0,00	0,00	0,00	0,00	0,00	0,00	0,00
N2	kg/hr	0,00	0,00	0,00	0,00	0,00	0,00	0,00	0,00	0,00	0,00	0,55	0,00	0,00	0,00	0,00	0,03	0,00	0,00
CELLULOS	kg/hr	0,00	0,00	790,97	1046,31	1837,28	0,00	0,00	0,00	0,00	0,00	0,00	0,00	0,00	0,00	0,00	0,00	0,00	0,00
MANNAN	kg/hr	0,00	0,00	3,07	4,06	7,14	0,00	0,00	0,00	0,00	0,00	0,00	0,00	0,00	0,00	0,00	0,00	0,00	0,00
GALACTAN	kg/hr	0,00	0,00	14,48	19,16	33,65	0,00	0,00	0,00	0,00	0,00	0,00	0,00	0,00	0,00	0,00	0,00	0,00	0,00
XYLAN	kg/hr	0,00	0,00	387,58	512,70	900,29	0,00	0,00	0,00	0,00	0,00	0,00	0,00	0,00	0,00	0,00	0,00	0,00	0,00
ARABINAN	kg/hr	0,00	0,00	32,04	42,39	74,43	0,00	0,00	0,00	0,00	0,00	0,00	0,00	0,00	0,00	0,00	0,00	0,00	0,00
LIGNIN	kg/hr	0,00	0,00	495,56	655,54	1151,10	0,00	0,00	0,00	0,00	0,00	0,00	0,00	0,00	0,00	0,00	0,00	0,00	0,00
EXTRACT	kg/hr	0,00	0,00	145,73	192,77	338,50	0,00	0,00	0,00	0,00	0,00	0,00	0,00	0,00	0,00	0,00	0,00	0,00	0,00
ASH	kg/hr	0,00	0,00	73,74	97,55	171,29	0,00	0,00	0,00	0,00	0,00	0,00	0,00	0,00	0,00	0,00	0,00	0,00	0,00
3B2O	kg/hr	0,00	0,00	0,00	0,00	0,00	0,00	0,01	0,00	0,01	0,00	0,00	0,00	0,00	0,00	13,99	0,00	0,00	0,00
MEK	kg/hr	0,00	0,00	0,00	0,00	0,00	0,00	1,26	0,00	0,52	0,00	0,00	0,00	0,00	0,00	488,08	0,00	0,00	0,00
IBA	kg/hr	0,03	0,00	0,00	0,00	0,00	0,00	0,10	0,00	0,02	0,00	0,00	0,00	0,00	0,00	20,89	0,00	0,00	0,00
1,3-BD	kg/hr	4568,97	0,00	0,00	0,00	0,00	0,00	12,25	0,00	0,28	0,00	0,00	0,00	0,00	0,00	272,68	0,00	0,00	0,00
BUTENE	kg/hr	20,99	0,00	0,00	0,00	0,00	0,00	0,12	0,00	0,00	0,00	0,00	0,00	0,00	0,00	3,43	0,00	0,00	0,00
METHPROP	kg/hr	0,00	0,00	0,00	0,00	0,00	0,00	0,00	0,00	0,00	0,00	0,00	0,00	0,00	0,00	0,00	0,00	0,00	0,00
NANO3	kg/hr	0,00	0,00	0,00	0,00	0,00	0,00	0,00	0,00	0,00	0,00	0,00	0,00	0,00	0,00	0,00	0,00	0,00	0,00
KNO3	kg/hr	0,00	0,00	0,00	0,00	0,00	0,00	0,00	0,00	0,00	0,00	0,00	0,00	0,00	0,00	0,00	0,00	0,00	0,00
C	kg/hr	0,00	0,00	0,00	0,00	0,00	0,00	0,00	0,00	0,00	0,00	0,00	0,00	0,00	0,00	0,00	0,00	0,00	0,00

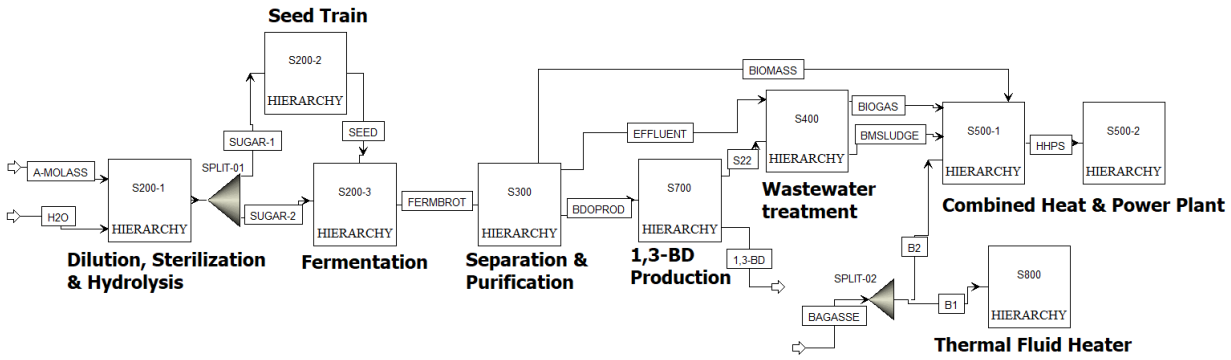

Figure 78: Scenario C, Main Flowsheet in Aspen Plus®

Table 63: Material Balances of Scenario D, Main Flowsheet

Material Balance - Scenario D															
Stream Name	**Units**	**1,3-BD**	**2,3-BDO**	**2GFEED**	**A-MOLASS**	**AIR**	**BIOGAS**	**BMSLUDGE**	**BYPASS**	**CELLULIG**	**GLUCOSE**	**GLUCSEED**	**H2O**	**H2O1**	**HEMICELL**
Description															
From		S700	S300				S400	S400	SPLIT	S100-2	S100-2	S100-2			S100-2
To			S700	SPLIT	S200-1	S100-1	S500-1	S500-1	S500-1	S500-1	S200-2	S200-2	S100-2	S200-1	S200-3
Stream Class		CONVEN	CONVEN	CONVEN	CONVEN	CONVEN	CONVEN	CONVEN	CONVEN	CONVEN	CONVEN	CONVEN	CONVEN	CONVEN	CONVEN
Total Stream															
Temperature	C	31,238	136,964	25,000	56,000	25,000	34,911	34,931	25,000	50,000	50,000	50,000	25,000	93,342	97,922
Pressure	bar	3,432	1,520	1,013	1,013	1,013	1,013	1,520	1,013	1,013	1,013	1,013	1,013	0,811	1,013
Mass Vapor Fraction		0,000	0,000	0,000	0,000	1,000	1,000	0,000	0,000	0,000	0,000	0,000	0,000	0,001	0,000
Mass Liquid Fraction		1,000	1,000	0,475	1,000	0,000	0,000	0,333	0,475	0,333	1,000	1,000	1,000	0,999	1,000
Mass Solid Fraction		0,000	0,000	0,525	0,000	0,000	0,000	0,667	0,525	0,667	0,000	0,000	0,000	0,000	0,000
Mass Enthalpy	cal/gm	395,493	-1327,963	-2430,014	-1984,655	-32,146	-1052,135	-1241,908	-2430,014	-1962,182	-3453,137	-3453,137	-3791,854	-3713,180	-3550,343
Mass Entropy	cal/gm-K	-0,936	-1,503	-1,485	-1,909	0,033	-0,033	-0,703	-1,485	-1,404	-1,994	-1,994	-2,163	-1,950	-2,047
Mass Density	gm/cc	0,606	0,803	1,140	0,923	0,001	0,001	1,117	1,140	1,254	1,014	1,014	0,997	0,460	0,998
Average MW		54,106	91,165	35,709	66,027	28,603	30,034	41,467	35,709	47,265	20,815	20,815	18,015	18,078	19,377
Mass Flows	kg/hr	6800,000	13300,000	63702,000	25433,000	2908,652	7049,553	580,606	21250,000	13929,474	46087,594	3362,019	42721,159	42669,000	57180,873
O2	kg/hr	0,000	0,000	0,000	0,000	610,817	0,771	0,000	0,000	0,000	0,000	0,000	0,000	0,000	0,000
SO2	kg/hr	0,000	0,000	0,000	0,000	0,000	39,552	0,029	0,000	0,083	0,824	0,060	0,000	9,575	10,949
FES2	kg/hr	0,000	0,000	0,000	0,000	0,000	0,000	0,000	0,000	0,000	0,000	0,000	0,000	0,000	0,000
H2O	kg/hr	0,000	0,001	27626,011	5613,063	29,087	235,160	189,414	9215,609	3948,722	39194,684	2859,192	42721,159	42458,388	52590,318
CELLULOS	kg/hr	0,000	0,000	14583,172	0,000	0,000	0,000	0,000	4864,720	391,399	0,000	0,000	0,000	0,000	0,000
MANNAN	kg/hr	0,000	0,000	56,132	0,000	0,000	0,000	0,000	18,725	34,189	0,000	0,000	0,000	0,000	0,000
GALACTAN	kg/hr	0,000	0,000	291,888	0,000	0,000	0,000	0,000	97,369	177,785	0,000	0,000	0,000	0,000	0,000
XYLAN	kg/hr	0,000	0,000	7807,998	0,000	0,000	0,000	0,000	2604,627	2358,329	0,000	0,000	0,000	0,000	0,000
ARABINAN	kg/hr	0,000	0,000	645,523	0,000	0,000	0,000	0,000	215,336	187,627	0,000	0,000	0,000	0,000	0,000
LIGNIN	kg/hr	0,000	0,000	8863,274	0,000	0,000	0,000	0,000	2956,651	5398,497	0,000	0,000	0,000	0,000	0,000
FURFURAL	kg/hr	0,000	0,292	0,000	0,000	0,000	0,003	0,030	0,000	0,369	3,660	0,267	0,000	14,216	48,610
ACETICAC	kg/hr	0,000	0,000	0,000	0,000	0,000	0,000	0,000	0,000	2,176	21,596	1,575	0,000	186,249	286,806
EXTRACT	kg/hr	0,000	112,871	2615,546	0,000	0,000	0,000	1,810	872,505	10,517	104,394	7,615	0,000	0,000	1386,407
CELLOBIO	kg/hr	0,000	6,805	0,000	0,000	0,000	0,000	0,005	0,000	7,904	78,451	5,723	0,000	0,000	0,000
ASH	kg/hr	0,000	0,000	1212,456	0,000	0,000	0,000	0,000	404,457	738,490	0,000	0,000	0,000	0,000	0,000
CO2	kg/hr	0,000	0,000	0,000	0,000	0,000	2794,777	0,061	0,000	0,000	0,000	0,000	0,000	0,114	0,000
2,3-BDO	kg/hr	0,000	12944,515	0,000	0,000	0,000	0,000	0,000	0,000	0,000	0,000	0,000	0,000	0,000	0,000
ETHANOL	kg/hr	0,000	0,000	0,000	0,000	0,000	0,000	0,000	0,000	0,000	0,000	0,000	0,000	0,000	0,000
GLYCEROL	kg/hr	0,000	20,898	0,000	0,000	0,000	0,000	0,000	0,000	0,000	0,000	0,000	0,000	0,000	0,000
XYLITOL	kg/hr	0,000	5,029	0,000	0,000	0,000	0,000	0,077	0,000	0,000	0,000	0,000	0,000	0,000	0,000
ACETOIN	kg/hr	0,000	0,077	0,000	0,000	0,000	0,012	0,080	0,000	0,000	0,000	0,000	0,000	0,000	0,000
SUCCINIC	kg/hr	0,000	46,846	0,000	0,000	0,000	0,000	0,000	0,000	0,000	0,000	0,000	0,000	0,000	0,000
FRUCTOSE	kg/hr	0,000	0,000	0,000	2988,378	0,000	0,000	0,000	0,000	0,000	0,000	0,000	0,000	0,000	0,000
SUCROSE	kg/hr	0,000	0,000	0,000	13843,182	0,000	0,000	0,000	0,000	0,000	0,000	0,000	0,000	0,000	0,000
FE2O3	kg/hr	0,000	0,000	0,000	0,000	0,000	0,000	0,000	0,000	0,000	0,000	0,000	0,000	0,000	0,000
SCEREVIS	kg/hr	0,000	0,000	0,000	0,000	0,000	0,000	0,000	0,000	0,000	0,000	0,000	0,000	0,000	0,000
KOXYTOCA	kg/hr	0,000	0,000	0,000	0,000	0,000	0,000	0,000	0,000	0,000	0,000	0,000	0,000	0,000	0,000
XYLOSE	kg/hr	0,000	24,748	0,000	0,000	0,000	0,000	0,000	0,000	17,383	172,543	12,587	0,000	0,003	2291,470
ARABINOS	kg/hr	0,000	17,101	0,000	0,000	0,000	0,000	0,013	0,000	1,542	15,306	1,117	0,000	0,036	203,272
GLUCOSE	kg/hr	0,000	120,817	0,000	2988,378	0,000	0,000	0,000	0,000	654,462	6496,131	473,883	0,000	0,000	362,992
NH3	kg/hr	0,000	0,000	0,000	0,000	0,000	0,073	0,002	0,000	0,000	0,000	0,000	0,000	0,371	0,000
PROPACID	kg/hr	0,000	0,000	0,000	0,000	0,000	0,009	0,041	0,000	0,000	0,000	0,000	0,000	0,000	0,000
BUTYRACI	kg/hr	0,000	0,000	0,000	0,000	0,000	0,000	0,000	0,000	0,000	0,000	0,000	0,000	0,000	0,000
CH4	kg/hr	0,000	0,000	0,000	0,000	0,000	605,743	0,455	0,000	0,000	0,000	0,000	0,000	0,000	0,000
H2	kg/hr	0,000	0,000	0,000	0,000	0,000	0,000	0,000	0,000	0,000	0,000	0,000	0,000	0,000	0,000
BMSLUDGE	kg/hr	0,000	0,000	0,000	0,000	0,000	0,000	387,070	0,000	0,000	0,000	0,000	0,000	0,000	0,000
ISOVACID	kg/hr	0,000	0,000	0,000	0,000	0,000	0,000	0,000	0,000	0,000	0,000	0,000	0,000	0,000	0,000
C3H6O2	kg/hr	0,000	0,000	0,000	0,000	0,000	0,676	0,144	0,000	0,000	0,000	0,000	0,000	0,000	0,000
N2	kg/hr	0,000	0,000	0,000	0,000	2268,749	3336,020	0,002	0,000	0,000	0,004	0,000	0,000	0,047	0,048
S	kg/hr	0,000	0,000	0,000	0,000	0,000	0,000	0,000	0,000	0,000	0,000	0,000	0,000	0,000	0,001
NO2	kg/hr	0,000	0,000	0,000	0,000	0,000	0,000	0,000	0,000	0,000	0,000	0,000	0,000	0,000	0,000
3B2O	kg/hr	0,000	0,000	0,000	0,000	0,000	0,041	0,025	0,000	0,000	0,000	0,000	0,000	0,000	0,000
1,3-BD	kg/hr	6765,888	0,000	0,000	0,000	0,000	32,357	0,420	0,000	0,000	0,000	0,000	0,000	0,000	0,000
IBA	kg/hr	1,987	0,000	0,000	0,000	0,000	0,272	0,035	0,000	0,000	0,000	0,000	0,000	0,000	0,000
MEK	kg/hr	0,825	0,000	0,000	0,000	0,000	3,745	0,885	0,000	0,000	0,000	0,000	0,000	0,000	0,000
METHPROP	kg/hr	0,000	0,000	0,000	0,000	0,000	0,000	0,000	0,000	0,000	0,000	0,000	0,000	0,000	0,000
BUTENE	kg/hr	31,300	0,000	0,000	0,000	0,000	0,341	0,006	0,000	0,000	0,000	0,000	0,000	0,000	0,000
NANO3	kg/hr	0,000	0,000	0,000	0,000	0,000	0,000	0,000	0,000	0,000	0,000	0,000	0,000	0,000	0,000
KNO3	kg/hr	0,000	0,000	0,000	0,000	0,000	0,000	0,000	0,000	0,000	0,000	0,000	0,000	0,000	0,000
CACO3	kg/hr	0,000	0,000	0,000	0,000	0,000	0,000	0,000	0,000	0,000	0,000	0,000	0,000	0,000	0,000
CASO4	kg/hr	0,000	0,000	0,000	0,000	0,000	0,000	0,000	0,000	0,000	0,000	0,000	0,000	0,000	0,000
CASO3	kg/hr	0,000	0,000	0,000	0,000	0,000	0,000	0,000	0,000	0,000	0,000	0,000	0,000	0,000	0,000
C	kg/hr	0,000	0,000	0,000	0,000	0,000	0,000	0,000	0,000	0,000	0,000	0,000	0,000	0,000	0,000

Material Balance - Scenario D															
Stream Name	**HHPS**	**KOXYTOCA**	**MSALTBYP**	**S1**	**S2**	**S3**	**S4**	**S13**	**S23**	**SCEREVIS**	**SO2**	**SULPHUR**	**WASTE**	**XFERM**	**XSEED**
Description															
From	S500-1	S200-2	SPLIT	S200-3	S200-2	S300	S700	SPLIT	S200-1	S200-3	S100-1		S100-2	S100-2	S100-2
To	S500-2	S500-1	S800	S300	S300	S400	S400	S100-2	S200-2	S500-1	S100-2	S100-1	S400	S200-3	S200-3
Stream Class	CONVEN	CONVEN	CONVEN	CONVEN	CONVEN	CONVEN	CONVEN	CONVEN	CONVEN	CONVEN	CONVEN	CONVEN	CONVEN	CONVEN	CONVEN
Total Stream															
Temperature	451,980	37,017	25,000	30,018	37,017	57,887	67,476	25,000	55,000	30,018	190,000	25,000	95,098	50,000	50,000
Pressure	63,024	1,013	1,013	1,013	1,013	0,203	1,373	1,013	1,013	1,013	1,013	1,013	1,013	1,013	1,013
Mass Vapor Fraction	1,000	0,000	0,000	0,000	0,000	0,000	0,000	0,000	0,000	0,000	1,000	0,000	0,466	0,000	0,000
Mass Liquid Fraction	0,000	0,010	0,475	1,000	1,000	1,000	1,000	0,475	1,000	0,010	0,000	1,000	0,534	1,000	1,000
Mass Solid Fraction	0,000	0,990	0,525	0,000	0,000	0,000	0,000	0,525	0,000	0,990	0,000	0,000	0,000	0,000	0,000
Mass Enthalpy	-3027,909	-1027,249	-2430,014	-3087,237	-3450,221	-3740,297	-3152,513	-2430,014	-3100,409	-1263,707	-365,968	1989,789	-3134,837	-3453,137	-3453,137
Mass Entropy	-0,650	-3,351	-1,485	-2,056	-2,047	-2,050	-1,849	-1,485	-2,382	-4,156	0,139	6,650	-1,194	-1,994	-1,994
Mass Density	0,020	1,099	1,140	1,037	0,986	0,980	0,911	1,140	1,057	1,099	0,001	0,404	0,001	1,014	1,014
Average MW	18,015	23,697	35,709	24,523	20,332	18,123	20,776	35,709	24,790	25,189	34,723	32,066	19,020	20,815	20,815
Mass Flows	131562,979	295,338	3652,000	10724,928	106701,312	99865,333	6489,662	38800,000	68217,360	77,764	3509,417	612,000	36489,715	3372,218	560,337
O2	0,000	0,000	0,000	0,008	0,000	0,000	0,000	0,000	0,000	0,000	0,183	0,000	0,771	0,000	0,000
SO2	0,000	0,000	0,000	0,000	1,164	0,594	0,000	0,000	9,575	0,000	1222,717	0,000	60,940	0,060	0,010
FES2	0,000	0,000	0,000	0,000	0,000	0,000	0,000	0,000	0,000	0,000	0,000	0,000	0,000	0,000	0,000
H2O	131562,979	2,513	1583,784	7338,072	91685,231	99013,037	5303,989	16826,618	47458,243	0,527	17,758	0,000	32035,998	2867,865	476,532
CELLULOS	0,000	0,000	836,045	0,000	0,000	0,000	0,000	8882,407	0,000	0,000	0,000	0,000	0,000	0,000	0,000
MANNAN	0,000	0,000	3,218	0,000	0,000	0,000	0,000	34,189	0,000	0,000	0,000	0,000	0,000	0,000	0,000
GALACTAN	0,000	0,000	16,734	0,000	0,000	0,000	0,000	177,785	0,000	0,000	0,000	0,000	0,000	0,000	0,000
XYLAN	0,000	0,000	447,628	0,000	0,000	0,000	0,000	4755,743	0,000	0,000	0,000	0,000	0,000	0,000	0,000
ARABINAN	0,000	0,000	37,007	0,000	0,000	0,000	0,000	393,179	0,000	0,000	0,000	0,000	0,000	0,000	0,000
LIGNIN	0,000	0,000	508,127	0,000	0,000	0,000	0,000	5398,497	0,000	0,000	0,000	0,000	0,000	0,000	0,000
FURFURAL	0,000	0,000	0,000	0,326	18,130	18,161	0,823	0,000	14,216	0,000	0,000	0,000	3,071	0,268	0,045
ACETICAC	0,000	0,010	0,000	25,949	367,223	393,157	0,000	0,000	186,249	0,002	0,000	0,000	49,956	1,580	0,263
EXTRACT	0,000	0,003	149,948	1395,214	112,006	0,000	10,158	1593,092	0,000	0,100	0,000	0,000	69,246	7,638	1,269
CELLOBIO	0,000	0,002	0,000	6,694	84,172	0,000	0,621	0,000	0,000	0,000	0,000	0,000	0,000	5,740	0,954
ASH	0,000	0,000	69,509	0,000	0,000	0,000	0,000	738,490	0,000	0,000	0,000	0,000	0,000	0,000	0,000
CO2	0,000	0,001	0,000	4,067	46,562	1,560	0,000	0,000	0,114	0,000	0,000	0,000	789,704	0,000	0,000
2,3-BDO	0,000	0,342	0,000	1006,699	12482,285	137,757	0,000	0,000	0,000	0,072	0,000	0,000	0,000	0,000	0,000
ETHANOL	0,000	0,001	0,000	186,163	41,787	227,837	0,000	0,000	0,000	0,013	0,000	0,000	0,000	0,000	0,000
GLYCEROL	0,000	0,000	0,000	259,935	0,000	0,002	2,134	0,000	0,000	0,019	0,000	0,000	0,000	0,000	0,000
XYLITOL	0,000	0,000	0,000	67,150	0,000	0,000	0,512	0,000	0,000	0,005	0,000	0,000	0,000	0,000	0,000
ACETOIN	0,000	0,000	0,000	64,926	0,000	64,849	0,004	0,000	0,000	0,005	0,000	0,000	0,000	0,000	0,000
SUCCINIC	0,000	0,002	0,000	0,000	63,748	5,266	3,166	0,000	0,000	0,000	0,000	0,000	0,000	0,000	0,000
FRUCTOSE	0,000	0,000	0,000	0,000	0,000	0,000	0,000	0,000	10274,252	0,000	0,000	0,000	0,000	0,000	0,000
SUCROSE	0,000	0,000	0,000	0,000	0,000	0,000	0,000	0,000	0,000	0,000	0,000	0,000	0,000	0,000	0,000
FE2O3	0,000	0,000	0,000	0,000	0,000	0,000	0,000	0,000	0,000	0,000	0,000	0,000	0,000	0,000	0,000
SCEREVIS	0,000	0,000	0,000	0,000	0,000	0,000	0,000	0,000	0,000	76,994	0,000	0,000	0,000	0,000	0,000
KOXYTOCA	0,000	292,413	0,000	0,000	0,000	0,000	0,000	0,000	0,000	0,000	0,000	0,000	0,000	0,000	0,000
XYLOSE	0,000	0,005	0,000	145,320	185,127	0,000	1,967	0,000	0,003	0,010	0,000	0,000	114,450	12,625	2,098
ARABINOS	0,000	0,000	0,000	204,521	16,459	0,000	2,017	0,000	0,036	0,015	0,000	0,000	10,153	1,120	0,186
GLUCOSE	0,000	0,044	0,000	18,376	1594,946	0,000	11,165	0,000	10274,252	0,001	0,000	0,000	18,130	475,320	78,980
NH3	0,000	0,000	0,000	1,432	1,729	3,113	0,000	0,000	0,371	0,000	0,000	0,000	0,000	0,000	0,000
PROPACID	0,000	0,000	0,000	0,000	0,000	0,000	0,000	0,000	0,000	0,000	0,000	0,000	0,000	0,000	0,000
BUTYRACI	0,000	0,000	0,000	0,000	0,000	0,000	0,000	0,000	0,000	0,000	0,000	0,000	0,000	0,000	0,000
CH4	0,000	0,000	0,000	0,000	0,000	0,000	0,000	0,000	0,000	0,000	0,000	0,000	0,000	0,000	0,000
H2	0,000	0,000	0,000	0,000	0,000	0,000	0,000	0,000	0,000	0,000	0,010	0,000	0,010	0,000	0,000
BMSLUDGE	0,000	0,000	0,000	0,000	0,000	0,000	0,000	0,000	0,000	0,000	0,000	0,000	0,000	0,000	0,000
ISOVACID	0,000	0,000	0,000	0,000	0,000	0,000	0,000	0,000	0,000	0,000	0,000	0,000	0,000	0,000	0,000
C3H6O2	0,000	0,000	0,000	0,000	0,000	0,000	0,000	0,000	0,000	0,000	0,000	0,000	0,000	0,000	0,000
N2	0,000	0,000	0,000	0,077	0,744	0,001	0,000	0,000	0,047	0,000	2268,748	0,000	3337,284	0,000	0,000
S	0,000	0,000	0,000	0,001	0,000	0,000	0,000	0,000	0,000	0,000	0,001	612,000	0,000	0,000	0,000
NO2	0,000	0,000	0,000	0,000	0,000	0,000	0,000	0,000	0,000	0,000	0,000	0,000	0,000	0,000	0,000
3B2O	0,000	0,000	0,000	0,000	0,000	0,000	20,714	0,000	0,000	0,000	0,000	0,000	0,000	0,000	0,000
1,3-BD	0,000	0,000	0,000	0,000	0,000	0,000	374,142	0,000	0,000	0,000	0,000	0,000	0,000	0,000	0,000
IBA	0,000	0,000	0,000	0,000	0,000	0,000	29,083	0,000	0,000	0,000	0,000	0,000	0,000	0,000	0,000
MEK	0,000	0,000	0,000	0,000	0,000	0,000	724,202	0,000	0,000	0,000	0,000	0,000	0,000	0,000	0,000
METHPROP	0,000	0,000	0,000	0,000	0,000	0,000	0,000	0,000	0,000	0,000	0,000	0,000	0,000	0,000	0,000
BUTENE	0,000	0,000	0,000	0,000	0,000	0,000	4,965	0,000	0,000	0,000	0,000	0,000	0,000	0,000	0,000
NANO3	0,000	0,000	0,000	0,000	0,000	0,000	0,000	0,000	0,000	0,000	0,000	0,000	0,000	0,000	0,000
KNO3	0,000	0,000	0,000	0,000	0,000	0,000	0,000	0,000	0,000	0,000	0,000	0,000	0,000	0,000	0,000
CACO3	0,000	0,000	0,000	0,000	0,000	0,000	0,000	0,000	0,000	0,000	0,000	0,000	0,000	0,000	0,000
CASO4	0,000	0,000	0,000	0,000	0,000	0,000	0,000	0,000	0,000	0,000	0,000	0,000	0,000	0,000	0,000
CASO3	0,000	0,000	0,000	0,000	0,000	0,000	0,000	0,000	0,000	0,000	0,000	0,000	0,000	0,000	0,000
C	0,000	0,000	0,000	0,000	0,000	0,000	0,000	0,000	0,000	0,000	0,000	0,000	0,000	0,000	0,000

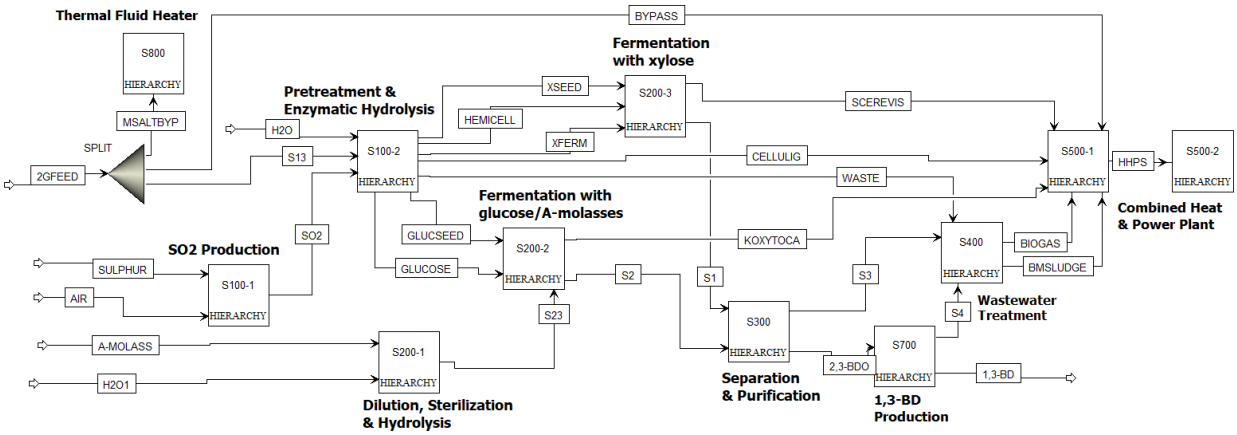

Figure 79: Scenario D, Main Flowsheet in Aspen Plus®

Table 64: Material Balances of Scenario E, Main Flowsheet

Material Balance - Scenario E																
Stream Name	**Units**	**1,3-BD**	**A-MOLAS**	**ACET**	**B1**	**B2**	**BAGASSE**	**BIOGAS**	**BIOMASS**	**BMSLUDGE**	**BTM1**	**ETH**	**ETHANOL**	**FERMBRTH**	**H2O**	**HHPS**
Description																
From		S700-5		S700-5	SPLIT-02	SPLIT-02		S400	S200-2	S400	S300-1	S700-5	S300-1	S200-2		S500-1
To			S200-1	S700-3	S800	S500-1	SPLIT-02	S500-1	S300-1	S500-1	S300-2	S700-3	SPLIT-01	S300-1	S200-1	S500-2
Stream Class		CONVEN	CONVEN	CONVEN	CONVEN	CONVEN	CONVEN	CONVEN	CONVEN	CONVEN	CONVEN	CONVEN	CONVEN	CONVEN	CONVEN	CONVEN
Total Stream																
Temperature	C	61,07	56,00	11,19	25,00	25,00	25,00	35,00	30,00	35,02	79,07	86,51	98,49	30,00	25,00	452,02
Pressure	bar	6,89	1,01	1,24	1,01	1,01	1,01	1,11	1,01	1,52	2,31	1,24	1,62	1,01	1,01	63,02
Mass Vapor Fraction		0,00	0,00	0,00	0,00	0,00	0,00	1,00	0,00	0,00	0,00	0,00	1,00	0,00	0,00	1,00
Mass Liquid Fraction		1,00	1,00	1,00	0,54	0,54	0,54	0,00	0,23	0,33	1,00	1,00	0,00	1,00	1,00	0,00
Mass Solid Fraction		0,00	0,00	0,00	0,46	0,46	0,46	0,00	0,77	0,67	0,00	0,00	0,00	0,00	0,00	0,00
Mass Enthalpy	cal/gm	408,46	-1961,86	-301,07	-2643,59	-2643,59	-2643,59	-1865,36	-1760,88	-1252,08	-3675,62	-1649,68	-1339,35	-3478,88	-3789,48	-3025,58
Mass Entropy	cal/gm-K	-0,88	-1,83	-1,33	-1,70	-1,70	-1,70	-0,30	-3,70	-0,71	-2,04	-1,49	-1,04	-2,11	-2,16	-0,65
Mass Density	gm/cc	0,57	1,22	0,66	1,09	1,09	1,09	0,00	1,07	1,12	0,98	0,77	0,00	0,98	1,00	0,02
Average MW		53,93	66,03	53,17	31,62	31,62	31,62	28,22	23,67	41,21	18,44	41,49	41,29	19,70	18,02	18,02
Mass Flows	kg/hr	2754,01	25433,00	957,76	5850,00	5343,70	11193,70	1287,60	146,23	281,16	66784,24	10942,03	10279,94	86073,04	70000,00	63560,16
H2O	kg/hr	4,00	5613,06	0,00	2972,13	2714,90	5687,03	42,03	29,30	92,86	64958,60	2072,04	761,12	74731,70	70000,00	63560,16
SUCROSE	kg/hr	0,00	13843,18	0,00	0,00	0,00	0,00	0,00	0,00	0,00	0,00	0,00	0,00	0,00	0,00	0,00
GLUCOSE	kg/hr	0,00	2988,38	0,00	0,00	0,00	0,00	0,00	0,16	0,00	410,95	0,00	0,00	410,79	0,00	0,00
FRUCTOSE	kg/hr	0,00	2988,38	0,00	0,00	0,00	0,00	0,00	0,38	0,00	976,71	0,00	0,00	977,69	0,00	0,00
ETHANOL	kg/hr	0,00	0,00	0,00	0,00	0,00	0,00	0,00	3,71	0,00	0,00	4330,96	9508,68	9455,65	0,00	0,00
CO2	kg/hr	0,00	0,00	0,00	0,00	0,00	0,00	866,27	0,05	0,05	0,00	0,00	8,08	122,01	0,00	0,00
CH4	kg/hr	0,00	0,00	0,00	0,00	0,00	0,00	378,66	0,00	0,00	0,00	0,00	0,00	0,00	0,00	0,00
O2	kg/hr	0,00	0,00	0,00	0,00	0,00	0,00	0,00	0,00	0,00	0,00	0,00	0,00	0,00	0,00	0,00
NH3	kg/hr	0,00	0,00	2,42	0,00	0,00	0,00	0,10	0,00	0,01	0,00	0,16	2,06	1,99	0,00	0,00
N2	kg/hr	0,00	0,00	0,00	0,00	0,00	0,00	0,00	0,00	0,00	0,00	0,00	0,00	0,00	0,00	0,00
BMSLUDGE	kg/hr	0,00	0,00	0,00	0,00	0,00	0,00	0,00	0,00	187,44	0,00	0,00	0,00	0,00	0,00	0,00
CELLULOS	kg/hr	0,00	0,00	0,00	1171,43	1070,05	2241,48	0,00	0,00	0,00	0,00	0,00	0,00	0,00	0,00	0,00
MANNAN	kg/hr	0,00	0,00	0,00	4,55	4,16	8,71	0,00	0,00	0,00	0,00	0,00	0,00	0,00	0,00	0,00
GALACTAN	kg/hr	0,00	0,00	0,00	21,45	19,60	41,05	0,00	0,00	0,00	0,00	0,00	0,00	0,00	0,00	0,00
XYLAN	kg/hr	0,00	0,00	0,00	574,01	524,33	1098,35	0,00	0,00	0,00	0,00	0,00	0,00	0,00	0,00	0,00
ARABINAN	kg/hr	0,00	0,00	0,00	47,46	43,35	90,80	0,00	0,00	0,00	0,00	0,00	0,00	0,00	0,00	0,00
LIGNIN	kg/hr	0,00	0,00	0,00	733,93	670,41	1404,34	0,00	0,00	0,00	0,00	0,00	0,00	0,00	0,00	0,00
EXTRACT	kg/hr	0,00	0,00	0,00	215,82	197,15	412,97	0,00	0,00	0,00	0,00	0,00	0,00	0,00	0,00	0,00
ASH	kg/hr	0,00	0,00	0,00	109,21	99,76	208,97	0,00	0,00	0,00	0,00	0,00	0,00	0,00	0,00	0,00
1,3-BD	kg/hr	2750,01	0,00	14,31	0,00	0,00	0,00	0,03	0,00	0,00	0,00	0,60	0,00	0,00	0,00	0,00
DIAMMON	kg/hr	0,00	0,00	0,00	0,00	0,00	0,00	0,00	0,00	0,00	3,73	0,00	0,00	3,73	0,00	0,00
GLYCEROL	kg/hr	0,00	0,00	0,00	0,00	0,00	0,00	0,00	0,09	0,21	233,71	0,00	0,00	233,63	0,00	0,00
UREA	kg/hr	0,00	0,00	0,00	0,00	0,00	0,00	0,00	0,02	0,06	53,75	0,00	0,00	53,73	0,00	0,00
SCEREVIS	kg/hr	0,00	0,00	0,00	0,00	0,00	0,00	0,00	112,48	0,00	112,48	0,00	0,00	0,00	0,00	0,00
SUCCINIC	kg/hr	0,00	0,00	0,00	0,00	0,00	0,00	0,00	0,01	0,00	33,47	0,00	0,00	33,47	0,00	0,00
ISOAMYL	kg/hr	0,00	0,00	0,00	0,00	0,00	0,00	0,00	0,02	0,05	0,00	0,00	0,00	47,82	0,00	0,00
ACETICAC	kg/hr	0,00	0,00	0,00	0,00	0,00	0,00	0,00	0,00	0,00	0,00	11,27	0,00	0,00	0,00	0,00
PROPAN	kg/hr	0,00	0,00	0,00	0,00	0,00	0,00	0,00	0,00	0,00	0,00	0,00	0,00	0,00	0,00	0,00
BUTYRIC	kg/hr	0,00	0,00	0,00	0,00	0,00	0,00	0,00	0,00	0,00	0,00	0,00	0,00	0,00	0,00	0,00
C3H6O2	kg/hr	0,00	0,00	0,00	0,00	0,00	0,00	0,02	0,00	0,01	0,00	0,00	0,00	0,00	0,00	0,00
ACETALDE	kg/hr	0,00	0,00	173,68	0,00	0,00	0,00	0,00	0,00	0,00	0,00	95,56	0,00	0,00	0,00	0,00
CO	kg/hr	0,00	0,00	0,00	0,00	0,00	0,00	0,00	0,00	0,00	0,00	0,00	0,00	0,00	0,00	0,00
DIETHYL	kg/hr	0,00	0,00	2,97	0,00	0,00	0,00	0,00	0,00	0,00	0,00	387,84	0,00	0,00	0,00	0,00
ETHYLACE	kg/hr	0,00	0,00	0,00	0,00	0,00	0,00	0,44	0,00	0,28	0,00	3114,57	0,00	0,00	0,00	0,00
N-BUT-01	kg/hr	0,00	0,00	0,00	0,00	0,00	0,00	0,03	0,00	0,18	0,00	29,17	0,00	0,00	0,00	0,00
ETHYL-01	kg/hr	0,00	0,00	0,00	0,00	0,00	0,00	0,00	0,00	0,00	0,00	0,00	0,00	0,00	0,00	0,00
2-BUT-01	kg/hr	0,00	0,00	764,38	0,00	0,00	0,00	0,00	0,00	0,00	0,00	74,31	0,00	0,00	0,00	0,00
1:5-H-01	kg/hr	0,00	0,00	0,00	0,00	0,00	0,00	0,00	0,00	0,00	0,00	825,57	0,00	0,00	0,00	0,00
H2SO4	kg/hr	0,00	0,00	0,00	0,00	0,00	0,00	0,00	0,00	0,00	0,83	0,00	0,00	0,83	0,00	0,00
H2	kg/hr	0,00	0,00	0,00	0,00	0,00	0,00	0,00	0,00	0,00	0,00	0,00	0,00	0,00	0,00	0,00
DIPHENOX	kg/hr	0,00	0,00	0,00	0,00	0,00	0,00	0,00	0,00	0,00	0,00	0,00	0,00	0,00	0,00	0,00
BIPHEN	kg/hr	0,00	0,00	0,00	0,00	0,00	0,00	0,00	0,00	0,00	0,00	0,00	0,00	0,00	0,00	0,00
NANO3	kg/hr	0,00	0,00	0,00	0,00	0,00	0,00	0,00	0,00	0,00	0,00	0,00	0,00	0,00	0,00	0,00
KNO3	kg/hr	0,00	0,00	0,00	0,00	0,00	0,00	0,00	0,00	0,00	0,00	0,00	0,00	0,00	0,00	0,00

Material Balance - Scenario E																
Stream Name	**Units**	**LIQ**	**MAKE-UP**	**S1**	**S2**	**S3**	**S5**	**S6**	**S7**	**S8**	**S9**	**S14**	**S16**	**S17**	**VAP**	**VENT**
Description																
From		S700-4	SPLIT-01	SPLIT-01	S700-1	S700-2	S200-1	S300-1	S700-3	S300-2	S300-2	S700-2	S700-5	S700-5	S700-4	S200-2
To		S700-5	S700-3	S700-1	S700-2	S700-3	S200-2	S400	S700-4	S500-1	S400	S500-1	S500-1	S400	S700-5	S300-1
Stream Class		CONVEN	CONVEN	CONVEN	CONVEN	CONVEN	CONVEN	CONVEN	CONVEN	CONVEN	CONVEN	CONVEN	CONVEN	CONVEN	CONVEN	CONVEN
Total Stream																
Temperature	C	110,53	98,49	98,49	66,67	55,97	39,05	113,75	145,64	64,27	76,85	55,97	32,67	105,06	93,33	30,00
Pressure	bar	8,62	1,62	1,62	2,41	10,69	1,01	1,62	6,41	1,01	1,52	10,69	1,24	1,24	9,17	1,01
Mass Vapor Fraction		0,00	1,00	1,00	0,49	0,00	0,00	0,00	0,70	0,00	0,00	1,00	0,13	0,00	0,88	1,00
Mass Liquid Fraction		1,00	0,00	0,00	0,51	1,00	1,00	1,00	0,30	0,46	1,00	0,00	0,87	1,00	0,12	0,00
Mass Solid Fraction		0,00	0,00	0,00	0,00	0,00	0,00	0,00	0,00	0,54	0,00	0,00	0,00	0,00	0,00	0,00
Mass Enthalpy	cal/gm	-1489,16	-1339,35	-1339,35	-1322,49	-1457,30	-3294,42	-3686,53	-1335,72	-1743,76	-3681,89	-805,42	-859,13	-3305,82	-219,04	-2148,04
Mass Entropy	cal/gm-K	-1,34	-1,04	-1,04	-1,10	-1,41	-2,05	-1,89	-0,97	-3,56	-2,04	-0,83	-1,38	-1,81	-0,72	0,01
Mass Density	gm/cc	0,69	0,00	0,00	0,00	0,76	1,05	0,90	0,01	1,17	0,98	0,00	0,02	0,20	0,01	0,00
Average MW		37,40	41,29	41,29	29,41	40,67	22,35	18,07	37,39	30,93	18,43	8,31	55,39	20,49	32,52	42,97
Mass Flows	kg/hr	21298,47	1435,86	8844,08	8844,08	7974,26	95433,00	13313,10	21315,06	206,42	64186,53	869,82	2860,03	3801,23	16,59	9293,28
H2O	kg/hr	5253,75	106,31	654,81	646,81	641,23	75613,06	13263,85	5254,27	33,47	62535,65	5,58	0,00	3178,23	0,52	157,50
SUCROSE	kg/hr	0,00	0,00	0,00	0,00	0,00	13843,18	0,00	0,00	0,00	0,00	0,00	0,00	0,00	0,00	0,00
GLUCOSE	kg/hr	0,00	0,00	0,00	0,00	0,00	2988,38	0,00	0,00	15,33	395,63	0,00	0,00	0,00	0,00	0,00
FRUCTOSE	kg/hr	0,00	0,00	0,00	0,00	0,00	2988,38	1,37	0,00	34,66	940,27	0,00	0,00	0,00	0,00	0,00
ETHANOL	kg/hr	5350,85	1328,14	8180,54	4090,27	4006,17	0,00	0,00	5352,40	0,00	0,00	84,10	886,26	135,18	1,54	49,32
CO2	kg/hr	2,32	1,13	6,95	36,26	1,69	0,00	0,00	2,82	0,00	0,00	34,57	2,82	0,00	0,50	9086,36
CH4	kg/hr	0,08	0,00	0,00	21,37	0,18	0,00	0,00	0,18	0,00	0,00	21,18	0,18	0,00	0,11	0,00
O2	kg/hr	0,00	0,00	0,00	0,00	0,00	0,00	0,00	0,00	0,00	0,00	0,00	0,00	0,00	0,00	0,00
NH3	kg/hr	2,96	0,29	1,77	1,77	1,20	0,00	0,00	2,96	0,00	0,00	0,58	0,38	0,00	0,01	0,08
N2	kg/hr	0,00	0,00	0,00	0,00	0,00	0,00	0,00	0,00	0,00	0,00	0,00	0,00	0,00	0,00	0,00
BMSLUDGE	kg/hr	0,00	0,00	0,00	0,00	0,00	0,00	0,00	0,00	0,00	0,00	0,00	0,00	0,00	0,00	0,00
CELLULOS	kg/hr	0,00	0,00	0,00	0,00	0,00	0,00	0,00	0,00	0,00	0,00	0,00	0,00	0,00	0,00	0,00
MANNAN	kg/hr	0,00	0,00	0,00	0,00	0,00	0,00	0,00	0,00	0,00	0,00	0,00	0,00	0,00	0,00	0,00
GALACTAN	kg/hr	0,00	0,00	0,00	0,00	0,00	0,00	0,00	0,00	0,00	0,00	0,00	0,00	0,00	0,00	0,00
XYLAN	kg/hr	0,00	0,00	0,00	0,00	0,00	0,00	0,00	0,00	0,00	0,00	0,00	0,00	0,00	0,00	0,00
ARABINAN	kg/hr	0,00	0,00	0,00	0,00	0,00	0,00	0,00	0,00	0,00	0,00	0,00	0,00	0,00	0,00	0,00
LIGNIN	kg/hr	0,00	0,00	0,00	0,00	0,00	0,00	0,00	0,00	0,00	0,00	0,00	0,00	0,00	0,00	0,00
EXTRACT	kg/hr	0,00	0,00	0,00	0,00	0,00	0,00	0,00	0,00	0,00	0,00	0,00	0,00	0,00	0,00	0,00
ASH	kg/hr	0,00	0,00	0,00	0,00	0,00	0,00	0,00	0,00	0,00	0,00	0,00	0,00	0,00	0,00	0,00
1,3-BD	kg/hr	2779,33	0,00	0,00	0,00	0,00	0,00	0,00	2786,09	0,00	0,00	0,00	20,05	1,12	6,75	0,00
DIAMMON	kg/hr	0,00	0,00	0,00	0,00	0,00	0,00	0,00	0,00	0,14	3,59	0,00	0,00	0,00	0,00	0,00
GLYCEROL	kg/hr	0,00	0,00	0,00	0,00	0,00	0,00	0,01	0,00	8,68	224,99	0,00	0,00	0,00	0,00	0,00
UREA	kg/hr	0,00	0,00	0,00	0,00	0,00	0,00	0,00	0,00	2,00	51,74	0,00	0,00	0,00	0,00	0,00
SCEREVIS	kg/hr	0,00	0,00	0,00	0,00	0,00	0,00	0,00	0,00	110,85	1,63	0,00	0,00	0,00	0,00	0,00
SUCCINIC	kg/hr	0,00	0,00	0,00	0,00	0,00	0,00	0,01	0,00	1,25	32,22	0,00	0,00	0,00	0,00	0,00
ISOAMYL	kg/hr	0,00	0,00	0,00	0,00	0,00	0,00	47,86	0,00	0,00	0,00	0,00	0,00	0,00	0,00	0,01
ACETICAC	kg/hr	64,28	0,00	0,00	53,32	53,03	0,00	0,00	64,29	0,00	0,00	0,29	0,00	53,02	0,00	0,00
PROPAN	kg/hr	0,00	0,00	0,00	0,00	0,00	0,00	0,00	0,00	0,00	0,00	0,00	0,00	0,00	0,00	0,00
BUTYRIC	kg/hr	0,00	0,00	0,00	0,00	0,00	0,00	0,00	0,00	0,00	0,00	0,00	0,00	0,00	0,00	0,00
C3H6O2	kg/hr	0,00	0,00	0,00	0,00	0,00	0,00	0,00	0,00	0,00	0,00	0,00	0,00	0,00	0,00	0,00
ACETALDE	kg/hr	588,48	0,00	0,00	3598,39	3081,01	0,00	0,00	589,39	0,00	0,00	517,38	320,15	0,00	0,92	0,00
CO	kg/hr	0,44	0,00	0,00	18,65	0,55	0,00	0,00	0,55	0,00	0,00	18,10	0,55	0,00	0,11	0,00
DIETHYL	kg/hr	1146,62	0,00	0,00	82,26	74,36	0,00	0,00	1147,69	0,00	0,00	7,91	756,88	0,00	1,08	0,00
ETHYLACE	kg/hr	3608,74	0,00	0,00	117,34	114,37	0,00	0,00	3609,65	0,00	0,00	2,97	233,87	261,21	0,91	0,00
N-BUT-01	kg/hr	201,39	0,00	0,00	0,00	0,00	0,00	0,00	201,40	0,00	0,00	0,00	0,00	172,23	0,01	0,00
ETHYL-01	kg/hr	129,32	0,00	0,00	0,00	0,00	0,00	0,00	130,67	0,00	0,00	0,00	130,67	0,00	1,34	0,00
2-BUT-01	kg/hr	961,00	0,00	0,00	0,00	0,00	0,00	0,00	962,95	0,00	0,00	0,00	124,26	0,00	1,95	0,00
1:5-H-01	kg/hr	1208,78	0,00	0,00	0,00	0,00	0,00	0,00	1209,29	0,00	0,00	0,00	383,47	0,25	0,50	0,00
H2SO4	kg/hr	0,00	0,00	0,00	0,00	0,00	0,00	0,00	0,00	0,03	0,80	0,00	0,00	0,00	0,00	0,00
H2	kg/hr	0,13	0,00	0,00	177,64	0,47	0,00	0,00	0,47	0,00	0,00	177,17	0,47	0,00	0,33	0,00
DIPHENOX	kg/hr	0,00	0,00	0,00	0,00	0,00	0,00	0,00	0,00	0,00	0,00	0,00	0,00	0,00	0,00	0,00
BIPHEN	kg/hr	0,00	0,00	0,00	0,00	0,00	0,00	0,00	0,00	0,00	0,00	0,00	0,00	0,00	0,00	0,00
NANO3	kg/hr	0,00	0,00	0,00	0,00	0,00	0,00	0,00	0,00	0,00	0,00	0,00	0,00	0,00	0,00	0,00
KNO3	kg/hr	0,00	0,00	0,00	0,00	0,00	0,00	0,00	0,00	0,00	0,00	0,00	0,00	0,00	0,00	0,00

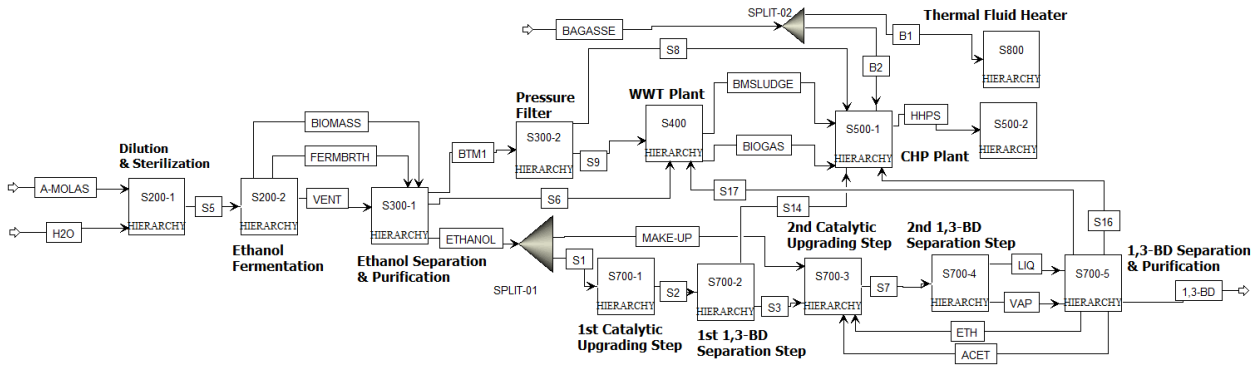

Figure 80: Scenario E, Main Flowsheet in Aspen Plus®

Table 65: Material Balances of Scenario F, Main Flowsheet

Material Balance - Scenario F																
Stream Name	**Units**	**1,3-BD**	**2GFEED**	**A-MOLASS**	**AC**	**AIR**	**BIOGAS**	**BIOMASS**	**BMSLUDGE**	**BYPASS**	**CO2EMIS**	**ETHANOL**	**FERMBROT**	**H2O**	**HHPS**	**LIQ**
Description																
From		S700-5			S700-5		S400	S200-2	S400	SPLIT-02	S200-2	S700-5	S200-2		S500-1	S700-4
To			SPLIT-02	S200-1	S700-3	S100-1	S500-1	S300-1	S500-1	S500-1	S300-1	S700-3	S300-1	S200-1	S500-2	S700-5
Stream Class		CONVEN	CONVEN	CONVEN	CONVEN	CONVEN	CONVEN	CONVEN	CONVEN	CONVEN	CONVEN	CONVEN	CONVEN	CONVEN	CONVEN	CONVEN
Total Stream																
Temperature	C	60,4	25,0	56,0	5,8	25,0	35,0	30,0	35,0	25,0	30,0	85,9	30,0	25,0	452,0	118,0
Pressure	bar	6,9	1,0	1,0	1,2	1,0	1,0	1,0	1,5	1,0	1,0	1,2	1,0	1,0	63,0	8,6
Mass Vapor Fraction		0,0	0,0	0,0	0,0	1,0	1,0	0,0	0,0	0,0	1,0	0,0	0,0	0,0	1,0	0,0
Mass Liquid Fraction		1,0	0,5	1,0	1,0	0,0	0,0	0,2	0,3	0,5	0,0	1,0	1,0	1,0	0,0	1,0
Mass Solid Fraction		0,0	0,5	0,0	0,0	0,0	0,0	0,8	0,7	0,5	0,0	0,0	0,0	0,0	0,0	0,0
Mass Enthalpy	cal/gm	406,9	-2454,5	-1976,7	-392,9	-32,1	-1891,5	-1760,8	-1350,2	-2454,5	-2147,9	-1621,0	-3478,7	-3789,5	-3025,6	-1461,1
Mass Entropy	cal/gm-K	-0,9	-1,8	-1,9	-1,1	0,0	-0,3	-3,7	-0,7	-1,8	0,0	-1,5	-2,1	-2,2	-0,7	-1,3
Mass Density	gm/cc	0,6	1,1	1,2	0,7	0,0	0,0	1,1	1,1	1,1	0,0	0,8	1,0	1,0	0,0	0,7
Average MW		53,9	30,7	66,0	56,5	28,6	28,9	23,7	41,2	30,7	43,0	41,6	19,7	18,0	18,0	37,6
Mass Flows	kg/hr	4603,4	63702,0	25433,0	1585,7	1119,4	3833,2	146,2	619,5	12702,0	9290,1	18983,2	86078,3	70000,0	171895,3	36060,0
O2	kg/hr	0,0	0,0	0,0	0,0	235,1	0,0	0,0	0,0	0,0	0,0	0,0	0,0	0,0	0,0	0,0
H2O	kg/hr	6,9	27626,0	5613,1	0,0	11,2	134,0	29,3	203,6	5508,5	157,4	3540,4	74731,1	70000,0	171895,3	8776,9
CELLULOS	kg/hr	0,0	14583,2	0,0	0,0	0,0	0,0	0,0	9,9	2907,8	0,0	0,0	0,0	0,0	0,0	0,0
MANNAN	kg/hr	0,0	56,1	0,0	0,0	0,0	0,0	0,0	0,1	11,2	0,0	0,0	0,0	0,0	0,0	0,0
GALACTAN	kg/hr	0,0	291,9	0,0	0,0	0,0	0,0	0,0	0,8	58,2	0,0	0,0	0,0	0,0	0,0	0,0
XYLAN	kg/hr	0,0	7808,0	0,0	0,0	0,0	0,0	0,0	11,2	1556,9	0,0	0,0	0,0	0,0	0,0	0,0
ARABINAN	kg/hr	0,0	645,5	0,0	0,0	0,0	0,0	0,0	1,3	128,7	0,0	0,0	0,0	0,0	0,0	0,0
LIGNIN	kg/hr	0,0	0,0	0,0	0,0	0,0	0,0	0,0	0,0	0,0	0,0	0,0	0,0	0,0	0,0	0,0
EXTRACT	kg/hr	0,0	2615,5	0,0	0,0	0,0	0,0	0,0	1,6	521,5	0,0	0,0	0,0	0,0	0,0	0,0
ASH	kg/hr	0,0	1212,5	0,0	0,0	0,0	0,0	0,0	10,9	241,8	0,0	0,0	0,0	0,0	0,0	0,0
CO2	kg/hr	0,0	0,0	0,0	0,0	0,0	2657,8	0,0	0,1	0,0	9082,5	0,0	121,9	0,0	0,0	4,8
ETHANOL	kg/hr	0,0	0,0	0,0	0,0	0,0	0,0	3,7	0,0	0,0	49,3	7611,7	9455,7	0,0	0,0	8996,8
GLYCEROL	kg/hr	0,0	0,0	0,0	0,0	0,0	0,0	0,1	0,2	0,0	0,0	0,0	240,3	0,0	0,0	0,0
FRUCTOSE	kg/hr	0,0	0,0	2988,4	0,0	0,0	0,0	0,4	0,0	0,0	0,0	0,0	977,7	0,0	0,0	0,0
SUCROSE	kg/hr	0,0	0,0	13843,2	0,0	0,0	0,0	0,0	0,0	0,0	0,0	0,0	0,0	0,0	0,0	0,0
GLUCOSE	kg/hr	0,0	0,0	2988,4	0,0	0,0	0,0	0,2	0,0	0,0	0,0	0,0	410,8	0,0	0,0	0,0
SCEREVIS	kg/hr	0,0	8863,3	0,0	0,0	0,0	0,0	112,5	0,0	1767,3	0,0	0,0	0,0	0,0	0,0	0,0
XYLOSE	kg/hr	0,0	0,0	0,0	0,0	0,0	0,0	0,0	0,0	0,0	0,0	0,0	0,0	0,0	0,0	0,0
ARABINOS	kg/hr	0,0	0,0	0,0	0,0	0,0	0,0	0,0	0,0	0,0	0,0	0,0	0,0	0,0	0,0	0,0
NH3	kg/hr	2,2	0,0	0,0	1,9	0,0	0,0	0,0	0,0	0,0	0,1	0,2	2,0	0,0	0,0	12,2
PROPAN	kg/hr	0,0	0,0	0,0	0,0	0,0	0,0	0,0	0,0	0,0	0,0	0,0	0,0	0,0	0,0	0,0
BUTYRIC	kg/hr	0,0	0,0	0,0	0,0	0,0	0,0	0,0	0,0	0,0	0,0	0,0	0,0	0,0	0,0	0,0
CH4	kg/hr	0,0	0,0	0,0	0,0	0,0	1040,4	0,0	0,0	0,0	0,0	0,0	0,0	0,0	0,0	0,1
H2	kg/hr	0,0	0,0	0,0	0,0	0,0	0,0	0,0	0,0	0,0	0,0	0,0	0,0	0,0	0,0	0,1
BMSLUDGE	kg/hr	0,0	0,0	0,0	0,0	0,0	0,0	0,0	378,8	0,0	0,0	0,0	0,0	0,0	0,0	0,0
ISOVALER	kg/hr	0,0	0,0	0,0	0,0	0,0	0,0	0,0	0,1	0,0	0,0	0,0	0,0	0,0	0,0	0,0
C3H6O2	kg/hr	0,0	0,0	0,0	0,0	0,0	0,1	0,0	0,0	0,0	0,0	0,0	0,0	0,0	0,0	0,0
1,3-BD	kg/hr	4592,0	0,0	0,0	30,6	0,0	0,1	0,0	0,0	0,0	0,0	1,7	0,0	0,0	0,0	4660,7
DIAMMON	kg/hr	0,0	0,0	0,0	0,0	0,0	0,0	0,0	0,0	0,0	0,0	0,0	3,7	0,0	0,0	0,0
SUCCINIC	kg/hr	0,0	0,0	0,0	0,0	0,0	0,0	0,0	0,0	0,0	0,0	0,0	33,5	0,0	0,0	0,0
ISOAMYL	kg/hr	0,0	0,0	0,0	0,0	0,0	0,0	0,0	0,0	0,0	0,8	105,3	47,0	0,0	0,0	158,9
ACETICAC	kg/hr	0,0	0,0	0,0	0,0	0,0	0,0	0,0	0,0	0,0	0,0	19,9	0,0	0,0	0,0	111,6
ACETALDE	kg/hr	0,0	0,0	0,0	86,3	0,0	0,0	0,0	0,0	0,0	0,0	175,8	0,0	0,0	0,0	971,8
CO	kg/hr	0,0	0,0	0,0	0,0	0,0	0,0	0,0	0,0	0,0	0,0	0,0	0,0	0,0	0,0	0,5
CIETHYL	kg/hr	0,0	0,0	0,0	1,2	0,0	0,0	0,0	0,0	0,0	0,0	723,9	0,0	0,0	0,0	2032,3
ETHYLACE	kg/hr	0,0	0,0	0,0	0,0	0,0	0,6	0,0	0,3	0,0	0,0	4945,0	0,0	0,0	0,0	5502,9
N-BUT-02	kg/hr	0,0	0,0	0,0	0,0	0,0	0,1	0,0	0,3	0,0	0,0	49,9	0,0	0,0	0,0	339,9
ETHYLENE	kg/hr	1,6	0,0	0,0	0,0	0,0	0,0	0,0	0,0	0,0	0,0	0,0	0,0	0,0	0,0	213,3
2-BUT-01	kg/hr	0,0	0,0	0,0	1147,8	0,0	0,0	0,0	0,0	0,0	0,0	145,7	0,0	0,0	0,0	1572,1
1:5-H-01	kg/hr	0,0	0,0	0,0	0,0	0,0	0,0	0,0	0,0	0,0	0,0	1663,3	0,0	0,0	0,0	2380,4
N2	kg/hr	0,0	0,0	0,0	0,0	873,1	0,0	0,0	0,0	0,0	0,0	0,0	0,0	0,0	0,0	0,0
S	kg/hr	0,0	0,0	0,0	0,0	0,0	0,0	0,0	0,0	0,0	0,0	0,0	0,0	0,0	0,0	0,0
SO2	kg/hr	0,6	0,0	0,0	318,0	0,0	0,0	0,0	0,0	0,0	0,0	0,6	0,0	0,0	0,0	324,7
CELLOBIO	kg/hr	0,0	0,0	0,0	0,0	0,0	0,0	0,0	0,0	0,0	0,0	0,0	0,0	0,0	0,0	0,0
GALACTOS	kg/hr	0,0	0,0	0,0	0,0	0,0	0,0	0,0	0,1	0,0	0,0	0,0	0,0	0,0	0,0	0,0
MANNOSE	kg/hr	0,0	0,0	0,0	0,0	0,0	0,0	0,0	0,0	0,0	0,0	0,0	0,0	0,0	0,0	0,0
FURFURAL	kg/hr	0,0	0,0	0,0	0,0	0,0	0,0	0,0	0,1	0,0	0,0	0,0	0,0	0,0	0,0	0,0
H2SO4	kg/hr	0,0	0,0	0,0	0,0	0,0	0,0	0,0	0,0	0,0	0,0	0,0	0,8	0,0	0,0	0,0
UREA	kg/hr	0,0	0,0	0,0	0,0	0,0	0,0	0,0	0,0	0,0	0,0	0,0	53,7	0,0	0,0	0,0
NANO3	kg/hr	0,0	0,0	0,0	0,0	0,0	0,0	0,0	0,0	0,0	0,0	0,0	0,0	0,0	0,0	0,0
KNO3	kg/hr	0,0	0,0	0,0	0,0	0,0	0,0	0,0	0,0	0,0	0,0	0,0	0,0	0,0	0,0	0,0

Material Balance - Scenario F										
Stream Name	**Units**	**MAKE-UP**	**S1**	**S2**	**S3**	**S4**	**S5**	**S6**	**S7**	**S8**
Description										
From		SPLIT	S100-2	S200-3	S300-1	SPLIT-02	S200-1	S100-2	S300-1	S300-2
To		S700-3	S200-3	S200-4	S300-2	S100-2	S200-2	S200-4	S400	S400
Stream Class		CONVEN	CONVEN	CONVEN	CONVEN	CONVEN	CONVEN	CONVEN	CONVEN	CONVEN
Total Stream										
Temperature	C	97,9	126,4	30,0	124,6	25,0	35,9	60,0	113,8	82,4
Pressure	bar	1,6	2,5	1,5	2,3	1,0	1,0	1,5	1,6	3,0
Mass Vapor Fraction		1,0	0,0	0,0	0,0	0,0	0,0	0,0	0,0	0,0
Mass Liquid Fraction		0,0	1,0	1,0	1,0	0,5	1,0	0,8	1,0	1,0
Mass Solid Fraction		0,0	0,0	0,0	0,0	0,5	0,0	0,2	0,0	0,0
Mass Enthalpy	cal/gm	-1320,5	-3094,0	-3161,9	-3508,0	-2454,5	-3301,1	-3232,2	-3678,8	-3655,7
Mass Entropy	cal/gm-K	-1,0	-2,3	-2,6	-1,9	-1,8	-2,1	-2,1	-1,9	-2,0
Mass Density	gm/cc	0,0	1,1	1,1	0,9	1,1	1,0	1,1	0,9	1,0
Average MW		41,9	23,9	23,9	19,0	30,7	22,3	21,6	18,1	18,6
Mass Flows	kg/hr	1756,8	2632,1	2671,3	194008,2	43800,0	95433,0	107427,5	22272,0	178296,8
O2	kg/hr	0,0	0,0	0,0	0,0	0,0	0,0	0,0	0,0	0,0
H2O	kg/hr	113,9	1886,1	1890,7	178483,8	18995,0	75613,1	82620,7	22137,6	171826,4
CELLULOS	kg/hr	0,0	0,0	0,0	759,6	10027,0	0,0	8631,3	0,0	11,0
MANNAN	kg/hr	0,0	0,0	0,0	11,1	38,6	0,0	11,1	0,0	0,2
GALACTAN	kg/hr	0,0	0,0	0,0	57,6	200,7	0,0	57,6	0,0	0,8
XYLAN	kg/hr	0,0	0,0	0,0	859,0	5368,6	0,0	859,0	0,0	12,5
ARABINAN	kg/hr	0,0	0,0	0,0	99,4	443,8	0,0	99,4	0,0	1,4
LIGNIN	kg/hr	0,0	0,0	0,0	0,0	0,0	0,0	0,0	0,0	0,0
EXTRACT	kg/hr	0,0	149,6	149,6	1798,4	1798,4	0,0	1648,8	0,0	1731,3
ASH	kg/hr	0,0	0,0	0,0	833,7	833,7	0,0	833,7	0,0	12,1
CO2	kg/hr	3,7	0,0	1,4	0,0	0,0	0,0	0,0	0,0	0,0
ETHANOL	kg/hr	1624,9	0,0	0,0	0,0	0,0	0,0	0,0	0,0	0,0
GLYCEROL	kg/hr	0,0	0,0	0,0	240,4	0,0	0,0	0,0	0,0	231,4
FRUCTOSE	kg/hr	0,0	0,0	0,0	977,2	0,0	2988,4	0,0	0,9	940,8
SUCROSE	kg/hr	0,0	0,0	0,0	0,0	0,0	13843,2	0,0	0,0	0,0
GLUCOSE	kg/hr	0,0	64,5	43,9	1232,6	0,0	2988,4	710,9	0,0	1186,7
SCEREVIS	kg/hr	0,0	0,0	16,5	6317,7	6094,2	0,0	6094,2	0,0	91,6
XYLOSE	kg/hr	0,0	410,6	410,6	945,1	0,0	0,0	4524,8	0,0	909,9
ARABINOS	kg/hr	0,0	32,6	32,6	391,3	0,0	0,0	358,8	0,0	376,7
NH3	kg/hr	1,5	0,0	15,7	0,0	0,0	0,0	0,0	0,0	0,0
PROPAN	kg/hr	0,0	0,0	0,0	0,0	0,0	0,0	0,0	0,0	0,0
BUTYRIC	kg/hr	0,0	0,0	0,0	0,0	0,0	0,0	0,0	0,0	0,0
CH4	kg/hr	0,0	0,0	0,0	0,0	0,0	0,0	0,0	0,0	0,0
H2	kg/hr	0,0	0,0	0,0	0,0	0,0	0,0	0,0	0,0	0,0
BMSLUDGE	kg/hr	0,0	0,0	0,0	0,0	0,0	0,0	0,0	0,0	0,0
ISOVALER	kg/hr	0,0	0,0	0,0	0,0	0,0	0,0	0,0	0,0	0,0
C3H6O2	kg/hr	0,0	0,0	0,0	0,0	0,0	0,0	0,0	0,0	0,0
1,3-BD	kg/hr	0,0	0,0	0,0	0,0	0,0	0,0	0,0	0,0	0,0
DIAMMON	kg/hr	0,0	0,0	21,7	25,4	0,0	0,0	0,0	0,0	24,5
SUCCINIC	kg/hr	0,0	0,0	0,0	33,5	0,0	0,0	0,0	0,0	32,2
ISOAMYL	kg/hr	4,9	0,0	0,0	0,0	0,0	0,0	0,0	0,0	0,0
ACETICAC	kg/hr	0,0	50,5	50,5	582,0	0,0	0,0	556,1	24,6	560,3
ACETALDE	kg/hr	0,0	0,0	0,0	0,0	0,0	0,0	0,0	0,0	0,0
CO	kg/hr	0,0	0,0	0,0	0,0	0,0	0,0	0,0	0,0	0,0
CIETHYL	kg/hr	0,0	0,0	0,0	0,0	0,0	0,0	0,0	0,0	0,0
ETHYLACE	kg/hr	0,0	0,0	0,0	0,0	0,0	0,0	0,0	0,0	0,0
N-BUT-02	kg/hr	0,0	0,0	0,0	0,0	0,0	0,0	0,0	0,0	0,0
ETHYLENE	kg/hr	0,0	0,0	0,0	0,0	0,0	0,0	0,0	0,0	0,0
2-BUT-01	kg/hr	0,0	0,0	0,0	0,0	0,0	0,0	0,0	0,0	0,0
1:5-H-01	kg/hr	0,0	0,0	0,0	0,0	0,0	0,0	0,0	0,0	0,0
N2	kg/hr	0,0	0,0	0,0	0,0	0,0	0,0	0,1	0,0	0,0
S	kg/hr	0,0	0,0	0,0	0,0	0,0	0,0	0,0	0,0	0,0
SO2	kg/hr	7,9	7,5	7,5	0,0	0,0	0,0	82,9	0,0	0,0
CELLOBIO	kg/hr	0,0	5,3	5,3	109,3	0,0	0,0	58,2	0,0	105,3
GALACTOS	kg/hr	0,0	13,2	13,2	159,0	0,0	0,0	145,8	0,0	153,1
MANNOSE	kg/hr	0,0	2,5	2,5	30,6	0,0	0,0	28,0	0,0	29,4
FURFURAL	kg/hr	0,0	9,6	9,6	7,4	0,0	0,0	106,0	108,2	7,1
H2SO4	kg/hr	0,0	0,0	0,0	1,0	0,0	0,0	0,2	0,0	1,0
UREA	kg/hr	0,0	0,0	0,0	53,1	0,0	0,0	0,0	0,6	51,1
NANO3	kg/hr	0,0	0,0	0,0	0,0	0,0	0,0	0,0	0,0	0,0
KNO3	kg/hr	0,0	0,0	0,0	0,0	0,0	0,0	0,0	0,0	0,0

Material Balance - Scenario F																	
Stream Name	**Units**	**S9**	**S10**	**S11**	**S12**	**S13**	**S14**	**S15**	**S16**	**S17**	**S23**	**S30**	**S31**	**SO2**	**SULPHUR**	**THERM**	**VAP**
Description																	
From		S300-2	S200-4	S200-4	S200-3	S300-1	S700-1	SPLIT	S700-2	S700-3	S700-5	S700-5	S700-2	S100-1		SPLIT-02	S700-4
To		S500-1	S300-1	S300-1	S300-1	SPLIT	S700-2	S700-1	S700-3	S700-4	S500-1	S400	S500-1	S100-2	S100-1	S800	S700-5
Stream Class		CONVEN	CONVEN	CONVEN	CONVEN	CONVEN	CONVEN	CONVEN	CONVEN	CONVEN	CONVEN	CONVEN	CONVEN	CONVEN	CONVEN	CONVEN	CONVEN
Total Stream																	
Temperature	C	66,4	51,6	51,6		97,9	66,7	97,9	56,8	142,4	28,1	105,4	56,8	195,0	25,0	25,0	93,3
Pressure	bar	1,0	1,0	1,0	1,0	1,6	2,2	1,6	10,7	6,4	1,2	1,2	10,7	1,0	1,0	1,0	9,2
Mass Vapor Fraction		0,0	0,0	1,0		1,0	0,6	1,0	0,0	0,5	0,1	0,0	1,0	1,0	0,0	0,0	0,9
Mass Liquid Fraction		0,0	0,9	0,0		0,0	0,4	0,0	1,0	0,5	0,9	1,0	0,0	0,0	1,0	0,5	0,1
Mass Solid Fraction		1,0	0,1	0,0		0,0	0,0	0,0	0,0	0,0	0,0	0,0	0,0	0,0	0,0	0,5	0,0
Mass Enthalpy	cal/gm	-1442,3	-3430,2	-2182,2		-1320,5	-1288,9	-1320,5	-1431,7	-1353,4	-796,9	-3379,3	-830,2	-364,7	1959,8	-2454,5	-220,0
Mass Entropy	cal/gm-K	-3,0	-2,1	0,0		-1,0	-1,1	-1,0	-1,4	-1,1	-1,3	-1,8	-0,8	0,1	1,6	-1,8	-0,7
Mass Density	gm/cc	1,2	1,0	0,0		0,0	0,0	0,0	0,8	0,0	0,0	0,2	0,0	0,0	2,1	1,1	0,0
Average MW		32,5	19,7	40,7		41,9	29,7	41,9	41,3	37,6	55,4	20,0	8,8	34,7	32,1	30,7	39,6
Mass Flows	kg/hr	9149,7	139913,9	6456,4	0,0	17195,1	15438,2	15438,2	13808,5	36136,4	4930,0	6034,1	1629,7	1350,6	235,5	7200,0	76,4
O2	kg/hr	0,0	0,0	0,0	0,0	0,0	0,0	0,0	0,0	0,0	0,0	0,0	0,0	0,0	0,0	0,0	0,0
H2O	kg/hr	119,5	119558,2	370,8	0,0	1115,1	987,2	1001,2	978,1	8778,6	0,0	5231,3	9,2	6,9	0,0	3122,5	1,7
CELLULOS	kg/hr	748,5	759,6	0,0	0,0	0,0	0,0	0,0	0,0	0,0	0,0	0,0	0,0	0,0	0,0	1648,3	0,0
MANNAN	kg/hr	10,9	11,1	0,0	0,0	0,0	0,0	0,0	0,0	0,0	0,0	0,0	0,0	0,0	0,0	6,3	0,0
GALACTAN	kg/hr	56,8	57,6	0,0	0,0	0,0	0,0	0,0	0,0	0,0	0,0	0,0	0,0	0,0	0,0	33,0	0,0
XYLAN	kg/hr	846,5	859,0	0,0	0,0	0,0	0,0	0,0	0,0	0,0	0,0	0,0	0,0	0,0	0,0	882,5	0,0
ARABINAN	kg/hr	98,0	99,4	0,0	0,0	0,0	0,0	0,0	0,0	0,0	0,0	0,0	0,0	0,0	0,0	73,0	0,0
LIGNIN	kg/hr	0,0	0,0	0,0	0,0	0,0	0,0	0,0	0,0	0,0	0,0	0,0	0,0	0,0	0,0	0,0	0,0
EXTRACT	kg/hr	67,1	1798,4	0,0	0,0	0,0	0,0	0,0	0,0	0,0	0,0	0,0	0,0	0,0	0,0	295,6	0,0
ASH	kg/hr	821,6	833,7	0,0	0,0	0,0	0,0	0,0	0,0	0,0	0,0	0,0	0,0	0,0	0,0	137,0	0,0
CO2	kg/hr	0,0	96,1	6022,3	0,0	36,7	84,1	32,9	4,0	7,7	7,7	0,0	80,1	0,0	0,0	0,0	2,9
ETHANOL	kg/hr	0,0	6347,6	46,9	0,0	15903,5	7139,3	14278,6	6980,8	9002,8	1254,5	136,5	158,5	0,0	0,0	0,0	6,0
GLYCEROL	kg/hr	8,9	0,0	0,0	0,0	0,0	0,0	0,0	0,0	0,0	0,0	0,0	0,0	0,0	0,0	0,0	0,0
FRUCTOSE	kg/hr	35,1	0,0	0,0	0,0	0,0	0,0	0,0	0,0	0,0	0,0	0,0	0,0	0,0	0,0	0,0	0,0
SUCROSE	kg/hr	0,0	0,0	0,0	0,0	0,0	0,0	0,0	0,0	0,0	0,0	0,0	0,0	0,0	0,0	0,0	0,0
GLUCOSE	kg/hr	46,0	821,7	0,0	0,0	0,0	0,0	0,0	0,0	0,0	0,0	0,0	0,0	0,0	0,0	0,0	0,0
SCEREVIS	kg/hr	6226,1	6205,2	0,0	0,0	0,0	0,0	0,0	0,0	0,0	0,0	0,0	0,0	0,0	0,0	1001,8	0,0
XYLOSE	kg/hr	35,3	945,1	0,0	0,0	0,0	0,0	0,0	0,0	0,0	0,0	0,0	0,0	0,0	0,0	0,0	0,0
ARABINOS	kg/hr	14,6	391,4	0,0	0,0	0,0	0,0	0,0	0,0	0,0	0,0	0,0	0,0	0,0	0,0	0,0	0,0
NH3	kg/hr	0,0	12,1	0,7	0,0	14,8	13,3	13,3	8,5	12,3	7,3	0,7	4,7	0,0	0,0	0,0	0,1
PROPAN	kg/hr	0,0	0,0	0,0	0,0	0,0	0,0	0,0	0,0	0,0	0,0	0,0	0,0	0,0	0,0	0,0	0,0
BUTYRIC	kg/hr	0,0	0,0	0,0	0,0	0,0	0,0	0,0	0,0	0,0	0,0	0,0	0,0	0,0	0,0	0,0	0,0
CH4	kg/hr	0,0	0,0	0,0	0,0	0,0	37,3	0,0	0,3	0,3	0,3	0,0	37,0	0,0	0,0	0,0	0,3
H2	kg/hr	0,0	0,0	0,0	0,0	0,0	310,1	0,0	0,8	0,8	0,8	0,0	309,2	0,0	0,0	0,0	0,7
BMSLUDGE	kg/hr	0,0	0,0	0,0	0,0	0,0	0,0	0,0	0,0	0,0	0,0	0,0	0,0	0,0	0,0	0,0	0,0
ISOVALER	kg/hr	0,0	0,0	0,0	0,0	0,0	0,0	0,0	0,0	0,0	0,0	0,0	0,0	0,0	0,0	0,0	0,0
C3H6O2	kg/hr	0,0	0,0	0,0	0,0	0,0	0,0	0,0	0,0	0,0	0,0	0,0	0,0	0,0	0,0	0,0	0,0
1,3-BD	kg/hr	0,0	0,0	0,0	0,0	0,0	0,0	0,0	0,0	4691,8	65,6	1,9	0,0	0,0	0,0	0,0	31,0
DIAMMON	kg/hr	0,9	21,7	0,0	0,0	0,0	0,0	0,0	0,0	0,0	0,0	0,0	0,0	0,0	0,0	0,0	0,0
SUCCINIC	kg/hr	1,2	0,0	0,0	0,0	0,0	0,0	0,0	0,0	0,0	0,0	0,0	0,0	0,0	0,0	0,0	0,0
ISOAMYL	kg/hr	0,0	0,0	0,0	0,0	47,8	42,9	42,9	40,8	159,0	53,8	0,0	2,1	0,0	0,0	0,0	0,2
ACETICAC	kg/hr	0,6	605,4	1,2	0,0	0,0	93,1	0,0	92,5	111,6	0,0	91,7	0,5	0,0	0,0	0,0	0,0
ACETALDE	kg/hr	0,0	0,0	0,0	0,0	0,0	6280,8	0,0	5327,7	975,8	713,8	0,0	953,1	0,0	0,0	0,0	4,0
CO	kg/hr	0,0	0,0	0,0	0,0	0,0	32,6	0,0	0,9	0,9	0,9	0,0	31,6	0,0	0,0	0,0	0,4
CIETHYL	kg/hr	0,0	0,0	0,0	0,0	0,0	143,6	0,0	129,0	2037,2	1312,1	0,0	14,6	0,0	0,0	0,0	4,8
ETHYLACE	kg/hr	0,0	0,0	0,0	0,0	0,0	204,8	0,0	199,3	5506,0	279,4	281,6	5,6	0,0	0,0	0,0	3,0
N-BUT-02	kg/hr	0,0	0,0	0,0	0,0	0,0	0,0	0,0	0,0	339,9	0,0	290,0	0,0	0,0	0,0	0,0	0,0
ETHYLENE	kg/hr	0,0	0,0	0,0	0,0	0,0	0,0	0,0	0,0	219,8	218,1	0,1	0,0	0,0	0,0	0,0	6,5
2-BUT-01	kg/hr	0,0	0,0	0,0	0,0	0,0	0,0	0,0	0,0	1580,7	287,3	0,0	0,0	0,0	0,0	0,0	8,6
1:5-H-01	kg/hr	0,0	0,0	0,0	0,0	0,0	0,0	0,0	0,0	2382,7	719,2	0,3	0,0	0,0	0,0	0,0	2,3
N2	kg/hr	0,0	0,0	0,1	0,0	0,0	0,0	0,0	0,0	0,0	0,0	0,0	0,0	873,1	0,0	0,0	0,0
S	kg/hr	0,0	0,0	0,0	0,0	0,0	0,0	0,0	0,0	0,0	0,0	0,0	0,0	0,0	235,5	0,0	0,0
SO2	kg/hr	0,0	76,1	14,4	0,0	77,2	69,3	69,3	45,9	328,5	9,2	0,0	23,5	470,6	0,0	0,0	3,8
CELLOBIO	kg/hr	4,1	109,3	0,0	0,0	0,0	0,0	0,0	0,0	0,0	0,0	0,0	0,0	0,0	0,0	0,0	0,0
GALACTOS	kg/hr	5,9	159,0	0,0	0,0	0,0	0,0	0,0	0,0	0,0	0,0	0,0	0,0	0,0	0,0	0,0	0,0
MANNOSE	kg/hr	1,1	30,6	0,0	0,0	0,0	0,0	0,0	0,0	0,0	0,0	0,0	0,0	0,0	0,0	0,0	0,0
FURFURAL	kg/hr	0,0	115,6	0,0	0,0	0,0	0,0	0,0	0,0	0,0	0,0	0,0	0,0	0,0	0,0	0,0	0,0
H2SO4	kg/hr	0,0	0,2	0,0	0,0	0,0	0,0	0,0	0,0	0,0	0,0	0,0	0,0	0,0	0,0	0,0	0,0
UREA	kg/hr	0,9	0,0	0,0	0,0	0,0	0,0	0,0	0,0	0,0	0,0	0,0	0,0	0,0	0,0	0,0	0,0
NANO3	kg/hr	0,0	0,0	0,0	0,0	0,0	0,0	0,0	0,0	0,0	0,0	0,0	0,0	0,0	0,0	0,0	0,0
KNO3	kg/hr	0,0	0,0	0,0	0,0	0,0	0,0	0,0	0,0	0,0	0,0	0,0	0,0	0,0	0,0	0,0	0,0

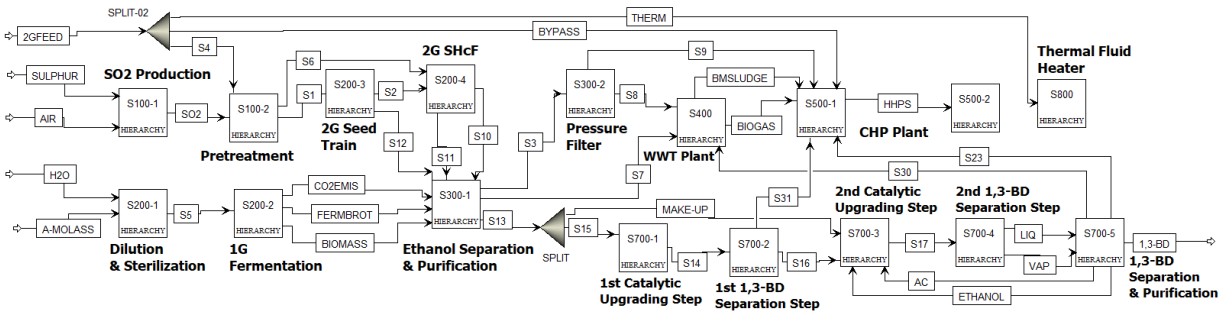

Figure 81: Scenario F, Main Flowsheet in Aspen Plus®

Table 66: Material Balances of Scenario G, Main Flowsheet

Material Balances - Scenario G														
Stream Name	**Units**	**A-MOLASS**	**FERMBRTH**	**H2O**	**MED1**	**MED2**	**MEDIUM**	**MOLAS1**	**MOLAS2**	**PHB**	**S3**	**S4**	**S5**	**S6**
Description														
From			S200-4		SPLIT-02	SPLIT-02		SPLIT	SPLIT	S300	S200-3	S200-2	S300	S200-1
To		S200-1	S300	S200-1	S200-3	S200-4	S200-2	S200-3	S200-4		S200-4	SPLIT-02	S400	SPLIT
Stream Class		CONVEN	CONVEN	CONVEN	CONVEN	CONVEN	CONVEN	CONVEN	CONVEN	CONVEN	CONVEN	CONVEN	CONVEN	CONVEN
Total Stream														
Temperature	C	56,00	37,01	25,00	121,00	121,00	25,00	55,00	55,00	100,00	37,01	121,00	37,01	55,00
Pressure	bar	1,00	1,52	1,01	1,01	1,01	1,01	1,01	1,01	1,01	1,52	1,01	1,01	1,01
Mass Vapor Fraction		0,00	0,00	0,00	0,00	0,00	0,00	0,00	0,00	0,00	0,00	0,00	0,00	0,00
Mass Liquid Fraction		1,00	0,96	1,00	1,00	1,00	1,00	1,00	1,00	0,01	0,96	1,00	0,99	1,00
Mass Solid Fraction		0,00	0,04	0,00	0,00	0,00	0,00	0,00	0,00	0,99	0,04	0,00	0,01	0,00
Mass Enthalpy	cal/gm	-1961,86	-3394,44	-3789,48	-660,21	-660,21	-674,31	-3352,35	-3352,35	60,07	-3406,46	-660,21	-3608,01	-3352,35
Mass Entropy	cal/gm-K	-1,83	-2,07	-2,16	0,63	0,63	0,56	-2,27	-2,27	0,23	-2,08	0,63	-2,12	-2,27
Mass Density	gm/cc	1,22	1,03	1,00	1,46	1,46	1,73	1,03	1,03	1,10	1,03	1,46	1,02	1,03
Average MW		66,03	20,45	18,02	227,32	227,32	227,32	21,67	21,67	84,46	20,40	227,32	19,15	21,67
Mass Flows	kg/hr	25433,00	102516,25	84000,00	97,71	909,50	7,52	10954,84	98593,52	3073,57	10716,25	1007,21	171205,76	109548,36
WATER	kg/hr	5613,06	87237,79	84000,00	0,00	0,00	0,00	8899,99	80099,87	15,70	9154,61	0,00	158348,47	88999,86
GLUCOSE	kg/hr	2988,38	3443,37	0,00	0,00	0,00	0,00	1027,43	9246,83	0,00	367,95	0,00	3443,37	10274,25
SUCROSE	kg/hr	13843,18	0,00	0,00	0,00	0,00	0,00	0,00	0,00	0,00	0,00	0,00	0,00	0,00
FRUCTOSE	kg/hr	2988,38	3610,50	0,00	0,00	0,00	0,00	1027,43	9246,83	0,00	385,14	0,00	3610,50	10274,25
O2	kg/hr	0,00	0,52	0,00	0,00	0,00	0,00	0,00	0,00	0,00	0,02	0,00	0,52	0,00
CH4	kg/hr	0,00	0,00	0,00	0,00	0,00	0,00	0,00	0,00	0,00	0,00	0,00	0,00	0,00
H2	kg/hr	0,00	0,00	0,00	0,00	0,00	0,00	0,00	0,00	0,00	0,00	0,00	0,00	0,00
CO2	kg/hr	0,00	2,25	0,00	0,00	0,00	0,00	0,00	0,00	0,00	1,32	0,00	2,25	0,00
PHB	kg/hr	0,00	3184,28	0,00	0,00	0,00	0,00	0,00	0,00	3057,87	306,92	0,00	126,42	0,00
NH3	kg/hr	0,00	0,06	0,00	0,00	0,00	0,00	0,00	0,00	0,00	0,06	0,00	0,06	0,00
N2	kg/hr	0,00	1,12	0,00	0,00	0,00	0,00	0,00	0,00	0,00	0,12	0,00	1,12	0,00
E.COLI	kg/hr	0,00	795,97	0,00	0,00	0,00	0,00	0,00	0,00	0,00	76,85	0,00	795,97	0,00
ACETIC	kg/hr	0,00	3233,17	0,00	0,00	0,00	0,00	0,00	0,00	0,00	325,54	0,00	3233,17	0,00
NA2HPO4	kg/hr	0,00	623,82	0,00	60,52	563,30	4,66	0,00	0,00	0,00	60,52	623,82	623,82	0,00
KH2PO4	kg/hr	0,00	344,40	0,00	33,41	310,99	2,57	0,00	0,00	0,00	33,41	344,40	344,40	0,00
MGSO4	kg/hr	0,00	38,99	0,00	3,78	35,21	0,29	0,00	0,00	0,00	3,78	38,99	38,99	0,00
NAOH	kg/hr	0,00	0,00	0,00	0,00	0,00	0,00	0,00	0,00	0,00	0,00	0,00	636,69	0,00
BMSLUDGE	kg/hr	0,00	0,00	0,00	0,00	0,00	0,00	0,00	0,00	0,00	0,00	0,00	0,00	0,00
PROPACID	kg/hr	0,00	0,00	0,00	0,00	0,00	0,00	0,00	0,00	0,00	0,00	0,00	0,00	0,00
BUTYRICA	kg/hr	0,00	0,00	0,00	0,00	0,00	0,00	0,00	0,00	0,00	0,00	0,00	0,00	0,00
CELLULOS	kg/hr	0,00	0,00	0,00	0,00	0,00	0,00	0,00	0,00	0,00	0,00	0,00	0,00	0,00
MANNAN	kg/hr	0,00	0,00	0,00	0,00	0,00	0,00	0,00	0,00	0,00	0,00	0,00	0,00	0,00
GALACTAN	kg/hr	0,00	0,00	0,00	0,00	0,00	0,00	0,00	0,00	0,00	0,00	0,00	0,00	0,00
XYLAN	kg/hr	0,00	0,00	0,00	0,00	0,00	0,00	0,00	0,00	0,00	0,00	0,00	0,00	0,00
ARABINAN	kg/hr	0,00	0,00	0,00	0,00	0,00	0,00	0,00	0,00	0,00	0,00	0,00	0,00	0,00
LIGNIN	kg/hr	0,00	0,00	0,00	0,00	0,00	0,00	0,00	0,00	0,00	0,00	0,00	0,00	0,00
EXTRACT	kg/hr	0,00	0,00	0,00	0,00	0,00	0,00	0,00	0,00	0,00	0,00	0,00	0,00	0,00
ASH	kg/hr	0,00	0,00	0,00	0,00	0,00	0,00	0,00	0,00	0,00	0,00	0,00	0,00	0,00

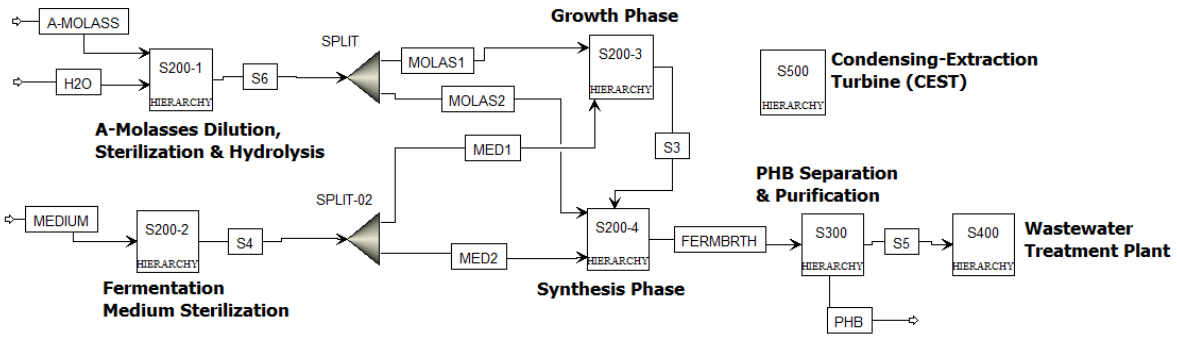

Figure 82: Scenario G, Main Flowsheet in Aspen Plus®

Table 67: Material Balances of Scenario H, Main Flowsheet

Material Balance - Scenario H													
Stream Name	**Units**	**2GFEED**	**A-MOLASS**	**BIOGAS**	**BMSLUDGE**	**EXCESS**	**H2O**	**HHPS**	**HYDROL**	**MED1**	**MED2**	**MEDIUM**	**MOLAS1**
Description													
From				S400	S400	SPLIT-03		S500-1	S100-1	SPLIT-02	SPLIT-02		SPLIT
To		S100-1	S200-1	SPLIT-03	WASTE		S200-1	S500-2	S400	S200-3	S200-4	S200-2	S200-3
Stream Class		CONVEN	CONVEN	CONVEN	CONVEN	CONVEN	CONVEN	CONVEN	CONVEN	CONVEN	CONVEN	CONVEN	CONVEN
Total Stream													
Temperature	C	25,0	56,0	34,9	34,9	34,9	25,0	452,0	87,4	121,0	121,0	25,0	51,5
Pressure	bar	1,0	1,0	1,0	1,5	1,0	1,0	63,0	1,5	1,0	1,0	1,0	1,0
Mass Vapor Fraction		0,0	0,0	1,0	0,0	1,0	0,0	1,0	0,0	0,0	0,0	0,0	0,0
Mass Liquid Fraction		0,5	1,0	0,0	0,3	0,0	1,0	0,0	1,0	1,0	1,0	1,0	1,0
Mass Solid Fraction		0,5	0,0	0,0	0,7	0,0	0,0	0,0	0,0	0,0	0,0	0,0	0,0
Mass Enthalpy	cal/gm	-2376,7	-1961,9	-1900,4	-1244,8	-1900,4	-3789,5	-3025,6	-3382,8	-332,1	-332,1	-341,1	-3341,8
Mass Entropy	cal/gm-K	-1,3	-1,8	-0,3	-0,7	-0,3	-2,2	-0,7	-2,2	0,6	0,6	0,6	-2,2
Mass Density	gm/cc	1,1	1,2	0,0	1,1	0,0	1,0	0,0	1,0	1,8	1,8	2,1	1,0
Average MW		35,7	66,0	29,2	41,5	29,2	18,0	18,0	20,9	277,9	277,9	277,9	21,9
Mass Flows	kg/hr	63702,0	25433,0	26086,8	3059,4	14347,8	64500,0	47355,4	77391,6	150,3	1375,5	7,5	16449,0
WATER	kg/hr	27626,0	5613,1	896,5	1001,8	493,1	64500,0	47355,4	64551,7	0,0	0,0	0,0	13215,1
GLUCOSE	kg/hr	0,0	2988,4	0,0	0,0	0,0	0,0	0,0	624,0	0,0	0,0	0,0	2063,0
SUCROSE	kg/hr	0,0	13843,2	0,0	0,0	0,0	0,0	0,0	0,0	0,0	0,0	0,0	0,0
FRUCTOSE	kg/hr	0,0	2988,4	0,0	0,0	0,0	0,0	0,0	0,0	0,0	0,0	0,0	1027,4
O2	kg/hr	0,0	0,0	0,8	0,0	0,4	0,0	0,0	0,0	0,0	0,0	0,0	0,0
CH4	kg/hr	0,0	0,0	6840,4	0,0	3762,2	0,0	0,0	0,0	0,0	0,0	0,0	0,0
H2	kg/hr	0,0	0,0	0,0	0,0	0,0	0,0	0,0	0,0	0,0	0,0	0,0	0,0
CO2	kg/hr	0,0	0,0	18347,2	0,6	10091,0	0,0	0,0	0,0	0,0	0,0	0,0	0,0
PHB	kg/hr	0,0	0,0	0,0	0,0	0,0	0,0	0,0	0,0	0,0	0,0	0,0	0,0
NH3	kg/hr	0,0	0,0	0,1	0,0	0,1	0,0	0,0	0,0	0,0	0,0	0,0	0,0
N2	kg/hr	0,0	0,0	1,7	0,0	0,9	0,0	0,0	0,0	0,0	0,0	0,0	0,0
E.COLI	kg/hr	0,0	0,0	0,0	0,0	0,0	0,0	0,0	0,0	0,0	0,0	0,0	0,0
ACETIC	kg/hr	0,0	0,0	0,0	0,0	0,0	0,0	0,0	2822,7	0,0	0,0	0,0	30,4
NA2HPO4	kg/hr	0,0	0,0	0,0	3,7	0,0	0,0	0,0	0,0	120,0	1098,0	6,0	0,0
KH2PO4	kg/hr	0,0	0,0	0,0	0,8	0,0	0,0	0,0	0,0	25,2	230,3	1,3	0,0
MGSO4	kg/hr	0,0	0,0	0,0	0,2	0,0	0,0	0,0	0,0	5,2	47,2	0,3	0,0
NAOH	kg/hr	0,0	0,0	0,0	2,4	0,0	0,0	0,0	0,0	0,0	0,0	0,0	0,0
BMSLUDGE	kg/hr	0,0	0,0	0,0	2039,6	0,0	0,0	0,0	0,0	0,0	0,0	0,0	0,0
PROPACID	kg/hr	0,0	0,0	0,0	0,3	0,0	0,0	0,0	0,0	0,0	0,0	0,0	0,0
BUTYRICA	kg/hr	0,0	0,0	0,0	0,0	0,0	0,0	0,0	0,0	0,0	0,0	0,0	0,0
CELLULOS	kg/hr	14583,2	0,0	0,0	0,0	0,0	0,0	0,0	0,0	0,0	0,0	0,0	0,0
MANNAN	kg/hr	56,1	0,0	0,0	0,0	0,0	0,0	0,0	0,0	0,0	0,0	0,0	0,0
GALACTAN	kg/hr	291,9	0,0	0,0	0,0	0,0	0,0	0,0	0,0	0,0	0,0	0,0	0,0
XYLAN	kg/hr	7808,0	0,0	0,0	0,0	0,0	0,0	0,0	0,0	0,0	0,0	0,0	0,0
ARABINAN	kg/hr	645,5	0,0	0,0	0,0	0,0	0,0	0,0	0,0	0,0	0,0	0,0	0,0
LIGNIN	kg/hr	8863,3	0,0	0,0	0,0	0,0	0,0	0,0	0,0	0,0	0,0	0,0	0,0
FURFURAL	kg/hr	0,0	0,0	0,1	1,4	0,1	0,0	0,0	394,7	0,0	0,0	0,0	4,2
EXTRACT	kg/hr	2615,5	0,0	0,0	7,8	0,0	0,0	0,0	2342,3	0,0	0,0	0,0	25,2
CELLOBIO	kg/hr	0,0	0,0	0,0	0,0	0,0	0,0	0,0	41,4	0,0	0,0	0,0	12,5
XYLOSE	kg/hr	0,0	0,0	0,0	0,0	0,0	0,0	0,0	5808,3	0,0	0,0	0,0	62,5
ARABINOS	kg/hr	0,0	0,0	0,0	0,1	0,0	0,0	0,0	533,4	0,0	0,0	0,0	5,7
ASH	kg/hr	1212,5	0,0	0,0	0,0	0,0	0,0	0,0	0,0	0,0	0,0	0,0	0,0
H2SO4	kg/hr	0,0	0,0	0,0	0,8	0,0	0,0	0,0	242,8	0,0	0,0	0,0	2,6
HMF	kg/hr	0,0	0,0	0,0	0,1	0,0	0,0	0,0	30,5	0,0	0,0	0,0	0,3
CITRICAC	kg/hr	0,0	0,0	0,0	0,0	0,0	0,0	0,0	0,0	0,0	0,0	0,0	0,0
DIAMMPH	kg/hr	0,0	0,0	0,0	0,0	0,0	0,0	0,0	0,0	0,0	0,0	0,0	0,0
ETHAN-01	kg/hr	0,0	0,0	0,0	0,0	0,0	0,0	0,0	0,0	0,0	0,0	0,0	0,0
ISOVA-01	kg/hr	0,0	0,0	0,0	0,0	0,0	0,0	0,0	0,0	0,0	0,0	0,0	0,0

Material Balance - Scenario H													
Stream Name	**Units**	**MOLAS2**	**PHB**	**S3**	**S4**	**S6**	**S14**	**S16**	**S19**	**S24**	**SWASTE**	**TOFERM**	**WASTEW**
Description													
From		SPLIT	S300	S200-3	S200-2	S200-1	S200-4	S300	SPLIT-03	WASTE	S100-1	S100-1	S100-1
To		S200-4		S200-4	SPLIT-02	SPLIT	S300	S400	S500-1		WASTE	SPLIT	S400
Stream Class		CONVEN	CONVEN	CONVEN	CONVEN	CONVEN	CONVEN	CONVEN	CONVEN	CONVEN	CONVEN	CONVEN	CONVEN
Total Stream													
Temperature	C	51,5	100,0	37,0	121,0	52,0	37,0	37,0	34,9	48,4	50,9	50,9	100,1
Pressure	bar	1,0	1,0	1,5	1,0	1,0	1,5	1,0	1,0	1,0	1,0	1,5	1,0
Mass Vapor Fraction		0,0	0,0	0,0	0,0	0,0	0,0	0,0	1,0	0,0	0,0	0,0	0,3
Mass Liquid Fraction		1,0	0,0	1,0	1,0	1,0	1,0	1,0	0,0	0,3	0,3	1,0	0,7
Mass Solid Fraction		0,0	1,0	0,0	0,0	0,0	0,0	0,0	0,0	0,7	0,7	0,0	0,0
Mass Enthalpy	cal/gm	-3341,8	57,0	-3388,9	-332,1	-3266,8	-3376,4	-3609,4	-1900,4	-1753,3	-1836,1	-3432,5	-3499,1
Mass Entropy	cal/gm-K	-2,2	0,2	-2,0	0,6	-2,3	-2,0	-2,1	-0,3	-1,1	-1,2	-2,0	-1,5
Mass Density	gm/cc	1,0	1,1	1,0	1,8	1,0	1,0	1,0	0,0	1,1	1,1	1,0	0,0
Average MW		21,9	84,2	20,6	277,9	22,7	20,6	19,2	29,2	46,5	47,5	21,0	18,4
Mass Flows	kg/hr	148041,2	4671,0	16086,1	1525,9	90048,4	153784,5	272047,9	11739,1	21859,2	18799,8	74441,8	12863,7
WATER	kg/hr	118936,2	27,7	13601,8	0,0	69499,9	129384,3	251508,2	403,4	6275,9	5274,1	62651,5	12453,7
GLUCOSE	kg/hr	18566,7	0,0	1085,8	0,0	10274,3	10343,1	10343,1	0,0	871,7	871,7	10355,4	0,0
SUCROSE	kg/hr	0,0	0,0	0,0	0,0	0,0	0,0	0,0	0,0	0,0	0,0	0,0	0,0
FRUCTOSE	kg/hr	9246,8	0,0	28,7	0,0	10274,3	258,8	258,8	0,0	0,0	0,0	0,0	0,0
O2	kg/hr	0,0	0,0	0,0	0,0	0,0	0,8	0,8	0,3	0,0	0,0	0,0	0,0
CH4	kg/hr	0,0	0,0	0,0	0,0	0,0	0,0	0,0	3078,2	0,0	0,0	0,0	0,0
H2	kg/hr	0,0	0,0	0,0	0,0	0,0	0,0	0,0	0,0	0,0	0,0	0,0	0,0
CO2	kg/hr	0,0	0,0	1,9	0,0	0,0	3,3	3,3	8256,2	0,6	0,0	0,0	0,0
PHB	kg/hr	0,0	4643,4	477,3	0,0	0,0	4786,0	142,6	0,0	0,0	0,0	0,0	0,0
NH3	kg/hr	0,0	0,0	0,7	0,0	0,0	0,6	0,6	0,0	0,0	0,0	0,0	0,0
N2	kg/hr	0,0	0,0	0,2	0,0	0,0	1,7	1,7	0,8	0,0	0,0	0,0	0,0
E.COLI	kg/hr	0,0	0,0	113,6	0,0	0,0	1196,5	1196,5	0,0	0,0	0,0	0,0	0,0
ACETIC	kg/hr	273,4	0,0	512,7	0,0	0,0	5152,9	5152,9	0,0	25,6	25,6	303,8	396,5
NA2HPO4	kg/hr	0,0	0,0	120,0	1218,0	0,0	1218,0	1218,0	0,0	3,7	0,0	0,0	0,0
KH2PO4	kg/hr	0,0	0,0	25,2	255,5	0,0	255,5	255,5	0,0	0,8	0,0	0,0	0,0
MGSO4	kg/hr	0,0	0,0	5,2	52,4	0,0	52,4	52,4	0,0	0,2	0,0	0,0	0,0
NAOH	kg/hr	0,0	0,0	0,0	0,0	0,0	0,0	782,9	0,0	2,4	0,0	0,0	0,0
BMSLUDGE	kg/hr	0,0	0,0	0,0	0,0	0,0	0,0	0,0	0,0	2039,6	0,0	0,0	0,0
PROPACID	kg/hr	0,0	0,0	0,0	0,0	0,0	0,0	0,0	0,0	0,3	0,0	0,0	0,0
BUTYRICA	kg/hr	0,0	0,0	0,0	0,0	0,0	0,0	0,0	0,0	0,0	0,0	0,0	0,0
CELLULOS	kg/hr	0,0	0,0	0,0	0,0	0,0	0,0	0,0	0,0	512,4	512,4	0,0	0,0
MANNAN	kg/hr	0,0	0,0	0,0	0,0	0,0	0,0	0,0	0,0	56,1	56,1	0,0	0,0
GALACTAN	kg/hr	0,0	0,0	0,0	0,0	0,0	0,0	0,0	0,0	291,9	291,9	0,0	0,0
XYLAN	kg/hr	0,0	0,0	0,0	0,0	0,0	0,0	0,0	0,0	1475,7	1475,7	0,0	0,0
ARABINAN	kg/hr	0,0	0,0	0,0	0,0	0,0	0,0	0,0	0,0	121,4	121,4	0,0	0,0
LIGNIN	kg/hr	0,0	0,0	0,0	0,0	0,0	0,0	0,0	0,0	8863,3	8863,3	0,0	0,0
FURFURAL	kg/hr	38,2	0,0	4,2	0,0	0,0	42,1	42,1	0,1	4,9	3,6	42,5	13,5
EXTRACT	kg/hr	226,9	0,0	25,2	0,0	0,0	252,1	252,1	0,0	29,0	21,2	252,1	0,0
CELLOBIO	kg/hr	112,2	0,0	12,5	0,0	0,0	124,7	124,7	0,0	10,5	10,5	124,7	0,0
XYLOSE	kg/hr	562,6	0,0	62,5	0,0	0,0	625,1	625,1	0,0	52,6	52,6	625,1	0,0
ARABINOS	kg/hr	51,7	0,0	5,7	0,0	0,0	57,4	57,4	0,0	4,9	4,8	57,4	0,0
ASH	kg/hr	0,0	0,0	0,0	0,0	0,0	0,0	0,0	0,0	1212,5	1212,5	0,0	0,0
H2SO4	kg/hr	23,5	0,0	2,6	0,0	0,0	26,1	26,1	0,0	3,0	2,2	26,1	0,0
HMF	kg/hr	3,0	0,0	0,3	0,0	0,0	3,3	3,3	0,0	0,4	0,3	3,3	0,0
CITRICAC	kg/hr	0,0	0,0	0,0	0,0	0,0	0,0	0,0	0,0	0,0	0,0	0,0	0,0
DIAMMPH	kg/hr	0,0	0,0	0,0	0,0	0,0	0,0	0,0	0,0	0,0	0,0	0,0	0,0
ETHAN-01	kg/hr	0,0	0,0	0,0	0,0	0,0	0,0	0,0	0,0	0,0	0,0	0,0	0,0
ISOVA-01	kg/hr	0,0	0,0	0,0	0,0	0,0	0,0	0,0	0,0	0,0	0,0	0,0	0,0

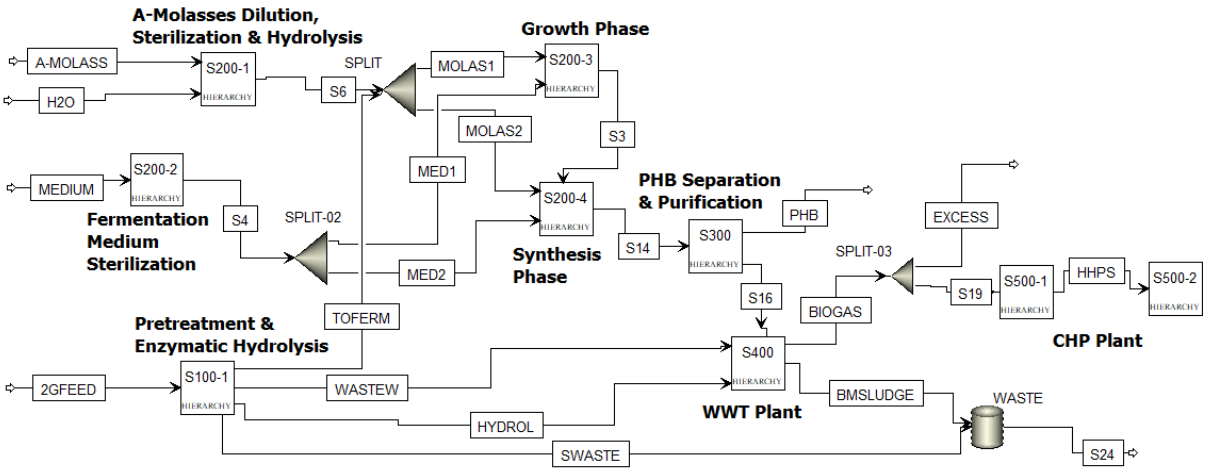

Figure 83: Scenario H, Main Flowsheet in Aspen Plus®

Table 68: Material Balances of Scenario I, Main Flowsheet

Material Balance - Scenario I																			
Stream Name	**Units**	**A-MOLASS**	**BAGASSE**	**BIOGAS**	**BIOMASS**	**BMSLDGE**	**CA**	**DILUTE**	**EFFL**	**FERM**	**FERMBRTH**	**HHPS**	**MEDIUM**	**MGSO4**	**S2**	**S3**	**S4**	**SEED**	**STMEDIUM**
Description																			
From				S400	S300	S400	S300		S300	SPLIT	S200-3	S500-1			S200-2	S200-1	S200-1,2	SPLIT	
To		SPLIT	S500-1	S500-1	S500-1	S500-1		S200-1	S400	S200-1	S300	S500-2	S200-1	S200-3	S200-3	S200-3	S200-2	S200-1,2	S200-1,2
Stream Class		CONVEN	CONVEN	CONVEN	CONVEN	CONVEN	CONVEN	CONVEN	CONVEN	CONVEN	CONVEN	CONVEN	CONVEN	CONVEN	CONVEN	CONVEN	CONVEN	CONVEN	CONVEN
Total Stream																			
Temperature	C	56,0	25,0	35,0	30,0	35,0	125,5	25,0	42,6	56,0	30,0	452,0	25,0	25,0	30,0	31,7	121,0	56,0	25,0
Pressure	bar	1,0	1,0	1,1	1,5	1,5	1,0	1,0	0,1	1,0	1,5	63,0	1,0	1,0	1,5	1,0	1,0	1,0	1,0
Mass Vapor Fraction		0,0	0,0	1,0	0,0	0,0	0,0	0,0	0,1	0,0	0,0	1,0	1,0	0,0	0,0	0,0	0,8	0,0	0,0
Mass Liquid Fraction		1,0	0,5	0,0	0,4	0,3	0,0	1,0	0,9	1,0	0,9	0,0	0,0	1,0	0,9	1,0	0,2	1,0	1,0
Mass Solid Fraction		0,0	0,5	0,0	0,6	0,7	1,0	0,0	0,0	0,0	0,1	0,0	0,0	0,0	0,1	0,0	0,0	0,0	0,0
Mass Enthalpy	cal/gm	-1961,9	-2565,4	-1895,2	-2249,2	-1259,0	-1883,1	-3789,5	-3644,9	-1961,9	-3449,7	-3025,6	-644,4	-39,2	-3464,2	-3414,4	-2915,7	-1961,9	-3778,0
Mass Entropy	cal/gm-K	-1,4	-1,4	-0,3	-3,1	-0,7	-1,2	-2,2	-1,9	-1,4	-2,0	-0,7	-1,4	1,0	-2,2	-2,0	-0,6	-1,4	-2,1
Mass Density	gm/cc	1,2	1,1	0,0	1,0	1,1	1,6	1,0	0,0	1,2	1,1	0,0	0,0	1,5	1,0	1,0	0,0	1,2	1,0
Average MW		66,0	31,6	29,2	22,6	41,0	192,1	18,0	18,7	66,0	21,3	18,0	17,0	192,4	19,7	21,1	20,9	66,0	18,1
Mass Flows	kg/hr	25433,0	11927,7	4442,2	2729,4	981,1	13042,1	97000,0	141413,3	24670,0	125909,1	57757,9	91,0	0,0	4156,7	121761,0	4185,2	763,0	3422,3
H2O	kg/hr	5613,1	6060,0	140,2	1036,6	326,8	0,0	97000,0	136038,1	5444,7	103656,2	57757,9	0,0	0,0	3594,1	102444,7	3569,7	168,4	3401,3
CO2	kg/hr	0,0	0,0	3129,2	0,0	0,2	0,0	0,0	0,1	0,0	0,1	0,0	0,0	0,0	0,1	0,0	0,0	0,0	0,0
O2	kg/hr	0,0	0,0	0,7	0,0	0,0	0,0	0,0	0,7	0,0	0,7	0,0	0,0	0,0	0,0	0,0	0,0	0,0	0,0
ACETAC	kg/hr	0,0	0,0	0,0	0,0	0,0	0,0	0,0	0,0	0,0	0,0	0,0	0,0	0,0	0,0	0,0	0,0	0,0	0,0
NH3	kg/hr	0,0	0,0	0,0	0,0	0,0	0,0	0,0	0,3	0,0	0,3	0,0	91,0	0,0	0,2	91,0	0,0	0,0	0,0
GLUCOSE	kg/hr	2988,4	0,0	0,0	0,0	0,0	0,0	0,0	0,0	2898,7	0,0	0,0	0,0	0,0	13,1	2898,7	89,7	89,7	0,0
FRUCTOSE	kg/hr	2988,4	0,0	0,0	54,1	0,0	0,0	0,0	5352,0	2898,7	5406,2	0,0	0,0	0,0	308,2	2898,7	89,7	89,7	0,0
SUCROSE	kg/hr	13843,2	0,0	0,0	0,0	0,0	0,0	0,0	0,0	13427,9	0,0	0,0	0,0	0,0	0,0	13427,9	415,3	415,3	0,0
BMSLUDGE	kg/hr	0,0	0,0	0,0	0,0	654,1	0,0	0,0	0,0	0,0	0,0	0,0	0,0	0,0	0,0	0,0	0,0	0,0	0,0
PROPACID	kg/hr	0,0	0,0	0,0	0,0	0,0	0,0	0,0	0,0	0,0	0,0	0,0	0,0	0,0	0,0	0,0	0,0	0,0	0,0
BUTYRACI	kg/hr	0,0	0,0	0,0	0,0	0,0	0,0	0,0	0,0	0,0	0,0	0,0	0,0	0,0	0,0	0,0	0,0	0,0	0,0
H2	kg/hr	0,0	0,0	0,0	0,0	0,0	0,0	0,0	0,0	0,0	0,0	0,0	0,0	0,0	0,0	0,0	0,0	0,0	0,0
CH4	kg/hr	0,0	0,0	1170,7	0,0	0,0	0,0	0,0	0,0	0,0	0,0	0,0	0,0	0,0	0,0	0,0	0,0	0,0	0,0
N2	kg/hr	0,0	0,0	1,4	0,0	0,0	0,0	0,0	1,4	0,0	1,4	0,0	0,0	0,0	0,0	0,0	0,0	0,0	0,0
MCITRICA	kg/hr	0,0	0,0	0,0	153,4	0,0	18,2	0,0	0,0	0,0	15338,1	0,0	0,0	0,0	0,0	0,0	0,0	0,0	0,0
A.NIGER	kg/hr	0,0	0,0	0,0	1485,2	0,0	0,0	0,0	0,0	0,0	1485,2	0,0	0,0	0,0	220,0	0,0	0,0	0,0	0,0
MGSO5H2O	kg/hr	0,0	0,0	0,0	0,0	0,0	0,0	0,0	0,0	0,0	0,0	0,0	0,0	0,0	0,0	0,0	0,0	0,0	0,0
MGSO4	kg/hr	0,0	0,0	0,0	0,0	0,0	0,0	0,0	0,8	0,0	0,8	0,0	0,0	0,0	0,8	0,0	0,8	0,0	0,8
TRISODCI	kg/hr	0,0	0,0	0,0	0,0	0,0	0,0	0,0	0,0	0,0	0,0	0,0	0,0	0,0	0,0	0,0	0,0	0,0	0,0
KH2PO4	kg/hr	0,0	0,0	0,0	0,2	0,0	0,0	0,0	20,0	0,0	20,2	0,0	0,0	0,0	20,2	0,0	20,2	0,0	20,2
ACITSOLI	kg/hr	0,0	0,0	0,0	0,0	0,0	13023,9	0,0	0,0	0,0	0,0	0,0	0,0	0,0	0,0	0,0	0,0	0,0	0,0
ACITLIQ	kg/hr	0,0	0,0	0,0	0,0	0,0	0,0	0,0	0,0	0,0	0,0	0,0	0,0	0,0	0,0	0,0	0,0	0,0	0,0
XYLAN	kg/hr	0,0	1170,4	0,0	0,0	0,0	0,0	0,0	0,0	0,0	0,0	0,0	0,0	0,0	0,0	0,0	0,0	0,0	0,0
ARABINAN	kg/hr	0,0	96,8	0,0	0,0	0,0	0,0	0,0	0,0	0,0	0,0	0,0	0,0	0,0	0,0	0,0	0,0	0,0	0,0
CELLULOS	kg/hr	0,0	2388,5	0,0	0,0	0,0	0,0	0,0	0,0	0,0	0,0	0,0	0,0	0,0	0,0	0,0	0,0	0,0	0,0
MANNAN	kg/hr	0,0	9,3	0,0	0,0	0,0	0,0	0,0	0,0	0,0	0,0	0,0	0,0	0,0	0,0	0,0	0,0	0,0	0,0
GALACTAN	kg/hr	0,0	43,7	0,0	0,0	0,0	0,0	0,0	0,0	0,0	0,0	0,0	0,0	0,0	0,0	0,0	0,0	0,0	0,0
EXTRACT	kg/hr	0,0	440,1	0,0	0,0	0,0	0,0	0,0	0,0	0,0	0,0	0,0	0,0	0,0	0,0	0,0	0,0	0,0	0,0
ASH	kg/hr	0,0	222,7	0,0	0,0	0,0	0,0	0,0	0,0	0,0	0,0	0,0	0,0	0,0	0,0	0,0	0,0	0,0	0,0
LIGNIN	kg/hr	0,0	1496,4	0,0	0,0	0,0	0,0	0,0	0,0	0,0	0,0	0,0	0,0	0,0	0,0	0,0	0,0	0,0	0,0
OCTANOL	kg/hr	0,0	0,0	0,0	0,0	0,0	0,0	0,0	0,0	0,0	0,0	0,0	0,0	0,0	0,0	0,0	0,0	0,0	0,0

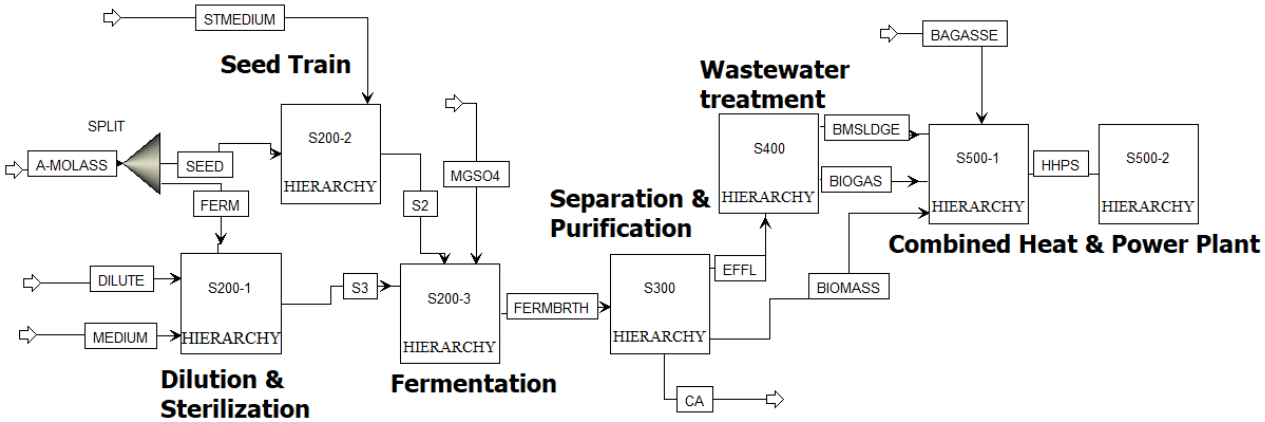

Figure 84: Scenario I, Main Flowsheet in Aspen Plus®

Table 69: Material Balances of Scenario J, Main Flowsheet

Material Balance - Scenario J														
Stream Name	**Units**	**2GFEED**	**A-MOLASS**	**AIR**	**BIOGAS**	**BIOMASS**	**BMSLDGE**	**BYPASS**	**CITRAC**	**DILUTE**	**GLUCFERM**	**GLUCSEED**	**H2O**	**HEMICELL**
Description														
From					S400	S300	S400	SPLIT-02	S300		S100-2	S100-2		S100-2
To		SPLIT-02	S200-1	S100-1	S500-1	S500-1	S500-1	S500-1		S200-1	S200-2,2	S200-2,1	S100-2	S200-4
Stream Class		CONVEN	CONVEN	CONVEN	CONVEN	CONVEN	CONVEN	CONVEN	CONVEN	CONVEN	CONVEN	CONVEN	CONVEN	CONVEN
Total Stream														
Temperature	C	25,0	56,0	25,0	35,0	29,8	35,0	25,0	125,3	25,0	50,0	50,0	25,0	78,3
Pressure	bar	1,0	1,0	1,0	1,1	1,0	1,5	1,0	1,0	1,0	1,0	1,0	1,0	1,0
Mass Vapor Fraction		0,0	0,0	1,0	1,0	0,0	0,0	0,0	0,0	0,0	0,0	0,0	0,0	0,0
Mass Liquid Fraction		0,5	1,0	0,0	0,0	0,4	0,3	0,5	0,0	1,0	1,0	1,0	1,0	1,0
Mass Solid Fraction		0,5	0,0	0,0	0,0	0,6	0,7	0,5	1,0	0,0	0,0	0,0	0,0	0,0
Mass Enthalpy	cal/gm	-2380,4	-1961,9	-32,1	-1441,4	-2606,3	-1254,8	-2380,4	-1883,1	-3789,5	-3452,5	-3452,5	-3789,5	-3594,1
Mass Entropy	cal/gm-K	-1,3	-1,4	0,0	-0,1	-4,3	-0,7	-1,3	-1,2	-2,2	-2,0	-2,0	-2,2	-2,1
Mass Density	gm/cc	1,1	1,2	0,0	0,0	1,0	1,1	1,1	1,6	1,0	1,0	1,0	1,0	1,0
Average MW		35,7	66,0	28,6	29,3	22,6	41,2	35,7	192,1	18,0	20,8	20,8	18,0	19,1
Mass Flows	kg/hr	63702,0	25433,0	2244,5	9840,5	4120,3	1407,6	33762,1	17469,8	70000,0	33162,4	6792,3	32965,7	67821,8
H2O	kg/hr	27626,0	5613,1	22,4	309,4	1577,3	466,1	14641,8	0,0	70000,0	28218,1	5779,6	32965,7	63256,6
CO2	kg/hr	0,0	0,0	0,0	5266,4	0,0	0,2	0,0	0,0	0,0	0,0	0,0	0,0	0,0
O2	kg/hr	0,0	0,0	471,3	1,1	0,0	0,0	0,0	0,0	0,0	0,0	0,0	0,0	0,0
ACETAC	kg/hr	0,0	0,0	0,0	0,0	0,5	0,0	0,0	0,0	0,0	11,1	2,3	0,0	296,4
NH3	kg/hr	0,0	0,0	0,0	0,4	0,1	0,0	0,0	0,0	0,0	0,0	0,0	0,0	0,0
GLUCOSE	kg/hr	0,0	2988,4	0,0	0,0	3,7	0,0	0,0	0,0	0,0	4730,4	968,9	0,0	374,1
FRUCTOSE	kg/hr	0,0	2988,4	0,0	0,0	71,6	0,0	0,0	0,0	0,0	0,0	0,0	0,0	0,0
SUCROSE	kg/hr	0,0	13843,2	0,0	0,0	0,0	0,0	0,0	0,0	0,0	0,0	0,0	0,0	0,0
BMSLUDGE	kg/hr	0,0	0,0	0,0	0,0	0,0	938,4	0,0	0,0	0,0	0,0	0,0	0,0	0,0
PROPACID	kg/hr	0,0	0,0	0,0	0,0	0,0	0,1	0,0	0,0	0,0	0,0	0,0	0,0	0,0
BUTYRACI	kg/hr	0,0	0,0	0,0	0,0	0,0	0,0	0,0	0,0	0,0	0,0	0,0	0,0	0,0
H2	kg/hr	0,0	0,0	0,0	0,0	0,0	0,0	0,0	0,0	0,0	0,0	0,0	0,0	0,0
CH4	kg/hr	0,0	0,0	0,0	1763,4	0,0	0,0	0,0	0,0	0,0	0,0	0,0	0,0	0,0
N2	kg/hr	0,0	0,0	1750,7	2486,5	0,0	0,0	0,0	0,0	0,0	0,0	0,0	0,0	0,0
MCITRICA	kg/hr	0,0	0,0	0,0	0,0	205,5	0,0	0,0	24,4	0,0	0,0	0,0	0,0	0,0
A.NIGER	kg/hr	0,0	0,0	0,0	0,0	1879,1	0,0	0,0	0,0	0,0	0,0	0,0	0,0	0,0
MGSO5H2O	kg/hr	0,0	0,0	0,0	0,0	0,0	0,0	0,0	0,0	0,0	0,0	0,0	0,0	0,0
MGSO4	kg/hr	0,0	0,0	0,0	0,0	0,1	0,0	0,0	0,0	0,0	0,0	0,0	0,0	0,0
TRISODCI	kg/hr	0,0	0,0	0,0	0,0	0,0	0,0	0,0	0,0	0,0	0,0	0,0	0,0	0,0
KH2PO4	kg/hr	0,0	0,0	0,0	0,0	1,9	0,3	0,0	0,0	0,0	0,0	0,0	0,0	0,0
ACITSOLI	kg/hr	0,0	0,0	0,0	0,0	0,0	0,0	0,0	17445,4	0,0	0,0	0,0	0,0	0,0
ACITLIQ	kg/hr	0,0	0,0	0,0	0,0	0,0	0,0	0,0	0,0	0,0	0,0	0,0	0,0	0,0
XYLAN	kg/hr	7808,0	0,0	0,0	0,0	0,0	0,0	4138,2	0,0	0,0	0,0	0,0	0,0	0,0
ARABINAN	kg/hr	645,5	0,0	0,0	0,0	0,0	0,0	342,1	0,0	0,0	0,0	0,0	0,0	0,0
CELLULOS	kg/hr	14583,2	0,0	0,0	0,0	0,0	0,0	7729,1	0,0	0,0	0,0	0,0	0,0	0,0
MANNAN	kg/hr	56,1	0,0	0,0	0,0	0,0	0,0	29,8	0,0	0,0	0,0	0,0	0,0	0,0
GALACTAN	kg/hr	291,9	0,0	0,0	0,0	0,0	0,0	154,7	0,0	0,0	0,0	0,0	0,0	0,0
EXTRACT	kg/hr	2615,5	0,0	0,0	0,0	12,2	2,0	1386,2	0,0	0,0	43,7	9,0	0,0	1169,6
ASH	kg/hr	1212,5	0,0	0,0	0,0	0,0	0,0	642,6	0,0	0,0	0,0	0,0	0,0	0,0
LIGNIN	kg/hr	8863,3	0,0	0,0	0,0	0,0	0,0	4697,5	0,0	0,0	0,0	0,0	0,0	0,0
SULPHUR	kg/hr	0,0	0,0	0,0	0,0	0,0	0,0	0,0	0,0	0,0	0,0	0,0	0,0	0,0
SO2	kg/hr	0,0	0,0	0,0	13,2	0,0	0,2	0,0	0,0	0,0	3,9	0,8	0,0	104,1
XYLOSE	kg/hr	0,0	0,0	0,0	0,0	1,1	0,0	0,0	0,0	0,0	88,3	18,1	0,0	2361,4
ARABINOS	kg/hr	0,0	0,0	0,0	0,0	2,2	0,0	0,0	0,0	0,0	7,8	1,6	0,0	209,5
FURFURAL	kg/hr	0,0	0,0	0,0	0,0	0,0	0,0	0,0	0,0	0,0	1,9	0,4	0,0	50,1
CACO3	kg/hr	0,0	0,0	0,0	0,0	0,0	0,0	0,0	0,0	0,0	0,0	0,0	0,0	0,0
CASO4	kg/hr	0,0	0,0	0,0	0,0	0,0	0,0	0,0	0,0	0,0	0,0	0,0	0,0	0,0
CASO3	kg/hr	0,0	0,0	0,0	0,0	0,0	0,0	0,0	0,0	0,0	0,0	0,0	0,0	0,0
CELLOB	kg/hr	0,0	0,0	0,0	0,0	0,7	0,1	0,0	0,0	0,0	57,2	11,7	0,0	0,0
Y.LIPOLY	kg/hr	0,0	0,0	0,0	0,0	363,5	0,0	0,0	0,0	0,0	0,0	0,0	0,0	0,0
XYLITOL	kg/hr	0,0	0,0	0,0	0,0	0,8	0,1	0,0	0,0	0,0	0,0	0,0	0,0	0,0
POTAS-01	kg/hr	0,0	0,0	0,0	0,0	0,0	0,0	0,0	0,0	0,0	0,0	0,0	0,0	0,0
MGSO47W	kg/hr	0,0	0,0	0,0	0,0	0,0	0,0	0,0	0,0	0,0	0,0	0,0	0,0	0,0
01-Oct-01	kg/hr	0,0	0,0	0,0	0,0	0,0	0,0	0,0	0,0	0,0	0,0	0,0	0,0	0,0
ISOVALAC	kg/hr	0,0	0,0	0,0	0,0	0,0	0,0	0,0	0,0	0,0	0,0	0,0	0,0	0,0

Material Balance - Scenario J																	
Stream Name	**Units**	**HHPS**	**MEDIUM**	**MGSO4**	**S1**	**S2**	**S3**	**S4**	**S5**	**S6**	**S7**	**S8**	**S9**	**S10**	**SOLIDS**	**STMEDIUM**	**SULPHUR**
Description																	
From		S500-1			S200-2,2	S200-2,1	S200-1	S300	S200-4	S100-2	SPLIT-02	S200-1,1	S200-4	S100-1	S100-2		
To		S500-2	S200-1	S200-2,2	S300	S200-2,2	S200-2,2	S400	S400	S400	S100-2	S200-2,1	S300	S100-2	S500-1	S200-1,1	S100-1
Stream Class		CONVEN	CONVEN	CONVEN	CONVEN	CONVEN	CONVEN	CONVEN	CONVEN	CONVEN	CONVEN	CONVEN	CONVEN	CONVEN	CONVEN	CONVEN	CONVEN
Total Stream																	
Temperature	C	452,0	25,0	25,0	30,0	30,0	68,6	42,6	93,5	95,0	25,0	100,5	28,0	190,0	50,0	25,0	25,0
Pressure	bar	63,0	1,0	1,0	1,5	1,5	1,0	0,1	0,8	1,0	1,0	1,0	1,0	1,0	1,0	1,0	1,0
Mass Vapor Fraction		1,0	1,0	0,0	0,0	0,0	0,0	0,1	0,0	0,6	0,0	1,0	0,0	1,0	0,0	0,0	0,0
Mass Liquid Fraction		0,0	0,0	1,0	0,9	1,0	1,0	0,9	1,0	0,4	0,5	0,0	0,9	0,0	0,3	1,0	1,0
Mass Solid Fraction		0,0	0,0	0,0	0,1	0,0	0,0	0,0	0,0	0,0	0,5	0,0	0,1	0,0	0,7	0,0	0,0
Mass Enthalpy	cal/gm	-3025,6	-644,4	-39,2	-3467,2	-3732,3	-3266,7	-3637,5	-3706,6	-2915,4	-2380,4	-3178,8	-3468,1	-365,8	-1874,3	-3779,9	1959,8
Mass Entropy	cal/gm-K	-0,7	-1,4	1,0	-2,0	-2,2	-1,8	-2,0	-1,9	-0,9	-1,3	-0,5	-2,4	0,1	-1,2	-2,1	1,6
Mass Density	gm/cc	0,0	0,0	1,5	1,0	1,0	1,0	0,0	0,2	0,0	1,1	0,0	1,0	0,0	1,1	1,0	2,1
Average MW		18,0	17,0	192,4	21,1	18,2	22,3	18,8	18,1	19,3	35,7	18,1	21,6	34,7	47,2	18,1	32,1
Mass Flows	kg/hr	177473,2	89,0	0,7	172692,5	44518,7	95522,0	212937,6	50003,9	19151,9	29939,9	37991,2	17312,1	2708,0	10072,3	37991,2	472,2
H2O	kg/hr	177473,2	0,0	0,0	143877,5	43543,1	75613,1	203546,3	49703,0	16046,1	12984,2	37797,4	13852,9	13,8	2856,9	37797,4	0,0
CO2	kg/hr	0,0	0,0	0,0	0,1	0,2	0,0	0,6	0,0	544,3	0,0	0,0	0,6	0,0	0,0	0,0	0,0
O2	kg/hr	0,0	0,0	0,0	0,9	0,3	0,0	1,0	0,0	0,1	0,0	0,0	0,1	0,1	0,0	0,0	0,0
ACETAC	kg/hr	0,0	0,0	0,0	12,9	2,3	0,0	50,3	184,9	34,1	0,0	0,0	37,9	0,0	1,1	0,0	0,0
NH3	kg/hr	0,0	89,0	0,0	1,9	1,1	89,0	5,6	0,0	0,0	0,0	0,0	3,8	0,0	0,0	0,0	0,0
GLUCOSE	kg/hr	0,0	0,0	0,0	0,0	55,2	2988,4	370,3	0,0	0,0	0,0	0,0	374,1	0,0	478,9	0,0	0,0
FRUCTOSE	kg/hr	0,0	0,0	0,0	7161,1	0,0	2988,4	7089,3	0,0	0,0	0,0	0,0	0,0	0,0	0,0	0,0	0,0
SUCROSE	kg/hr	0,0	0,0	0,0	0,0	0,0	13843,2	0,0	0,0	0,0	0,0	0,0	0,0	0,0	0,0	0,0	0,0
BMSLUDGE	kg/hr	0,0	0,0	0,0	0,0	0,0	0,0	0,0	0,0	0,0	0,0	0,0	0,0	0,0	0,0	0,0	0,0
PROPACID	kg/hr	0,0	0,0	0,0	0,0	0,0	0,0	0,0	0,0	0,0	0,0	0,0	0,0	0,0	0,0	0,0	0,0
BUTYRACI	kg/hr	0,0	0,0	0,0	0,0	0,0	0,0	0,0	0,0	0,0	0,0	0,0	0,0	0,0	0,0	0,0	0,0
H2	kg/hr	0,0	0,0	0,0	0,0	0,0	0,0	0,0	0,0	0,0	0,0	0,0	0,0	0,0	0,0	0,0	0,0
CH4	kg/hr	0,0	0,0	0,0	0,0	0,0	0,0	0,0	0,0	0,0	0,0	0,0	0,0	0,0	0,0	0,0	0,0
N2	kg/hr	0,0	0,0	0,0	1,9	0,6	0,0	2,1	0,0	2485,7	0,0	0,0	0,2	1750,7	0,0	0,0	0,0
MCITRICA	kg/hr	0,0	0,0	0,0	19322,4	0,0	0,0	0,0	0,0	0,0	0,0	0,0	1223,0	0,0	0,0	0,0	0,0
A.NIGER	kg/hr	0,0	0,0	0,0	1879,1	681,0	0,0	0,0	0,0	0,0	0,0	0,0	0,0	0,0	0,0	0,0	0,0
MGSO5H2O	kg/hr	0,0	0,0	0,7	0,7	0,0	0,0	0,6	0,0	0,0	0,0	0,0	0,0	0,0	0,0	0,0	0,0
MGSO4	kg/hr	0,0	0,0	0,0	7,5	7,5	0,0	7,4	0,0	0,0	0,0	7,5	0,0	0,0	0,0	7,5	0,0
TRISODCI	kg/hr	0,0	0,0	0,0	0,0	0,0	0,0	0,0	0,0	0,0	0,0	0,0	0,0	0,0	0,0	0,0	0,0
KH2PO4	kg/hr	0,0	0,0	0,0	186,4	186,4	0,0	184,5	0,0	0,0	0,0	186,4	0,0	0,0	0,0	186,4	0,0
ACITSOLI	kg/hr	0,0	0,0	0,0	0,0	0,0	0,0	0,0	0,0	0,0	0,0	0,0	0,0	0,0	0,0	0,0	0,0
ACITLIQ	kg/hr	0,0	0,0	0,0	0,0	0,0	0,0	0,0	0,0	0,0	0,0	0,0	0,0	0,0	0,0	0,0	0,0
XYLAN	kg/hr	0,0	0,0	0,0	0,0	0,0	0,0	0,0	0,0	0,0	3669,8	0,0	0,0	0,0	1410,0	0,0	0,0
ARABINAN	kg/hr	0,0	0,0	0,0	0,0	0,0	0,0	0,0	0,0	0,0	303,4	0,0	0,0	0,0	109,6	0,0	0,0
CELLULOS	kg/hr	0,0	0,0	0,0	0,0	0,0	0,0	0,0	0,0	0,0	6854,1	0,0	0,0	0,0	296,0	0,0	0,0
MANNAN	kg/hr	0,0	0,0	0,0	0,0	0,0	0,0	0,0	0,0	0,0	26,4	0,0	0,0	0,0	26,4	0,0	0,0
GALACTAN	kg/hr	0,0	0,0	0,0	0,0	0,0	0,0	0,0	0,0	0,0	137,2	0,0	0,0	0,0	137,2	0,0	0,0
EXTRACT	kg/hr	0,0	0,0	0,0	52,7	9,0	0,0	1210,0	0,0	0,0	1229,3	0,0	1169,6	0,0	4,4	0,0	0,0
ASH	kg/hr	0,0	0,0	0,0	0,0	0,0	0,0	0,0	0,0	0,0	569,9	0,0	0,0	0,0	569,9	0,0	0,0
LIGNIN	kg/hr	0,0	0,0	0,0	0,0	0,0	0,0	0,0	0,0	0,0	4165,7	0,0	0,0	0,0	4165,7	0,0	0,0
SULPHUR	kg/hr	0,0	0,0	0,0	0,0	0,0	0,0	0,0	0,0	0,0	0,0	0,0	0,0	0,0	0,0	0,0	472,2
SO2	kg/hr	0,0	0,0	0,0	0,7	0,4	0,0	0,7	104,1	41,0	0,0	0,0	0,0	943,5	0,4	0,0	0,0
XYLOSE	kg/hr	0,0	0,0	0,0	106,3	18,1	0,0	105,3	0,0	0,0	0,0	0,0	0,0	0,0	8,9	0,0	0,0
ARABINOS	kg/hr	0,0	0,0	0,0	9,4	1,6	0,0	216,7	0,0	0,0	0,0	0,0	209,4	0,0	0,8	0,0	0,0
FURFURAL	kg/hr	0,0	0,0	0,0	2,2	0,4	0,0	2,6	11,9	0,6	0,0	0,0	0,4	0,0	0,2	0,0	0,0
CACO3	kg/hr	0,0	0,0	0,0	0,0	0,0	0,0	0,0	0,0	0,0	0,0	0,0	0,0	0,0	0,0	0,0	0,0
CASO4	kg/hr	0,0	0,0	0,0	0,0	0,0	0,0	0,0	0,0	0,0	0,0	0,0	0,0	0,0	0,0	0,0	0,0
CASO3	kg/hr	0,0	0,0	0,0	0,0	0,0	0,0	0,0	0,0	0,0	0,0	0,0	0,0	0,0	0,0	0,0	0,0
CELLOB	kg/hr	0,0	0,0	0,0	68,9	11,7	0,0	68,2	0,0	0,0	0,0	0,0	0,0	0,0	5,8	0,0	0,0
Y.LIPOLY	kg/hr	0,0	0,0	0,0	0,0	0,0	0,0	0,0	0,0	0,0	0,0	0,0	363,5	0,0	0,0	0,0	0,0
XYLITOL	kg/hr	0,0	0,0	0,0	0,0	0,0	0,0	75,9	0,0	0,0	0,0	0,0	76,7	0,0	0,0	0,0	0,0
POTAS-01	kg/hr	0,0	0,0	0,0	0,0	0,0	0,0	0,0	0,0	0,0	0,0	0,0	0,0	0,0	0,0	0,0	0,0
MGSO47W	kg/hr	0,0	0,0	0,0	0,0	0,0	0,0	0,0	0,0	0,0	0,0	0,0	0,0	0,0	0,0	0,0	0,0
01-Oct-01	kg/hr	0,0	0,0	0,0	0,0	0,0	0,0	0,0	0,0	0,0	0,0	0,0	0,0	0,0	0,0	0,0	0,0
ISOVALAC	kg/hr	0,0	0,0	0,0	0,0	0,0	0,0	0,0	0,0	0,0	0,0	0,0	0,0	0,0	0,0	0,0	0,0

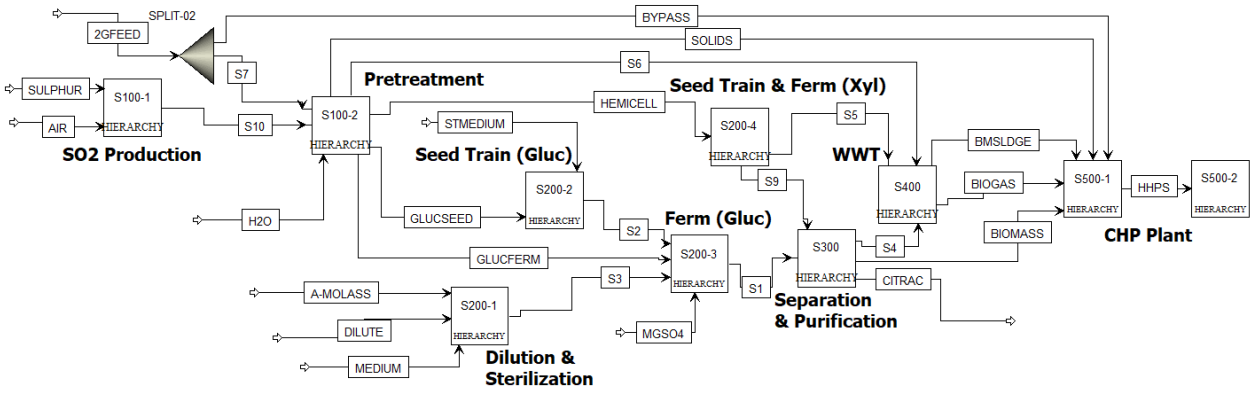

Figure 85: Scenario J, Main Flowsheet in Aspen Plus®

APPENDIX D – CAPITAL EXPENDITURES

Table 70: Capital Expenditures of the 2,3-BDO Scenarios

	TOTAL PURCHASED EQUIPMENT COST (M$)		TOTAL INSTALLED EQUIPMENT COST (M$)	
SECTION OF PLANT	**A**	**B**	**A**	**B**
S100-1&2	-	18.62	-	27.33
S200-1	0.36	0.28	0.62	0.5
S200-2&3	8.53	15.61	13.13	24.58
S300	6.43	8.99	15.08	19.63
S400	18.98	32	19.51	32.81
S500-1&2	8.56	28.24	15.54	51.28
S600	2.17	3.44	3.57	5.75
TOTAL INSTALLED EQUIPMENT COST	**45.02**	**107.17**	**67.45**	**161.87**
ISBL: INSTALLED COST INSIDE BATTERY LIMITS (EXCLUDING UTILITIES)			**28.83**	**72.03**
			COST (M$)	
WAREHOUSE	4% OF ISBL		1.15	2.88
SITE DEVELOPMENT	9% OF ISBL		2.59	6.48
ADDITIONAL PIPING	4.5% OF ISBL		1.3	3.24
STORAGE	5% OF ISBL		1.44	3.6
INITIAL REFRIGERANT COST			-	0.002
TOTAL DIRECT COST (TDC)			73.94	178.08
PRORATEABLE COSTS	10% OF TDC		7.39	17.81
FIELD EXPENSES	10% OF TDC		7.39	17.81
HOME OFFICE AND CONSTRUCTION	20% OF TDC		14.79	35.62
PROJECT CONTINGENCY	10% OF TDC		7.39	17.81
OTHER COSTS	10% OF TDC		7.39	17.81
TOTAL INDIRECT COST			44.36	106.85
FIXED CAPITAL INVESTMENT (FCI)	**TDC+TIC**		118.3	284.93
WORKING CAPITAL	5% OF FCI		5.92	14.25
TOTAL CAPITAL INVESTMENT (TCI)			**124.2**	**299.18**
TOTAL CAPITAL INVESTMENT$_{per\ unit}$	$/kg per year		**2.73**	**4.4**

Table 71: Capital Expenditures of 1,3-BD Scenarios

	TOTAL PURCHASED EQUIPMENT COST (M$)				TOTAL INSTALLED EQUIPMENT COST (M$)			
SECTION OF PLANT	**C**	**D**	**E**	**F**	**C**	**D**	**E**	**F**
S100-1&2	-	17.9	-	14.81	-	26.3	-	21.9
S200-1	0.38	0.31	0.03	0.03	0.74	0.54	0.18	0.14
S200-2&3(2-4)	8.75	15.33	5.38	8.15	13.4	24.2	8.11	12.78
S300-1(&2)	6.15	9	3.71	6.1	14.5	19.4	7.04	11.15
S400	19.59	30.33	21	36.2	19.9	31	21.4	36.8
S500-1&2	10.3	27.24	18.4	32.75	18.7	49.6	33.3	59.35
S600	2.3	3.28	4.62	6.27	3.8	5.47	6.05	8.4
S700(-1-5)	1.68	1.63	5.01	6.21	3.47	3.82	10.8	16.15
S800	0.88	0.95	0.99	1.23	1.94	2.19	2.18	2.71
TOTAL EQUIPMENT COST	**49.9**	**106**	**59.1**	**111.7**	**76.5**	**163**	**89.1**	**169**
ISBL: INSTALLED COST INSIDE BATTERY LIMITS (EXCLUDING UTILITIES)					**32.1**	**74.3**	**26.1**	**62.1**
					COST (M$)			
WAREHOUSE	4% OF ISBL				1.29	2.97	1.04	2.48
SITE DEVELOPMENT	9% OF ISBL				2.89	6.69	2.35	5.59
ADDITIONAL PIPING	4.5% OF ISBL				1.45	3.34	1.17	2.79
STORAGE	5% OF ISBL				1.61	3.71	1.3	3.1
INITIAL REFRIGERANT COST					-	0.002	0.09	0.13
INITIAL MOLTEN SALT COST					0.01	0.01	0.01	0.02
CATALYST COST					2.7	4.41	0.95	2.93
TOTAL DIRECT COST (TDC)					86.4	184	96	186
PRORATEABLE COSTS	10% OF TDC				8.64	18.4	9.6	18.6
FIELD EXPENSES	10% OF TDC				8.64	18.4	9.6	18.6
HOME OFFICE AND CONSTRUCTION	20% OF TDC				17.3	36.7	19.2	37.27
PROJECT CONTINGENCY	10% OF TDC				8.64	18.4	9.6	18.6
OTHER COSTS	10% OF TDC				8.64	18.4	9.6	18.6
TOTAL INDIRECT COST					51.9	110	57.59	111.8
FIXED CAPITAL INVESTMENT (FCI)	**TDC+TIC**				138	294	154	298.1
WORKING CAPITAL	5% OF FCI				6.91	14.7	7.68	14.9
TOTAL CAPITAL INVESTMENT (TCI)					**145**	**308**	**161**	**313**
TOTAL CAPITAL INVESTMENT$_{per\ unit}$	$/kg per year				**6.33**	**9.07**	**11.71**	**13.6**

Table 72: Capital Expenditures of the PHB Scenarios

	TOTAL PURCHASED EQUIPMENT COST (M$)		TOTAL INSTALLED EQUIPMENT COST (M$)	
SECTION OF PLANT	**G**	**H**	**G**	**H**
S100	-	15.39	-	21.69
S200-1&2	0.48	0.44	0.91	0.96
S200-3&4	18.66	25.5	33.65	47.3
S300	3.76	5.29	6.16	8.51
S400	30.6	47.78	30.94	48.19
S500-(1&2)	2.08	16.72	3.75	30.38
S600	4.06	2.78	5.3	4.56
TOTAL EQUIPMENT COST	**59.64**	**113.9**	**80.71**	**161.56**
ISBL: INSTALLED COST INSIDE BATTERY LIMITS (EXCLUDING UTILITIES)			**40.72**	**78.43**
			COST (M$)	
WAREHOUSE	4% OF ISBL		1.63	3.14
SITE DEVELOPMENT	9% OF ISBL		3.66	7.06
ADDITIONAL PIPING	4.5% OF ISBL		1.83	3.53
STORAGE	5% OF ISBL		2.04	3.92
INITIAL REFRIGERANT COST			0.001	0.0014
TOTAL DIRECT COST (TDC)			89.87	179.2
PRORATEABLE COSTS	10% OF TDC		8.99	17.92
FIELD EXPENSES	10% OF TDC		8.99	17.92
HOME OFFICE AND CONSTRUCTION	20% OF TDC		17.97	35.84
PROJECT CONTINGENCY	10% OF TDC		8.99	17.92
OTHER COSTS	10% OF TDC		8.99	17.92
TOTAL INDIRECT COST			53.92	107.53
FIXED CAPITAL INVESTMENT (FCI)	**TDC+TIC**		143.8	286.73
WORKING CAPITAL	5% OF FCI		7.19	14.34
TOTAL CAPITAL INVESTMENT (TCI)			**150.99**	**301.07**
TOTAL CAPITAL INVESTMENT$_{\text{per unit}}$	$/kg per year		**9.82**	**12.89**

Table 73: Capital Expenditures of the Citric Acid Scenarios

	TOTAL PURCHASED EQUIPMENT COST (M$)		TOTAL INSTALLED EQUIPMENT COST (M$)	
SECTION OF PLANT	**I**	**J**	**I**	**J**
S100-1&2	-	16.8	-	24.62
S200-1	0.03	0.025	0.184	0.167
S200-2&3	67.9	96.54	138.87	190.3
S300	4.9	7.22	8.73	11.95
S400	27.59	43.28	28	43.66
S500-1&2	17.78	33.86	32.16	61.27
S600	3.53	5.45	5,78	8.94
TOTAL EQUIPMENT COST	**121.69**	**181.25**	**213.72**	**340.9**
ISBL: INSTALLED COST INSIDE BATTERY LIMITS (EXCLUDING UTILITIES)			**147.79**	**227**
			COST (M$)	
WAREHOUSE	4% OF ISBL		5.9	9.08
SITE DEVELOPMENT	9% OF ISBL		13.3	20.43
ADDITIONAL PIPING	4.5% OF ISBL		6.65	10.2
STORAGE	5% OF ISBL		7.4	11.4
INITIAL REFRIGERANT COST			-	0.002
TOTAL DIRECT COST (TDC)			246.97	392
PRORATEABLE COSTS	10% OF TDC		24.7	39.2
FIELD EXPENSES	10% OF TDC		24.7	39.2
HOME OFFICE AND CONSTRUCTION	20% OF TDC		49.4	78.4
PROJECT CONTINGENCY	10% OF TDC		24.7	39.2
OTHER COSTS	10% OF TDC		24.7	39.2
TOTAL INDIRECT COST			148.18	235.2
FIXED CAPITAL INVESTMENT (FCI)	**TDC+TIC**		395.15	627.2
WORKING CAPITAL	5% OF FCI		19.78	31.4
TOTAL CAPITAL INVESTMENT (TCI)			**414.91**	**658.6**
TOTAL CAPITAL INVESTMENT$_{\text{per unit}}$	$/kg per year		**6.36**	**6.88**

APPENDIX E – FIXED OPERATIONAL COSTS

Table 74: Fixed Operating Costs of Scenario A

FIXED OPERATING COST			
LABOR AND SUPERVISION			
JOB TITLE IN SOUTH AFRICA	**2019 SALARY $/year**	**AMOUNT REQUIRED**	**TOTAL SALARIES ($/year)**
PROCESS MANAGER	43730	1	43730
PROCESS ENGINEER	27183	2	54366
MAINTENANCE ENGINEER	27040	1	27040
MACHINE SETTER	19283	8	154264
CHEMICAL ENGINEER	22277	1	22277
CHEMICAL LAB TECHNICIAN	16143	2	32286
CHEM LAB TECHNICIAN (ENZYME)	NOT APPLICABLE TO 1G		
FOREMAN	22917	4	91668
MACHINE OPERATORS	16088	12	193056
MACHINE OPERATORS - ENZYME	NOT APPLICABLE TO 1G		
LABOURER	13984	3	41952
HELPDESK OPERATOR	16994	3	50982
TOTAL SALARIES		**31**	**711621**
OTHER OVERHEAD COSTS			
MAINTENANCE	3% OF ISBL		864840.41
PROPERTY INSURANCE AND TAX	0,7% OF FCI		828104.59
TOTAL OVERHEAD COSTS			**1692945.01**
TOTAL FIXED OPERATING COSTS			**2404566.01**

Table 75: Fixed Operating Costs of Scenario B

FIXED OPERATING COST			
LABOR AND SUPERVISION			
JOB TITLE IN SOUTH AFRICA	**2019 SALARY $/year**	**AMOUNT REQUIRED**	**TOTAL SALARIES ($/year)**
PROCESS MANAGER	43730	1	43730
PROCESS ENGINEER	27183	2	54366
MAINTENANCE ENGINEER	27040	1	27040
MACHINE SETTER	19283	8	154264
CHEMICAL ENGINEER	22277	1	22277
CHEMICAL LAB TECHNICIAN	16143	2	32286
CHEM LAB TECHNICIAN (ENZYME)	16143	2	32286
FOREMAN	22917	4	91668
MACHINE OPERATORS	16088	32	514816
MACHINE OPERATORS - ENZYME	16088	11	176968
LABOURER	13984	3	41952
HELPDESK OPERATOR	16994	3	50982
TOTAL SALARIES		**70**	**1242635**
OTHER OVERHEAD COSTS			
MAINTENANCE	3% OF ISBL		2138543.93
PROPERTY INSURANCE AND TAX	0,7% OF FCI		1984235.74
TOTAL OVERHEAD COSTS			**4122779.67**

TOTAL FIXED OPERATING COSTS	5365414.67

Table 76: Fixed Operating Costs of Scenario C

FIXED OPERATING COST			
LABOR AND SUPERVISION			
JOB TITLE IN SOUTH AFRICA	2019 SALARY $/year	AMOUNT REQUIRED	TOTAL SALARIES ($/year)
PROCESS MANAGER	43730	1	43730
PROCESS ENGINEER	27183	2	54366
MAINTENANCE ENGINEER	27040	1	27040
MACHINE SETTER	19283	8	154264
CHEMICAL ENGINEER	22277	1	22277
CHEMICAL LAB TECHNICIAN	16143	2	32286
CHEM LAB TECHNICIAN (ENZYME)	NOT APPLICABLE TO 1G		
FOREMAN	22917	4	91668
MACHINE OPERATORS	16088	13	209144
MACHINE OPERATORS - ENZYME	NOT APPLICABLE TO 1G		
LABOURER	13984	3	41952
HELPDESK OPERATOR	16994	3	50982
TOTAL SALARIES		**32**	**727709**
OTHER OVERHEAD COSTS			
MAINTENANCE	3% OF ISBL		964613.80
PROPERTY INSURANCE AND TAX	0,7% OF FCI		967869.15
TOTAL OVERHEAD COSTS			**1932482.96**
TOTAL FIXED OPERATING COSTS			**2660191.96**

Table 77: Fixed Operating Costs of Scenario D

FIXED OPERATING COST			
LABOR AND SUPERVISION			
JOB TITLE IN SOUTH AFRICA	2019 SALARY $/year	AMOUNT REQUIRED	TOTAL SALARIES ($/year)
PROCESS MANAGER	43730	1	43730
PROCESS ENGINEER	27183	2	54366
MAINTENANCE ENGINEER	27040	1	27040
MACHINE SETTER	19283	8	154264
CHEMICAL ENGINEER	22277	1	22277
CHEMICAL LAB TECHNICIAN	16143	2	32286
CHEM LAB TECHNICIAN	16143	2	32286
FOREMAN	22917	4	91668
MACHINE OPERATORS	16088	32	514816
MACHINE OPERATORS -	16088	11	176968
LABOURER	13984	3	41952
HELPDESK OPERATOR	16994	3	50982
TOTAL SALARIES		**64**	**1242635**
OTHER OVERHEAD COSTS			
MAINTENANCE	3% OF ISBL		2228205.91
PROPERTY INSURANCE AND TAX	0,7% OF FCI		2056570.46
TOTAL OVERHEAD COSTS			**4284776.37**
TOTAL FIXED OPERATING COSTS			**5527411.37**

Table 78: Fixed Operating Costs of Scenario E

FIXED OPERATING COST			
LABOR AND SUPERVISION			
JOB TITLE IN SOUTH AFRICA	**2019 SALARY $/year**	**AMOUNT REQUIRED**	**TOTAL SALARIES ($/year)**
PROCESS MANAGER	43730	1	43730
PROCESS ENGINEER	27183	2	54366
MAINTENANCE ENGINEER	27040	1	27040
MACHINE SETTER	19283	8	154264
CHEMICAL ENGINEER	22277	1	22277
CHEMICAL LAB TECHNICIAN	16143	2	32286
CHEM LAB TECHNICIAN (ENZYME)	NOT APPLICABLE TO 1G		
FOREMAN	22917	4	91668
MACHINE OPERATORS	16088	12	193056
MACHINE OPERATORS - ENZYME	NOT APPLICABLE TO 1G		
LABOURER	13984	3	41952
HELPDESK OPERATOR	16994	3	50982
TOTAL SALARIES		**31**	**711621**
OTHER OVERHEAD COSTS			
MAINTENANCE	3% OF ISBL		782724.11
PROPERTY INSURANCE AND TAX	0,7% OF FCI		1075038.66
TOTAL OVERHEAD COSTS			**1857762.77**
TOTAL FIXED OPERATING COSTS			**2569383.77**

Table 79: Fixed Operating Costs of Scenario F

FIXED OPERATING COST			
LABOR AND SUPERVISION			
JOB TITLE IN SOUTH AFRICA	**2019 SALARY $/year**	**AMOUNT REQUIRED**	**TOTAL SALARIES ($/year)**
PROCESS MANAGER	43730	1	43730
PROCESS ENGINEER	27183	2	54366
MAINTENANCE ENGINEER	27040	1	27040
MACHINE SETTER	19283	8	154264
CHEMICAL ENGINEER	22277	1	22277
CHEMICAL LAB TECHNICIAN	16143	2	32286
CHEM LAB TECHNICIAN (ENZYME)	16143	2	32286
FOREMAN	22917	4	91668
MACHINE OPERATORS	16088	32	514816
MACHINE OPERATORS - ENZYME	16088	11	176968
LABOURER	13984	3	41952
HELPDESK OPERATOR	16994	3	50982
TOTAL SALARIES		**70**	**1242635**
OTHER OVERHEAD COSTS			
MAINTENANCE	3% OF ISBL		1863140.65
PROPERTY INSURANCE AND TAX	0,7% OF FCI		2086922.16
TOTAL OVERHEAD COSTS			**3950062.81**
TOTAL FIXED OPERATING COSTS			**5192697.81**

Table 80: Fixed Operating Costs of Scenario G

FIXED OPERATING COST			
LABOR AND SUPERVISION			
JOB TITLE IN SOUTH AFRICA	**2019 SALARY $/year**	**AMOUNT REQUIRED**	**TOTAL SALARIES ($/year)**
PROCESS MANAGER	43730	1	43730
PROCESS ENGINEER	27183	2	54366
MAINTENANCE ENGINEER	27040	1	27040
MACHINE SETTER	19283	8	154264
CHEMICAL ENGINEER	22277	1	22277
CHEMICAL LAB TECHNICIAN	16143	2	32286
CHEM LAB TECHNICIAN (ENZYME)	NOT APPLICABLE TO 1G		
FOREMAN	22917	4	91668
MACHINE OPERATORS	16088	11	176968
MACHINE OPERATORS - ENZYME	NOT APPLICABLE TO 1G		
LABOURER	13984	3	41952
HELPDESK OPERATOR	16994	3	50982
TOTAL SALARIES		**30**	**695533**
OTHER OVERHEAD COSTS			
MAINTENANCE	3% OF ISBL		1221623.77
PROPERTY INSURANCE AND TAX	0,7% OF FCI		1006587.62
TOTAL OVERHEAD COSTS			**2228211.39**
TOTAL FIXED OPERATING COSTS			**2923744.39**

Table 81: Fixed Operating Costs of Scenario H

FIXED OPERATING COST			
LABOR AND SUPERVISION			
JOB TITLE IN SOUTH AFRICA	**2019 SALARY $/year**	**AMOUNT REQUIRED**	**TOTAL SALARIES ($/year)**
PROCESS MANAGER	43730	1	43730
PROCESS ENGINEER	27183	2	54366
MAINTENANCE ENGINEER	27040	1	27040
MACHINE SETTER	19283	8	154264
CHEMICAL ENGINEER	22277	1	22277
CHEMICAL LAB TECHNICIAN	16143	2	32286
CHEM LAB TECHNICIAN (ENZYME)	16143	2	32286
FOREMAN	22917	4	91668
MACHINE OPERATORS	16088	32	514816
MACHINE OPERATORS - ENZYME	16088	11	176968
LABOURER	13984	3	41952
HELPDESK OPERATOR	16994	3	50982
TOTAL SALARIES		**70**	**1242635**
OTHER OVERHEAD COSTS			
MAINTENANCE	3% OF ISBL		2352884.32
PROPERTY INSURANCE AND TAX	0,7% OF FCI		2007133.82
TOTAL OVERHEAD COSTS			**4360018.13**
TOTAL FIXED OPERATING COSTS			**5602653.13**

Table 82: Fixed Operating Costs of Scenario I

FIXED OPERATING COST			
LABOR AND SUPERVISION			
JOB TITLE IN SOUTH AFRICA	**2019 SALARY $/year**	**AMOUNT REQUIRED**	**TOTAL SALARIES ($/year)**
PROCESS MANAGER	43730	1	43730
PROCESS ENGINEER	27183	2	54366
MAINTENANCE ENGINEER	27040	1	27040
MACHINE SETTER	19283	8	154264
CHEMICAL ENGINEER	22277	1	22277
CHEMICAL LAB TECHNICIAN	16143	2	32286
CHEM LAB TECHNICIAN (ENZYME)	NOT APPLICABLE TO 1G		
FOREMAN	22917	4	91668
MACHINE OPERATORS	16088	14	225232
MACHINE OPERATORS - ENZYME	NOT APPLICABLE TO 1G		
LABOURER	13984	3	41952
HELPDESK OPERATOR	16994	3	50982
TOTAL SALARIES		**33**	**743797**
OTHER OVERHEAD COSTS			
MAINTENANCE	3% OF ISBL		4506961.14
PROPERTY INSURANCE AND TAX	0,7% OF FCI		2818367.39
TOTAL OVERHEAD COSTS			**7325328.53**
TOTAL FIXED OPERATING COSTS			**8069125.53**

Table 83: Fixed Operating Costs of Scenario J

FIXED OPERATING COST			
LABOR AND SUPERVISION			
JOB TITLE IN SOUTH AFRICA	**2019 SALARY $/year**	**AMOUNT REQUIRED**	**TOTAL SALARIES ($/year)**
PROCESS MANAGER	43730	1	43730
PROCESS ENGINEER	27183	2	54366
MAINTENANCE ENGINEER	27040	1	27040
MACHINE SETTER	19283	8	154264
CHEMICAL ENGINEER	22277	1	22277
CHEMICAL LAB TECHNICIAN	16143	2	32286
CHEM LAB TECHNICIAN (ENZYME)	16143	2	32286
FOREMAN	22917	4	91668
MACHINE OPERATORS	16088	32	514816
MACHINE OPERATORS - ENZYME	16088	11	176968
LABOURER	13984	3	41952
HELPDESK OPERATOR	16994	3	50982
TOTAL SALARIES		**64**	**1242635**
OTHER OVERHEAD COSTS			
MAINTENANCE	3% OF ISBL		7450785.35
PROPERTY INSURANCE AND TAX	0,7% OF FCI		4684042.48
TOTAL OVERHEAD COSTS			**12134827.83**
TOTAL FIXED OPERATING COSTS			**13377462.83**

APPENDIX F – GHG EMISSIONS

Table 84: GHG Emissions of Scenario A

	Emissions of each step (kg/h)						
	Feedstock cultivation	Transport, blending & storage	Processing 1	Existing CHP	Processing 2	New CHP	Total emissions
Emissions allocated to A-molasses production	3861,61	677,17	332,53	14595,05			
Emissions allocated to Raw sugar production	6562,78	1150,84	565,13	24804,19			33082,94
Emissions allocated to Bagasse production	2086,06	365,81	179,63	7884,32			
Emissions allocated to 2,3-Butanediol production	3861,61	677,17	332,53	14595,05	1069,51	14545,03	35080,90
Emissions allocated to None production	0,00	0,00	0,00	0,00	0,00	0,00	0,00
Emissions allocated to None production	0,00	0,00	0,00	0,00	0,00	0,00	0,00

Table 85: GHG Emissions of Scenario B

	Emissions of each step (kg/h)						
	Feedstock cultivation	Transport, blending & storage	Processing 1	Existing CHP	Processing 2	New CHP	Total emissions
Emissions allocated to A-molasses/2G production	3543,59	805,18	384,92	14955,15			
Emissions allocated to Raw sugar production	5219,94	1186,09	567,01	22029,89			29002,92
Emissions allocated to Bagasse production	1659,22	377,01	180,23	7002,48			
Emissions allocated to 1,3-Butadiene production	3543,59	805,18	384,92	14955,15	8628,39	57341,37	85658,60
Emissions allocated to None production	0,00	0,00	0,00	0,00	0,00	0,00	0,00
Emissions allocated to None production	0,00	0,00	0,00	0,00	0,00	0,00	0,00

Table 86: GHG Emissions of Scenario C

	Emissions of each step (kg/h)						
	Feedstock cultivation	**Transport, blending & storage**	**Processing 1**	**Existing CHP**	**Processing 2**	**New CHP**	**Total emissions**
Emissions allocated to A-molasses production	4047,77	677,17	332,53	14615,64			
Emissions allocated to Raw sugar production	6879,15	1150,84	565,13	24839,18			33434,31
Emissions allocated to Bagasse production	2186,63	365,81	179,63	7895,45			
Emissions allocated to 1,3-Butadiene production	4047,77	677,17	332,53	14615,64	1108,33	16837,36	37618,79
Emissions allocated to None production	0,00	0,00	0,00	0,00	0,00	0,00	0,00
Emissions allocated to None production	0,00	0,00	0,00	0,00	0,00	0,00	0,00

Table 87: GHG Emissions of Scenario D

	Emissions of each step (kg/h)						
	Feedstock cultivation	**Transport, blending & storage**	**Processing 1**	**Existing CHP**	**Processing 2**	**New CHP**	**Total emissions**
Emissions allocated to A-molasses/2G production	4581,91	827,62	395,92	15431,70			
Emissions allocated to Raw sugar production	6472,21	1169,06	559,26	21798,18			29998,71
Emissions allocated to Bagasse production	2057,27	371,60	177,77	6928,83			
Emissions allocated to 2,3-Butanediol production	4581,91	827,62	395,92	15431,70	10335,90	62404,70	93977,75
Emissions allocated to None production	0,00	0,00	0,00	0,00	0,00	0,00	0,00
Emissions allocated to None production	0,00	0,00	0,00	0,00	0,00	0,00	0,00

Table 88: GHG Emissions of Scenario E

	Emissions of each step (kg/h)						
	Feedstock cultivation	**Transport, blending & storage**	**Processing 1**	**Existing CHP**	**Processing 2**	**New CHP**	**Total emissions**
Emissions allocated to A-molasses production	4047,77	676,09	332,97	14615,57			
Emissions allocated to Raw sugar production	6879,15	1149,00	565,89	24839,06			33433,11
Emissions allocated to Bagasse production	2186,63	365,22	179,87	7895,41			
Emissions allocated to 1,3-Butadiene production	4047,77	676,09	332,97	14615,57	3078,44	23251,71	46002,55
Emissions allocated to None production	0,00	0,00	0,00	0,00	0,00	0,00	0,00
Emissions allocated to None production	0,00	0,00	0,00	0,00	0,00	0,00	0,00

Table 89: GHG Emissions of Scenario F

	Emissions of each step (kg/h)						
	Feedstock cultivation	**Transport, blending & storage**	**Processing 1**	**Existing CHP**	**Processing 2**	**New CHP**	**Total emissions**
Emissions allocated to A-molasses/2G production	3636,36	826,26	410,12	15343,12			
Emissions allocated to Raw sugar production	5149,54	1170,09	580,79	21727,81			28628,23
Emissions allocated to Bagasse production	1636,85	371,93	184,61	6906,46			
Emissions allocated to 1,3-Butadiene production	3636,36	826,26	410,12	15343,12	8397,34	60614,45	89227,66
Emissions allocated to None production	0,00	0,00	0,00	0,00	0,00	0,00	0,00
Emissions allocated to None production	0,00	0,00	0,00	0,00	0,00	0,00	0,00

Table 90: GHG Emissions of Scenario G

	Emissions of each step (kg/h)						
	Feedstock cultivation	**Transport, blending & storage**	**Processing 1**	**Existing CHP**	**Processing 2**	**New CHP**	**Total emissions**
Emissions allocated to A-molasses production	3861,26	676,09	332,97	14594,94			
Emissions allocated to Raw sugar production	6562,19	1149,00	565,89	24804,00			33081,08
Emissions allocated to Bagasse production	2085,87	365,22	179,87	7884,27			
Emissions allocated to Polyhydroxybutyrate production	3861,26	676,09	332,97	14594,94	65503,00	13845,86	98814,13
Emissions allocated to None production	0,00	0,00	0,00	0,00	0,00	0,00	0,00
Emissions allocated to None production	0,00	0,00	0,00	0,00	0,00	0,00	0,00

Table 91: GHG Emissions of Scenario H

	Emissions of each step (kg/h)						
	Feedstock cultivation	**Transport, blending & storage**	**Processing 1**	**Existing CHP**	**Processing 2**	**New CHP**	**Total emissions**
Emissions allocated to A-molasses/2G production	4599,73	871,13	430,40	16217,06			
Emissions allocated to Raw sugar production	5998,56	1136,05	561,29	21148,84			28844,74
Emissions allocated to Bagasse production	1906,72	361,11	178,41	6722,43			
Emissions allocated to Polyhydroxybutyrate production	4599,73	871,13	430,40	16217,06	431517,04	36351,13	489986,48
Emissions allocated to None production	0,00	0,00	0,00	0,00	0,00	0,00	0,00
Emissions allocated to None production	0,00	0,00	0,00	0,00	0,00	0,00	0,00

Table 92: GHG Emissions of Scenario I

	Emissions of each step (kg/h)						
	Feedstock cultivation	**Transport, blending & storage**	**Processing 1**	**Existing CHP**	**Processing 2**	**New CHP**	**Total emissions**
Emissions allocated to A-molasses production	3861,26	676,09	332,97	14594,94			
Emissions allocated to Raw sugar production	6562,19	1149,00	565,89	24804,00			33081,08
Emissions allocated to Bagasse production	2085,87	365,22	179,87	7884,27			
Emissions allocated to Citric Acid production	3861,26	676,09	332,97	14594,94	1627,65	20969,22	42062,14
Emissions allocated to None production	0,00	0,00	0,00	0,00	0,00	0,00	0,00
Emissions allocated to None production	0,00	0,00	0,00	0,00	0,00	0,00	0,00

Table 93: GHG Emissions of Scenario J

	Emissions of each step (kg/h)						
	Feedstock cultivation	**Transport, blending & storage**	**Processing 1**	**Existing CHP**	**Processing 2**	**New CHP**	**Total emissions**
Emissions allocated to A-molasses/2G production	4224,16	800,00	246,40	14899,70			
Emissions allocated to Raw sugar production	6283,55	1190,02	366,52	22163,72			30003,81
Emissions allocated to Bagasse production	1997,31	378,26	116,50	7045,02			
Emissions allocated to Citric Acid production	4224,16	800,00	246,40	14899,70	8016,91	63636,07	91823,23
Emissions allocated to None production	0,00	0,00	0,00	0,00	0,00	0,00	0,00
Emissions allocated to None production	0,00	0,00	0,00	0,00	0,00	0,00	0,00